



HAL
open science

Solubility of a hydrophobic model drug in a binary solvent system of interest for industrial freeze-drying

Fabrice Aman-Pommier

► **To cite this version:**

Fabrice Aman-Pommier. Solubility of a hydrophobic model drug in a binary solvent system of interest for industrial freeze-drying. Chemical and Process Engineering. Université de Lyon, 2017. English. NNT : 2017LYSE1220 . tel-01717820

HAL Id: tel-01717820

<https://theses.hal.science/tel-01717820>

Submitted on 26 Feb 2018

HAL is a multi-disciplinary open access archive for the deposit and dissemination of scientific research documents, whether they are published or not. The documents may come from teaching and research institutions in France or abroad, or from public or private research centers.

L'archive ouverte pluridisciplinaire **HAL**, est destinée au dépôt et à la diffusion de documents scientifiques de niveau recherche, publiés ou non, émanant des établissements d'enseignement et de recherche français ou étrangers, des laboratoires publics ou privés.

N°d'ordre NNT : xxx



THESE de DOCTORAT DE L'UNIVERSITE DE LYON

opérée au sein de
l'Université Claude Bernard Lyon 1

**Ecole Doctorale de Chimie de Lyon
(ED 206, Chimie, Procédés, Environnement)**

**Spécialité de doctorat : Chimie
Disciplines : Physico-Chimie/Génie des Procédés**

Soutenue publiquement le 26/10/2017, par :
Fabrice Aman-Pommier

Solubilité d'un principe actif hydrophobe modèle dans un système de solvant binaire d'intérêt pour la lyophilisation industrielle.

Devant le jury composé de :

Briançon, Stéphanie	PU	Université Lyon 1	Présidente
Gruy, Frédéric	PU	Ecole des Mines de St Etienne	Rapporteur
Puel, François	PU	CentraleSupélec	Rapporteur
Bakri, Aziz	PU	Université Grenoble-Alpes	Examinateur
Tayakout-Fayolle, Mélaz	PU	Université Lyon 1	Examinatrice
Jallut, Christian	PU	Université Lyon 1	Directeur de thèse

UNIVERSITE CLAUDE BERNARD - LYON 1

Président de l'Université

Président du Conseil Académique

Vice-président du Conseil d'Administration

Vice-président du Conseil Formation et Vie Universitaire

Vice-président de la Commission Recherche

Directrice Générale des Services

M. le Professeur Frédéric FLEURY

M. le Professeur Hamda BEN HADID

M. le Professeur Didier REVEL

M. le Professeur Philippe CHEVALIER

M. Fabrice VALLÉE

Mme Dominique MARCHAND

COMPOSANTES SANTE

Faculté de Médecine Lyon Est – Claude Bernard

Faculté de Médecine et de Maïeutique Lyon Sud – Charles Mérieux

Faculté d'Odontologie

Institut des Sciences Pharmaceutiques et Biologiques

Institut des Sciences et Techniques de la Réadaptation

Département de formation et Centre de Recherche en Biologie Humaine

Directeur : M. le Professeur G.RODE

Directeur : Mme la Professeure C. BURILLON

Directeur : M. le Professeur D. BOURGEOIS

Directeur : Mme la Professeure C. VINCIGUERRA

Directeur : M. X. PERROT

Directeur : Mme la Professeure A-M. SCHOTT

COMPOSANTES ET DEPARTEMENTS DE SCIENCES ET TECHNOLOGIE

Faculté des Sciences et Technologies

Département Biologie

Département Chimie Biochimie

Département GEP

Département Informatique

Département Mathématiques

Département Mécanique

Département Physique

UFR Sciences et Techniques des Activités Physiques et Sportives

Observatoire des Sciences de l'Univers de Lyon

Polytech Lyon

Ecole Supérieure de Chimie Physique Electronique

Institut Universitaire de Technologie de Lyon 1

Ecole Supérieure du Professorat et de l'Education

Institut de Science Financière et d'Assurances

Directeur : M. F. DE MARCHI

Directeur : M. le Professeur F. THEVENARD

Directeur : Mme C. FELIX

Directeur : M. Hassan HAMMOURI

Directeur : M. le Professeur S. AKKOUICHE

Directeur : M. le Professeur G. TOMANOV

Directeur : M. le Professeur H. BEN HADID

Directeur : M. le Professeur J-C PLENET

Directeur : M. Y. VANPOULLE

Directeur : M. B. GUIDERDONI

Directeur : M. le Professeur E.PERRIN

Directeur : M. G. PIGNAULT

Directeur : M. le Professeur C. VITON

Directeur : M. le Professeur A. MOUGNIOTTE

Directeur : M. N. LEBOISNE

This page is intentionally left blank.

Abstract

The aim of this work is to investigate the solubility behavior of a hydrophobic model drug, diazepam, in a binary solvent of industrial interest for freeze-drying, the water + *tert*-butyl alcohol mixture. Firstly, a model describing the dependence of the excess volume of the solvent on both composition and temperature was validated from experimental data obtained during this work and literature data. This model was used to derive expressions for excess partial thermodynamic quantities and their variations with respect to composition and temperature were discussed in terms of molecular interactions and structural arrangements in solution. Secondly, the solubility of diazepam in neat solvents and different binary solvent mixtures was determined. The density of drug-saturated mixtures was also determined as well as the thermophysical properties of original diazepam crystals and excess solid phases from solid-liquid equilibria. The thermodynamic properties relative to the dissolution process of the drug under saturation condition were obtained from solubility temperature dependence using van't Hoff plots. From these, the excess partial thermodynamic properties of diazepam in saturated mixtures were computed and the forces driving the drug solubility variation with respect to the solvent composition were identified. Finally, two excess Gibbs energy models, the Scatchard-Hildebrand and combined Scatchard-Hildebrand/Flory-Huggins models were tested to represent the solubility data. Their capabilities in correlating the dependence of the drug solubility on both the solvent composition and temperature were evaluated and compared.

Key words: diazepam; water; *tert*-butyl alcohol; solubility; density; solid-liquid equilibrium; thermodynamic analysis; thermodynamic modeling; excess thermodynamic quantities

Résumé

L'objectif de ce travail est l'étude de la solubilité d'un principe actif hydrophobe modèle, le diazépam, dans un solvant binaire d'intérêt pour la lyophilisation industrielle, le mélange eau + *tert*-butanol. Un modèle décrivant la dépendance du volume d'excès du solvant vis-à-vis de sa composition et de sa température a été validé à partir de données mesurées au cours de ce travail et de données de la littérature. Les variations de diverses propriétés partielles d'excès issues de ce modèle en fonction de la composition du solvant et de sa température ont été interprétées en termes d'interactions moléculaires et d'arrangements structuraux. Ensuite, la solubilité du diazépam dans le solvant a été mesurée en fonction de sa composition et de sa température. La masse volumique des phases liquides saturées ainsi que les propriétés thermophysiques des cristaux de principe actif originels et des phases solides en excès issues des équilibres solide-liquide ont été déterminées. Les propriétés thermodynamiques caractéristiques du processus de dissolution du diazépam en condition d'équilibre ont été obtenues à partir de la dépendance de sa solubilité vis-à-vis de la température. À partir de ces données, les propriétés thermodynamiques d'excès du diazépam dans les différents mélanges saturés ont été calculées et les forces responsables de la variation de la solubilité du principe actif avec la composition du solvant ont été identifiées. Enfin, la capacité de deux modèles d'enthalpie libre d'excès, le modèle de Scatchard-Hildebrand combiné ou non au modèle de Flory-Huggins, à corréliser les données expérimentales de solubilité a été évaluée et comparée.

Mots-clés : diazépam ; eau ; *tert*-butanol ; solubilité ; masse volumique ; équilibre solide-liquide ; analyse thermodynamique ; modélisation thermodynamique ; quantités thermodynamiques d'excès

Laboratoire d'Automatique et de Génie des Procédés

CNRS/UCBL UMR 5007

Université de Lyon, Université Claude Bernard Lyon 1

43 Bd du 11 novembre 1918

69622 – VILLEURBANNE CEDEX

This page is intentionally left blank.

To Sophie and Cléo.

This page is intentionally left blank.

Acknowledgements

I want to express my deeply-felt thanks to my thesis advisor, Professor Christian Jallut, for his genuine caring attitude, supervision and thoughtful guidance throughout the long and windy road to complete my graduate degree. I also thank the other members of my thesis committee, namely, Professor Frédéric Gruy, Professor François Puel, Professor Aziz Bakri, Professor Stéphanie Briançon and Professor Mélaz Tayakout-Fayolle for their positive comments about the research work presented herein.

I am very grateful to all knowledgeable and friendly people who helped me over these academic years, and especially to my office mate, Audrey Juban, and other fellow graduate students Laure Ridel, Jessica Bile and Barthélémy Brunier, as well as their respective spouses. In addition to their friendship, I offer my sincere thanks to Emmanuel Bayle for assistance with data processing and to Simon Grand for driving a very special day to my better half and me. I will not forget the support, both technical and moral, provided by Jean-Pierre Valour and Sébastien Urbaniak.

I also want to acknowledge Anton Paar GmbH for the generous loan of the vibrating-tube digital density meter, anonymous reviewers for their careful reading of the manuscripts submitted for publication and their insightful suggestions for improving them as well as the French ‘Ministère de l’Enseignement Supérieur et de la Recherche’ for supporting this work financially.

Finally, I thank my close friends and family members whose love and support enabled me to attain this long-awaited goal.

This page is intentionally left blank.

Solubility of a hydrophobic model drug in a binary solvent system of interest for industrial freeze-drying.

This page is intentionally left blank.

Contents

Preface.....	17
Chapter 1.....	21
Excess specific volume of water + <i>tert</i>-butyl alcohol solvent mixtures: Experimental data, modeling and derived excess thermodynamic quantities	
1.1. Introduction.....	23
1.2. Material and methods.....	25
1.2.1. Chemicals.....	25
1.2.2. Solvent mixtures preparation.....	27
1.2.3. Density measurements.....	27
1.2.4. Statistical analysis.....	27
1.3. Results.....	28
1.3.1. Experimental excess specific volume data of water + <i>tert</i> -butyl alcohol solvent mixtures..	28
1.3.2. Modeling of the temperature and composition dependence of excess specific volume of water + <i>tert</i> -butyl alcohol solvent mixtures.....	35
1.3.2.1. Determination of model coefficients and their temperature dependencies.....	35
1.3.2.2. Evaluation of correlative and predictive capabilities of the model.....	43
1.3.3. Derived excess partial specific thermodynamic quantities.....	57
1.4. Discussion.....	65
1.4.1. Components in their pure state.....	65
1.4.2. Components in their mixed state.....	66
1.5. Conclusion.....	72
Nomenclature.....	75
References.....	77
Chapter 2.....	83
Solubility of diazepam in water + <i>tert</i>-butyl alcohol solvent mixtures: Experimental data and thermodynamic analysis	
2.1. Introduction.....	85
2.2. Theory.....	88
2.2.1. Solid-liquid equilibrium.....	88
2.2.2. Solubility temperature dependence.....	90
2.3. Material and methods.....	92
2.3.1. Chemicals.....	92
2.3.2. Solvent mixtures preparation.....	92
2.3.3. Solid-liquid equilibria.....	92

2.3.4. Solubility measurements.....	94
2.3.4.1. Preparation of calibration standards and quality control samples.....	94
2.3.4.2. Preparation of solubility samples.....	96
2.3.4.3. Instrumentation and analytical conditions.....	96
2.3.4.4. Method validation.....	96
2.3.4.5. Quantification of diazepam in solubility samples.....	97
2.3.5. Density measurements.....	98
2.3.6. Differential scanning calorimetry measurements.....	100
2.3.7. Calculations.....	100
2.3.8. Statistical analysis.....	102
2.4. Results and discussion.....	102
2.4.1. Experimental data.....	102
2.4.1.1. Thermal analysis of original drug crystals and excess solid phases from solubility samples.....	102
2.4.1.2. Density of diazepam-free and diazepam-saturated water + <i>tert</i> -butyl alcohol solvent mixtures.....	103
2.4.1.3. Solubility of diazepam in water + <i>tert</i> -butyl alcohol solvent mixtures.....	106
2.4.1.4. Temperature dependence of the solubility of diazepam in water + <i>tert</i> -butyl alcohol solvent mixtures.....	108
2.4.2. Thermodynamics of the solubility of diazepam in water + <i>tert</i> -butyl alcohol solvent mixtures.....	111
2.4.2.1. Activity coefficient of diazepam in water + <i>tert</i> -butyl alcohol solvent mixtures...111	
2.4.2.2. Excess partial molar thermodynamic quantities of diazepam in water + <i>tert</i> -butyl alcohol solvent mixtures.....	113
2.5. Conclusion and perspectives.....	117
Nomenclature.....	119
References.....	121
Chapter 3.....	125
Solubility of diazepam in water + <i>tert</i>-butyl alcohol solvent mixtures: Correlation using Scatchard-Hildebrand and combined Scatchard-Hildebrand/Flory-Huggins excess Gibbs energy models	
3.1. Introduction.....	127
3.2. Theory.....	129
3.2.1. Solid-liquid equilibria.....	129
3.2.2. Excess Gibbs energy models.....	130
3.2.2.1. Scatchard-Hildebrand model.....	131
3.2.2.2. Combined Scatchard-Hildebrand/Flory-Huggins model.....	132
3.3. Methods.....	133
3.3.1. Calculations.....	133
3.3.2. Data reduction.....	137
3.3.3. Models comparison and selection.....	140

3.3.4. Statistical analysis.....	141
3.4. Results and discussion.....	141
3.4.1. Correlation of the temperature and composition dependence of the activity coefficient of diazepam in water + <i>tert</i> -butyl alcohol solvent mixtures.....	141
3.4.2. Accuracy and precision of calculated solubility of diazepam in water + <i>tert</i> -butyl alcohol solvent mixtures.....	152
3.4.3. Practical considerations.....	159
3.5. Conclusion and perspectives.....	159
Nomenclature.....	163
References.....	165
Appendix A.....	173
Supplementary materials related to Chapter 1	
Appendix B.....	191
Supplementary materials related to Chapter 2	
Appendix C.....	201
Supplementary materials related to Chapter 3	

This page is intentionally left blank.

Preface

Despite formulation approaches and technologies developed by scientists over the past decades to enhance the solubility and/or the dissolution rate of hydrophobic drugs in aqueous media, the design of an optimal, reliable and scalable formulation for poorly water-soluble drugs delivery remains extremely challenging, especially when these drugs exhibit physical and/or chemical instability. Freeze-drying, the process by which solvent or dispersion media is removed from a frozen solution or suspension by sublimation and desorption under vacuum, is traditionally used in the pharmaceutical industry for the manufacturing of solid dosage forms of heat-labile and/or water-labile drugs. The first step in the manufacturing process of most lyophilized pharmaceutical compositions consists in preparing a homogeneous solution of the ingredients to be dried, and for this purpose, water is almost universally used as solvent. When considering freeze-drying of high-dosage hydrophobic drugs, for which the concentration in the solution to be lyophilized must be high enough to make the whole process economically viable for a large-scale production, cosolvency, the addition of a miscible organic solvent to water, appears to be the most effective and widely used solubilization approach. Among the cosolvents that have been investigated over the past years in the field of freeze-drying, *tert*-butyl alcohol is the one that attracted the most attention from researchers in both academic and industrial settings. As a matter of fact, *tert*-butyl alcohol is miscible with water over the whole composition range at any temperature, has a low toxicity profile and exhibits suitable physical properties with regard to the freeze drying process including a high fusion temperature, a high solid vapor pressure and a low sublimation enthalpy. All water + *tert*-butyl alcohol solvent mixture compositions share these desirable properties as well and, consequently, they freeze under operating conditions for conventional commercial freeze-dryers and they sublime at a higher rate than neat water for identical process parameters.

A survey of the literature on poorly water-soluble drug formulations freeze-dried from water + *tert*-butyl alcohol solvent mixtures yields the following observations. First, indisputable evidence is given that any kind of poorly water-soluble drug formulation that might be prepared by solvent evaporation method could be produced by freeze-drying from this cosolvent system, but it could or could not be manufactured at the industrial level with

respect to the technology currently available. Second, and despite the fact that actual knowledge allows a rational and effective development of lyophilization cycles, attention is focused on formulation aspects so that apart from very few studies, freeze-drying appears to be a push-button affair, regardless of the process complexity. In the pharmaceutical industry, empirical selection of process parameters and development of freeze-drying cycles on a trial-and-error basis is a risky choice, always time-consuming and cost-effective. This is all the more surprising given that for specific formulation approaches, their successes in improving the solubility and/or the dissolution rate of hydrophobic drugs in aqueous media are conditioned by the process parameters settings. Third, and as a consequence of the second observation made above, the nature of single or multiple excipients included in the pharmaceutical composition as well as their relative amount to the drug of interest are deeply investigated as formulation parameters whereas the composition of the water + *tert*-butyl alcohol solvent mixture used as freeze-drying medium, the total concentration of solutes into and the filling volume of vials or containers of any type are almost never studied as such. Since successful application of freeze-drying is driven by the interplay between formulation and process parameters, it is essential to design such liquid formulations of poorly water-soluble drugs not only according to their end-use properties, but also according to the lyophilization process. In this context, a rational selection of the composition of water + *tert*-butyl alcohol solvent mixtures is to be made. This requires detailed knowledge of the influence of the mixed solvent system composition on many outcomes such as solubility and stability of drugs and excipients, thermophysical properties of maximally freeze-concentrated phases, sublimation kinetics under specified shelf temperature and chamber pressure conditions or even on mechanical properties of freeze-dried cakes.

The primary interest of using *tert*-butyl alcohol as a cosolvent to water being to enhance the solubility of hydrophobic drugs to allow them to be freeze-dried from a restricted volume of solvent, the ability to predict the composition and temperature dependence of the solubility of poorly water-soluble drugs in this cosolvent system with a qualitative level of accuracy and precision would be of a great value. Obviously, comparative evaluation of existing models in this aim requires the availability of a large experimental data set, but at this time, solubility data of drugs in water + *tert*-butyl alcohol solvent mixtures are very scarce and often limited to a narrow solvent composition range. In this framework and as a first step toward this goal, the aim of this thesis is to investigate the solubility behavior of a

hydrophobic model drug, diazepam, in this mixed solvent system of industrial interest for freeze-drying. The thesis-by-publication format was selected for the presentation of the current research findings. Following this preface, the remainder of this document is divided into three independent chapters with nomenclature and references listed at their ends. Chapter 1 presents a validated model describing the dependence of the excess specific volume of the binary solvent mixture on both composition and temperature and discusses the variations of excess partial specific thermodynamic quantities with respect to temperature and composition in terms of molecular interactions and structural arrangements in solution. Chapter 2 provides experimental solubility data of diazepam in water + *tert*-butyl alcohol solvent mixtures as well as other experimental data allowing performing the thermodynamic analysis used to identify the forces driving the variation of the drug solubility with respect to the binary solvent mixture composition and temperature. Chapter 3 investigates the capability of the Scatchard-Hildebrand and combined Scatchard-Hildebrand/Flory-Huggins excess Gibbs energy models in correlating the composition and temperature dependence of the solubility of diazepam in water + *tert*-butyl alcohol solvent mixtures and the use of an approach based on information-theoretic concepts to select the temperature dependence of model parameters with respect to the parsimony principle. The first two chapters are published in an international peer-reviewed journal. Nevertheless, it is thought that this does not negate the possibility to criticize their respective contents.

This page is intentionally left blank.

Chapter 1

Excess specific volume of water + *tert*-butyl alcohol solvent mixtures: Experimental data, modeling and derived excess partial specific thermodynamic quantities

Abstract

The aim of this work is to develop a model for the dependence of the excess specific volume of the water + *tert*-butyl alcohol system on both composition and temperature under the temperature and pressure conditions relevant to the manufacturing and processing of poorly water-soluble drug formulations intended to be freeze-dried. For this purpose, experimental excess volumes of binary solvent mixtures were obtained from density measurements performed with a vibrating-tube density meter and carried out at atmospheric pressure for thirty-nine compositions covering the whole composition range and at five temperatures over the range from 293.15 to 313.15 K. For every temperature investigated, experimental excess volume data were fitted by a Redlich-Kister-based equation. By considering the temperature dependence of the regression coefficient estimates thus determined, the complete model equation was obtained and further validated by testing its correlative and predictive capabilities against data from this work and those from literature, respectively. Then, it was used to derive expressions for the excess partial thermodynamic quantities and their variations with respect to composition and temperature were discussed in terms of molecular interactions and structural arrangements in solution.

This page is intentionally left blank.

1.1. Introduction

Solvent mixtures are of widespread use in the pharmaceutical industry as reaction, crystallization, extraction, separation or formulation media [1]. Over the past decades, water + *tert*-butyl alcohol solvent mixtures have received an increasing interest from scientists in both academic and industrial settings as lyophilization vehicle for the preparation of freeze-dried pharmaceutical compositions [2-4]. In addition to be fully miscible with water under ambient temperature and pressure conditions, *tert*-butyl alcohol is a low toxicity [5] and environmentally friendly solvent relatively safe in use [6] which exhibits suitable physical properties with regard to the freeze-drying process including a high fusion temperature, a high solid vapor pressure and a low sublimation enthalpy [2-4]. Binary mixtures of this monohydric alcohol with water share these desirable properties as well so that, unlike other aqueous organic cosolvent systems, they can be frozen under operating conditions for conventional industrial-scale freeze-dryers [7-11] and, for identical process parameters, they sublime faster than neat water [12, 13]. Since the first step in the manufacturing process of most lyophilized pharmaceutical compositions consists in preparing a homogeneous solution of the ingredients to be dried, the use of water + *tert*-butyl alcohol solvent mixtures is especially valuable when considering freeze-drying of high-dosage hydrophobic drugs, for which the concentration in the solution to be lyophilized must be high enough to make the whole process economically viable for a large-scale production [2-4, 14]. To further increase the concentration of such drugs, the solubilization step is preferably carried out with slight heating [15, 16], provided that the drug dissolution in the excipient-free and/or -containing binary solvent mixture of defined composition is an endothermic process, and that the stability of the individual solute components in the resulting solution at the selected temperature is ensured until completion of pre-lyophilization unit operations.

These multicomponent liquid mixtures, comprising at least water, *tert*-butyl alcohol and a hydrophobic drug, but more generally also including one or more hydrophilic and/or amphiphilic excipients [15-20], are expected to exhibit strong deviations from ideal mixing behavior. Indeed, in addition to the difference in size and shape of individual mixture components, a wide range of specific intermolecular interactions is very likely to occur in such solutions since, on the one hand, both solvent components are associated liquids, and on the other hand, most drug and excipient molecules present single or multiple hydrogen bond acceptor and/or donor functional groups in their structures. Although precise knowledge of excess thermodynamic properties of these multicomponent liquid mixtures is essential for both theoretical and practical considerations, they are unlikely to be found in the literature, let alone under temperature conditions of interest, owing to the large number of possible qualitative and quantitative mixture compositions. Experimental determination of excess thermodynamic properties of liquid mixtures becoming increasingly more difficult, time-consuming and cost-intensive with each additional component, the development of model equations enabling to reliably estimate them has

always been an overarching goal of research in solution thermodynamics [21-24] and a countless number of empirical and semi-empirical expressions have been proposed and evaluated in the past with this aim [25-39]. Above and beyond their capabilities and limitations, one common feature of these mathematical models is that they are all built-up in such a way that the excess thermodynamic properties of a multicomponent liquid mixture of defined composition can be predicted only from knowledge of those of every possible contributing binary subsystem, commonly parameterized using the Redlich-Kister formalism [27]. Therefore, generating highly accurate excess thermodynamic data for the water + *tert*-butyl alcohol binary system and providing a suitable analytical representation of their dependencies on both mixture composition and temperature are essential steps toward predicting excess thermodynamic properties of drug formulations intended to be freeze-dried from this cosolvent system.

Among thermodynamic properties of liquid mixtures, volumetric and related derived quantities as well as the extent of their deviations from ideal mixing behavior are of special importance from both fundamental and applied viewpoints [40]. Indeed, knowledge of volumetric properties is not only indispensable for properly converting volume-based quantities into mass- or amount-of-substance-based quantities and performing all material balance calculations required for designing, operating, controlling and scaling-up technological processes, but also provides insights into the nature of intermolecular interactions taking place in the mixed systems. Although a great number of volumetric data at atmospheric pressure for the water + *tert*-butyl alcohol binary mixture have been reported by numerous investigators over the last sixty years [41-55], it was necessary for us to perform complementary experiments in the temperature range relevant to the industrial manufacturing of pharmaceutical composition freeze-dried from this co-solvent system, which is the field in which we are focus in this work. As a matter of fact, as pointed out by Egorov and Makarov [54], most of these experimental data were obtained either at a single temperature, or over limited composition and/or temperature ranges, or over the whole composition and/or wide temperature ranges but with large intervals, and even in some instances, they were only graphically displayed. To remedy these shortcomings, these authors carried out density measurements at atmospheric pressure on up to thirty-six water + *tert*-butyl alcohol binary mixture compositions per temperature, ranging from 274.15 to 348.15 K [54], and also performed isothermal compressibility measurements over the temperature range from 278.15 to 323.15 K and pressures up to 100 MPa [56, 57]. However, despite the substantial amount of experimental data provided in these studies, those covering the whole composition range under atmospheric pressure conditions are available only for four temperatures, of which solely one is inside the range of from 293.15 to 313.15 K in which we are interested in, whereas the remaining three are substantially higher than the said upper temperature range limit. Furthermore, although from these data modeling of the isothermal dependence of the excess volume of the water + *tert*-butyl alcohol system on composition was performed, that of its dependence on both temperature and composition

was not considered, so that no extrapolation beyond the temperature range covered can be made. Nevertheless, even if this were practicable, it would be unwise unless the reliability in as such extrapolated excess volume values were assessed, which in turn would require availability of sufficient experimental data covering the whole composition and relevant temperature ranges to ensure a fair evaluation.

The aim of this study is to provide a single equation allowing for the simultaneous modeling of both the composition and temperature dependence of the excess volume of the water + *tert*-butyl alcohol system under the temperature and pressure conditions relevant to the manufacturing and processing of poorly water-soluble drug formulations intended to be freeze-dried. For this purpose, experimental excess volumes of binary solvent mixtures were obtained from density measurements performed with a vibrating-tube density meter and carried out at atmospheric pressure on thirty-nine compositions covering the whole composition range and at five temperatures over the range from 293.15 to 313.15 K. The model equation was developed by considering, first, the composition dependence of excess volume of the liquid mixture on composition under isothermal conditions, and second, the temperature dependence of the model parameter estimates, and was further validated by testing its correlative and predictive capabilities against data from this work and those from literature, respectively. Finally, the changes in derived excess partial thermodynamic quantities with respect to the composition and temperature were computed and discussed in terms of molecular interactions in the light of findings from structural and dynamical studies published to date. Before proceeding further, one should specify that throughout this work, specific units were preferred over molar units to express thermodynamic quantities because, in addition to be more convenient for practical purposes in the field, they allow to detect [50, 58] and model [54] more subtly extrema in the composition dependence of excess partial thermodynamic quantities. Although less conventional, this does not represent any particular issue since conversion of data provided in this work from mass units to molar ones is straightforward.

1.2. Material and methods

1.2.1. Chemicals

Ultra-pure water, otherwise known as type 1 water, ([CAS 7732-18-5], 18.2 M Ω ·cm resistivity at 298.15 K, total organic carbon < 10 ppb, sodium < 1 ppb, chlorine < 1 ppb and silica < 3 ppb, W, component 1) was produced by a Synergy water purification system (Merck Millipore, Molsheim, France) whereas *tert*-butyl alcohol (2-methylpropan-2-ol, [CAS 75-65-0], purity: 0.99 in mass fraction, TBA, component 2) was purchased from Fisher Scientific (Loughborough, United Kingdom) and used as received with no further purification. Overview of chemicals used in this study is summarized in Table 1.1.

Table 1.1. Overview of chemicals used in this study.

Chemical	CAS RN	Formula	Molar mass ($\text{g}\cdot\text{mol}^{-1}$)	Source	Mass purity (%)	Analysis method
<i>tert</i> -butyl alcohol	75-65-0	$(\text{CH}_3)_3\text{COH}$	74.12	Fisher Chemical	> 99	Gas chromatography
Water Type I	7732-18-5	H_2O	18.02	In-house	Ultra-pure	Resistivity

Table 1.2. Density of neat water ρ_1^* and *tert*-butyl alcohol ρ_2^* at system temperature T and pressure $P = 0.1$ MPa.

T (K)	This work ^a	Literature
ρ_1^* ($\text{g}\cdot\text{cm}^{-3}$)		
293.15	$9.98205(0.00001)\cdot 10^{-1}$	$9.98203\cdot 10^{-1}$ [47]; $9.982067\cdot 10^{-1}$ [64]; $9.98207\cdot 10^{-1}$ [65]
299.15	$9.96784(0.00001)\cdot 10^{-1}$	$9.967857\cdot 10^{-1}$ [64]; $9.96786\cdot 10^{-1}$ [65]
303.15	$9.95647(0.00001)\cdot 10^{-1}$	$9.956\cdot 10^{-1}$ [53]; $9.956488\cdot 10^{-1}$ [64]; $9.95649\cdot 10^{-1}$ [65]
308.15	$9.94031(0.00001)\cdot 10^{-1}$	$9.94029\cdot 10^{-1}$ [54]; $9.940326\cdot 10^{-1}$ [64]; $9.94033\cdot 10^{-1}$ [65]; $9.9404\cdot 10^{-1}$ [52]
313.15	$9.92213(0.00002)\cdot 10^{-1}$	$9.922152\cdot 10^{-1}$ [64]; $9.92216\cdot 10^{-1}$ [65]; $9.9224\cdot 10^{-1}$ [41]
ρ_2^* ($\text{g}\cdot\text{cm}^{-3}$)		
299.15	$7.79477(0.00001)\cdot 10^{-1}$	$7.7940\cdot 10^{-1}$ [50]; $7.7948\cdot 10^{-1}$ [54]
303.15	$7.75378(0.00002)\cdot 10^{-1}$	$7.752\cdot 10^{-1}$ [53]; $7.7521\cdot 10^{-1}$ [51]; $7.7524\cdot 10^{-1}$ [61]; $7.7529\cdot 10^{-1}$ [50]; $7.7539\cdot 10^{-1}$ [54]; $7.7620\cdot 10^{-1}$ [66]
308.15	$7.70168(0.00001)\cdot 10^{-1}$	$7.6997\cdot 10^{-1}$ [51]; $7.7008\cdot 10^{-1}$ [50]; $7.7014\cdot 10^{-1}$ [54]; $7.7019\cdot 10^{-1}$ [62]; $7.7022\cdot 10^{-1}$ [52]; $7.7090\cdot 10^{-1}$ [63]
313.15	$7.64863(0.00002)\cdot 10^{-1}$	$7.6469\cdot 10^{-1}$ [51]; $7.6476\cdot 10^{-1}$ [50]; $7.6484\cdot 10^{-1}$ [54]; $7.6503\cdot 10^{-1}$ [41]; $7.651\cdot 10^{-1}$ [60]; $7.652\cdot 10^{-1}$ [67]
318.15	$7.59472(0.00002)\cdot 10^{-1}$	$7.5937\cdot 10^{-1}$ [50, 51]; $7.5946\cdot 10^{-1}$ [54]; $7.5965\cdot 10^{-1}$ [52]
323.15	$7.54012(0.00002)\cdot 10^{-1}$	$7.5394\cdot 10^{-1}$ [54]; $7.5401\cdot 10^{-1}$ [51]; $7.5409\cdot 10^{-1}$ [49]; $7.5448\cdot 10^{-1}$ [41]

^a Values in parentheses are standard deviations, $u(T) = 0.005$ K and $u_r(P) = 0.05$.

1.2.2. Solvent mixtures preparation

Since pure TBA is in the solid state at room temperature, the original container was warmed in a water bath a few degrees above its fusion temperature until the entire content was melted and was further homogenized prior to use. Samples of 100 g of W + TBA solvent mixtures were prepared by gravimetric method using a CP225D analytical balance (Sartorius, Goettingen, Germany) with an accuracy of $\pm 1 \cdot 10^{-1}$ mg. The mass fraction of TBA in solvent mixtures ranged from 0.025 to 0.975 with increments of 0.025. The uncertainty in mixture composition expressed in mass fraction was less than $1 \cdot 10^{-5}$ for each component. In order to minimize errors in mixture composition due to preferential evaporation of the organic solvent, water was weighed in first, followed by *tert*-butyl alcohol. For the same reason, binary mixtures were kept in hermetically sealed vials until analysis, performed within the same or following day.

1.2.3. Density measurements

Density measurements were performed with a DMA 5000 M vibrating-tube digital density meter (Anton Paar, Graz, Austria). Apparatus was operated in the dynamic temperature mode under atmospheric pressure condition and an incorporated Peltier system was used to control the temperature of the measuring cell. According to the technical specifications provided by the manufacturer for this instrument, accuracy and repeatability standard deviation in density measurement are of $5 \cdot 10^{-6}$ and $1 \cdot 10^{-6}$ g·cm⁻³ whereas those in temperature of the measuring cell are of $1 \cdot 10^{-2}$ and $1 \cdot 10^{-3}$ K, respectively. The density of neat water as well as investigated solvent binary mixtures was measured at 293.15, 299.15, 303.15, 308.15 and 313.15 K. The density of neat *tert*-butyl alcohol was measured at the same temperatures starting from 299.15 K and at two additional temperatures, namely 318.15 and 323.15 K. Every measurement was performed in triplicate and was preceded by density meter calibration with dry air and ultra-pure water. The standard uncertainty in density measurement and measuring cell temperature were found to be at most of $3 \cdot 10^{-6}$ g·cm⁻³ and less than $5 \cdot 10^{-3}$ K, respectively.

1.2.4. Statistical analysis

Standard error propagation equations were used to estimate the standard deviations in values calculated from those obtained from experimental measurements [59]. Regression analyses were performed using ordinary least-squares method. Goodness-of-fit of regression equations was evaluated by the adjusted squared correlation coefficient and its statistical significance was assessed by one-tailed Fisher's *F*-test whereas statistical significance of estimated regression coefficients was determined by two-tailed Student's *t*-test. Accuracy and precision of regression equations were appraised from standard deviation of the residuals and range of relative standard deviation of the

dependent variable estimates, respectively. All calculations were carried out using Microsoft Excel 2010 software (Microsoft, Redmond, USA).

1.3. Results

1.3.1. Experimental excess specific volume data of water + *tert*-butyl alcohol solvent mixtures

The experimental density values of pure water ρ_1^* and *tert*-butyl alcohol ρ_2^* are provided according to the temperature in Table 1.2 whereas those of W + TBA binary mixtures ρ are presented in Table 1.3 according to the temperature and the TBA mass fraction w_2 . For comparison purposes are also included in Table 1.2 the experimental density data of pure components taken from literature [41, 47, 49-54, 60-62] as well as from reference works and handbooks [63-67]. It can be observed that the results presented in this work are in perfect agreement with those reported by others, our measured values being in the range of published ones for every investigated temperature. Based on these data, the experimental excess specific volume of the binary mixtures was calculated for each isotherm from its definition [68, 69]:

$$v^E = v - v^{id} = v - [v_1^* + w_2(v_2^* - v_1^*)] \quad (1.1)$$

where $v = v(T, P, X) = [\rho(T, P, X)]^{-1}$, $v^E = v^E(T, P, X) = \Delta_{mix}v(T, P, X)$ and $v^{id} = v^{id}(T, P, X)$ are respectively the actual, the excess and the ideal specific volume of the mixture, $v_i^* = v_i^*(T, P) = [\rho_i^*(T, P)]^{-1}$ is the specific volume of the pure liquid *i*-th component, *T* is the system temperature, *P* is the system pressure, *X* is the mixture composition, the Δ symbol denotes the change in an extensive thermodynamic quantity associated with a process, the subscript mix refers to mixing process whereas the superscripts E, id and * stand for excess quantities, ideal quantities and pure component, respectively.

Since the fusion temperature of pure TBA is reported to be in the range of 298.65-298.87 K at atmospheric pressure [11, 41, 51, 67, 70-72], the density value of the hypothetical pure liquid TBA at 293.15 K required to calculate the excess specific volume of the W + TBA mixtures from Eq. (1.1) at this temperature must be extrapolated. This can be achieved by considering either the dependence of the binary mixture density on composition at the relevant temperature or the dependence of the pure component density on temperature. The latter approach was adopted in this work. As illustrated in Figure 1.1, the density of neat TBA exhibits a linear dependence on temperature over the range 299.15-323.15 K and could be regressed into a straight line whose slope and intercept were found to be equal to $-1.061 \pm 0.006 \cdot 10^{-3} \text{ K}^{-1}$ and $1.097 \pm 0.002 \text{ g}\cdot\text{cm}^{-3}$, respectively. Both these parameters as well as the adjusted squared correlation coefficient r_{adj}^2 , which value exceeds 0.9998, were found to be

Table 1.3. Density of the water + *tert*-butyl alcohol mixtures ρ at system temperature T and pressure $P = 0.1$ MPa^a.

w_2	$T = 293.15$ K	$T = 299.15$ K	$T = 303.15$ K	$T = 308.15$ K	$T = 313.15$ K
ρ (g·cm ⁻³)					
0.025	9.93922 (0.00001) · 10 ⁻¹	9.92481 (0.00001) · 10 ⁻¹	9.91318 (0.00001) · 10 ⁻¹	9.89650 (0.00002) · 10 ⁻¹	9.87794 (0.00002) · 10 ⁻¹
0.050	9.90088 (0.00001) · 10 ⁻¹	9.88554 (0.00001) · 10 ⁻¹	9.87329 (0.00001) · 10 ⁻¹	9.85570 (0.00002) · 10 ⁻¹	9.83617 (0.00003) · 10 ⁻¹
0.075	9.86645 (0.00001) · 10 ⁻¹	9.84955 (0.00001) · 10 ⁻¹	9.83625 (0.00002) · 10 ⁻¹	9.81754 (0.00002) · 10 ⁻¹	9.79671 (0.00003) · 10 ⁻¹
0.100	9.83472 (0.00001) · 10 ⁻¹	9.81555 (0.00002) · 10 ⁻¹	9.80074 (0.00002) · 10 ⁻¹	9.78019 (0.00002) · 10 ⁻¹	9.75750 (0.00002) · 10 ⁻¹
0.125	9.80319 (0.00002) · 10 ⁻¹	9.78094 (0.00002) · 10 ⁻¹	9.76412 (0.00001) · 10 ⁻¹	9.74108 (0.00003) · 10 ⁻¹	9.71599 (0.00003) · 10 ⁻¹
0.150	9.77225 (0.00002) · 10 ⁻¹	9.74588 (0.00002) · 10 ⁻¹	9.72643 (0.00002) · 10 ⁻¹	9.70029 (0.00003) · 10 ⁻¹	9.67235 (0.00003) · 10 ⁻¹
0.175	9.73742 (0.00002) · 10 ⁻¹	9.70625 (0.00002) · 10 ⁻¹	9.68393 (0.00002) · 10 ⁻¹	9.65463 (0.00002) · 10 ⁻¹	9.62392 (0.00002) · 10 ⁻¹
0.200	9.69629 (0.00002) · 10 ⁻¹	9.66064 (0.00002) · 10 ⁻¹	9.63580 (0.00001) · 10 ⁻¹	9.60384 (0.00003) · 10 ⁻¹	9.57095 (0.00003) · 10 ⁻¹
0.225	9.64936 (0.00002) · 10 ⁻¹	9.61024 (0.00002) · 10 ⁻¹	9.58346 (0.00003) · 10 ⁻¹	9.54940 (0.00002) · 10 ⁻¹	9.51458 (0.00002) · 10 ⁻¹
0.250	9.59834 (0.00001) · 10 ⁻¹	9.55698 (0.00001) · 10 ⁻¹	9.52890 (0.00002) · 10 ⁻¹	9.49333 (0.00002) · 10 ⁻¹	9.45714 (0.00002) · 10 ⁻¹
0.275	9.54431 (0.00001) · 10 ⁻¹	9.50130 (0.00001) · 10 ⁻¹	9.47229 (0.00001) · 10 ⁻¹	9.43567 (0.00002) · 10 ⁻¹	9.39858 (0.00003) · 10 ⁻¹
0.300	9.48868 (0.00002) · 10 ⁻¹	9.44443 (0.00002) · 10 ⁻¹	9.41459 (0.00002) · 10 ⁻¹	9.37705 (0.00003) · 10 ⁻¹	9.33922 (0.00003) · 10 ⁻¹
0.325	9.43195 (0.00001) · 10 ⁻¹	9.38688 (0.00001) · 10 ⁻¹	9.35650 (0.00003) · 10 ⁻¹	9.31833 (0.00002) · 10 ⁻¹	9.27956 (0.00002) · 10 ⁻¹
0.350	9.37373 (0.00002) · 10 ⁻¹	9.32787 (0.00002) · 10 ⁻¹	9.29697 (0.00002) · 10 ⁻¹	9.25803 (0.00003) · 10 ⁻¹	9.21863 (0.00003) · 10 ⁻¹
0.375	9.31610 (0.00001) · 10 ⁻¹	9.26964 (0.00001) · 10 ⁻¹	9.23831 (0.00002) · 10 ⁻¹	9.19872 (0.00003) · 10 ⁻¹	9.15865 (0.00003) · 10 ⁻¹
0.400	9.25788 (0.00002) · 10 ⁻¹	9.21086 (0.00002) · 10 ⁻¹	9.17911 (0.00002) · 10 ⁻¹	9.13903 (0.00002) · 10 ⁻¹	9.09845 (0.00002) · 10 ⁻¹
0.425	9.19996 (0.00001) · 10 ⁻¹	9.15233 (0.00001) · 10 ⁻¹	9.12016 (0.00001) · 10 ⁻¹	9.07950 (0.00002) · 10 ⁻¹	9.03833 (0.00002) · 10 ⁻¹
0.450	9.14153 (0.00002) · 10 ⁻¹	9.09352 (0.00002) · 10 ⁻¹	9.06106 (0.00002) · 10 ⁻¹	9.02006 (0.00003) · 10 ⁻¹	8.97849 (0.00003) · 10 ⁻¹
0.475	9.08281 (0.00002) · 10 ⁻¹	9.03393 (0.00002) · 10 ⁻¹	9.00084 (0.00002) · 10 ⁻¹	8.95897 (0.00003) · 10 ⁻¹	8.91652 (0.00003) · 10 ⁻¹
0.500	9.02429 (0.00001) · 10 ⁻¹	8.97548 (0.00001) · 10 ⁻¹	8.94241 (0.00003) · 10 ⁻¹	8.90060 (0.00002) · 10 ⁻¹	8.85816 (0.00003) · 10 ⁻¹
0.525	8.96577 (0.00002) · 10 ⁻¹	8.91659 (0.00002) · 10 ⁻¹	8.88328 (0.00002) · 10 ⁻¹	8.84110 (0.00002) · 10 ⁻¹	8.79830 (0.00002) · 10 ⁻¹

^a Values in parentheses are standard deviations, $u(T) = 0.005$ K, $u_i(P) = 0.05$, $u(w_2) = 0.00001$.

Table 1.3. Density of the water + *tert*-butyl alcohol mixtures ρ at system temperature T and pressure $P = 0.1$ MPa (*continued*)^a.

w_2	$T = 293.15$ K	$T = 299.15$ K	$T = 303.15$ K	$T = 308.15$ K	$T = 313.15$ K
ρ (g·cm ⁻³)					
0.550	8.90795 (0.00001) · 10 ⁻¹	8.85845 (0.00001) · 10 ⁻¹	8.82488 (0.00001) · 10 ⁻¹	8.78237 (0.00002) · 10 ⁻¹	8.73920 (0.00003) · 10 ⁻¹
0.575	8.84983 (0.00001) · 10 ⁻¹	8.79995 (0.00002) · 10 ⁻¹	8.76610 (0.00002) · 10 ⁻¹	8.72319 (0.00002) · 10 ⁻¹	8.67966 (0.00002) · 10 ⁻¹
0.600	8.79091 (0.00001) · 10 ⁻¹	8.74051 (0.00001) · 10 ⁻¹	8.70627 (0.00002) · 10 ⁻¹	8.66284 (0.00003) · 10 ⁻¹	8.61867 (0.00003) · 10 ⁻¹
0.625	8.73330 (0.00002) · 10 ⁻¹	8.68264 (0.00002) · 10 ⁻¹	8.64820 (0.00003) · 10 ⁻¹	8.60460 (0.00002) · 10 ⁻¹	8.56029 (0.00002) · 10 ⁻¹
0.650	8.67448 (0.00001) · 10 ⁻¹	8.62352 (0.00001) · 10 ⁻¹	8.58890 (0.00001) · 10 ⁻¹	8.54499 (0.00002) · 10 ⁻¹	8.50036 (0.00003) · 10 ⁻¹
0.675	8.61666 (0.00002) · 10 ⁻¹	8.56538 (0.00002) · 10 ⁻¹	8.53054 (0.00002) · 10 ⁻¹	8.48634 (0.00002) · 10 ⁻¹	8.44138 (0.00003) · 10 ⁻¹
0.700	8.55815 (0.00001) · 10 ⁻¹	8.50649 (0.00001) · 10 ⁻¹	8.47135 (0.00001) · 10 ⁻¹	8.42678 (0.00003) · 10 ⁻¹	8.38143 (0.00003) · 10 ⁻¹
0.725	8.49953 (0.00001) · 10 ⁻¹	8.44745 (0.00002) · 10 ⁻¹	8.41206 (0.00003) · 10 ⁻¹	8.36713 (0.00003) · 10 ⁻¹	8.32138 (0.00003) · 10 ⁻¹
0.750	8.44112 (0.00002) · 10 ⁻¹	8.38864 (0.00002) · 10 ⁻¹	8.35296 (0.00002) · 10 ⁻¹	8.30766 (0.00002) · 10 ⁻¹	8.26153 (0.00002) · 10 ⁻¹
0.775	8.38260 (0.00001) · 10 ⁻¹	8.32967 (0.00001) · 10 ⁻¹	8.29366 (0.00001) · 10 ⁻¹	8.24795 (0.00003) · 10 ⁻¹	8.20143 (0.00003) · 10 ⁻¹
0.800	8.32329 (0.00002) · 10 ⁻¹	8.26989 (0.00002) · 10 ⁻¹	8.23357 (0.00003) · 10 ⁻¹	8.18746 (0.00002) · 10 ⁻¹	8.14054 (0.00003) · 10 ⁻¹
0.825	8.26467 (0.00001) · 10 ⁻¹	8.21077 (0.00001) · 10 ⁻¹	8.17414 (0.00001) · 10 ⁻¹	8.12762 (0.00003) · 10 ⁻¹	8.08025 (0.00003) · 10 ⁻¹
0.850	8.20506 (0.00002) · 10 ⁻¹	8.15065 (0.00002) · 10 ⁻¹	8.11367 (0.00002) · 10 ⁻¹	8.06671 (0.00002) · 10 ⁻¹	8.01889 (0.00002) · 10 ⁻¹
0.875	8.14575 (0.00001) · 10 ⁻¹	8.09078 (0.00001) · 10 ⁻¹	8.05340 (0.00001) · 10 ⁻¹	8.00594 (0.00002) · 10 ⁻¹	7.95763 (0.00003) · 10 ⁻¹
0.900	8.08564 (0.00001) · 10 ⁻¹	8.03011 (0.00001) · 10 ⁻¹	7.99235 (0.00002) · 10 ⁻¹	7.94442 (0.00003) · 10 ⁻¹	7.89565 (0.00003) · 10 ⁻¹
0.925	8.02553 (0.00002) · 10 ⁻¹	7.96938 (0.00002) · 10 ⁻¹	7.93119 (0.00003) · 10 ⁻¹	7.88275 (0.00003) · 10 ⁻¹	7.83340 (0.00003) · 10 ⁻¹
0.950	7.96552 (0.00002) · 10 ⁻¹	7.90861 (0.00002) · 10 ⁻¹	7.86995 (0.00002) · 10 ⁻¹	7.82083 (0.00002) · 10 ⁻¹	7.77081 (0.00003) · 10 ⁻¹
0.975	7.90751 (0.00001) · 10 ⁻¹	7.84957 (0.00002) · 10 ⁻¹	7.81016 (0.00002) · 10 ⁻¹	7.76007 (0.00002) · 10 ⁻¹	7.70907 (0.00003) · 10 ⁻¹

^a Values in parentheses are standard deviations, $u(T) = 0.005$ K, $u_r(P) = 0.05$, $u(w_2) = 0.00001$.

statistically significant with p -values lesser than $1 \cdot 10^{-8}$. From this, the density value of the hypothetical pure supercooled liquid TBA was estimated to be $\rho_2^*(T = 293.15 \text{ K}, P = 0.1 \text{ MPa}) = 7.860 \pm 0.001 \cdot 10^{-1} \text{ g} \cdot \text{cm}^{-3}$.

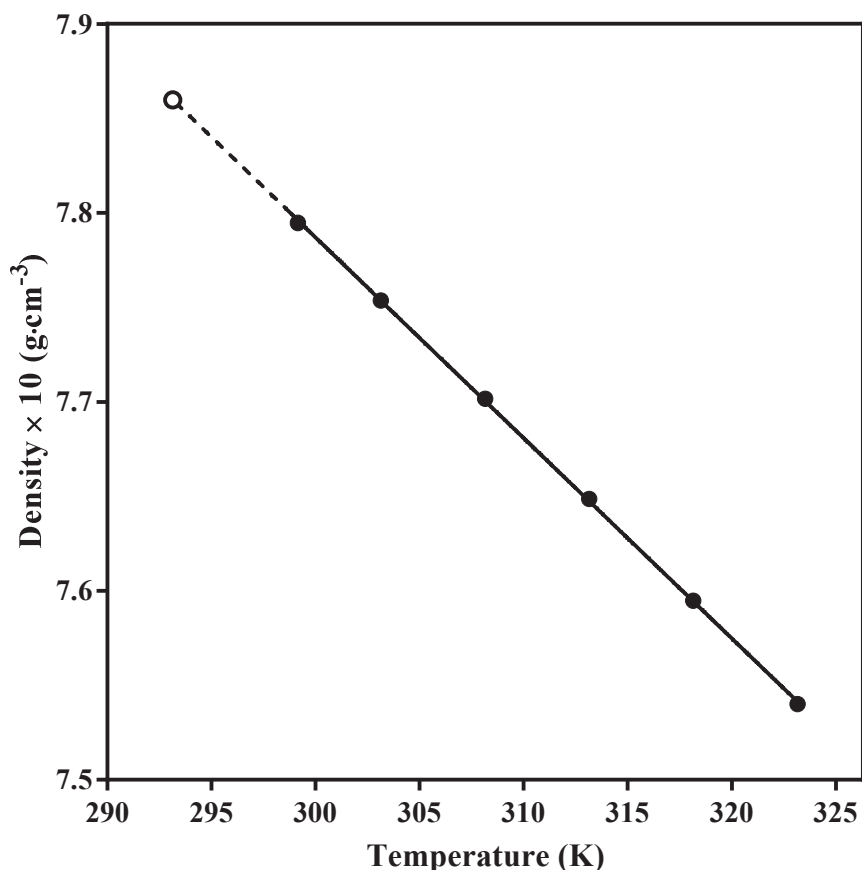


Figure 1.1. Density of pure *tert*-butyl alcohol as function of the absolute temperature (●): experimental values; (○): extrapolated value at $T = 293.15 \text{ K}$ (the solid line is a linear fit to experimental data; the dashed line is the continuation of the solid line to temperatures lower than the fusion temperature of the pure component; error bars corresponding to plus and minus one standard deviation are smaller than symbol size).

The experimental values of the excess specific volume of the W + TBA binary mixtures are listed in Table A.1 and displayed in Figure 1.2 according to the TBA mass fraction and the temperature. The relative standard deviations of excess specific volume values are less than 1% for almost all mixture compositions, irrespective of the temperature condition. The only exception to this concerns the excess specific volume values of TBA-rich mixtures at 293.15 K for which the relative standard deviations are at most of 20%, because of the uncertainty associated with the extrapolated density value of the pure TBA which is about one hundred times higher than those of the experimental density for these

mixtures at this temperature. Provided that mixture composition and excess volume are converted into the same units, the variations of the W + TBA mixtures excess volume obtained in this work with respect to the temperature and composition well agree with those reported by others [41-43, 46, 49-51, 53, 54]. However, direct comparison of experimental values provided by these authors with those obtained in the present work is limited due to difference in both investigated mixture compositions and system temperatures so that it can only be achieved for a very limited number of data. Instead, we think more appropriate to consider indirect comparison by means of a model expressing the dependence of the excess specific volume of the W + TBA system on both mixture composition and temperature as described in the section 1.3.2.

One can see from Table A.1 and Figure 1.2 that the excess specific volume of the W + TBA mixtures is negative over the entire composition range indicating that the mixing of the individual components always results in volumetric contraction for this system in the temperature range investigated. As illustrated in Figure 1.2, the variation of v^E with the mixture composition for a given system temperature exhibits an asymmetric U-shaped profile in agreement with the general features of water and monohydric alcohols binary mixtures. Depending on temperature, the maximum deviation from ideal mixing behavior with respect to volume change is found to occur in binary mixtures with w_2 ranging from 0.40 to 0.45 and appears to shift to mixtures of higher TBA content as the temperature increases. The variation of the magnitude of v^E with the system temperature for a given mixture composition can be better discussed by considering the values of the excess specific isobaric expansivity e_p^E , defined as $e_p^E(T, P, X) = (\partial v^E / \partial T)_{P, X}$. To investigate for the temperature dependence of this quantity at a given composition, the experimental values of v^E were regressed against the temperature. It was found that a linear dependence of v^E on the temperature provide the best regression results, evidencing that the temperature range covered in this work is narrow enough so that the temperature dependence of e_p^E over the whole composition range can be neglected. The experimental values of $e_p^E = e_p^E(P, X)$ over the range $T = 293.15-313.15$ K and at a given composition are the slope of the straight lines obtained from least-squares linear regression of the experimental excess specific volume data on temperature according to:

$$e_p^E = A = \frac{1}{T}(v^E - B) \quad (1.2)$$

where A and B are the slope and intercept of the linear function, respectively. The corresponding values of e_p^E are provided as supplementary material in Appendix A (Table A.2) and depicted in Figure 1.3 according to the TBA mass fraction in the solvent mixture. The variation of e_p^E with mixture composition displays a W-shaped profile. For binary mixtures with a TBA mass fraction lower than 0.15 and higher than 0.50, e_p^E values are negative so that the magnitude of v^E decreases with

temperature whereas in the composition range in between, e_p^E values are positive and the opposite occurs. Within these TBA mass fraction intervals, extrema are found for TBA mass fractions of 0.075, 0.250 and 0.875 for which e_p^E values are -0.5 , 1.1 and $-1.2 \cdot 10^{-4} \text{ cm}^3 \cdot \text{g}^{-1} \cdot \text{K}^{-1}$, respectively.

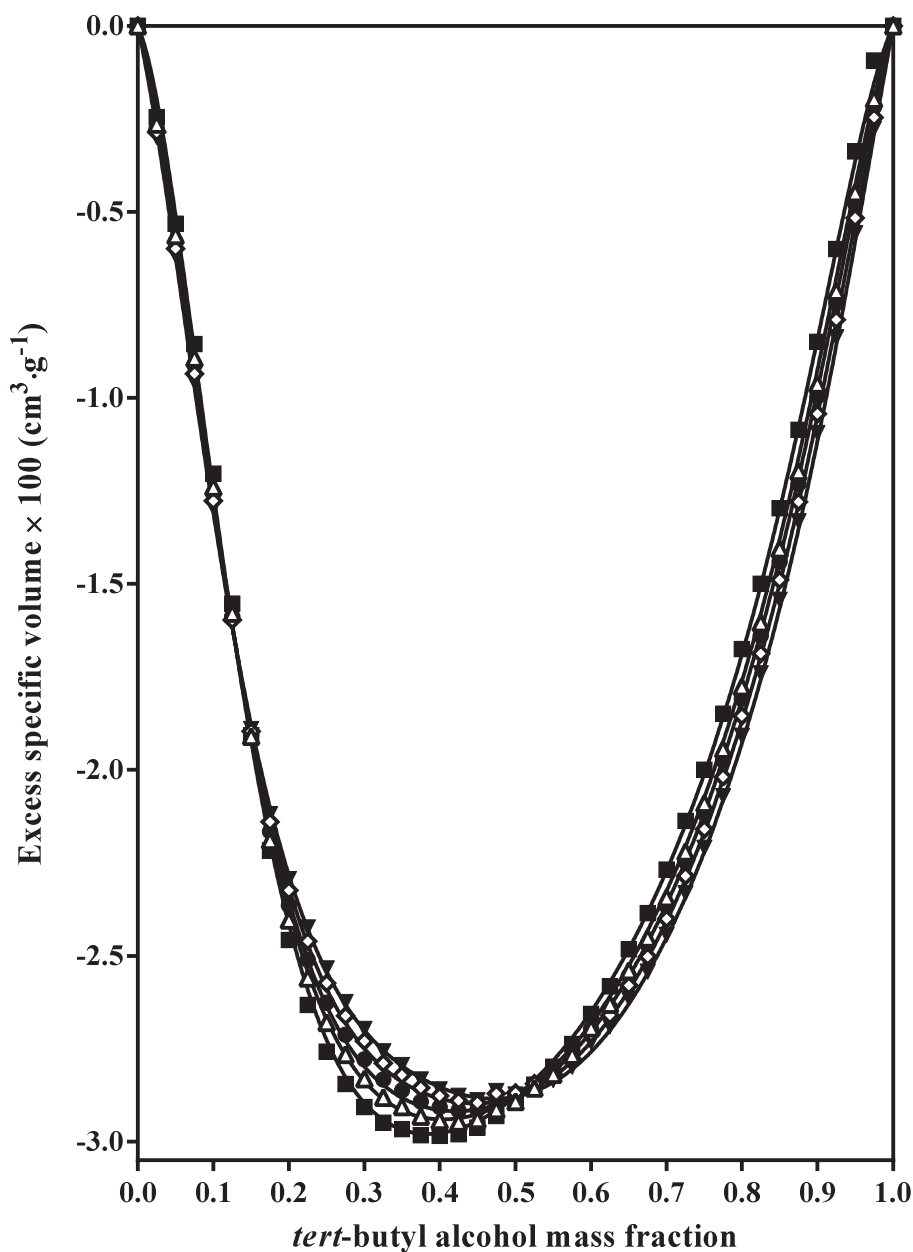


Figure 1.2. Experimental excess specific volume of water + *tert*-butyl alcohol solvent mixtures as function of the *tert*-butyl alcohol mass fraction (■): $T = 293.15 \text{ K}$; (△): $T = 299.15 \text{ K}$; (●): $T = 303.15 \text{ K}$; (◇): $T = 308.15 \text{ K}$; (▼): $T = 313.15 \text{ K}$ (error bars corresponding to plus and minus one standard deviation are smaller than symbol size, the solid lines are calculated from Eq. (1.4)).

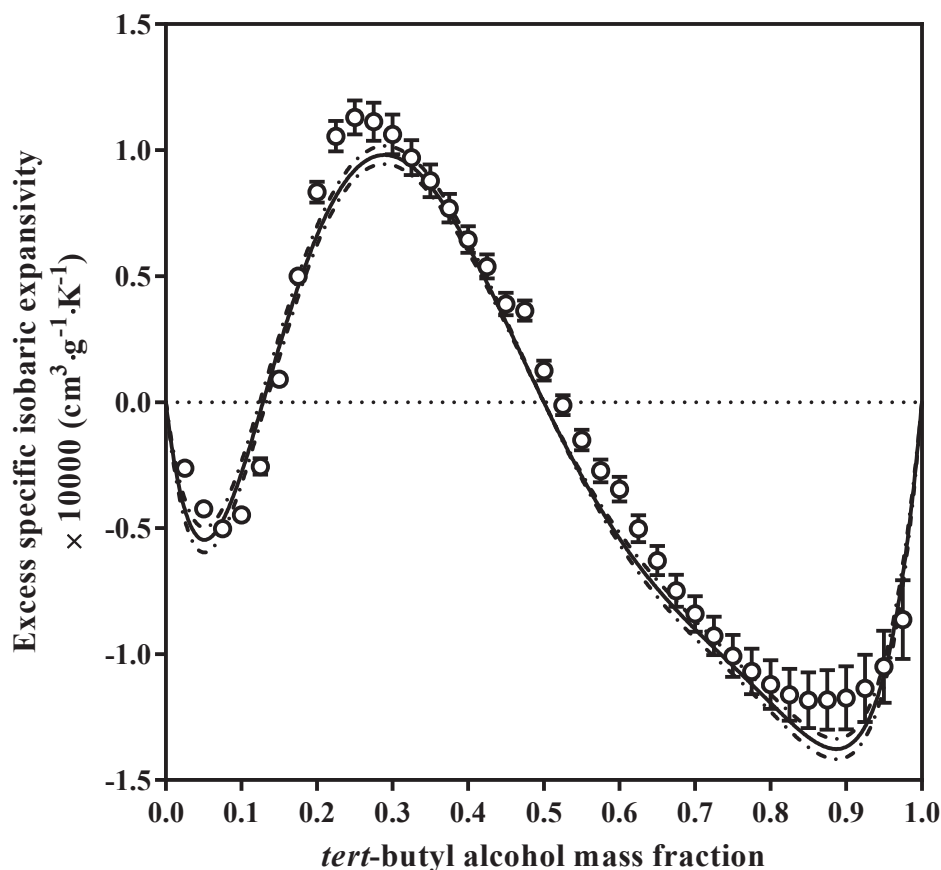


Figure 1.3. Excess specific isobaric expansivity of water + *tert*-butyl alcohol solvent mixtures over the temperature range $T = 293.15\text{-}313.15$ K as function of the *tert*-butyl alcohol mass fraction (○): experimental values calculated from Eq. (1.2); (solid line): modelled values calculated from Eq. (1.5) (error bars and dashed-dotted lines correspond to plus and minus one standard deviation).

Accordingly, as it can be seen on Figure 1.2, in the temperature range investigated, the magnitude of the maximum deviation from ideal mixing behavior with respect to volume change is highest at 293.15 K and lowest at 313.15 K for which temperatures $v^E = -2.98 \cdot 10^{-2} \text{ cm}^3 \cdot \text{g}^{-1}$ and $v^E = -2.88 \cdot 10^{-2} \text{ cm}^3 \cdot \text{g}^{-1}$, respectively. Consequently, the dependence of the mixture excess specific volume on temperature over the range investigated is not very strong in the water-rich region while it is more pronounced in the remaining part of the composition range, without exceeding $2.5 \cdot 10^{-3} \text{ cm}^3 \cdot \text{g}^{-1}$.

The large negative excess specific volume observed for the W + TBA system indicates that the difference in shape and size of the unlike molecules as well as the specific and non-specific intermolecular interactions between like and unlike molecules in the mixture impose overall structural changes upon mixing of the individual components. These molecular rearrangements, although being composition and temperature dependent, always result in an effective packing of the mixture leading to system contraction. The structural changes of individual mixture components with respect to their

pure liquid state leading to the observed dependence of the W + TBA excess specific volume on mixture composition and temperature can be more appropriately interpreted in light to those of excess partial specific volumes and their variation with temperature at a given pressure and composition. This obviously requires beforehand to model the variation of the binary mixture excess specific volume with respect to its composition over the temperature range investigated.

1.3.2. Modeling of the temperature and composition dependence of excess specific volume of water + *tert*-butyl alcohol solvent mixtures

1.3.2.1. Determination of model coefficients and their temperature dependencies

For each of the five temperatures studied, the composition dependence of the mixture excess specific volume was correlated with a Redlich-Kister-like polynomial equation [27]:

$$v^E = w_2(1 - w_2) \sum_{i=0}^k A_i(1 - 2w_2)^i \quad (1.3)$$

where $A_i = A_i(T, P)$ are the model coefficients, k is the degree of the polynomial and where other terms are as previously defined. One can see that this equation is structurally expressed in such a way that $v^E(T, P, w_2 = 1) = v^E(T, P, w_2 = 0) = 0$. The coefficients of Eq. (1.3) were obtained by regressing v^E against each of the $w_2(1 - w_2)(1 - 2w_2)^i$ terms for the different isotherms. In order to avoid overfitting, extra-sum-of-squares F -test was used to check whether stepwise increment in k value from zero up to six results in a statistically significant better fit of Eq. (1.3) to the data. The results, including relative differences in residual sum-of-squares $SS(e)$ and degrees of freedom df between compared models as well as corresponding F -scores and associated p -values reported as asterisks, are summarized in Table 1.4 for the different temperature investigated in the framework of this study. Full statistical analysis results are provided in Appendix A (Table A.3). For every isotherm studied, one can see from Table 1.4 that despite the loss in degrees of freedom, increasing the polynomial degree value from k to $k + 1$ always leads to a statistically significant improvement in the fit of Eq. (1.3) to the data at the 95 percent level of confidence. A noticeable exception to this occurs when the value of the polynomial degree is increased from two to three but at the same time, a fourth-order polynomial expression fit the data significantly better than does a second-order one, with associated p -values lesser than $1 \cdot 10^{-6}$. In addition to this approach based on traditional statistical hypothesis testing, second-order Akaike's information criterion corrected for small sample size (AIC_c), which is based on information-theoretical concepts, was used to compare and rank the different nested candidate models according to the parsimony principle. Full explanation and details of calculation procedures for computing AIC_c scores and derived indices from the results of least-squares

regression analysis can be found in the reference book by Burnham and Anderson [73]. The results are presented in Table 1.5 and lead to the exact same conclusion than that drawn from extra-sum-of-squares F -tests. Indeed, for each of the different temperatures considered, the sixth-order polynomial model presents the lowest AIC_c score among alternative models tested, indicating that Eq. (1.3) with the highest polynomial degree performs better than with any of the lower ones in balancing the decrease in the residual sum-of-squares against the number of adjustable coefficients. In addition to $SS(e)$ values and AIC_c scores, are also presented in Table 1.5 Akaike weights w_A which are the weight of evidence in favor of each model being the actual Kullback-Leibler best model in the model set considered, given the data, normalized to sum to unity so that they may be interpreted as probabilities [73]. It can be observed from Table 1.5 that, for the five temperatures investigated, the value of w_A corresponding to Eq. (1.3) with $k = 6$ is higher than 0.9999, providing compelling support that it is the most parsimonious model among those examined. Hence, from the results of both statistical- and information theory-based approaches, a sixth-order polynomial was selected as the optimal model.

The least-squares regression parameters are presented in Table 1.6, including p -values of estimated regression and adjusted squared correlation coefficients reported as asterisks. Full statistical analysis results are summarized in Appendix A (Tables A.4 and A.5), including the respective variance-covariance matrices. It can be observed from Table 1.6 that the values of the adjusted squared determination r_{adj}^2 are higher than 0.9999 with associated p -values of less than $1 \cdot 10^{-4}$ in all cases, indicating that for every investigated temperature, almost all of the total variation in the dependent variable is accounted for by the model. Regarding to the model coefficient estimates, they are found to be statistically significant at the 95 percent level of confidence with p -values mostly lower than $1 \cdot 10^{-4}$, however, with notable exception of the quartic coefficient estimates for $T = 293.15$ K and $T = 299.15$ K.

From Table 1.6, the accuracy and precision of Eq. (1.3) in modeling the excess specific volume of the W + TBA system from its composition at a given investigated temperature can be considered satisfactory. Indeed, the values of the standard deviation of the residuals from regression $s(e)$ ranges from $2.22 \cdot 10^{-4}$ to less than $1 \cdot 10^{-4}$ $\text{cm}^3 \cdot \text{g}^{-1}$ whereas the maximum values for the relative standard deviation of the calculated excess specific volume $s_r(v_{calc}^E)$ ranges from 2.9 to 18.1%. In comparison with the uncertainty in experimental v^E data, the values of these two parameters are found to be slightly higher, whatever the temperature, but both the accuracy and precision of mixture excess specific volume values calculated from Eq. (1.3) increase with temperature [42, 43].

Table 1.4. Results of extra-sum-of-squares analysis for pairwise comparisons of Eq. (1.3) with increasing values of polynomial degree k in fitting the excess specific volume of the water + *tert*-butyl alcohol mixtures v^E at system temperature T and pressure $P = 0.1$ MPa^a.

Eq. (1.3)	Parameters ^a	$T = 293.15$ K	$T = 299.15$ K	$T = 303.15$ K	$T = 308.15$ K	$T = 313.15$ K
$k = 0$ vs. $k = 1$	RD SS(e) (%)	585.85	367.95	275.24	171.64	96.49
	RD df (%)	2.56	2.56	2.56	2.56	2.56
	F -score	228.48 ****	143.50 ****	107.34 ****	66.94 ****	37.63 ****
$k = 1$ vs. $k = 2$	RD SS(e) (%)	13.62	77.75	140.75	266.70	473.73
	RD df (%)	2.63	2.63	2.63	2.63	2.63
	F -score	5.17 *	29.54 ****	53.49 ****	101.35 ****	180.02 ****
$k = 2$ vs. $k = 3$	RD SS(e) (%)	6.81	6.44	3.00	0.63	0.01
	RD df (%)	2.70	2.70	2.70	2.70	2.70
	F -score	2.52	2.38	1.11	0.23	<0.01
$k = 2$ vs. $k = 4$	RD SS(e) (%)	586.76	397.49	323.68	247.44	186.57
	RD df (%)	5.56	5.56	5.56	5.56	5.56
	F -score	105.62 ****	71.55 ****	58.26 ****	44.54 ****	33.58 ****
$k = 3$ vs. $k = 4$	RD SS(e) (%)	542.99	367.40	311.32	245.28	186.54
	RD df (%)	2.78	2.78	2.78	2.78	2.78
	F -score	195.48 ****	132.26 ****	112.08 ****	88.30 ****	67.15 ****
$k = 4$ vs. $k = 5$	RD SS(e) (%)	61.98	138.80	142.41	148.33	154.14
	RD df (%)	2.86	2.86	2.86	2.86	2.86
	F -score	21.69 ****	48.58 ****	49.85 ****	51.92 ****	53.95 ****
$k = 5$ vs. $k = 6$	RD SS(e) (%)	96.67	172.59	264.14	389.53	396.85
	RD df (%)	2.94	2.94	2.94	2.94	2.94
	F -score	32.87 ****	58.68 ****	89.81 ****	132.44 ****	134.93 ****

**** $p \leq 0.0001$, *** $p \leq 0.001$, ** $p \leq 0.01$, * $p \leq 0.05$.

^a RD: relative difference in quantity; SS(e): residual sum-of-squares; df: degree of freedom; F : Fisher statistic.

Table 1.5. Results of Akaike's information criterion analysis for comparison of Eq. (1.3) with different values of polynomial degree k in fitting the excess specific volume of the water + *tert*-butyl alcohol mixtures v^E at system temperature T and pressure $P = 0.1$ MPa^a.

Rank	1	2	3	4	5	6	7
$T = 293.15$ K							
Eq. (1.3)	$k = 6$	$k = 5$	$k = 4$	$k = 3$	$k = 2$	$k = 1$	$k = 0$
SS(e) (cm ⁶ ·g ⁻²)	1.67·10 ⁻⁶	3.28·10 ⁻⁶	5.32·10 ⁻⁶	3.42·10 ⁻⁵	3.65·10 ⁻⁵	4.15·10 ⁻⁵	2.85·10 ⁻⁴
AIC _c	-677.19	-652.57	-635.72	-562.17	-562.08	-559.31	-482.69
w_A	> 0.9999	< 0.0001	< 0.0001	< 0.0001	< 0.0001	< 0.0001	< 0.0001
$T = 299.15$ K							
Eq. (1.3)	$k = 6$	$k = 5$	$k = 4$	$k = 2$	$k = 3$	$k = 1$	$k = 0$
SS(e) (cm ⁶ ·g ⁻²)	6.97·10 ⁻⁷	1.90·10 ⁻⁶	4.53·10 ⁻⁶	2.26·10 ⁻⁵	2.12·10 ⁻⁵	4.01·10 ⁻⁵	1.88·10 ⁻⁴
AIC _c	-713.02	-675.01	-642.24	-581.82	-581.78	-560.70	-499.76
w_A	> 0.9999	< 0.0001	< 0.0001	< 0.0001	< 0.0001	< 0.0001	< 0.0001
$T = 303.15$ K							
Eq. (1.3)	$k = 6$	$k = 5$	$k = 4$	$k = 2$	$k = 3$	$k = 1$	$k = 0$
SS(e) (cm ⁶ ·g ⁻²)	4.59·10 ⁻⁷	1.67·10 ⁻⁶	4.05·10 ⁻⁶	1.72·10 ⁻⁵	1.67·10 ⁻⁵	4.13·10 ⁻⁵	1.55·10 ⁻⁴
AIC _c	-730.11	-680.23	-646.85	-593.01	-591.62	-559.45	-507.57
w_A	> 0.9999	< 0.0001	< 0.0001	< 0.0001	< 0.0001	< 0.0001	< 0.0001
$T = 308.15$ K							
Eq. (1.3)	$k = 6$	$k = 5$	$k = 4$	$k = 2$	$k = 3$	$k = 1$	$k = 0$
SS(e) (cm ⁶ ·g ⁻²)	2.95·10 ⁻⁷	1.44·10 ⁻⁶	3.59·10 ⁻⁶	1.25·10 ⁻⁵	1.24·10 ⁻⁵	4.57·10 ⁻⁵	1.24·10 ⁻⁴
AIC _c	-748.24	-686.23	-651.86	-606.16	-603.81	-555.35	-516.71
w_A	> 0.9999	< 0.0001	< 0.0001	< 0.0001	< 0.0001	< 0.0001	< 0.0001
$T = 313.15$ K							
Eq. (1.3)	$k = 6$	$k = 5$	$k = 4$	$k = 2$	$k = 3$	$k = 1$	$k = 0$
SS(e) (cm ⁶ ·g ⁻²)	2.51·10 ⁻⁷	1.25·10 ⁻⁶	3.17·10 ⁻⁶	9.09·10 ⁻⁶	9.09·10 ⁻⁶	5.21·10 ⁻⁵	1.02·10 ⁻⁴
AIC _c	-754.84	-692.22	-656.90	-619.09	-616.49	-549.93	-524.57
w_A	> 0.9999	< 0.0001	< 0.0001	< 0.0001	< 0.0001	< 0.0001	< 0.0001

^a SS(e): residual sum-of-squares; AIC_c: second-order Akaike's information criterion; w_A : Akaike weight.

Table 1.6. Results of the multiple linear least-squares regressions of the excess specific volume of the water + *tert*-butyl alcohol mixtures v^E on *tert*-butyl alcohol mass fraction w_2 at system temperature T and pressure $P = 0.1$ MPa fitted with Eq. (1.3)^a.

Parameters ^b	$T = 293.15$ K	$T = 299.15$ K	$T = 303.15$ K	$T = 308.15$ K	$T = 313.15$ K
n	41	41	41	41	41
A_0 ($\text{cm}^3 \cdot \text{g}^{-1}$)	-1.1561 (0.0034) $\cdot 10^{-1}$ ****	-1.1559 (0.0022) $\cdot 10^{-1}$ ****	-1.1500 (0.0018) $\cdot 10^{-1}$ ****	-1.1472 (0.0014) $\cdot 10^{-1}$ ****	-1.1490 (0.0013) $\cdot 10^{-1}$ ****
A_1 ($\text{cm}^3 \cdot \text{g}^{-1}$)	-3.4007 (0.1526) $\cdot 10^{-2}$ ****	-2.3721 (0.0986) $\cdot 10^{-2}$ ****	-1.9004 (0.0800) $\cdot 10^{-2}$ ****	-1.3644 (0.0641) $\cdot 10^{-2}$ ****	-8.8226 (0.5918) $\cdot 10^{-3}$ ****
A_2 ($\text{cm}^3 \cdot \text{g}^{-1}$)	-5.1986 (0.6156) $\cdot 10^{-2}$ ****	-4.9438 (0.3977) $\cdot 10^{-2}$ ****	-4.6184 (0.3229) $\cdot 10^{-2}$ ****	-4.3632 (0.2588) $\cdot 10^{-2}$ ****	-4.2562 (0.2388) $\cdot 10^{-2}$ ****
A_3 ($\text{cm}^3 \cdot \text{g}^{-1}$)	-3.7700 (0.8923) $\cdot 10^{-2}$ ****	-4.9387 (0.5764) $\cdot 10^{-2}$ ****	-5.1530 (0.4680) $\cdot 10^{-2}$ ****	-5.3353 (0.3751) $\cdot 10^{-2}$ ****	-5.3950 (0.3461) $\cdot 10^{-2}$ ****
A_4 ($\text{cm}^3 \cdot \text{g}^{-1}$)	-0.2139 (2.3580) $\cdot 10^{-2}$ ****	-1.5266 (1.5234) $\cdot 10^{-2}$ *	-2.8525 (1.2367) $\cdot 10^{-2}$ *	-3.9626 (0.9914) $\cdot 10^{-2}$ ****	-4.4858 (0.9148) $\cdot 10^{-2}$ ****
A_5 ($\text{cm}^3 \cdot \text{g}^{-1}$)	7.1637 (1.1128) $\cdot 10^{-2}$ ****	8.1536 (0.7189) $\cdot 10^{-2}$ ****	7.7495 (0.5836) $\cdot 10^{-2}$ ****	7.3508 (0.4678) $\cdot 10^{-2}$ ****	6.9658 (0.4317) $\cdot 10^{-2}$ ****
A_6 ($\text{cm}^3 \cdot \text{g}^{-1}$)	1.3175 (0.2298) $\cdot 10^{-1}$ ****	1.1373 (0.1485) $\cdot 10^{-1}$ ****	1.1422 (0.1205) $\cdot 10^{-1}$ ****	1.1119 (0.0966) $\cdot 10^{-1}$ ****	1.0355 (0.0891) $\cdot 10^{-1}$ ****
r_{adj}^2	>0.9999 ****	>0.9999 ****	>0.9999 ****	>0.9999 ****	>0.9999 ****
$s(e)$ ($\text{cm}^3 \cdot \text{g}^{-1}$)	$2.22 \cdot 10^{-4}$	$1.43 \cdot 10^{-4}$	$1.16 \cdot 10^{-4}$	$9.31 \cdot 10^{-5}$	$8.59 \cdot 10^{-5}$
$s_r(v_{\text{calc}}^E)$ (%) ^c	0.27 – 18.11	0.18 – 7.62	0.15 – 5.28	0.12 – 3.63	0.11 – 2.94

**** $p \leq 0.0001$, *** $p \leq 0.001$, ** $p \leq 0.01$, * $p \leq 0.05$.

^a Values in parentheses are standard deviations.

^b n : number of regressed data points; A_i : equation coefficients; r_{adj}^2 : adjusted squared determination coefficients; $s(e)$: standard deviations of the residuals from regression; $s_r(v_{\text{calc}}^E)$: relative standard deviations of the excess specific volume estimates over the whole composition range.

^c Null values corresponding to v_{calc}^E for pure components excluded.

In order to describe the dependence of the excess specific volume of the W + TBA system on both temperature and mixture composition with a single equation, the temperature dependence of the estimated coefficients A_i of Eq. (1.3) was considered on the basis of a linear relationship because of the narrow temperature range covered in the present work so that Eq. (1.3) can be written as:

$$v^E = w_2(1 - w_2) \sum_{i=0}^6 (B_i T + C_i)(1 - 2w_2)^i \quad (1.4)$$

where $B_i = B_i(P)$ and $C_i = C_i(P)$ are the slope and intercept of the considered linear functions, respectively, and are independent of composition as well as temperature over the experimental temperature range and where other terms are as defined above. It should be noted that, despite being found statistically insignificant at the probability level of 0.05 for two of the five isotherms investigated, the temperature dependence of the coefficient estimate A_4 was considered over the full temperature range. The plots of the coefficient estimates of Eq. (1.3) against temperature are shown in Figure 1.4 and the least-squares linear regression parameters are given in Table 1.7. As for the previous regression analysis, the statistical significance of estimated regression and adjusted squared correlation coefficients reported as asterisks are included in this table whereas complete statistical analysis results are provided in Appendix A (Tables A.6 and A.7). From Figure 1.4 and Table 1.7, it can be observed that five of the seven regression coefficient estimates of Eq. (1.3) exhibit a linear dependence to the absolute temperature over the experimental temperature range as assessed by the p -values of less than 0.05 associated with the respective adjusted squared correlation coefficients whose values range from 0.6324 to 0.9708. Oppositely, the degree of association between the values of the remaining two regression coefficient estimates A_0 and A_5 and the temperature was not found to be statistically significant at the 95 percent level of confidence suggesting that the variation of these parameters with temperature is not linear. Considering the graphical plots and the p -values associated with the slopes and intercepts as obtained from linear regression of A_0 and A_5 values against temperature, it follows that the former coefficient estimate is almost constant over the temperature range considered whereas the poor correlation observed for the latter one results because of a single data point. Consequently, these two parameters were considered to be temperature independent over the range $T = 293.15\text{-}313.15$ K and their mean values with respect to temperature were used for subsequent calculations so that, from the results provided in Table 1.6, $C_0 = -1.1516 \cdot 10^{-1} \text{ cm}^3 \cdot \text{g}^{-1}$ and $C_5 = 7.4767 \cdot 10^{-2} \text{ cm}^3 \cdot \text{g}^{-1}$ with $B_0 = B_5 = 0 \text{ K}^{-1}$.

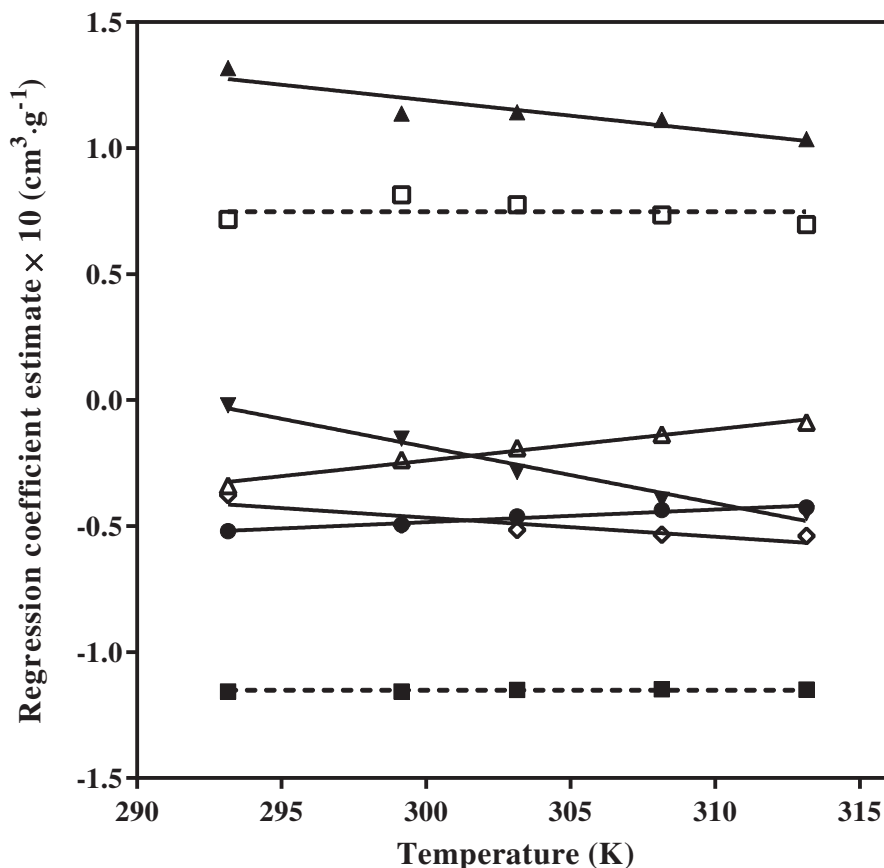


Figure 1.4. Regression coefficient estimates of Eq. (1.3) as a function of the absolute temperature (■): A_0 ; (Δ): A_1 ; (●): A_2 ; (\diamond): A_3 ; (\blacktriangledown): A_4 ; (\square): A_5 ; (\blacktriangle): A_6 (the solid lines are linear fits to data; the dashed lines are the arithmetic mean values of data; error bars corresponding to plus and minus one standard deviation are smaller than symbol size).

The curves of the excess specific volume of W + TBA binary mixtures as calculated from Eq. (1.4) for the different experimental temperatures are drawn in Figure 1.2. At a first glance, experimental data appeared to be well described by the model equation from which the minimum values in v^E are calculated to occur in binary mixtures with a TBA mass fraction of 0.384, 0.421 and 0.472 at temperatures of 293.15, 303.15 and 313.15 K, respectively. Considering the variation of the first derivative of Eq. (1.4) with respect to w_2 as a function of the binary mixture composition, it appears that the curves relating the composition dependence of v^E for any temperature in the range considered exhibits two inflexion points, one in the water-rich region and another in the *tert*-butyl alcohol-rich region of the composition range. As the temperature increases, the former is shifted toward mixtures of lower TBA content whereas the latter is shifted toward mixtures of higher TBA content. The binary mixture compositions corresponding to the occurrence of these inflexions in the curves describing the dependence of v^E on composition are computed to be $w_2 = 0.080$ and $w_2 = 0.916$ for $T = 293.15$ K and $w_2 = 0.060$ and $w_2 = 0.974$ for $T = 313.15$ K.

Table 1.7. Results of the linear least-squares regressions of the coefficients A_i from Eq. (1.3) on system temperature T at pressure $P = 0.1$ MPa^a.

Parameters ^b	n	B_i (K ⁻¹)	C_i (cm ³ ·g ⁻¹)	r_{adj}^2	$s(e)$ (cm ³ ·g ⁻¹)	$s_r(A_{i,\text{calc}})$ (%)
A_0 (cm ³ ·g ⁻¹) ^c	5	4.5825 (1.5075) · 10 ⁻⁵	-1.2907 (0.0457) · 10 ⁻³ ****	0.5915	2.34 · 10 ⁻⁴	0.09 – 0.16
A_1 (cm ³ ·g ⁻¹)	5	1.2390 (0.0955) · 10 ⁻³ ****	-3.9569 (0.2898) · 10 ⁻¹ ****	0.9708 ****	1.48 · 10 ⁻³	3.07 – 14.90
A_2 (cm ³ ·g ⁻¹)	5	5.0080 (0.5032) · 10 ⁻⁴ **	-1.9868 (0.1527) · 10 ⁻¹ ****	0.9510 **	7.81 · 10 ⁻⁴	0.74 – 1.44
A_3 (cm ³ ·g ⁻¹)	5	-7.5803 (2.3280) · 10 ⁻⁴ *	1.8076 (0.7064) · 10 ⁻¹	0.6324 *	3.61 · 10 ⁻³	3.27 – 6.93
A_4 (cm ³ ·g ⁻¹)	5	-2.2349 (0.2018) · 10 ⁻³ **	6.5189 (0.6122) · 10 ⁻¹ **	0.9602 **	3.13 · 10 ⁻³	4.61 – 75.74
A_5 (cm ³ ·g ⁻¹) ^c	5	-2.2073 (3.3070) · 10 ⁻⁴	1.4173 (1.0035) · 10 ⁻¹	-0.4512	5.13 · 10 ⁻³	3.07 – 5.47
A_6 (cm ³ ·g ⁻¹)	5	-1.2283 (0.2996) · 10 ⁻³ *	4.8748 (0.9091) · 10 ⁻¹ *	0.7476 *	4.65 · 10 ⁻³	1.80 – 3.50

**** $p \leq 0.0001$, *** $p \leq 0.001$, ** $p \leq 0.01$, * $p \leq 0.05$.

^a Values in parentheses are standard deviations.

^b n : number of regressed data points; B_i : slope; C_i : intercept; r_{adj}^2 : adjusted squared determination coefficients; $s(e)$: standard deviations of the residuals from regression; $s_r(A_{i,\text{calc}})$: relative standard deviations of the equation coefficient estimates over the whole temperature range.

^c Equation coefficient A_i was considered to be temperature independent for subsequent calculations so that $B_i = 0$ K⁻¹ and $C_i = \overline{A_i(T)}$ cm³·g⁻¹. See results and discussion section 1.3.1.2 for details and used values of C_0 and C_5 .

In addition, the composition dependence of e_p^E over the whole composition range can be obtained by differentiation of Eq. (1.4) with respect to the temperature:

$$e_p^E = w_2(1 - w_2) \sum_{i=0}^6 B_i(1 - 2w_2)^i \quad (1.5)$$

The variation of e_p^E with the TBA mass fraction, as calculated from Eq. (1.5), is illustrated in Figure 1.3 in order to compare the curve profile computed in this way with the values obtained from fitting Eq. (1.2) to experimental v^E data. It can be observed from Figure 1.3 that e_p^E values calculated by the two methods are in good agreement from a qualitative point of view but show some quantitative differences, especially at the extrema of the curve and in the composition range $w_2 = 0.5-0.7$. The values of e_p^E corresponding to the experimental binary mixture composition calculated from Eq. (1.5) are provided in Appendix A (Table A.2) along with those calculated from Eq. (1.2) for comparison purpose. Due to the high order of the polynomial Eq. (1.5), the values obtained from Eq. (1.2) are expected to be more accurate but, nevertheless, the absolute difference between the e_p^E values calculated by the two methods is at most of $0.2 \cdot 10^{-4} \text{ cm}^3 \cdot \text{g}^{-1} \cdot \text{K}^{-1}$. The extrema in the curve describing the composition dependence of e_p^E as calculated from Eq. (1.5) are computed to occur in binary mixtures with a TBA mass fraction of 0.051, 0.289 and 0.887 whereas null values of e_p^E are found for $w_2 \cong 0.129$ and, as expected, $w_2 = 0.500$.

1.3.2.2. Evaluation of correlative and predictive capabilities of the model

The effectiveness of Eq. (1.4) in modeling the dependence of the excess specific volume of W + TBA solvent mixtures on both composition and temperature was evaluated by considering the experimental data obtained in this work as well as those reported in published papers. These two experimental data sets are hereinafter referred as training and testing sets, respectively.

The testing set was constituted by all available numerical experimental values of either density or excess volume for the binary system under consideration in the range $T = 293.15-313.15 \text{ K}$ at atmospheric pressure published up to December 2015 for a total of 393 data points taken from [41-45, 47, 48, 51, 52, 54]. Experimental data from [49] and [53], although originally included in the testing set, were excluded because over half of experimental data from each of these references turned out to be detected as outliers on the basis of how we defined them, which is detailed below. The experimental excess specific volume values of W + TBA solvent mixtures, when not directly provided, were calculated from Eq. (1.1) using binary mixtures and pure components density values as reported in the original publication. When missing in the original publication, the experimental density

values of pure components measured in this work were used if available at the relevant temperature. If not, reference values from [64] were used for neat water whereas extrapolated values from least-squares linear regression of pure component density on temperature were used for neat *tert*-butyl alcohol, employing the density values measured in this work. The only exception is for the data from [54] for which all density values of pure TBA reported in were regressed with respect to temperature using a quadratic polynomial function and extrapolated density values of hypothetical pure supercooled TBA were calculated from the corresponding equation coefficient estimates. It should also be mentioned that the excess specific volume values for compositions corresponding to pure components, which by definition are null and perfectly predicted by the Redlich-Kister-like polynomial expansion were not included, neither in the training nor in the testing data sets, for not positively biasing the results.

In order to assess the correlative and predictive capabilities of Eq. (1.4), experimental data points from both the training and testing sets were compared with values computed from the model equation using the fixed coefficients values predetermined in section 1.3.2.1 and the model performances were evaluated from the least-squares fitting parameters including goodness-of-fit and its statistical significance as well as accuracy and precision of the calculated excess specific volume values, in the exact same way that for previous regression analyses. The results are summarized in Table 1.8 and the statistical outcomes are set out in Appendix A (Table A.8).

Table 1.8. Results of the least-squares comparison of Eq. (1.4) with fixed coefficient values to the excess specific volume of the water + *tert*-butyl alcohol mixtures v^E data from this work (training set) and from literature (testing set)^a.

Experimental data set		n	r_{adj}^2	$s(e)$ ($\text{cm}^3 \cdot \text{g}^{-1}$)	$s_r(v_{\text{calc}}^E)$ (%) ^b
Training set	Full	195	0.9999 *****	$1.76 \cdot 10^{-4}$	0.10 – 8.96
	Outliers excluded	184	>0.9999 *****	$1.41 \cdot 10^{-4}$	0.08 – 8.44
Testing set	Full	393	0.9994 *****	$4.66 \cdot 10^{-4}$	0.22 – 16.78
	Outliers excluded	368	0.9997 *****	$3.36 \cdot 10^{-4}$	0.16 – 13.11

**** $p \leq 0.0001$, *** $p \leq 0.001$, ** $p \leq 0.01$, * $p \leq 0.05$.

^a n : number of regressed data points; r_{adj}^2 : adjusted squared determination coefficients; $s(e)$: standard deviations of the residuals from regression; $s_r(v_{\text{calc}}^E)$: relative standard deviations of the excess specific volume estimates over the whole composition and temperature ranges.

^b Null values corresponding to v_{calc}^E for pure components excluded.

One can see from Table 1.8 that experimental data of v^E from both training and testing sets are well represented by Eq. (1.4) as indicated from the closeness of r_{adj}^2 values to unity. The good agreement between experimental values obtained in this work as well as those reported by others and the ones calculated from Eq. (1.4) can be appreciated in Figure 1.5 where it can be observed that all the training data points and almost all the testing data points fall along the identity line. Regarding to the accuracy of the model equation, the values of the standard deviation of the residuals from regression for the training set was found to be $1.76 \cdot 10^{-4} \text{ cm}^3 \cdot \text{g}^{-1}$ which, depending on the temperature considered and with exception of the lowest one, is 1.2 to 2.0-fold higher than the values obtained from the use of Eq. (1.3). For the testing set, the value of $s(e)$ was found to be less than $5 \cdot 10^{-4} \text{ cm}^3 \cdot \text{g}^{-1}$ which seems reasonable but, unfortunately, direct comparison with experimental uncertainties is hindered because measurement error is unavailable in most of the references from which the data were pooled. The uncertainty in calculated excess specific volume values for the training and testing data sets, computed from their respective variance-covariance matrices according to the general error propagation equation, are depicted in Figure 1.6 as a function of the composition of the W + TBA mixture for temperatures corresponding to the mean temperature of the range currently under discussion and at this temperature plus and minus 5 and 10 K. Because for both data sets the overall covariance term is always found to be negative with an absolute value slightly lower than that of the overall variance term over the whole composition and temperature ranges, it can be observed from Figure 1.6 that uncertainty values in calculated excess specific volume are very small and never exceed $7.3 \cdot 10^{-5} \text{ cm}^3 \cdot \text{g}^{-1}$ for the training set and $1.6 \cdot 10^{-4} \text{ cm}^3 \cdot \text{g}^{-1}$ for the testing set. Regarding to the composition and temperature dependence of the uncertainty in v_{calc}^E computed for the training set, as expected, the standard deviation of v_{calc}^E exhibits a symmetrical profile with respect to the composition corresponding to the mixture of equal mass of components over the whole temperature range whereas for a given mixture composition, the uncertainty in v_{calc}^E increases going away from the mean temperature of the range. In comparison, for a given mixture composition and system temperature, the uncertainty in v_{calc}^E computed for the testing set are always higher. Furthermore, although the uncertainty in v_{calc}^E is still converging toward the same value as the mass fraction of TBA in the mixture tends to 0.5 for the different isotherms, the symmetry of both sides of this composition is lost. In addition, considering the whole composition range, for the same deviation in temperature around the mean temperature of the range, the difference in uncertainty values are more pronounced than those observed for the training set. This obviously arises from the fact that the fitted data set is not the one that was used to estimate the model equation coefficients which results in different values in the matrix error. Whatever, the precision of the excess specific volume values calculated from Eq. (1.4) is proved to be extremely satisfactory considering the magnitude of the thermodynamic quantity of interest, the relative standard deviations of v_{calc}^E being lesser than 9% and 17% for the training and the testing sets, respectively.

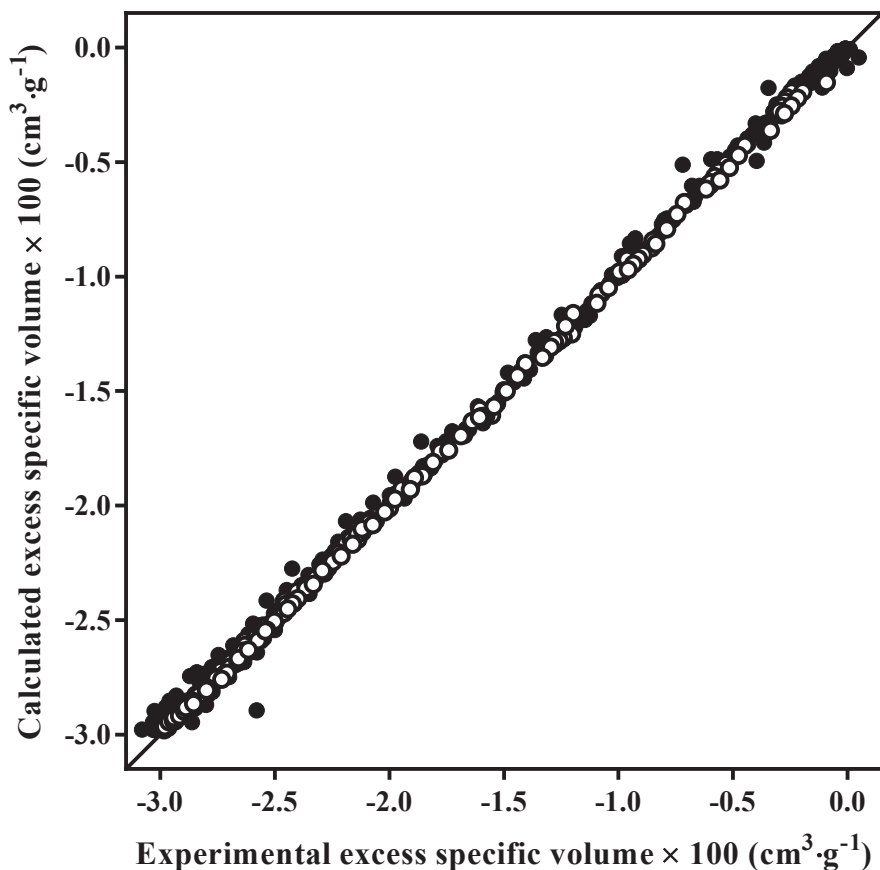


Figure 1.5. Scatter plot of the values of the excess specific volume of water + *tert*-butyl alcohol solvent mixtures calculated from Eq. (1.4) against the experimental values from this work (○): training set and from literature (●): testing set (the solid line is the identity line).

Before any other considerations, analyses of residuals from regression for both the training and testing sets were graphically performed to ensure that assumptions underlying the least-squares regression method were satisfied and to detect the presence of potential outliers in the experimental data sets. To assess whether or not residual errors from the model equation corresponding to the two the data sets under consideration are approximately normally distributed, the standardized residuals were plotted against theoretical *z*-scores derived from the Gaussian distribution. The resulting normal probability plots are depicted in Figure 1.7.A and 1.7.B for the training and testing sets, respectively. From these, one can note that for both data sets, the probability plots exhibit a straight-line pattern in the center of the data but that the first and last few data points in the lower and upper extremes of the plot show respectively an increasing departure from linearity below and above the fitted line, typical of a long-tailed distribution with respect to the normal one. Departure from linearity is more marked in the upper extreme of the distribution for the training set whereas the opposite occurs for the testing set. Furthermore, the middle of the probability plot of the residuals from the testing data set presents an S-like pattern while this not obvious on the plot corresponding to the residuals from the training data set.

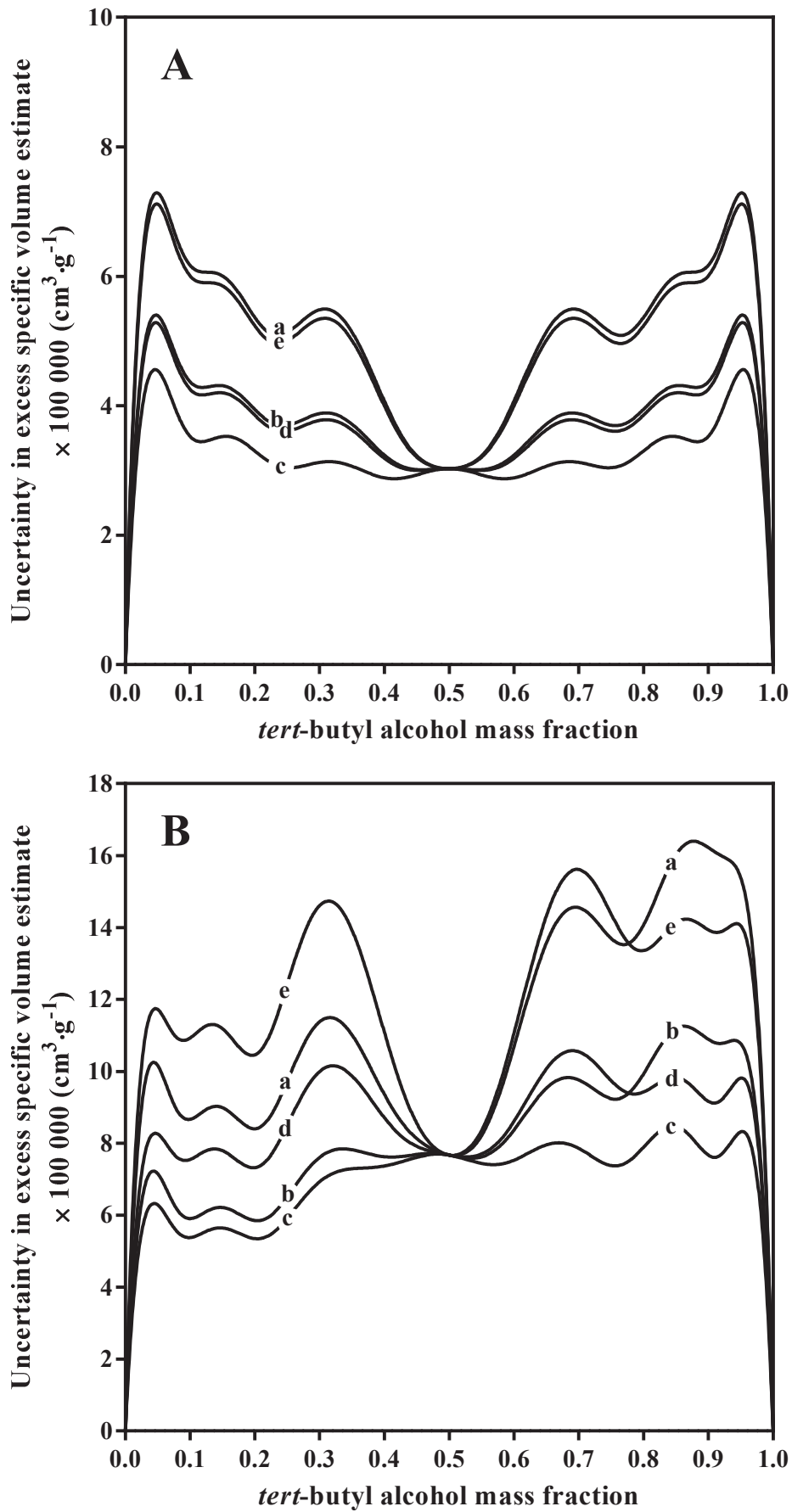


Figure 1.6. Uncertainty in excess specific volume estimates of water + *tert*-butyl alcohol solvent mixtures calculated from Eq. (1.4) as function of the *tert*-butyl alcohol mass fraction (A): training set; (B): testing set; (a): $T = 293.15$ K; (b): $T = 298.15$ K; (c): $T = 303.15$ K; (d): $T = 308.15$ K; (e): $T = 313.15$ K.

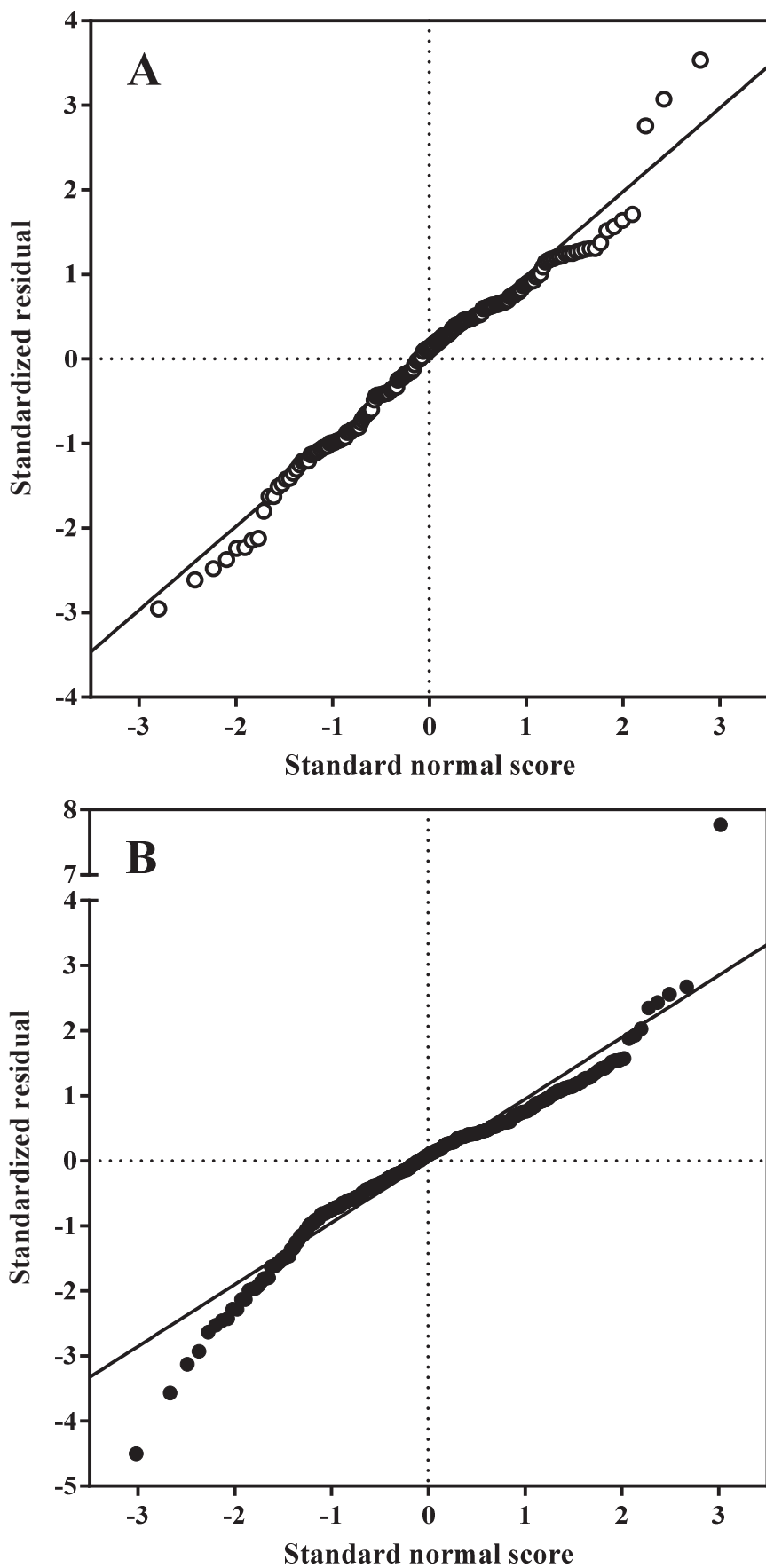


Figure 1.7. Normal probability plots of the residuals from Eq. (1.4) corresponding to experimental values of the excess specific volume of water + *tert*-butyl alcohol solvent mixtures from this work (A): training set and from literature (B): testing set (residuals are standardized with respect to mean and standard deviation; the solid lines are linear fits to data).

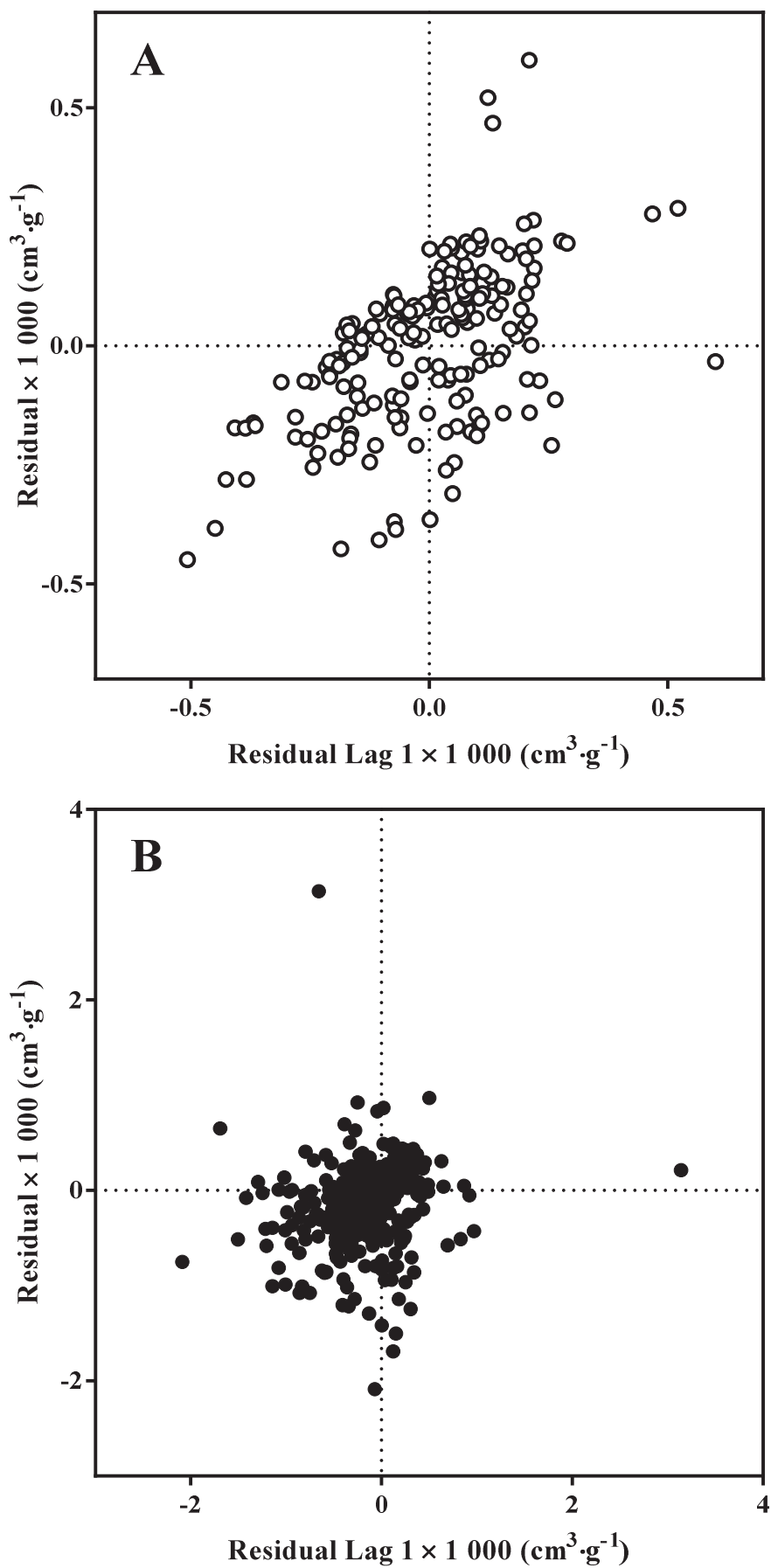


Figure 1.8. Lag plots of the residuals from Eq. (1.4) corresponding to experimental values of the excess specific volume of water + *tert*-butyl alcohol solvent mixtures from this work (A): training set and from literature (B): testing set (residuals are ranked in an increasing order first with respect to the *tert*-butyl alcohol mass fraction and second with respect to the absolute temperature).

Despite the values of the squared correlation coefficient associated with the linear fit to the data are found to be equal to 0.9776 and 0.9022 for the training and testing data sets, respectively, the profiles of the probability plots suggest the presence in them of outliers relative to a Gaussian distribution. Since in the present work, and supposedly in others, the order of experiments was not randomized with respect to both binary mixture composition and temperature, serial independence of residuals was checked by plotting for the two data sets each i -th residual value against the corresponding $(i - 1)$ -th one as depicted in Figure 1.8. The residual values were ranked first with respect to TBA mass fraction and second with respect to temperature so that the resulting final order correspond to the order of experiments of this work where density measurements were performed in an increasing order of TBA content and where for a given binary mixture composition, the density was measured in an increasing order of temperature. For the residuals obtained from the comparison of Eq. (1.4) to the data constituting the testing set, this ordering can be judged to be arbitrary but in absence of relevant information in the different published studies, we assumed that experimental scientists, especially those who used vibrating-tube digital density meters, performed the density measurements of W + TBA mixtures in the same way we did. It can be seen in Figures 1.8.A and 1.8.B that, neither for the training set nor for the testing set, the lag plots exhibit any identifiable pattern which assess of the independence of residuals from regression of experimental v^E data on temperature and composition using the model equation. In addition, the presence of some outliers in the data sets is confirmed from these plots. Detection of outliers was performed in the usual way by plotting standardized residuals as a function of calculated values of the dependent variable, as illustrated in Figure 1.9. However, in the present work, standardization of residuals was done with respect to the median and median absolute deviation of the residuals distributions rather than with respect to their means and standard deviations. This was preferred because, on the one hand, residuals are observed to be not completely normally distributed, and on the other hand, because median and median absolute deviation are respectively central tendency and dispersion indicators which are both almost insensitive to the presence of outlying values, in contrary to mean and standard deviation. Full explanation and details of the calculation procedure for absolute deviation around the median of a distribution are available in the paper by Leys and coworkers [74]. As recommended by these authors, a threshold value of 2.5 was selected as rejection criterion value so that any data point for which the corresponding standardized residual value was found to be either strictly superior to 2.5 or strictly inferior to -2.5 was considered as outlier^{1,2}.

¹ The interval of two and a half absolute deviations from either side of the median population do not correspond to the one enclosing a certain percentage of the observations based on any distribution assumption but qualitatively to a moderately conservative one.

² It should be emphasized that the experimental data identified as outliers in this work should not, in any way, be systematically considered as erroneous experimental values, but well as they are defined, that is, data points whose perpendicular distance from the fitted line of regression is two and half times greater than the median distance value.

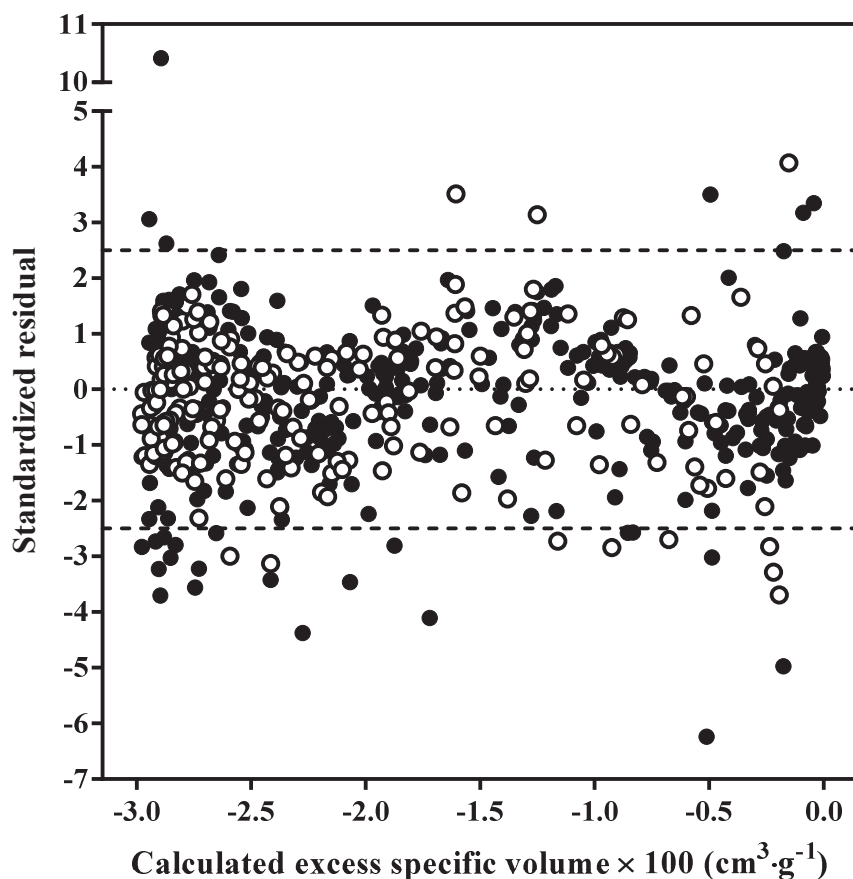


Figure 1.9. Scatter plot of the standardized residuals from Eq. (1.4) corresponding to experimental values of the excess specific volume of water + *tert*-butyl alcohol solvent mixtures from this work (○): training set and from literature (●): testing set, against the calculated mixture excess specific volume (residuals are standardized with respect to median and median absolute deviation; the dashed lines are the threshold values used for defining outliers).

Accordingly, it can be observed from Figure 1.9 the presence of 11 outlying values in the training set and 25 ones in the testing set which correspond, respectively, to 5.6 and 6.4% of the experimental data sets. In Figure 1.10 is depicted a scatter plot of the experimental data points identified as outliers which allows for mapping their presence with respect to both mixture composition and temperature. Considering outliers from the training data set, it appears that they are clustered in the water-rich and *tert*-butyl alcohol part of the composition range and are more prevalent in the lower part of the temperature range. Those from the testing are more scattered with respect to the mixture composition but not with respect to the temperature, but it should be kept in mind that for this data set, experimental excess specific volume values measured at temperatures lower than 303.15 K are proportionally more numerous than those measured at higher temperatures. Once outliers were identified and removed from the two data sets, goodness of representation of experimental excess specific volume values with Eq. (1.4) and accuracy and precision of excess specific volume values

calculated from the model equation were recomputed and the results are presented in Table 1.8 for comparison purposes.

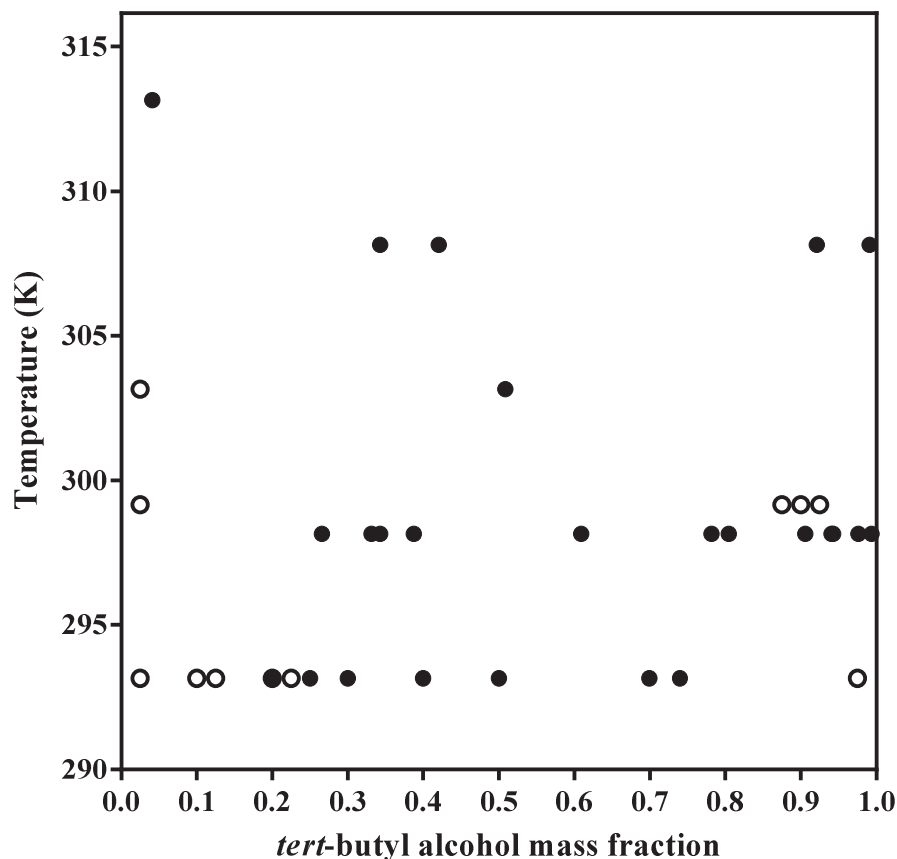


Figure 1.10. Distribution of the identified outlying experimental data points of excess specific volume of water + *tert*-butyl alcohol solvent mixtures from this work (○): training set and from literature (●): testing set, as function of the *tert*-butyl alcohol mass fraction and absolute temperature.

For both data sets, removal of outliers results in a slight enhancement of the model performance indicators, as expected. The normality of the distribution of the residuals was also reassessed using the same procedure as described before. The squared correlation coefficients from linear regression between standardized residuals and normal *z*-scores for the outlier-free training and testing sets were found to be closer to unity in comparison to those obtained for the full data sets, with values of 0.9804 and 0.9953, respectively. It can be reasonably concluded that the distribution of residuals from both outlier-free data sets is nearly normal so that the corresponding means and standard deviations can be used as central tendency and dispersion estimators, respectively. The values of $s(e)$ are provided in Table 1.8 and were found to be equal to $1.4 \cdot 10^{-4} \text{ cm}^3 \cdot \text{g}^{-1}$ for the training set and to $3.4 \cdot 10^{-4} \text{ cm}^3 \cdot \text{g}^{-1}$ for the testing set whereas the those of \bar{e} were calculated to be $6.1 \cdot 10^{-6} \text{ cm}^3 \cdot \text{g}^{-1}$ for the former data set and

$-1.4 \cdot 10^{-4} \text{ cm}^3 \cdot \text{g}^{-1}$ for the latter one. Scatter plots of the residuals from regression against the model response and predictor variables for the two outlier-free data sets are depicted in Figure 1.11. Considering the plots of the residuals against the excess specific volume of binary mixtures calculated from Eq. (1.4), it appears that for both data sets, individual data points are randomly distributed from either sides of the mean value and that requirement of homoscedasticity of errors is met overall. This is also true when considering the distribution of the residuals as a function of the temperature but it is less evident when one examines Figures 1.11.A.3 and 1.11.B.3 where the residuals are plotted against the TBA mass fraction in the binary mixture. Regarding to the outlier-free training set, the distribution of the residuals appears to be globally satisfactory, with exception of the water-rich region of the composition range where depending on the considered composition, residuals are clustered on one side of the mean or the other but the magnitude of the deviations around the mean value in this specific part of the composition range is similar to that observed in the remaining one. This clustering is also observed for the outlier-free testing set but the magnitude of the deviation around the mean value is no more nearly constant over the whole composition range and is accompanied by a shift toward negative residual values as the TBA content in the mixture increases. Nevertheless, considering all the results highlighted in this subsection, it can reasonably be stated that assumptions underlying the least-squares regression method are, at least substantially, satisfied.

The performances of Eq. (1.4) in modeling the temperature and composition dependences of v^E were further evaluated by considering the absolute relative deviation (ARD) between calculated values and the experimental ones from both outlier-free data sets. The distribution of ARD in v_{calc}^E is graphically presented as scatter and box-and-whiskers plots in Figures 1.12.A and 12.B, respectively. Looking to Figure 1.12.A, where ARD values of individual data points are plotted against the mixture composition, one can see that for both data sets, the ARD values are lower than 5% over almost all of the composition range. In comparison, the values of the ARD in v_{calc}^E are considerably higher in both the water-rich and *tert*-butyl alcohol-rich regions, without exceeding 10% for the training set but being up to about 175% for the testing set. This must be considered in the light of the very low absolute value of the excess specific volume for these mixtures. Turning to Figure 1.12.B to examine the distribution of the ARD among the individual data sets, it can be observed that the mean ARD value is less than 1% for the training set and of about 7% for the testing set. Although appreciable, these values are substantially higher than the corresponding median ARD values because of extremely large values outweigh the smaller and more numerous ones so that it appears more pertinent to consider percentiles values of the ARD distributions. The values of the 25th, 50th and 75th percentiles were found to be equal to 0.25, 0.47 and 0.87% for the training set and to 0.77, 1.64 and 5.95% for the testing set, respectively.

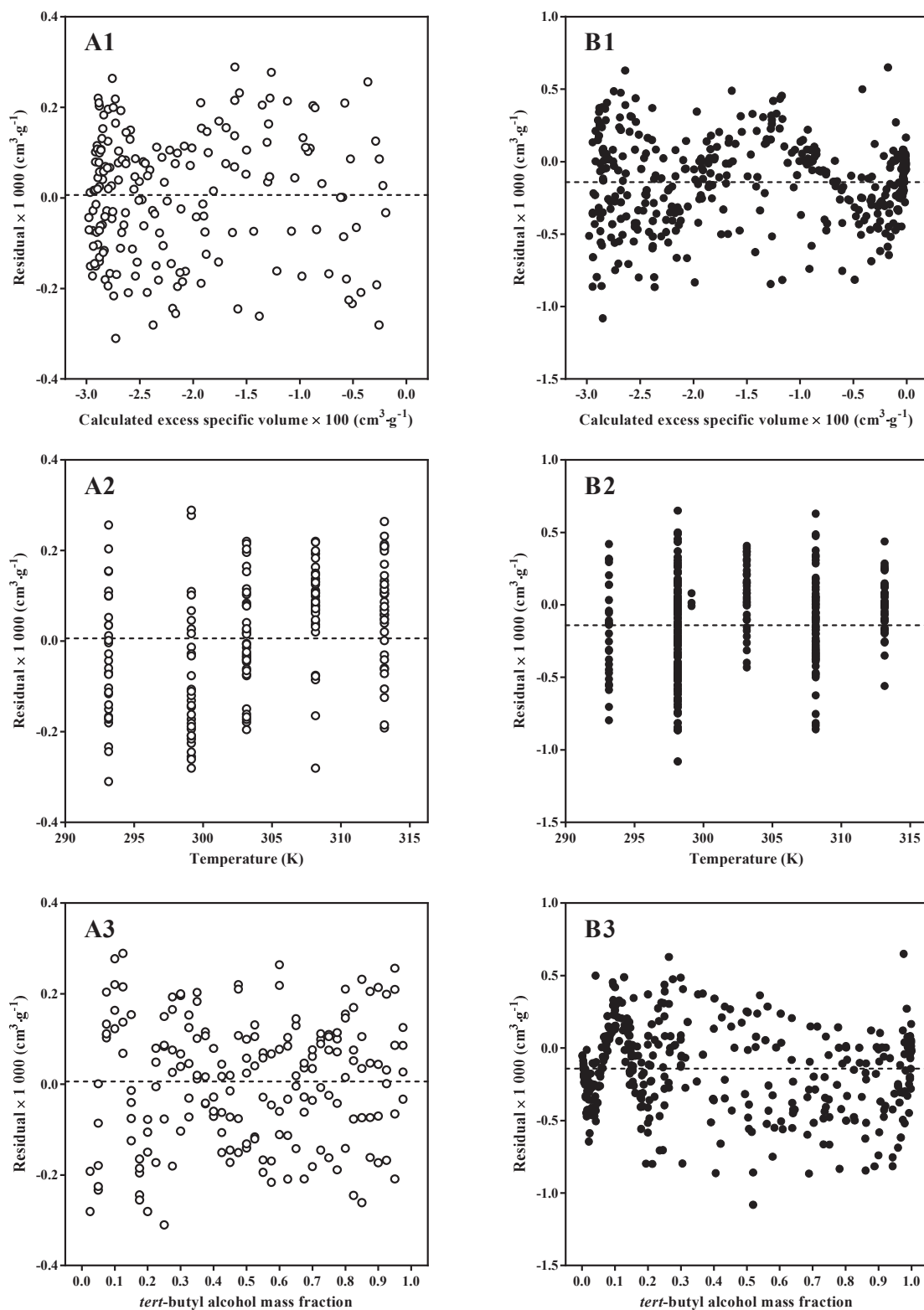


Figure 1.11. Scatter plots of the residuals from Eq. (1.4) corresponding to experimental values of the excess specific volume of water + *tert*-butyl alcohol solvent mixtures from this work (A): training set and from literature (B): testing set, against (1): calculated excess specific volume of the binary mixture; (2): absolute temperature and (3): *tert*-butyl alcohol mass fraction (the dashed lines are the means of the residuals from regression; data points identified as outliers are not included in the data sets).

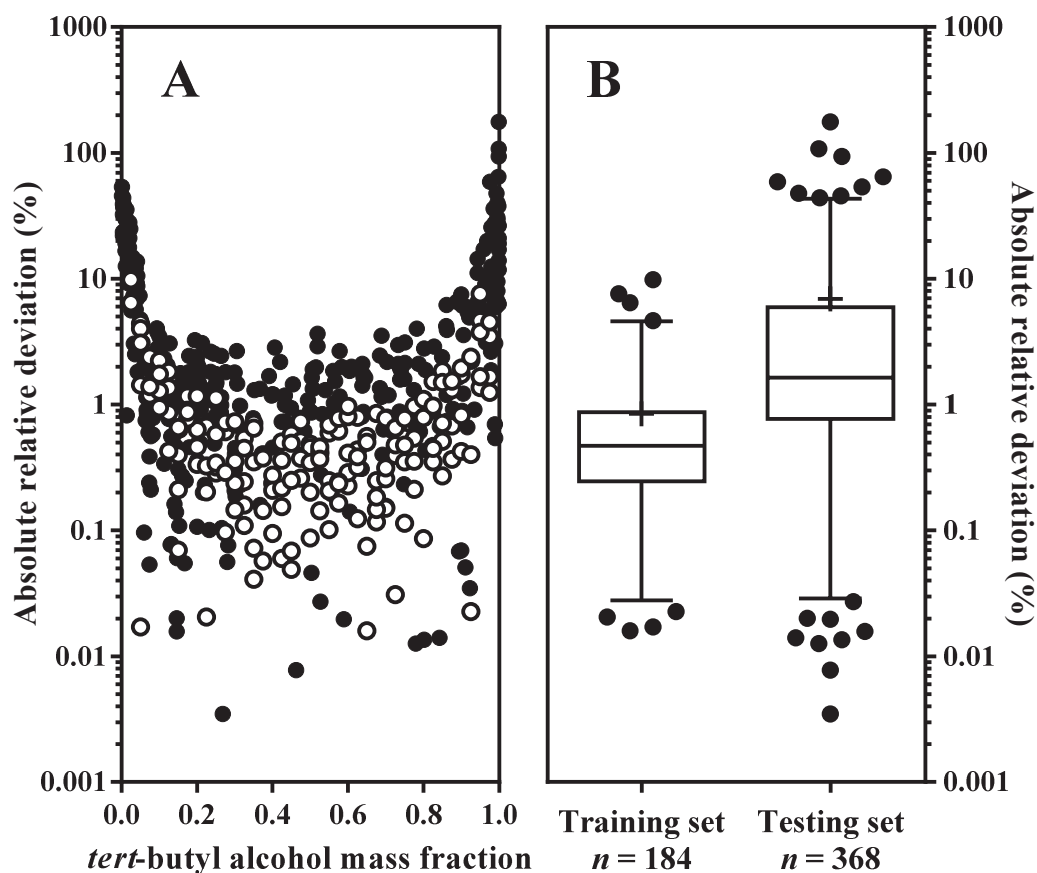


Figure 1.12. Absolute relative deviation in values of the excess specific volume of water + *tert*-butyl alcohol solvent mixtures calculated with Eq. (1.4) from experimental values from this work and from literature displays as (A): scatter plot against *tert*-butyl alcohol mass fraction (○): training set; (●): testing set and (B): box-and-whiskers plots (the upper and lower hinges of the boxes indicate the 25th and 75th percentiles, respectively, the lines within the boxes represent the 50th percentiles, the whiskers extend from the 2.5th to the 97.5th percentiles, the crosses denote the means and the dots correspond to individual values which are outside the range delimited by whiskers; data points identified as outliers are not included in the data sets).

Finally, evaluation of the forecasting ability of Eq. (1.4) was performed by considering the coverage rate of the 99% prediction interval of the model, constructed on the basis of the least-squared regression parameters corresponding to the outlier-free training set using a Student's distribution. The proportion of experimental excess specific volume values from the outlier-free testing set falling into was computed to be of 80.7% which can be considered satisfactory in regard to the narrowness of the prediction interval width which does not exceed $8 \cdot 10^{-4} \text{ cm}^3 \cdot \text{g}^{-1}$ and to the fact that considered excess specific volume values are obviously accompanied by an experimental error. In Figures 1.13.A and 1.13.B are shown the coverage rates of the 99% model prediction interval over the binary mixture composition and temperature ranges partitioned into discrete classes.

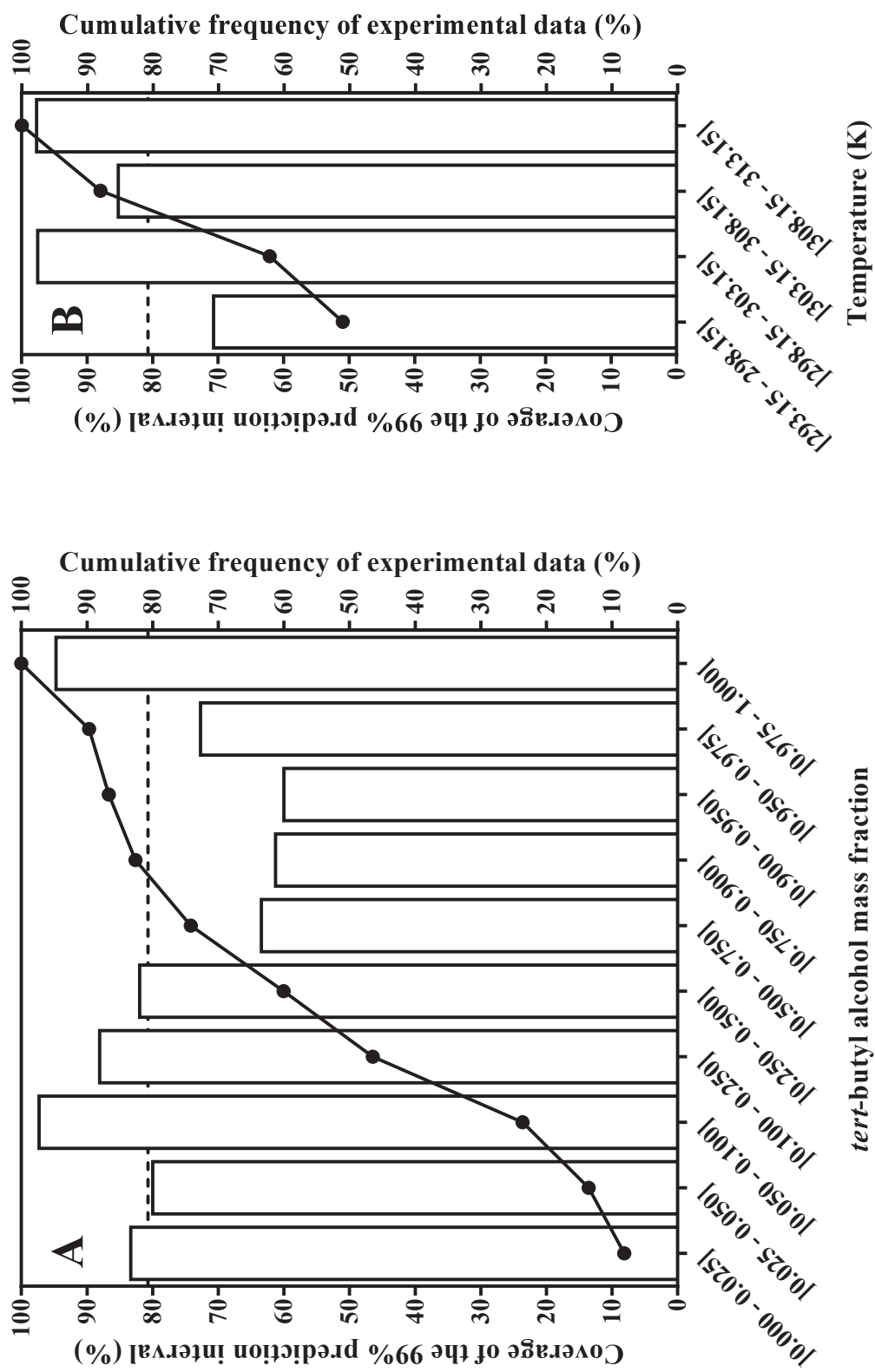


Figure 1.13. Relative frequency distributions of the coverage rate by experimental values from literature of the excess specific volume of water + *tert*-butyl alcohol solvent mixtures calculated from Eq. (1.4) (bars) and corresponding cumulative relative frequency distributions of experimental data (dots), per class of system composition (A) and temperature (B) (the dashed lines are the coverage rate for the whole composition and temperature ranges; data points identified as outliers are not included in the data set).

Because they are of unequal size, the cumulative frequencies of experimental data per interval are also presented in these figures. From Figure 1.13.A it can be observed that coverage rate values are highest for binary mixtures with a TBA mass fraction of less than 0.5 or higher than 0.975 and are least for those of composition in between with values ranging from 60 to 73%. For classes corresponding to the water-rich and *tert*-butanol-rich ends of the composition interval, the proportion of experimental values falling into the model prediction interval are found to be of about 83% and 94%, respectively, indicating that Eq. (1.4) is able to correctly describe the composition dependence of v^E at near infinite dilution conditions. It can also be seen from Figure 1.13.B that, for temperatures higher than 298.15 K, the coverage rate values range from 85 to 98% whereas at lower or equal temperatures, only about 71% of the observations were covered by the 99% prediction interval

From these results, it can be concluded that the experimental data provided in this work are in perfect agreement with those previously reported in the literature. Furthermore, the model Eq. (1.4) can be considered to be reliable in predicting the dependence of the excess specific of W + TBA solvent mixtures on composition and temperature over the range investigated so that it can be used to compute related excess partial specific thermodynamic quantities of water and *tert*-butyl alcohol in their binary mixtures.

1.3.3. Derived excess partial specific thermodynamic quantities

Excess partial thermodynamic quantities, as differential properties, allow separating the contribution of individual mixture components to the deviation of the system from ideal behavior and quantifying for each component the changes accompanying their transfer from the pure state to the mixture. The composition and temperature dependences of the excess partial specific volumes of water $v_1^E = (\partial V^E / \partial m_1)_{T,P,m_2}$ and *tert*-butyl alcohol $v_2^E = (\partial V^E / \partial m_2)_{T,P,m_1}$ in mixtures were determined on the basis of Eq. (1.4) through the use of the well-known method of intercepts [21, 22]. It can be readily shown that the intercepts of the tangent line to the curve relating the isothermal variation of v^E with w_2 at mixture composition w'_2 on the axis at $w_2 = 0$ and $w_2 = 1$ are $v_1^E(w'_2)$ and $v_2^E(w'_2)$, respectively, and they can therefore be computed from the following equations:

$$v_1^E(w'_2) = v^E(w'_2) - w'_2 \frac{dv^E}{dw_2}(w'_2) \quad (1.6.a)$$

$$v_2^E(w'_2) = v^E(w'_2) + (1 - w'_2) \frac{dv^E}{dw_2}(w'_2) \quad (1.6.b)$$

where $v^E(w_2')$ and $dv^E/dw_2(w_2')$ are the binary mixture excess specific volume and its derivative with respect to w_2 for $w_2 = w_2'$, respectively. Appropriate differentiation of Eq. (1.4) and substitution with Eq. (1.4) into Eq. (1.6.a) and Eq. (1.6.b) lead, after rearrangement, to:

$$v_1^E = (w_2)^2 \sum_{i=0}^6 (B_i T + C_i) [(1 - 2w_2)^i + 2i(1 - w_2)(1 - 2w_2)^{i-1}] \quad (1.7.a)$$

$$v_2^E = (1 - w_2)^2 \sum_{i=0}^6 (B_i T + C_i) [(1 - 2w_2)^i - 2iw_2(1 - 2w_2)^{i-1}] \quad (1.7.b)$$

where $v_i^E = v_i^E(T, P, X) = \Delta_{\text{mix}} v_i(T, P, X)$ and where all other terms are as previously defined. The temperature dependence of the excess partial specific volumes over the range $T = 293.15\text{-}313.15$ K can be accounted for by using the quantities $e_{p,1}^E = (\partial v_1^E / \partial T)_{P,X}$ for water and $e_{p,2}^E = (\partial v_2^E / \partial T)_{P,X}$ for *tert*-butyl alcohol. They are computed from differentiation of Eqs. (1.7.a) and (1.7.b) with respect to temperature:

$$e_{p,1}^E = (w_2)^2 \sum_{i=0}^6 B_i [(1 - 2w_2)^i + 2i(1 - w_2)(1 - 2w_2)^{i-1}] \quad (1.8.a)$$

$$e_{p,2}^E = (1 - w_2)^2 \sum_{i=0}^6 B_i [(1 - 2w_2)^i - 2iw_2(1 - 2w_2)^{i-1}] \quad (1.8.b)$$

From Eqs. (1.8.a) and (1.8.b) and within the framework of the model we propose, it can be seen that $e_{p,i}^E = e_{p,i}^E(P, X) = \Delta_{\text{mix}} e_{p,i}(P, X)$ are independent of the temperature over the range considered. The values of v_i^E and $e_{p,i}^E$ calculated for our experimental compositions at different temperatures are provided in Appendix A (Tables A.9, A.10 and A.11). In Figure 1.14 and Figure 1.15 are displayed respectively the variations of v_1^E and v_2^E and those of $e_{p,1}^E$ and $e_{p,2}^E$ with the mass fraction of alcohol over the whole experimental composition and temperature ranges. According to the Gibbs-Duhem relation [75, 76] applied to a binary system, any change in a given partial property of one of the mixture component is accompanied by an opposite one, but not necessarily equal, in that of the other component. Thus, extrema in the curves describing the composition dependence of the partial properties of the individual mixture components occur at the same composition, which corresponds into an inflexion in the curve of the corresponding mixture property against composition. In addition, equalization of the values of the partial quantity of the two component occurring at a given mixture composition is reflected as an extremum in the curve relating the binary mixture property to its composition.

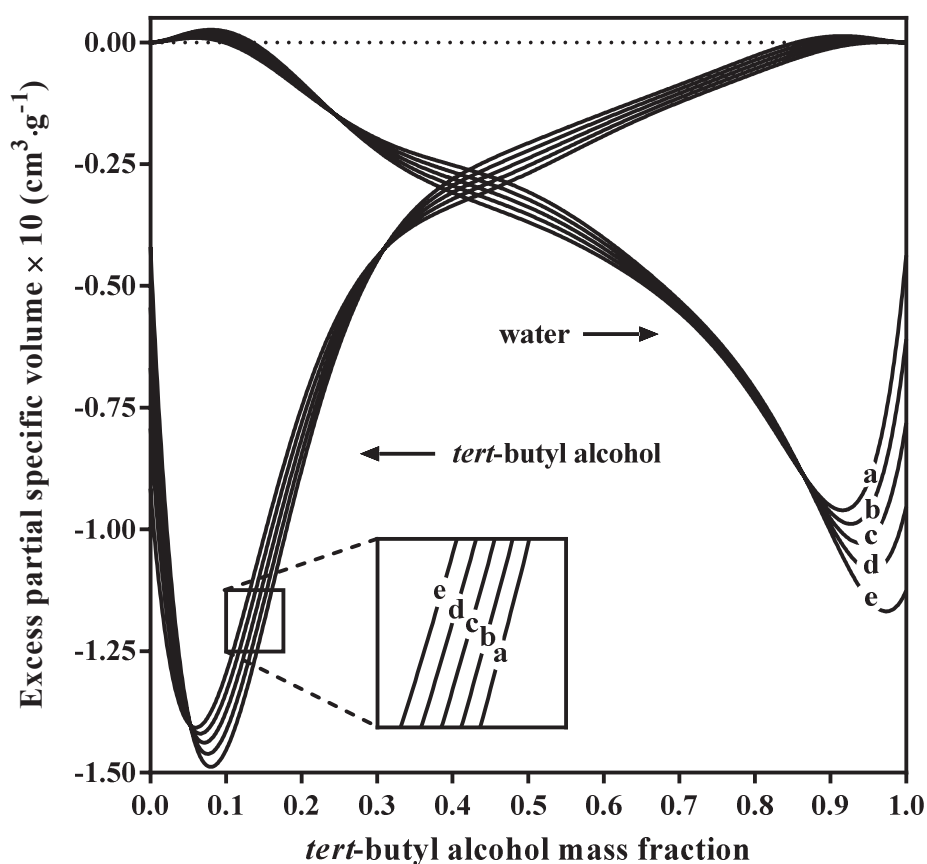


Figure 1.14. Excess partial specific volume of water and *tert*-butyl alcohol in their mixtures as function of the *tert*-butyl alcohol mass fraction (a): $T = 293.15$ K; (b): $T = 298.15$ K; (c): $T = 303.15$ K; (d): $T = 308.15$ K; (e): $T = 313.15$ K (the solid lines are calculated from Eq. (1.7.a) and Eq. (1.7.b)).

From Figure 1.14, one can observe the presence of extrema in the curves of v_1^E and v_2^E plotted against the mass fraction of TBA at both ends of the composition range. Whereas the sharp minimum in v_2^E curves in the water-rich region is a characteristic feature of aqueous solutions of non-electrolytes containing both polar and non-polar groups, that in v_1^E curves in the *tert*-butyl alcohol-rich region, although certainly less pronounced but nonetheless well defined, is generally not reported in the literature, except in the work of Sakurai [50] whose curve profiles of v_1^E and v_2^E depicted in are in perfect agreement with those shown in Figure 1.14. As pointed out and demonstrated by this author almost thirty years ago, this arises from the mixture composition scale and volume unit used to investigate the volumetric behavior of the W + TBA system. Indeed, the molar mass of *tert*-butyl alcohol being about four times greater than that of water, expressing the mixture composition and volume in mole fraction and molar units, respectively, results in concealing the extrema in the curves describing the composition dependence of v_1^E and v_2^E in the *tert*-butyl alcohol-rich region whereas

expressing mixture composition in mass fraction and volume in mass units allows to reveal them. The unusual volumetric behavior of the W + TBA system in the *tert*-butyl alcohol-rich region, as reflected by the occurrence of a minimum in the curve relating the dependence of the apparent partial molar volume of water on mixture composition, was also evidenced by Kipkemboi and Eastal for different isotherms [52]. However, since apparent partial thermodynamic quantities of a given mixture component are calculated in such a way that all the deviations in the corresponding mixture properties from ideal mixing behavior are attributed solely to this component, this extremum was not accompanied by one in the curve describing the composition dependence of the apparent partial molar volume of *tert*-butyl alcohol.

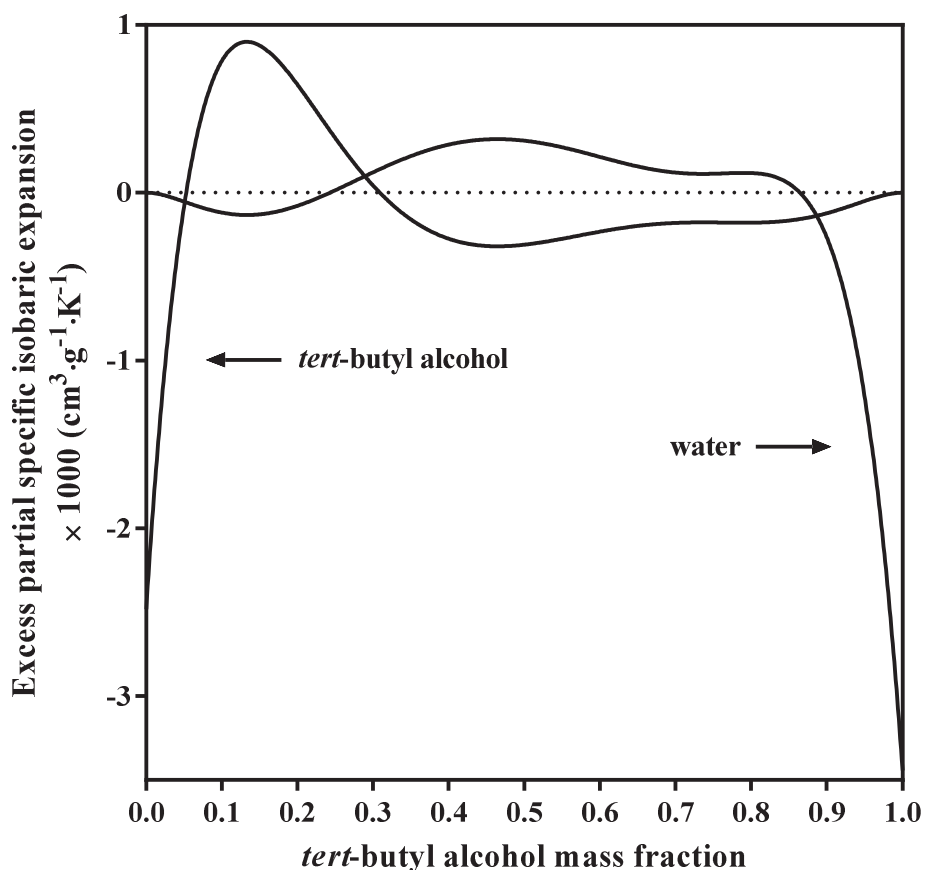


Figure 1.15. Excess partial specific isobaric expansivity of water and *tert*-butyl alcohol in their mixtures over the temperature range $T = 293.15\text{-}313.15\text{ K}$ as function of the *tert*-butyl alcohol mass fraction (the solid lines are calculated from Eq. (1.8.a) and Eq. (1.8.b)).

Regarding to the sign of the excess partial specific volumes of both components, it follows that they are negative over the most of the composition range meaning that the specific volume of water and *tert*-butyl alcohol in their binary mixtures is lower than that in their pure liquid states. Oppositely, they are found to be positive only over a narrow range on both sides of their respective maximum at either one or another ends of the composition range so that in these restricted zones, the specific volume of water and *tert*-butyl alcohol in mixture appears to expand in comparison with their pure counterparts. Focusing on the extreme values of v_1^E and v_2^E in the water-rich and *tert*-butyl alcohol-rich regions, one can notice that the magnitude of the minima in both v_1^E and v_2^E curves are substantially larger than that of the corresponding maxima. As the system temperature increases, the composition of the mixture corresponding to the extrema in the water-rich region are shifted toward lower alcohol content whereas that corresponding to the extrema in the *tert*-butyl alcohol-rich region are shifted toward higher one. Furthermore, increasing the temperature results in a decrease in the magnitude of the extrema in both v_1^E and v_2^E curves in the water-rich region while in the *tert*-butyl alcohol-rich region, this also entails a decrease in the magnitude of the maxima in the v_2^E curve but an increase in the magnitude of the minima in that of v_1^E . However, the magnitude of the maxima in either v_1^E or v_2^E curves is not as dependent as that of the corresponding minima on temperature.

Turning to Figure 1.15, it can be seen that the curve relating the dependence of $e_{p,2}^E$ to the mass fraction of alcohol exhibits a pronounced maximum in the water-rich region which, in comparison to the minima in the v_2^E isothermal curves, occurs for a mixture composition of slightly higher TBA content. This maximum is obviously accompanied by minimum in the $e_{p,1}^E$ curve but the magnitude of this latter is relatively small compared to that of the former. Consequently, within the composition range on both sides of these extrema, the values of $e_{p,2}^E$ are positive whereas those of $e_{p,1}^E$ are negative so that in this composition range, the magnitude of the variation of the partial specific volumes of *tert*-butyl alcohol and water in mixture with temperature is respectively greater and lesser than that of the components in their pure liquid states. The excess partial specific isobaric expansivity of both mixture components are found to change in sign twice across the whole composition range and the mixtures compositions at which this occurs expectedly correspond to those for which the respective excess partial specific volume values are temperature independent within the range of interest. Furthermore, at these particular compositions, the dependence of the partial specific volume of the relevant component on temperature is the same than that in its pure liquid state. The values of $e_{p,1}^E$ and $e_{p,2}^E$ are found to be positive for TBA mass fraction ranging about from 0.243 to 0.865 and from 0.053 to 0.309, respectively, and negative over the remaining composition range. Over the range of mixture composition from about 0.35 to 0.75 in mass fraction of TBA, one can notice the presence of small-amplitude fluctuations in both $e_{p,1}^E$ and $e_{p,2}^E$ curves. From visual inspection of Figure 1.3, it appears that within this particular composition range, the variation of e_p^E with respect to the binary mixture

composition is almost linear whereas it is described by a concave upward curve through the use of Eq. (1.5). This reflects in the corresponding first-order partial derivative curves as fluctuations which almost certainly have non-physical meaning so that $e_{p,1}^E$ and $e_{p,2}^E$ should more likely exhibit a monotonic variation with mixture composition in the range considered. The more suitable way to confirm it would be to straightforwardly regress e_p^E data calculated from Eq. (1.2) on alcohol concentration in mixture in order to express the composition dependence of this thermodynamic quantity with a proper equation from which corresponding excess partial specific isobaric thermal expansivity of individual mixture components could be determined. However, since no convenient procedure appears to be readily available for such a curve fitting procedure, one must be satisfied with the present data and, from our opinion, their use must be restricted to a qualitative interpretation, especially over the composition range in which fluctuations in $e_{p,1}^E$ and $e_{p,2}^E$ curves are observed. Considering now the water-rich and *tert*-butanol-rich ends of the composition range, one can observe from Figure 1.15 that as the concentration of one of the mixture component tends to toward infinite dilution, the excess partial specific isobaric expansivity of that component decreases in a sharp manner to an extreme negative value.

Numerical values of infinite dilution excess partial specific volumes of water $v_1^{E,\infty} = \lim_{w_1 \rightarrow 0} (v_1^E)$ and of *tert*-butyl alcohol $v_2^{E,\infty} = \lim_{w_2 \rightarrow 0} (v_2^E)$ can be readily computed over the range $T = 293.15\text{-}313.15$ K by setting, respectively, $w_2 = 1$ into Eq. (1.7.a) and $w_2 = 0$ into Eq. (1.7.b) so that:

$$v_1^{E,\infty} = \sum_{i=0}^6 (B_i T + C_i) (-1)^i \quad (1.9.a)$$

$$v_2^{E,\infty} = \sum_{i=0}^6 (B_i T + C_i) \quad (1.9.b)$$

where $v_i^{E,\infty} = v_i^{E,\infty}(T, P) = \Delta_{\text{mix}} v_i^{\infty}(T, P)$. Hence, the temperature dependence of the limiting excess partial specific volumes over the temperature range under consideration can be envisioned by considering the quantities $e_{p,1}^{E,\infty} = (\partial v_1^{E,\infty} / \partial T)_p$ for water and $e_{p,2}^{E,\infty} = (\partial v_2^{E,\infty} / \partial T)_p$ for *tert*-butyl alcohol which are easily obtained from direct differentiation of Eqs. (1.9.a) and (1.9.b) with respect to temperature:

$$e_{p,1}^{E,\infty} = \sum_{i=0}^6 B_i (-1)^i \quad (1.10.a)$$

$$e_{p,2}^{E,\infty} = \sum_{i=0}^6 B_i \quad (1.10.b)$$

where $e_{p,i}^{E,\infty} = e_{p,i}^{E,\infty}(P) = \Delta_{\text{mix}} e_{p,i}^{\infty}(P)$ are inherently constant over the temperature range considered. In Figure 1.16 are displayed the variations of $v_1^{E,\infty}$ and $v_2^{E,\infty}$ with respect to temperature as calculated from Eq. (1.9) over the temperature range of applicability. The values of $v_1^{E,\infty}$ and $v_2^{E,\infty}$ are computed to range from -0.44 ± 0.04 to $-1.12 \pm 0.03 \cdot 10^{-1} \text{ cm}^3 \cdot \text{g}^{-1}$ and from -0.42 ± 0.04 to $-0.92 \pm 0.03 \cdot 10^{-1} \text{ cm}^3 \cdot \text{g}^{-1}$, respectively. As expected from Eq. (1.9), both these thermodynamic quantities decrease linearly with temperature over the temperature range investigated with a constant slope of $-3.4 \pm 0.03 \text{ cm}^3 \cdot \text{g}^{-1} \cdot \text{K}^{-1}$ and $-2.5 \pm 0.03 \text{ cm}^3 \cdot \text{g}^{-1} \cdot \text{K}^{-1}$, equal to $e_{p,1}^{E,\infty}$ and $e_{p,2}^{E,\infty}$, respectively. In Figure 1.16 are also shown for comparison purposes values of $v_1^{E,\infty}$ and $v_2^{E,\infty}$ taken from literature. It can be observed that the values of $v_1^{E,\infty}$ calculated from Eq. (1.9) show good agreement with those reported in [50-52] but considerable differences with those reported in [41] and [54], whereas values of $v_2^{E,\infty}$ obtained in this work are found to be substantially higher than those previously published [41, 46, 47, 52, 54, 58, 77]. Although, such discrepancies between values of infinite dilution partial thermodynamic quantities are commonly ascribed to difference in methodology used for extrapolation to zero concentration, one cannot ignore that, unless proven otherwise, extrapolated infinite dilution values estimated from a fitting equation applied to data covering the whole composition range are less accurate than the ones obtained from the same fitting equation with a smaller number of coefficients but restricted to data covering the very-diluted composition range [78]. Because of the particular application domain of interest to us, very-diluted regions of the W + TBA system were not of prime importance in the present work so that they were not experimentally covered. Hence, and despite the fact that Eq. (1.4) was shown to be able to adequately describe the composition dependence of v^E at near infinite dilution conditions, the values of $v_1^{E,\infty}$ and $v_2^{E,\infty}$ derived from this equation are certainly less reliable than those obtained from measurements carried out on extremely diluted binary mixtures [54].

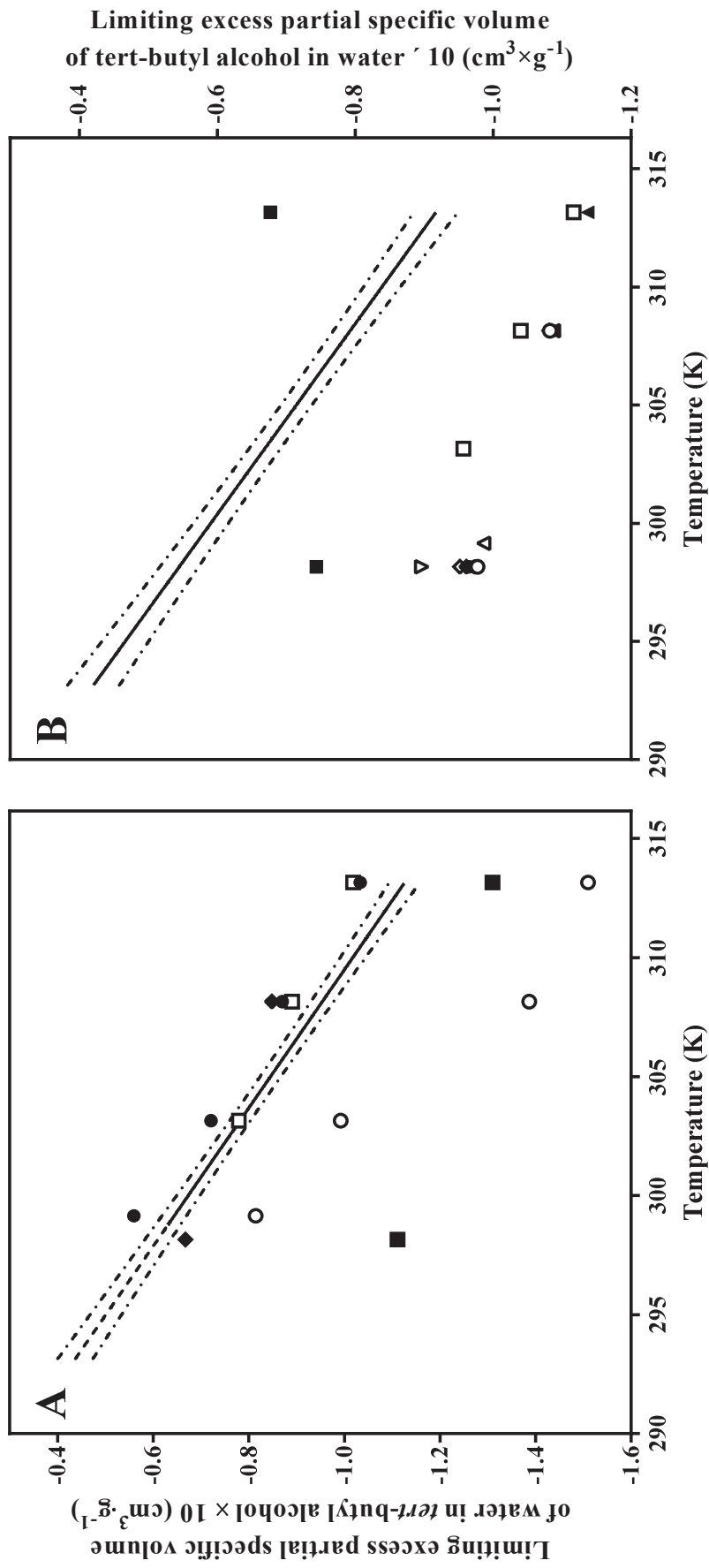


Figure 1.16. Comparison of infinite dilution excess partial volume values of water (A) and *tert*-butyl alcohol (B) over the temperature range $T = 293.15$ - 313.15 K determined in this work with those from literature (○): [54]; (●): [51]; (□): [50]; (■): [41]; (▼): [47]; (◆): [52]; (△): [46]; (◇): [77] (the solid lines are calculated from Eq. (1.9.a) and Eq. (1.9.b); the dashed line is the extrapolation of the infinite dilution excess partial volume of water in hypothetical pure supercooled *tert*-butyl alcohol; the dashed-dotted lines correspond to plus and minus one standard deviation).

1.4. Discussion

The variations of the excess partial specific volume and isobaric expansivity of water and *tert*-butyl alcohol with respect to the composition reflect the structural changes of individual components occurring in mixture in comparison to their pure liquid state. Both water and *tert*-butyl alcohol are associated liquids with their own structures which are expected to be rearranged and/or disrupted upon mixing as a result of a complex interplay of specific and non-specific intermolecular interactions between like and unlike molecules as well as of packing and steric effects. From these, infinite dilution excess partial thermodynamic quantities allow nevertheless to isolate unlike intermolecular interactions between solute and solvent molecules [79]. Undeniably, extrema in the curves relating the dependence of excess partial volumetric properties of individual mixture components on composition evidence the occurrence of transitions in mixing schemes. However, because thermodynamic data describe a system at the macroscopic scale, their interpretation at the molecular level remains extremely challenging. Fortunately, the structure and dynamics of the W + TBA system have been the subject of numerous studies over the past decades and, despite being obtained by methods focusing on a limited number of molecules, the results from these investigations provide direct information about the changes in intermolecular interactions leading to molecular reordering from which the variations of the excess partial volumetric properties of water and *tert*-butyl alcohol with mixture composition originate.

1.4.1. Components in their pure state

Before considering the binary mixtures, some comments may be given on the two components in their pure liquid state. On the one hand, water molecule is characterized by its very small size and its ability to form up to four intermolecular hydrogen bonds through the two hydrogen atoms and the two lone electron pairs on the oxygen atom allowing for different local structural arrangements [80, 81]. Despite decades of effort, the exact structure of bulk liquid water, even under ambient conditions, is still not fully understood and remains the subject of extensive research and debate [82, 83]. According to one of the presently accepted views, the structure of liquid water under ambient temperature and pressure conditions consists in a dynamic and inhomogeneous three-dimensional hydrogen-bonded network within which most of water molecules present a closer packing than tetrahedral with distorted hydrogen bonds, but with local clusters of tetrahedrally hydrogen-bonded molecules existing as fluctuations on some time scale whose occurrence and size increase with decreasing temperature [84-86]. On the other hand, *tert*-butyl alcohol molecule is of relatively large size in comparison to a water one and presents a strong amphiphilic character due to the presence of three hydrophobic methyl groups and a fourth hydrophilic hydroxyl group attached to a central carbon atom. This amphiphilic nature is evidenced by the fact that, when placed at a water-oil interface, a *tert*-butyl alcohol molecule

aligns itself equally between the two phases with the hydroxyl and alkyl moieties being respectively in the water and oil phases [87]. The three methyl groups being in symmetrical positions with respect to the carbon-oxygen axis, the TBA molecule exhibits a tetrahedral geometry with the hydroxyl group pointing in opposite direction from that of the alkyl moieties. The structure of this alcohol in its pure liquid state has received much less attention than that of water, nevertheless, the most recent studies performed at temperatures slightly higher than the component fusion temperature have revealed that the structure of the neat liquid is less dominated by intermolecular hydrogen-bonding interactions than generally postulated [88, 89]. Indeed, it was proven the presence of a significant level of other intermolecular interactions including polar to polar interactions between hydroxyl groups, polar to non-polar interactions between hydroxyl and methyl groups as well non-polar to non-polar interactions between alkyls moieties of alcohol molecules [88]. The formation of extensive intermolecular hydrogen bonds appears to be restricted and hindered by the bulky methyl groups so that each TBA molecule, despite being able to participate up to three intermolecular hydrogen bonds, forms no more than two with neighboring molecules [89]. This complex balance of intermolecular interactions results in the formation of dynamic molecular clusters involving from three to six molecules which can adopt either a cyclic or a chain hydrogen-bonding pattern [90-92]. At room temperature, the cyclic hydrogen-bonding pattern is the one preferentially adopted by TBA molecules but the occurrence of the chain hydrogen-bonding pattern increases with increasing temperature [92]. However, hydrogen-bonded chains of TBA molecules remain relatively short in comparison to linear alcohols due to the steric hindrance imposed by the configuration of the methyl groups [93].

1.4.2. Components in their mixed state

Turning back to the binary W + TBA system and considering the water-rich region of the composition range, all the results obtained from theoretical analyses [94-99], nuclear magnetic resonance spectroscopy [100-103], infrared [101, 104, 105] and near-infrared [106] spectroscopy, Raman spectroscopy [107, 108], mass spectroscopy [109] and light scattering [110-115] experiments as well as from molecular dynamics [103, 114, 116-122] and Monte Carlo [123] simulations converge to the fact that the composition at which extrema in the curve profiles of v_1^E and v_2^E occur corresponds to a boundary separating the water-rich region into two distinct parts involving different mixing schemes. In extremely dilute aqueous solutions, *tert*-butyl alcohol molecules are essentially hydrated as single individual molecules with water molecules adopting a configuration allowing to incorporate the solute hydroxyl group into its hydrogen-bonded network and to surround the alcohol alkyl moieties in a cage-like manner. Due to the steric conformation of the three methyl groups, the hydrophobic moiety of a TBA molecule exhibits a nearly spherical surface which curvature allows limiting the distortion of the hydrogen bond angles between water molecules in its vicinity and hence helping to maintain the integrity of the hydrogen-bonded cage-like structure [124, 125]. According to the conclusion drawn by

Nakanishi and coworkers [123] who investigated the nature of intermolecular interactions occurring in an aqueous solution close to infinite dilution conditions, two strong hydrogen bonds are formed between the hydroxyl group of a *tert*-butyl alcohol molecule and neighboring water molecules while there are no interaction of this kind between solute molecules. This is in agreement with the negative values of $v_2^{E,\infty}$ which indicate that intermolecular interactions between the solute and solvent molecules are stronger than that between solute molecules in the pure liquid state. Also, the negative value of $e_{p,2}^{E,\infty}$ reveals that, in the temperature range investigated, the difference in intermolecular interactions strength between, on the one hand, solute and solvent molecules in infinite dilute solutions, and on the other hand, solute molecules in the pure liquid state, increases with temperature. This complies with the findings that the strength of the hydrogen bonds between *tert*-butyl alcohol and water molecules is stronger than that between two alcohol molecules and/or that intermolecular interactions weaker than hydrogen-bonding account for a significant part of the overall intermolecular interactions taking place in pure liquid *tert*-butyl alcohol. Although in such dilute aqueous solutions not every alcohol polar moieties are involved in hydrogen-bonding formation, they can still interact with water molecules through strong dipole-dipole forces. Besides, it is expected that water molecules could interact with the methyl groups of the alcohol molecule through weak dipole-induced dipole forces and that those belonging to the hydration shell at the interface with the hydrophobic surface of the solute molecule would rearrange and adopt the tangential configuration characteristic of hydrophobic hydration allowing maintaining the integrity of three-dimensional hydrogen-bonded network around [124, 126, 127]. Whether or not, relative to that of the bulk water, the *tert*-butyl alcohol hydrophobic surface induces an enhancement of the hydrogen-bonded network of water molecules in contact with, is still a controversial issue and the results from different groups appear to be contradictory. Whatever, in the water-rich end of the composition range, the hydration shell structure around individual TBA molecules remains thermodynamically stable to suppress any direct contacts between hydrophobic moieties of different solute molecules [107] and the sign and variation of v_1^E and v_2^E with mixture composition arise from this interplay between hydrophilic and hydrophobic hydrations of alcohol molecules as well as from volume exclusion effects [124]. As the mass fraction of TBA in the mixture increases from infinite dilution to the herein above defined threshold composition, an increasing number of alcohol molecules are interstitially accommodated in the dynamic open structure of water. Solute molecules hydrated in such a way being much more efficiently packed than in their pure liquid state, this manifests by a sharp decrease and negative sign of v_2^E . At the same time, rearrangement of the three-dimensional water hydrogen-bonded network accompanying the accommodation of the bulky TBA molecules and exclusion of water molecules from the volume they formerly occupied lead to a slight expansion of the water structure as reflected by the small increase and positive sign of v_1^E . Because in this narrow composition range the mixing process is mainly governed by the structural features of water and occurrence of specific short-range interactions between unlike molecules, the

weak temperature dependence of v_1^E and v_2^E mostly results from the strength of the hydrogen bonds between solvent molecules and those between solute and solvent molecules. At the threshold composition, there are no longer enough water molecules to form any additional separate hydration shell around a solute molecule [128] so that upon further addition of alcohol, they are expelled from water and start to self-associate through the so-called hydrophobic effect [124, 127, 129]. By this process, the total surface area of the volume occupied by the solute molecules decreases relative to a non-associated state so that less water molecules are required to form a complete hydration shell around an equal number of *tert*-butyl alcohol molecules. Furthermore, the amphiphilic alcohol molecules are expected to adopt a micelle-like configuration which, by shielding the non-polar moieties formerly exposed to the bulk water, allows minimizing the contact surface area between the *tert*-butyl groups of solute molecules and surrounding water molecules [130]. Consequently, in more concentrated aqueous solutions, that is, binary mixtures with an alcohol content higher than the threshold composition, *tert*-butyl alcohol molecules are hydrated as small-sized molecular clusters existing as fluctuations on some time scale [112, 113, 131, 132] and the system, despite being macroscopically homogeneous, exhibits an incomplete mixing at the molecular level³. Such a self-association process being driven by the difference between the hydration Gibbs energy of a molecular aggregate and the overall hydration Gibbs energy of the individual solute molecules constituting it, clustering of solute molecules occurs spontaneously when their concentration in aqueous solution is large enough to make this difference negative and, under ambient conditions, the driving force for forming this kind of assembly strengthens as the temperature increases [124, 130]. Hence, the mixture composition corresponding to the transition between the two mixing schemes is shifted toward lower TBA content as the system temperature is increased. Consequently, as the extent of the water-rich region where TBA molecules are individually hydrated decreases, the absolute value of v_1^E and v_2^E at the threshold mixture composition also decreases. The variations of $e_{p,1}^E$ and $e_{p,2}^E$ with respect to mixture composition in the water-rich region, characterized by passing through an extremum value, result from and reflect this temperature influence on the self-association process. Additionally, it should be pointed out that, for any temperature in the range studied, the binary mixture composition for which self-association of TBA molecules is predicted to occur from Eqs. (1.7.a) or (1.7.b) by v_1^E and v_2^E taking respectively a maximum and a minimum value, is in perfect agreement with that determined from scattering and spectroscopy experiments. The extent of the second part of the water-rich region can be better appreciated by considering the first derivatives of these equations with respect to the mass fraction of TBA in the binary mixture, which composition dependences over the

³ As a remark, one can highlight that binary systems of water and other butanol isomers, for which curves relating the dependence of the partial specific volume of the respective alcohols on mixture composition also display a pronounced minimum in the water-rich region, undergo a macroscopic liquid-liquid phase separation that occurs in aqueous alcohol solutions slightly more concentrated than that corresponding to the said extremum [42-43].

entire range are depicted in Figure 1.17 for different isotherms, as calculated from the following expressions:

$$\frac{dv_1^E}{dw_2} = 2w_2 \sum_{i=0}^6 (B_i T + C_i)(1 - 2w_2)^{i-1} [(1 + 2i)(1 - 2w_2) - 2iw_2(i - 1)(1 - w_2)(1 - 2w_2)^{-1}] \quad (1.11.a)$$

$$\frac{dv_2^E}{dw_2} = 2(1 - w_2) \sum_{i=0}^6 (B_i T + C_i)(1 - 2w_2)^{i-1} [(1 + 2i)(2w_2 - 1) + 2iw_2(i - 1)(1 - w_2)(1 - 2w_2)^{-1}] \quad (1.11.b)$$

where all terms are as previously defined.

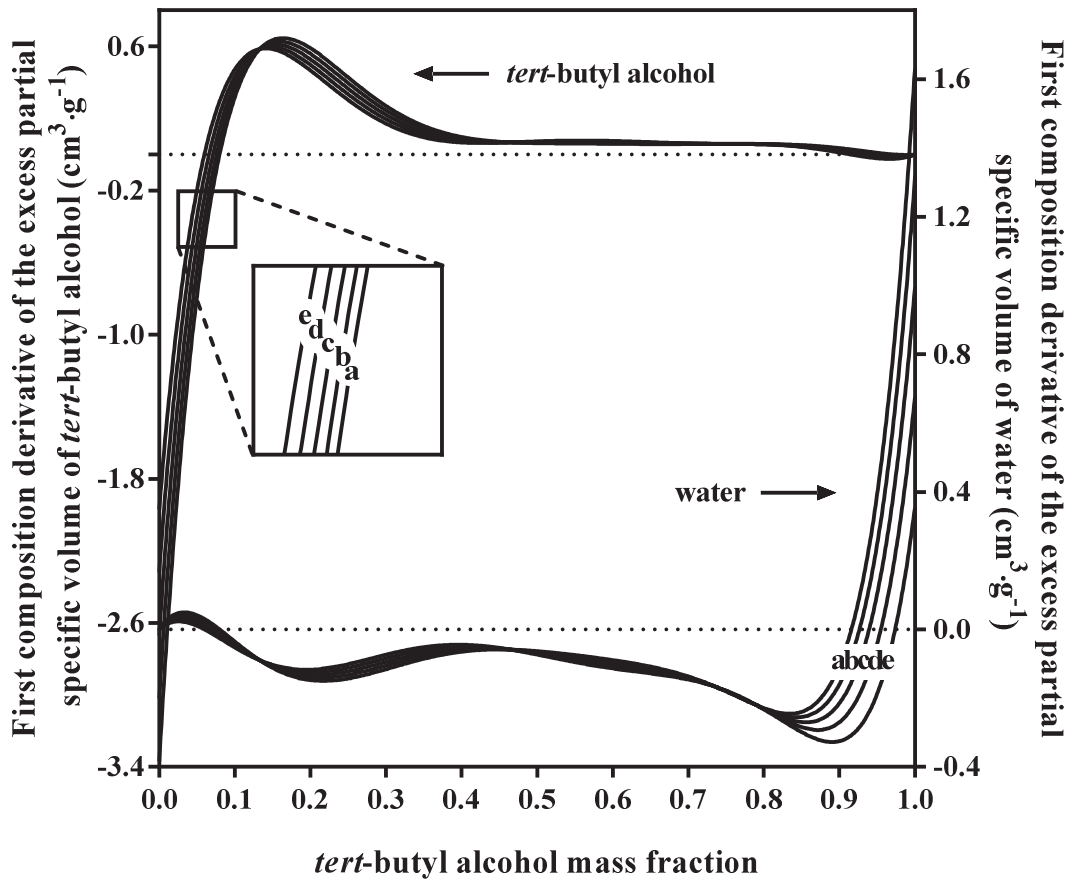


Figure 1.17. First composition derivative of the excess partial specific volume of water and *tert*-butyl alcohol in their mixtures as function of the *tert*-butyl alcohol mass fraction (a): $T = 293.15$ K; (b): $T = 298.15$ K; (c): $T = 303.15$ K; (d): $T = 308.15$ K; (e): $T = 313.15$ K (the solid lines are calculated from Eq. (1.11.a) and Eq. (1.11.b)).

From Figure 1.17, one can observe that the first composition derivative of v_2^E stops changing with increasing alcohol concentration in solution when the mass fraction of TBA reaches a value in between 0.40 to 0.45, depending on the temperature considered, indicative of a threshold composition marking changeover to a steady-state in which the magnitude of the excess partial specific volume of *tert*-butyl alcohol is inversely proportional to its content in the mixture. Regardless of being a coincidence or not, it should be mentioned that when the mixture composition is expressed in terms of volume fraction, *tert*-butyl alcohol becomes the major component in the system beyond a mixture composition whose alcohol content is almost exactly the same than that corresponding to the step change in the dependence of v_2^E on the alcohol mass fraction. Whatever, this threshold mixture composition is here defined as the upper limit of the second part of the water-rich region and the lower one as that for which the first composition derivative of v_2^E changes in sign. In this composition range, isotopic substitution neutron diffraction experiments and Monte Carlo-based simulations with empirical potential structure refinement procedure performed by Bowron, Finney and Soper [133-135] provided evidence of direct molecular contacts between clustered *tert*-butyl alcohol molecules involving only van der Waals intermolecular interactions, the formation of hydrogen bonds through the hydroxyl groups of alcohol molecules taking place solely with water molecules. The interface between *tert*-butyl alcohol molecular clusters and water molecules belonging to their respective hydration shells was proven to be similar to that of individually hydrated solute molecules with water molecules in the vicinity of the methyl and hydroxyl groups of alcohol molecules adopting tangential and hydrogen-bonding orientations, respectively. Hence, the molecular clusters of TBA are surrounded by a hydrogen-bonded network of water molecules into which the alcohol hydroxyl groups are incorporated. These results have been supported by molecular dynamics simulations from independent laboratories [113, 116, 132] as well as from infrared and nuclear magnetic resonance spectroscopic studies [101, 106] and discard the hypothesis of a water-separated association scheme such as the formation of clathrate-like alcohol hydrates originally postulated from some early X-ray diffraction [128, 136-138] and light scattering [110, 111] experiments. In aqueous alcohol solutions of compositions close to that corresponding to the lower limit of the composition range under consideration, is present a small number of solute clusters undergoing continual change on short times scales that are constituted by two to four TBA molecules interacting with each other predominantly through instantaneous dipole-induced dipole forces between methyl groups whereas the hydrogen-bonding requirements of the hydroxyl groups of every clustered alcohol molecules are exclusively and almost fully satisfied by available water molecules [99, 113, 116, 120, 132-135]. As the mass fraction of TBA increases up to the upper limit of the second part of the water-rich region, the molecular clusters not only increase in number but also growth in size with a number of TBA molecules per cluster being as high as six to eight [113, 134]. Even if non-polar to non-polar interactions between clustered TBA molecules remains predominant over this composition range, the increase of the alcohol content in the mixture is accompanied by the occurrence and increase in number of polar to

non-polar interactions. Although substitution of hydrogen bond interactions between hydroxyl groups of water and alcohol molecules by dipole-induced dipole interactions between hydroxyl group of one TBA molecule and methyl groups of a neighboring one is suboptimal, this is compelled by the rise in number of alcohol molecule within clusters, but partially compensated by the ability of the neighboring TBA molecule to retain its hydrogen bonds with surrounding water molecules [134]. Hence, the progressive disruption of hydrogen bonds between water and alcohol molecules and the shift toward a more complex balance of intermolecular interactions between TBA molecules closer to those observed in the pure liquid alcohol is reflected by a sharp decrease in the magnitude of v_2^E . Concomitantly, these are accompanied by a progressive overlap of the hydration shells of adjacent solute molecules and an increase in the number of distorted hydrogen bonds between water molecules belonging to the first hydration layers [116, 117, 120, 122] which manifests by the smooth decrease of v_1^E with respect to the increase of the TBA content in the mixture. The upper limit of the second part of the water-rich region corresponds to a threshold composition beyond which short-lived, short-ranged micelle-like structural fluctuations are no more detected in binary mixtures [113, 122] and marks the cross-over to an usual non-ideal mixing scheme where molecular clusters of *tert*-butyl alcohol and water coexist and are bridge together though hydrogen-bonding but exhibit a growing tendency to be apart from each other [113]. At this threshold composition, intermolecular interactions between *tert*-butyl alcohol and water molecules become less prevalent than those between *tert*-butyl alcohol molecules whose pattern differs from that found in the pure liquid almost only in the number of polar to polar interactions between the hydroxyl groups of alcohol molecules [133, 134]. Indeed, the strength of the hydrogen bonds between water and alcohol molecules being much larger than that between alcohol molecules, the hydrogen-bonding requirement of TBA molecules remains fully satisfied by available water molecules. However, even if they are of comparable strength, hydrogen-bonding between water molecules are always preferred over hydrogen-bonding between water and alcohol molecules. Thus, as the TBA content in the mixture increases further beyond this threshold composition and the number of water molecules available to fully satisfy the hydrogen-bond requirement of the alcohol hydroxyl groups decreases, the level of polar to polar interactions between alcohol molecules continuously increases so that the difference in pattern of intermolecular interactions between TBA molecules in solution and in pure liquid state decreases which translates into the monotonic increase of negative v_2^E values toward zero. Besides, at the same time the large spanning hydrogen-bonded clusters of water molecules break up into smaller ones solvated by the hydroxyl groups of alcohol molecules, in which the near tetrahedral hydrogen-bonded structure is preserved wherever possible [99, 120, 139, 140]. This progressive disruption of the three dimensional hydrogen-bonded network of water is reflected by the marked decrease of v_1^E with respect to the increase in the content of alcohol in mixture from the threshold composition considered up to the one at which extrema in the curve profiles of v_1^E and v_2^E occur. Over this composition range, a point would

be reached where, like it happens in concentrated aqueous solution of other monohydric alcohols [141], the number of water molecules in mixture would no longer be sufficient to reach full connectivity and a transition from a percolating to a non-percolating three dimensional hydrogen-bonded network of water would occur but manifestation of this phenomenon in the curves relating the composition dependence of either v_1^E or its first composition derivative is not obvious at all. Because the alcohol-rich region of composition range has received to date much less attention than the water-rich one, interpreting the temperature and composition dependences of partial specific volume of individual mixture components in extremely concentrated aqueous solution of *tert*-butyl alcohol remains especially challenging. One can argue that what is manifested through the minima in the curve profiles of v_2^E in the water-rich end should be reciprocated in the minima in the curve profiles of v_1^E and it does not appear incongruous to presume that they correspond to a strongly temperature-dependent threshold composition beyond which water molecules are no more solvated as hydrogen-bonded molecular clusters but rather as individual molecules. Hence, the sharp decrease in v_1^E values observed upon the first addition of water to neat *tert*-butyl alcohol is linked to the interstitial accommodation of individual water molecules within the alcohol structure and arises from the absence of any hydrogen-bonded structure between solute molecules in the extremely *tert*-butyl alcohol-rich region. However, the fact that a given change in temperature leads to an opposite effect on both occurring composition and magnitude of the minimum in the curve profile of v_1^E as compared to that of v_2^E clearly evidences that different mechanisms are involved. On this basis, the shift of the extrema in the alcohol-rich region toward mixture compositions of higher content upon increase in temperature would indicate that as the system temperature increases, the extent of the composition range where water molecules are individually solvated decreases. Since the negative values of $v_1^{E,\infty}$ cannot be attributed to a larger strength of the hydrogen bonds between water and *tert*-butyl alcohol molecules than between two water molecules, it can reasonably be stated the structural features of the alcohol, and especially the variation of its hydrogen-bonding pattern with respect to temperature, might be the prime determinant of the observed variations in excess partial specific volume values of individual mixture components with respect to composition and temperature in extremely concentrated aqueous solutions of *tert*-butyl alcohol.

1.5. Conclusion

In the present investigation, experimental excess specific volumes of water + *tert*-butyl alcohol solvent mixtures were obtained from density measurements carried out over the whole composition range and temperature range from 293.15 to 313.15 K. For every temperature investigated, the composition dependence of the excess specific volume of the binary system was adequately described by a sixth-order Redlich-Kister-like polynomial equation. By considering the temperature dependence of the regression coefficient estimates, a single equation allowing for the simultaneous modeling of both the

composition and temperature dependence of the excess specific volume of the water + *tert*-butyl alcohol system was obtained. The correlative and predictive performances of the proposed model were further evaluated against experimental data from this work and those taken from literature, respectively. Both were deemed to be particularly satisfactory with mean and median absolute relative deviations of less than 0.5 and 0.9% for the outlier-free training set and less than 1.7 and 7.0% for the outlier-free testing set, which were respectively constituted by 184 and 368 experimental data. From the developed equation, excess partial specific volume and excess partial specific isobaric expansivity of water and *tert*-butyl alcohol in their binary mixtures were derived and their variations with mixture composition over the temperature range investigated were used to evidence transitions in mixing schemes. Accordingly, the composition range can be divided into distinct regions differing from one another by the nature and magnitude of intermolecular interactions between like and unlike molecules as well as the molecular arrangements in solution. These were discussed in the light of the results from structural and dynamical studies performed to date on the water + *tert*-butyl alcohol system with which the threshold composition values delimiting the boundaries between different mixing schemes as predicted by equations derived from the proposed model were found to be in perfect agreement. As far the application of this model to freeze-drying of poorly water-soluble formulations from water + *tert*-butyl alcohol mixtures is concerned, it would provide a solid basis to predict the excess volumetric properties of such multicomponent liquid mixtures, provided that, in addition to those reported herein for the cosolvent system, excess volumetric properties of every other possible contributing binary subsystem would be known and described using the Redlich-Kister formalism. Furthermore, it could also be used to forecast the specific volume or density of the binary solvent mixture of any composition over the temperature range of applicability by simply adding into the ideal contribution at the desired system composition and temperature. Similarly, the composition and temperature dependences of the partial specific quantities of individual mixture components could be easily obtained from relevant derived equations by introducing into the pure component counterpart at the relevant temperature. This allows, for example, performing rigorous conversion of mixture composition from either mass or mole fractions to volume fractions which are preferred by pharmaceutical scientists to expressed solvent blend composition. Finally, the proposed equation set would also constitute for physico-chemical scientists involved in the structural and dynamical characterization of the system a useful tool for designing experiments.

This page is intentionally left blank.

Nomenclature

Latin letters

A	parameter of Equation (1.2) ($\text{cm}^3 \cdot \text{g}^{-1} \cdot \text{K}^{-1}$)
A_i	parameters of Equation (1.3) ($\text{cm}^3 \cdot \text{g}^{-1}$)
B	parameter of Equation (1.2) ($\text{cm}^3 \cdot \text{g}^{-1}$)
B_i	parameters of Equation (1.4) and derived expressions (K^{-1})
C_i	parameters of Equation (1.4) and derived expressions ($\text{cm}^3 \cdot \text{g}^{-1}$)
e	residual from least-squares regression (varies)
e_p	specific isobaric expansivity of the mixture ($\text{cm}^3 \cdot \text{g}^{-1} \cdot \text{K}^{-1}$)
$e_{p,i}$	partial specific isobaric expansivity of the i -th mixture component ($\text{cm}^3 \cdot \text{g}^{-1} \cdot \text{K}^{-1}$)
F	Fisher statistic
k	polynomial order of Equation (1.3) and derived expressions
m_i	mass of the i -th mixture component (g)
n	number of data points
P	pressure (MPa)
p	statistical probability
r_{adj}^2	adjusted squared correlation coefficient
s	standard deviation (varies)
s_r	relative standard deviation
T	temperature (K)
t	Student statistic
u	standard uncertainty (varies)
U_c	combined expanded uncertainty (varies)
u_r	relative standard uncertainty
V	volume of the mixture (cm^3)
v	specific volume of the mixture ($\text{cm}^3 \cdot \text{g}^{-1}$)
v_i	partial specific volume of the i -th mixture component ($\text{cm}^3 \cdot \text{g}^{-1}$)
w_A	Akaike weight
w_i	mass fraction of the i -th mixture component
X	phase composition
z	normal statistic

Greek letters

Δ	change in quantity
ρ	density of the mixture ($\text{g} \cdot \text{cm}^{-3}$)

Superscripts

*	pure component
∞	infinite dilution
E	excess quantity
id	ideal quantity

Subscripts

1	component 1
2	component 2
calc	back-calculated from a model equation
mix	mixing process

Abbreviations

AIC _c	second-order Akaike's information criterion
ARD	absolute relative deviation
df	statistical degree of freedom
RD	relative difference
SS	sum-of-squares
TBA	<i>tert</i> -butyl alcohol
vs.	versus
W	water

References

- [1] P. Kolář, J.-W. Shen, A. Tsuboi, T. Ishikawa, Solvent selection for pharmaceuticals, *Fluid Phase Equilibria*, 194–197 (2002) 771-782.
- [2] D.L. Teagarden, D.S. Baker, Practical aspects of lyophilization using non-aqueous co-solvent systems, *European Journal of Pharmaceutical Sciences*, 15 (2002) 115-133.
- [3] D.L. Teagarden, W. Wang, D.S. Baker, Practical aspects of freeze-drying of pharmaceutical and biological products using nonaqueous cosolvent systems, in: *Freeze Drying/Lyophilization of Pharmaceutical and Biological Products*, third ed., Informa Healthcare, 2010, pp. 254-287.
- [4] S. Vessot, J. Andrieu, A review on freeze drying of drugs with tert-butanol (TBA) + water systems: Characteristics, advantages, drawbacks, *Drying Technology*, 30 (2012) 377-385.
- [5] ICH harmonized tripartite guideline Q3C (R5), Impurities: guideline for residual solvents, in: *International Conference on the Harmonization of Technical Requirements for the Registration of Pharmaceuticals for Human Use*, 2011.
- [6] D. Prat, O. Pardigon, H.-W. Flemming, S. Letestu, V. Ducandas, P. Isnard, E. Guntrum, T. Senac, S. Ruisseau, P. Cruciani, P. Hosek, Sanofi's solvent selection guide: A step toward more sustainable processes, *Organic Process Research & Development*, 17 (2013) 1517-1525.
- [7] D.L. Teagarden, W.J. Petre, P.M. Gold, Stabilized prostaglandin E1, US Patent No. 5,741,523, (1998).
- [8] R. Daoussi, E. Bogdani, S. Vessot, J. Andrieu, O. Monnier, Freeze-drying of an active principle ingredient using organic co-solvent formulations: Influence of freezing conditions and formulation on solvent crystals morphology, thermodynamics data, and sublimation kinetics, *Drying Technology*, 29 (2011) 1858-1867.
- [9] E. Bogdani, S. Vessot, J. Andrieu, Experimental and modeling study during freeze drying of aqueous tert-butanol-based formulations in vials, *Drying Technology*, 31 (2013) 1772-1779.
- [10] E. Bogdani, S. Vessot, G. Do, J. Andrieu, G. Degobert, Optimization of freeze-drying cycle for tert-butanol-based formulations of ibuprofen, *Drying Technology*, 31 (2013) 308-313.
- [11] K. Kasraian, P.P. DeLuca, Thermal analysis of the tertiary butyl alcohol-water system and its implications on freeze-drying, *Pharmaceutical Research*, 12 (1995) 484-490.
- [12] K. Kasraian, P.P. DeLuca, The effect of tertiary butyl alcohol on the resistance of the dry product layer during primary drying, *Pharmaceutical Research*, 12 (1995) 491-495.
- [13] R. Daoussi, S. Vessot, J. Andrieu, O. Monnier, Sublimation kinetics and sublimation end-point times during freeze-drying of pharmaceutical active principle with organic co-solvent formulations, *Chemical Engineering Research and Design*, 87 (2009) 899-907.
- [14] S.T. Jay, Solubilization using cosolvent approach, in: *Water-insoluble Drug Formulation*, second ed., CRC Press, 2008, pp. 161-194.
- [15] H. de Waard, W.L.J. Hinrichs, M.R. Visser, C. Bologna, H.W. Frijlink, Unexpected differences in dissolution behavior of tablets prepared from solid dispersions with a surfactant physically mixed or incorporated, *International Journal of Pharmaceutics*, 349 (2008) 66-73.
- [16] H. de Waard, W.L.J. Hinrichs, H.W. Frijlink, A novel bottom-up process to produce drug nanocrystals: Controlled crystallization during freeze-drying, *Journal of Controlled Release*, 128 (2008) 179-183.
- [17] D.J. van Drooge, W.L.J. Hinrichs, H.W. Frijlink, Incorporation of lipophilic drugs in sugar glasses by lyophilization using a mixture of water and tertiary butyl alcohol as solvent, *Journal of Pharmaceutical Sciences*, 93 (2004) 713-725.
- [18] D.J. van Drooge, W.L.J. Hinrichs, K.A.M. Wegman, M.R. Visser, A.C. Eissens, H.W. Frijlink, Solid dispersions based on inulin for the stabilisation and formulation of Δ^9 -tetrahydrocannabinol, *European Journal of Pharmaceutical Sciences*, 21 (2004) 511-518.
- [19] J.J. Moes, S.L.W. Koolen, A.D.R. Huitema, J.H.M. Schellens, J.H. Beijnen, B. Nuijen, Pharmaceutical development and preliminary clinical testing of an oral solid dispersion formulation of docetaxel (ModraDoc001), *International Journal of Pharmaceutics*, 420 (2011) 244-250.
- [20] J. Moes, S. Koolen, A. Huitema, J. Schellens, J. Beijnen, B. Nuijen, Development of an oral solid dispersion formulation for use in low-dose metronomic chemotherapy of paclitaxel, *European Journal of Pharmaceutics and Biopharmaceutics*, 83 (2013) 87-94.
- [21] W.E. Acree Jr., Empirical expressions for estimating multicomponent properties from binary data, in: *Thermodynamic Properties of Nonelectrolyte Solutions*, Academic Press, 1984, pp. 62-73.
- [22] S.I. Sandler, The thermodynamics of multi-component mixtures, in: *Chemical and Engineering Thermodynamics*, third ed., John Wiley & Sons Ltd, 1999, pp. 324-387.
- [23] R.L. Gardas, J.A.P. Coutinho, Extension of the Ye and Shreeve group contribution method for density estimation of ionic liquids in a wide range of temperatures and pressures, *Fluid Phase Equilibria*, 263 (2008) 26-32.

- [24] K. Padaszyński, U. Domańska, A new group contribution method for prediction of density of pure ionic liquids over a wide range of temperature and pressure, *Industrial & Engineering Chemistry Research*, 51 (2012) 591-604.
- [25] G. Scatchard, S.E. Wood, J.M. Mochel, Vapor-liquid equilibrium. V. Carbon tetrachloride-benzene mixtures, *Journal of the American Chemical Society*, 62 (1940) 712-716.
- [26] K. Wohl, Thermodynamic evaluation of binary and ternary liquid systems, *Transactions of the American Institute of Chemical Engineers* 42 (1946) 215-249.
- [27] O. Redlich, A.T. Kister, Algebraic representation of thermodynamic properties and the classification of solutions, *Industrial & Engineering Chemistry*, 40 (1948) 345-348.
- [28] C. Tsao, J. Smith, Applied thermodynamics, *Chemical Engineering Progress Symposium Series*, 49 (1953) 107-117.
- [29] A.R. Mathieson, J.C.J. Thynne, Thermodynamics of hydrocarbon mixtures. Part II. The heats of mixing of the binary mixtures formed by benzene, cyclohexane, n-heptane, toluene, and n-hexane, *Journal of the Chemical Society*, (1956) 3708-3713.
- [30] A.R. Mathieson, J.C.J. Thynne, Thermodynamics of hydrocarbon mixtures. Part III. The heats of mixing of ternary, quaternary, and quinary mixtures formed by benzene, cyclohexane, heptane, toluene, and hexane, *Journal of the Chemical Society*, (1956) 3713-3716.
- [31] F. Kohler, Zur berechnung der thermodynamischen daten eines ternären systems aus den zugehörigen binären systemen, *Monatshefte für Chemie und verwandte Teile anderer Wissenschaften*, 91 (1960) 738-740.
- [32] G.W. Toop, Predicting ternary activities using binary data, *Transactions of the Metallurgical Society of AIME*, 233 (1965) 850-855.
- [33] C. Colinet, Estimation des grandeurs thermodynamiques des alliages ternaires, M.Sc. thesis, University of Grenoble, France, 1967.
- [34] K.T. Jacob, K. Fitzner, The estimation of the thermodynamic properties of ternary alloys from binary data using the shortest distance composition path, *Thermochimica Acta*, 18 (1977) 197-206.
- [35] R.P. Rastogi, J. Nath, S.S. Das, Thermodynamic properties of ternary mixtures. 2. The excess volumes of mixing of ternary mixtures of cyclohexane, aromatics, and halomethanes, *Journal of Chemical & Engineering Data*, 22 (1977) 249-252.
- [36] I. Cibulka, Estimation of excess volume and density of ternary liquid mixtures of non-electrolytes from binary data, *Collection of Czechoslovak Chemical Communications*, 47 (1982) 1414-1419.
- [37] G.L. Bertrand, W.E. Acree, T.E. Burchfield, Thermochemical excess properties of multicomponent systems: Representation and estimation from binary mixing data, *Journal of Solution Chemistry*, 12 (1983) 327-346.
- [38] P.P. Singh, R.K. Nigam, S.P. Sharma, S. Aggarwal, Molar excess volumes of ternary mixtures of nonelectrolytes, *Fluid Phase Equilibria*, 18 (1984) 333-344.
- [39] I. Nagata, K. Tamura, Excess molar enthalpies of {methanol or ethanol + (2-butanone + benzene)} at 298.15 K, *The Journal of Chemical Thermodynamics*, 22 (1990) 279-283.
- [40] I. Cibulka, L. Hnědkovský, J.-C. Fontaine, K. Sosnkowska-Kehiaian, H.V. Kehiaian, Introduction, in: *Volumetric Properties of Mixtures and Solutions*, subvol. A, Springer Science & Business Media, 2009, pp. 1-24.
- [41] J. Kenttämäa, M. Martti, E. Tommila, Some thermodynamic properties of the system t-butanol+ water, *Annales Academiae Scientiarum Fennicae A*, 93 (1959) 1-20.
- [42] K. Nakanishi, Partial molal volumes of butyl alcohols and of related compounds in aqueous solution, *Bulletin of the Chemical Society of Japan*, 33 (1960) 793-797.
- [43] K. Nakanishi, N. Kato, M. Maruyama, Excess and partial volumes of some alcohol-water and glycol-water solutions, *The Journal of Physical Chemistry*, 71 (1967) 814-818.
- [44] T.L. Broadwater, R.L. Kay, Solvent structure in aqueous mixtures. II. Ionic mobilities in tert-butyl alcohol-water mixtures at 25°, *The Journal of Physical Chemistry*, 74 (1970) 3802-3812.
- [45] L. Avédikian, G. Perron, J.E. Desnoyers, Apparent molal volumes and heat capacities of some alkali halides and tetraalkylammonium bromides in aqueous tert-butanol solutions, *Journal of Solution Chemistry*, 4 (1975) 331-346.
- [46] C. de Visser, G. Perron, J.E. Desnoyers, The heat capacities, volumes, and expansibilities of tert-butyl alcohol – water mixtures from 6 to 65 °C, *Canadian Journal of Chemistry*, 55 (1977) 856-862.
- [47] A. Hvidt, R. Moss, G. Nielsen, Volume properties of aqueous solutions of tert-butyl alcohol at temperatures between 5 and 25 °C, *Acta Chemica Scandinavica B*, 32 (1978) 274-280.
- [48] J.F. Alary, M.A. Simard, J. Dumont, C. Jolicoeur, Simultaneous flow measurement of specific heats and thermal expansion coefficients of liquids: Aqueous t-BuOH mixtures and neat alkanols and alkanediols at 25°C, *Journal of Solution Chemistry*, 11 (1982) 755-776.

- [49] H. Kubota, Y. Tanaka, T. Makita, Volumetric behavior of pure alcohols and their water mixtures under high pressure, *International Journal of Thermophysics*, 8 (1987) 47-70.
- [50] M. Sakurai, Partial molar volumes in aqueous mixtures of nonelectrolytes. I. t-butyl alcohol, *Bulletin of the Chemical Society of Japan*, 60 (1987) 1-7.
- [51] E.S. Kim, K.N. Marsh, Excess volumes for 2-methyl-2-propanol + water at 5 K intervals from 303.15 to 323.15 K, *Journal of Chemical & Engineering Data*, 33 (1988) 288-292.
- [52] P.K. Kipkemboi, A.J. Easteal, Densities and viscosities of binary aqueous mixtures of nonelectrolytes: tert-butyl alcohol and tert-butylamine, *Canadian Journal of Chemistry*, 72 (1994) 1937-1945.
- [53] F. Rived, M. Roses, E. Bosch, Densities, refractive indices, absolute viscosities, and static dielectric constants of 2-methylpropan-2-ol + hexane, + benzene, + propan-2-ol, + methanol, + ethanol, and + water at 303.2 K, *Journal of Chemical & Engineering Data*, 40 (1995) 1111-1114.
- [54] G.I. Egorov, D.M. Makarov, Densities and volume properties of (water + tert-butanol) over the temperature range of (274.15 to 348.15) K at pressure of 0.1 MPa, *The Journal of Chemical Thermodynamics*, 43 (2011) 430-441.
- [55] K. Tamura, A. Osaki, Y. Koga, Compressibilities of aqueous tert-butanol in the water-rich region at 25°C: Partial molar fluctuations and mixing schemes, *Physical Chemistry Chemical Physics*, 1 (1999) 121-126.
- [56] G.I. Egorov, D.M. Makarov, A.M. Kolker, Liquid phase PVTx properties of (water + tert-butanol) binary mixtures at temperatures from 278.15 to 323.15 K and pressures from 0.1 to 100 MPa. II. Molar isothermal compressions, molar isobaric expansions, molar thermal pressure coefficients, and internal pressure, *The Journal of Chemical Thermodynamics*, 61 (2013) 169-179.
- [57] G.I. Egorov, D.M. Makarov, A.M. Kolker, Liquid phase PVTx properties of (water + tert-butanol) binary mixtures at temperatures from 278.15 to 323.15 K and pressures from 0.1 to 100 MPa: I. Experimental results, excess and partial molar volumes, *The Journal of Chemical Thermodynamics*, 61 (2013) 161-168.
- [58] M. Sakurai, K. Nakamura, K. Nitta, Volumetric properties of dilute aqueous solutions at different temperatures, *Bulletin of the Chemical Society of Japan*, 67 (1994) 1580-1587.
- [59] P.R. Bevington, D.K. Robinson, *Data Reduction and Error Analysis for the Physical Sciences*, third ed., McGraw-Hill, 2003.
- [60] F. Franks, H.T. Smith, Volumetric properties of alcohols in dilute aqueous solutions, *Transactions of the Faraday Society*, 64 (1968) 2962-2972.
- [61] I. Brown, F. Smith, Volume changes on mixing. I. alcohol + benzene solutions, *Australian Journal of Chemistry*, 15 (1962) 1-8.
- [62] H.T. French, Thermodynamic and dielectric studies of alcohols in non-polar solvents and their interpretation in terms of hydrogen bonded association, Ph.D. thesis, University of New England, Australia, 1980.
- [63] J. Timmermans, *Physico-Chemical Constants of Pure Organic Compounds*, vol. 1, Elsevier Publishing Company, 1950.
- [64] M. Tanaka, G. Girard, R. Davis, A. Peuto, N. Bignell, Recommended table for the density of water between 0 °C and 40 °C based on recent experimental reports, *Metrologia*, 38 (2001) 301.
- [65] E.W. Lemmon, M.O. McLinden, D.G. Friend, Thermophysical properties of fluid systems, in: *NIST Chemistry WebBook*, NIST Standard Reference Database Number 69, National Institute of Standards and Technology, 2003.
- [66] J. Timmermans, Y. Delcourt, *Travaux du bureau international d'étalons physico-chimiques*. 6. Etude des constantes physiques de vingt composés organiques, *Journal de Chimie Physique*, 31 (1934) 85-124.
- [67] J.M. Costello, S.T. Bowden, The temperature variation of orthobaric density difference in liquid-vapour systems. III. Alcohols, *Recueil des Travaux Chimiques des Pays-Bas*, 77 (1958) 36-46.
- [68] W.E. Acree Jr., Ideal and nonideal solutions, in: *Thermodynamic Properties of Nonelectrolyte Solutions*, Academic Press, 1984, pp. 30-61.
- [69] S.I. Sandler, The estimation of the Gibbs free energy and fugacity of a component in a mixture, in: *Chemical and Engineering Thermodynamics*, third ed., John Wiley & Sons Ltd, 1999, pp. 388-477.
- [70] D.R. Simonsen, E.R. Washburn, The ternary system: t-butyl alcohol, benzene and water at 25°, *Journal of the American Chemical Society*, 68 (1946) 235-237.
- [71] R.C. Wilhoit, B.J. Zwolinski, Physical and thermodynamic properties of aliphatic alcohols, *Journal of Physical and Chemical Reference Data*, 2, suppl. 1 (1973) 113-123.
- [72] J.B. Ott, J.R. Goates, B.A. Waite, (Solid + liquid) phase equilibria and solid-hydrate formation in water + methyl, + ethyl, + isopropyl, and + tertiary butyl alcohols, *The Journal of Chemical Thermodynamics*, 11 (1979) 739-746.
- [73] K.P. Burnham, D.R. Anderson, *Model Selection and Multimodel Inference: A Practical Information-Theoretic Approach*, second ed., Springer-Verlag New York, Inc., 2002.

- [74] C. Leys, C. Ley, O. Klein, P. Bernard, L. Licata, Detecting outliers: Do not use standard deviation around the mean, use absolute deviation around the median, *Journal of Experimental Social Psychology*, 49 (2013) 764-766.
- [75] J.W. Gibbs, On the Equilibrium of Heterogeneous Substances, *Transactions of the Connecticut Academy of Arts and Sciences*, 3 (1876) 108-248.
- [76] P. Duhem, *Le Potentiel Thermodynamique et Ses Applications à la Mécanique Chimique et à l'Etude des Phénomènes Electriques*, A. Hermann, 1886.
- [77] P. Hynčica, L. Hnědkovský, I. Cibulka, Partial molar volumes of organic solutes in water. XIII. Butanols (aq) at temperatures $T = 298$ K to 573 K and at pressures up to 30 MPa, *The Journal of Chemical Thermodynamics*, 38 (2006) 418-426.
- [78] Â.F.S. Santos, I.M.S. Lampreia, How reliable are extrapolations to infinite dilution of partial molar properties using Redlich–Kister fittings?, *Thermochimica Acta*, 512 (2011) 268-272.
- [79] P. Alessi, M. Fermeglia, I. Kikic, Significance of dilute regions, *Fluid Phase Equilibria*, 70 (1991) 239-250.
- [80] K.A. Sharp, *Water: Structure and properties*, in: eLS, John Wiley & Sons, Ltd, 2001.
- [81] B. Bagchi, *Water in Biological and Chemical Processes*, first ed., Cambridge University Press, 2013.
- [82] C. Huang, K.T. Wikfeldt, T. Tokushima, D. Nordlund, Y. Harada, U. Bergmann, M. Niebuhr, T.M. Weiss, Y. Horikawa, M. Leetmaa, M.P. Ljungberg, O. Takahashi, A. Lenz, L. Ojamäe, A.P. Lyubartsev, S. Shin, L.G.M. Pettersson, A. Nilsson, The inhomogeneous structure of water at ambient conditions, *Proceedings of the National Academy of Sciences*, 106 (2009) 15214-15218.
- [83] G.N.I. Clark, G.L. Hura, J. Teixeira, A.K. Soper, T. Head-Gordon, Small-angle scattering and the structure of ambient liquid water, *Proceedings of the National Academy of Sciences*, 107 (2010) 14003-14007.
- [84] G.G. Malenkov, Structure and dynamics of liquid water, *Journal of Structural Chemistry*, 47 (2006) S1-S31.
- [85] A. Nilsson, L.G.M. Pettersson, Perspective on the structure of liquid water, *Chemical Physics*, 389 (2011) 1-34.
- [86] A. Nilsson, L.G.M. Pettersson, The structural origin of anomalous properties of liquid water, *Nature Communications*, 6 (2015) 8998.
- [87] A. Fiore, V. Venkateshwaran, S. Garde, Trimethylamine N-oxide (TMAO) and tert-butyl alcohol (TBA) at hydrophobic interfaces: Insights from molecular dynamics simulations, *Langmuir*, 29 (2013) 8017-8024.
- [88] B.D.T. Bowron, J.L. Finney, A.K. Soper, The structure of pure tertiary butanol, *Molecular Physics*, 93 (1998) 531-543.
- [89] P.G. Kusalik, A.P. Lyubartsev, D.L. Bergman, A. Laaksonen, Computer simulation study of tert-butyl alcohol. 1. Structure in the pure liquid, *The Journal of Physical Chemistry B*, 104 (2000) 9526-9532.
- [90] D.W. Aksnes, L.L. Kimtys, High-field magnetic resonance studies of tert-butanol in liquid and solid phases, *Magnetic Resonance in Chemistry*, 29 (1991) 698-705.
- [91] A.K. Karmakar, S. Sarkar, R.N. Joarder, Molecular clusters in liquid tert-butyl alcohol at room temperature, *The Journal of Physical Chemistry*, 99 (1995) 16501-16503.
- [92] C.R. Yonker, S.L. Wallen, B.J. Palmer, B.C. Garrett, Effects of pressure and temperature on the dynamics of liquid tert-butyl alcohol, *The Journal of Physical Chemistry A*, 101 (1997) 9564-9570.
- [93] M.C.R. Symons, H.L. Robinson, A near infrared and NMR spectroscopic study of the solvation of basic aprotic solvents and anions in tert-butanol, *Physical Chemistry Chemical Physics*, 3 (2001) 535-541.
- [94] B. Lee, Partial molar volume from the hard-sphere mixture model, *The Journal of Physical Chemistry*, 87 (1983) 112-118.
- [95] P. Ruelle, U.W. Kesselring, The hydrophobic propensity of water toward amphiprotic solutes: Prediction and molecular origin of the aqueous solubility of aliphatic alcohols, *Journal of Pharmaceutical Sciences*, 86 (1997) 179-186.
- [96] P. Ruelle, U.W. Kesselring, The hydrophobic effect. 1. A consequence of the mobile order in H-bonded liquids, *Journal of Pharmaceutical Sciences*, 87 (1998) 987-997.
- [97] I. Shulgin, E. Ruckenstein, Kirkwood–Buff integrals in aqueous alcohol systems: Comparison between thermodynamic calculations and X-ray scattering experiments, *The Journal of Physical Chemistry B*, 103 (1999) 2496-2503.
- [98] I. Shulgin, E. Ruckenstein, Kirkwood–Buff Integrals in aqueous alcohol systems: Aggregation, correlation volume, and local composition, *The Journal of Physical Chemistry B*, 103 (1999) 872-877.
- [99] K. Yoshida, T. Yamaguchi, A. Kovalenko, F. Hirata, Structure of tert-Butyl Alcohol–Water Mixtures Studied by the RISM Theory, *The Journal of Physical Chemistry B*, 106 (2002) 5042-5049.

- [100] M. Mayele, M. Holz, A. Sacco, NMR studies on hydrophobic interactions in solution Part 4. Temperature and concentration dependence of the hydrophobic self-association of tert-butanol in water, *Physical Chemistry Chemical Physics*, 1 (1999) 4615-4618.
- [101] K. Mizuno, Y. Kimura, H. Morichika, Y. Nishimura, S. Shimada, S. Maeda, S. Imafuji, T. Ochi, Hydrophobic hydration of tert-butyl alcohol probed by NMR and IR, *Journal of Molecular Liquids*, 85 (2000) 139-152.
- [102] W.S. Price, H. Ide, Y. Arata, Solution dynamics in aqueous monohydric alcohol systems, *The Journal of Physical Chemistry A*, 107 (2003) 4784-4789.
- [103] R. Sinibaldi, C. Casieri, S. Melchionna, G. Onori, A.L. Segre, S. Viel, L. Mannina, F. De Luca, The role of water coordination in binary mixtures. A study of two model amphiphilic molecules in aqueous solutions by molecular dynamics and NMR, *The Journal of Physical Chemistry B*, 110 (2006) 8885-8892.
- [104] M. Freda, G. Onori, A. Santucci, Infrared study of the hydrophobic hydration and hydrophobic interactions in aqueous solutions of tert-butyl alcohol and trimethylamine-N-oxide, *The Journal of Physical Chemistry B*, 105 (2001) 12714-12718.
- [105] M. Freda, G. Onori, A. Santucci, Hydrophobic hydration and hydrophobic interaction in aqueous solutions of tert-butyl alcohol and trimethylamine-N-oxide: a correlation with the effect of these two solutes on the micellization process, *Physical Chemistry Chemical Physics*, 4 (2002) 4979-4984.
- [106] A. Di Michele, M. Freda, G. Onori, A. Santucci, Hydrogen bonding of water in aqueous solutions of trimethylamine-N-oxide and tert-butyl alcohol: A near-infrared spectroscopy study, *The Journal of Physical Chemistry A*, 108 (2004) 6145-6150.
- [107] D.S. Wilcox, B.M. Rankin, D. Ben-Amotz, Distinguishing aggregation from random mixing in aqueous t-butyl alcohol solutions, *Faraday Discussions*, 167 (2013) 177-190.
- [108] A. Di Michele, M. Freda, G. Onori, M. Paolantoni, A. Santucci, P. Sassi, Modulation of hydrophobic effect by cosolutes, *The Journal of Physical Chemistry B*, 110 (2006) 21077-21085.
- [109] T. Fukasawa, Y. Tominaga, A. Wakisaka, Molecular association in binary mixtures of tert-butyl alcohol-water and tetrahydrofuran-heavy water studied by mass spectrometry of clusters from liquid droplets, *The Journal of Physical Chemistry A*, 108 (2004) 59-63.
- [110] K. Iwasaki, T. Fujiyama, Light-scattering study of clathrate hydrate formation in binary mixtures of tert-butyl alcohol and water, *The Journal of Physical Chemistry*, 81 (1977) 1908-1912.
- [111] K. Iwasaki, T. Fujiyama, Light-scattering study of clathrate hydrate formation in binary mixtures of tert-butyl alcohol and water. 2. Temperature effect, *The Journal of Physical Chemistry*, 83 (1979) 463-468.
- [112] D. Subramanian, D.A. Ivanov, I.K. Yudin, M.A. Anisimov, J.V. Sengers, Mesoscale inhomogeneities in aqueous solutions of 3-methylpyridine and tertiary butyl alcohol, *Journal of Chemical & Engineering Data*, 56 (2011) 1238-1248.
- [113] D. Subramanian, C.T. Boughter, J.B. Klauda, B. Hammouda, M.A. Anisimov, Mesoscale inhomogeneities in aqueous solutions of small amphiphilic molecules, *Faraday Discussions*, 167 (2013) 217-238.
- [114] L. Comez, M. Paolantoni, L. Lupi, P. Sassi, S. Corezzi, A. Morresi, D. Fioretto, Hydrophobic hydration in water-tert-butyl alcohol solutions by extended depolarized light scattering, *The Journal of Physical Chemistry B*, 119 (2015) 9236-9243.
- [115] M.F. Vuks, L.V. Shurupova, The scattering of light and phase transition in solutions of tertiary butyl alcohol in water, *Optics Communications*, 5 (1972) 277-278.
- [116] P.G. Kusalik, A.P. Lyubartsev, D.L. Bergman, A. Laaksonen, Computer simulation study of tert-butyl alcohol. 2. Structure in aqueous solution, *The Journal of Physical Chemistry B*, 104 (2000) 9533-9539.
- [117] A. Fornili, M. Civera, M. Sironi, S.L. Fornili, Molecular dynamics simulation of aqueous solutions of trimethylamine-N-oxide and tert-butyl alcohol, *Physical Chemistry Chemical Physics*, 5 (2003) 4905-4910.
- [118] S. Paul, G.N. Patey, Why tert-butyl alcohol associates in aqueous solution but trimethylamine-N-oxide does not, *The Journal of Physical Chemistry B*, 110 (2006) 10514-10518.
- [119] R. Gupta, G.N. Patey, Aggregation in dilute aqueous tert-butyl alcohol solutions: Insights from large-scale simulations, *The Journal of Chemical Physics*, 137 (2012) 034509.
- [120] S. Banerjee, J. Furtado, B. Bagchi, Fluctuating micro-heterogeneity in water-tert-butyl alcohol mixtures and lambda-type divergence of the mean cluster size with phase transition-like multiple anomalies, *The Journal of Chemical Physics*, 140 (2014) 194502.
- [121] H. Tanaka, K. Nakanishi, H. Touhara, Computer experiments on aqueous solutions. VI. Potential energy function for tert-butyl alcohol dimer and molecular dynamics calculation of 3 mol % aqueous solution of tert-butyl alcohol, *The Journal of Chemical Physics*, 81 (1984) 4065-4073.
- [122] H. Tanaka, K. Nakanishi, Structure of aqueous solutions of amphiphilics: t-butyl alcohol and urea solutions, *Fluid Phase Equilibria*, 83 (1993) 77-84.

- [123] K. Nakanishi, K. Ikari, S. Okazaki, H. Touhara, Computer experiments on aqueous solutions. III. Monte Carlo calculation on the hydration of tertiary butyl alcohol in an infinitely dilute aqueous solution with a new water–butanol pair potential, *The Journal of Chemical Physics*, 80 (1984) 1656-1670.
- [124] D. Chandler, Interfaces and the driving force of hydrophobic assembly, *Nature*, 437 (2005) 640-647.
- [125] F.H. Stillinger, Structure in aqueous solutions of nonpolar solutes from the standpoint of scaled-particle theory, *Journal of Solution Chemistry*, 2 (1973) 141-158.
- [126] N.T. Southall, K.A. Dill, A.D.J. Haymet, A view of the hydrophobic effect, *The Journal of Physical Chemistry B*, 106 (2002) 521-533.
- [127] T. Lazaridis, Hydrophobic effect, in: *eLS*, John Wiley & Sons, Ltd, 2013.
- [128] K. Nishikawa, T. Iijima, Structural study of tert-butyl alcohol and water mixtures by x-ray diffraction, *The Journal of Physical Chemistry*, 94 (1990) 6227-6231.
- [129] M.B. Hillyer, B.C. Gibb, Molecular shape and the hydrophobic effect, *Annual Review of Physical Chemistry*, 67 (2016) 307-329.
- [130] L. Maibaum, A.R. Dinner, D. Chandler, Micelle formation and the hydrophobic effect, *The Journal of Physical Chemistry B*, 108 (2004) 6778-6781.
- [131] G.W. Euliss, C.M. Sorensen, Dynamic light scattering studies of concentration fluctuations in aqueous t-butyl alcohol solutions, *The Journal of Chemical Physics*, 80 (1984) 4767-4773.
- [132] D. Subramanian, J.B. Klauda, J. Leys, M.A. Anisimov, Thermodynamic anomalies and structural fluctuations in aqueous solutions of tertiary butyl alcohol, *Herald of St. Petersburg University* (2013) 139-153.
- [133] D.T. Bowron, J.L. Finney, A.K. Soper, Structural investigation of solute–solute interactions in aqueous solutions of tertiary butanol, *The Journal of Physical Chemistry B*, 102 (1998) 3551-3563.
- [134] J.L. Finney, D.T. Bowron, A.K. Soper, The structure of aqueous solutions of tertiary butanol, *Journal of Physics: Condensed Matter*, 12 (2000) A123.
- [135] D.T. Bowron, A.K. Soper, J.L. Finney, Temperature dependence of the structure of a 0.06 mole fraction tertiary butanol-water solution, *The Journal of Chemical Physics*, 114 (2001) 6203-6219.
- [136] K. Nishikawa, Y. Kodera, T. Iijima, Fluctuations in the particle number and concentration and the Kirkwood-Buff parameters of tert-butyl alcohol and water mixtures studied by small-angle x-ray scattering, *The Journal of Physical Chemistry*, 91 (1987) 3694-3699.
- [137] K. Nishikawa, H. Hayashi, T. Iijima, Temperature dependence of the concentration fluctuation, the Kirkwood-Buff parameters, and the correlation length of tert-butyl alcohol and water mixtures studied by small-angle x-ray scattering, *The Journal of Physical Chemistry*, 93 (1989) 6559-6565.
- [138] H. Tanaka, K. Nakanishi, K. Nishikawa, Clathrate-like structure of water around some nonelectrolytes in dilute solution as revealed by computer simulation and X-ray diffraction studies, *Journal of inclusion phenomena*, 2 (1984) 119-126.
- [139] D.T. Bowron, S.D.a. Moreno, The structure of a concentrated aqueous solution of tertiary butanol: Water pockets and resulting perturbations, *The Journal of Chemical Physics*, 117 (2002) 3753-3762.
- [140] D.T. Bowron, S.D. Moreno, Structural correlations of water molecules in a concentrated alcohol solution, *Journal of Physics: Condensed Matter*, 15 (2003) S121.
- [141] A. Ghoufi, F. Artzner, P. Malfreyt, Physical properties and hydrogen-bonding network of water–ethanol mixtures from molecular dynamics simulations, *The Journal of Physical Chemistry B*, 120 (2016) 793-802.

Chapter 2

Solubility of diazepam in water + *tert*-butyl alcohol solvent mixtures: Experimental data and thermodynamic analysis

Abstract

The aim of this work is to provide solubility data of a poorly water-soluble drug, diazepam, in water + *tert*-butyl alcohol solvent mixtures that could be used to train existing cosolvency models and to identify the forces driving the drug solubility variation with the cosolvent content in the solvent mixture. The solubility of diazepam was determined in nine binary solvent mixtures and in both neat solvents at temperatures ranging from 293.15 to 313.15 K under atmospheric pressure. The density of diazepam-free and diazepam-saturated solvent mixtures were also determined as well as the thermophysical properties of original drug crystals and excess solid phases from solid-liquid equilibria. The thermodynamic quantities relative to the dissolution process of diazepam under saturation condition were obtained from solubility temperature dependence using the van't Hoff plot. From these data, the changes in thermodynamic quantities of diazepam upon fusion and mixing as well as the excess thermodynamic quantities of the drug in the different saturated solvent compositions over the temperature range investigated were determined using classical thermodynamic approaches. The mole fraction solubility of diazepam increases with the *tert*-butyl alcohol content in the solvent mixture to reach a maximum in the solvent mixture with a cosolvent mass fraction of 0.90. For every solvent compositions investigated, the transfer of the drug molecules from the pure crystalline solid to the saturated liquid mixtures was found to be endothermic so that the solubility of the drug increases with the temperature. Moreover, for every solvent compositions investigated, enthalpy is the main contributor to the deviation of the systems from ideal behavior, with noticeable exception of neat water. The solubility enhancement of the drug upon increase of the *tert*-butyl alcohol content in the solvent is then linked to a simultaneous evolution of the partial molar excess entropy and enthalpy of the drug with respect to the solvent composition.

This chapter was published in *Fluid Phase Equilibria*, volume 408, 25 January 2016, pages 284–298.

This page is intentionally left blank.

2.1. Introduction

Current methods used in drug discovery programs are leading to the selection of an increasing number of new small-molecule drug candidates with high pharmaceutical potency but low aqueous solubility [1-3]. Poor aqueous solubility is a major hurdle to successful drug development owing to formulation issues associated with water-insoluble drugs [4]. Over the past decades, numerous formulation approaches and technologies were developed by scientists to enhance the solubility and/or the dissolution rate of hydrophobic drugs in aqueous media [5-7]. However, the design of an optimal, reliable and scalable formulation for poorly water-soluble drugs delivery remains extremely challenging, especially when these drugs exhibit physical and/or chemical instability [8]. For heat-labile and/or water-labile hydrophobic drugs, the combination of functional excipients with freeze-drying process was proven to be an effective strategy to develop solid dosage forms with long-term stability and improved end-use properties [9-19].

The first step in the manufacturing process of such lyophilized pharmaceutical compositions is the preparation of a homogeneous solution containing an appropriate amount of drug and excipients in a fixed ratio in order to obtain, after freeze-drying, the required dose of formulated drug per unit dosage form. Due to the poor aqueous solubility of hydrophobic drugs, the use of neat water as solvent is not adequate to prepare the bulk solution intended to be freeze-dried, especially when considering high-dosage drugs. Indeed, the tremendous amount of solvent that would need to be removed from such very dilute solutions would require lengthy freeze-drying cycle times, which would result in unacceptably high operating costs [20, 21]. In addition, the batch size capacity would be drastically limited due to the vial geometry necessary to accommodate these dilute solutions [20, 21]. To achieve a sufficiently high drug concentration in the solution to be freeze-dried and make the whole process economically viable for a large-scale production, cosolvency, the addition of a miscible organic solvent to water, appears to be the most effective and widely used solubilization approach [22-25]. Besides to enable to incorporate the intended amount of drug per unit dosage form in an acceptable volume of solvent, it can also decrease the hydrolytic degradation rate of water-labile drugs in solution [25-27]. This allows performing pre-lyophilization unit operations over an extended temperature range and/or time-period, thus adding flexibility in the manufacturing process as well as in the production scheduling of such freeze-dried pharmaceutical compositions [20, 21].

Among the cosolvents that have been investigated over the past years in the field of freeze-drying, *tert*-butyl alcohol is the one that attracted the most attention from researchers in both academic and industrial settings [22-24]. As a matter of fact, *tert*-butyl alcohol is miscible with water over the whole composition range at any temperature, has a low toxicity profile and exhibits suitable physical properties with regard to the freeze drying process including a high fusion temperature, a high solid vapor pressure and a low sublimation enthalpy [22-24]. All water + *tert*-butyl alcohol solvent mixture

compositions share these desirable properties as well and, consequently, they freeze under operating conditions for conventional commercial freeze-dryers and they sublime at a higher rate than neat water for identical process parameters [28-31].

Experimental determination of drug solubility is a time-consuming and cost-effective procedure being mostly unworkable for drug candidates in the early stages of development [32-34]. For these reasons, numerous mathematical models have been developed and expanded over decades to correlate and/or predict the solubility of drugs in mixed solvents. Their underlying basis and assumptions as well as their capability, limitation and accuracy for correlating and/or predicting the solubility of drugs in water + cosolvent mixtures have been reviewed elsewhere [35]. Above and beyond the specificity of well-established models commonly employed in the pharmaceutical industry, their use to predict the solubility of drugs in water + cosolvent mixtures necessitate knowledge of numerical values of cosolvent-specific model constants [36-41]. Unfortunately, as far as we know, those for *tert*-butyl alcohol have not been reported to date in the literature. Moreover, their determination would require the availability of a large experimental data set, but at this time, solubility data of drugs in water + *tert*-butyl alcohol solvent mixtures are very scarce and often limited to a narrow solvent composition range [27, 42, 43]. Thus, it is of a crucial importance to create a large enough database on experimental solubility of hydrophobic drugs in this cosolvent system.

In the present work, diazepam (7-chloro-1,3-dihydro-1-methyl-5-phenyl-2H-1,4-benzodiazepin-2-one; $M = 284.74 \text{ g}\cdot\text{mol}^{-1}$; Figure 2.1) was used as hydrophobic model drug. Its physico-chemical properties, synthesis routes, pharmacology and pharmacokinetic characteristics as well as clinical uses were recently reviewed [44]. Solubility enhancement of diazepam through the use of common organic solvents, either neat or mixed with water, was reported by many authors. Common organic solvents investigated include ethanol [45-48], propane-1,2-diol [48-51], 1-methyl-2-pyrrolidinone [48, 52, 53] and 1,4-dioxane [54]. Oppositely, the use of alternative solvents such as supercritical fluids [55] and ionic liquids [56], which are of increasing interest in the pharmaceutical industry [57-59], is more limited. So far, solubility data of diazepam have been reported only in supercritical carbon dioxide [60].

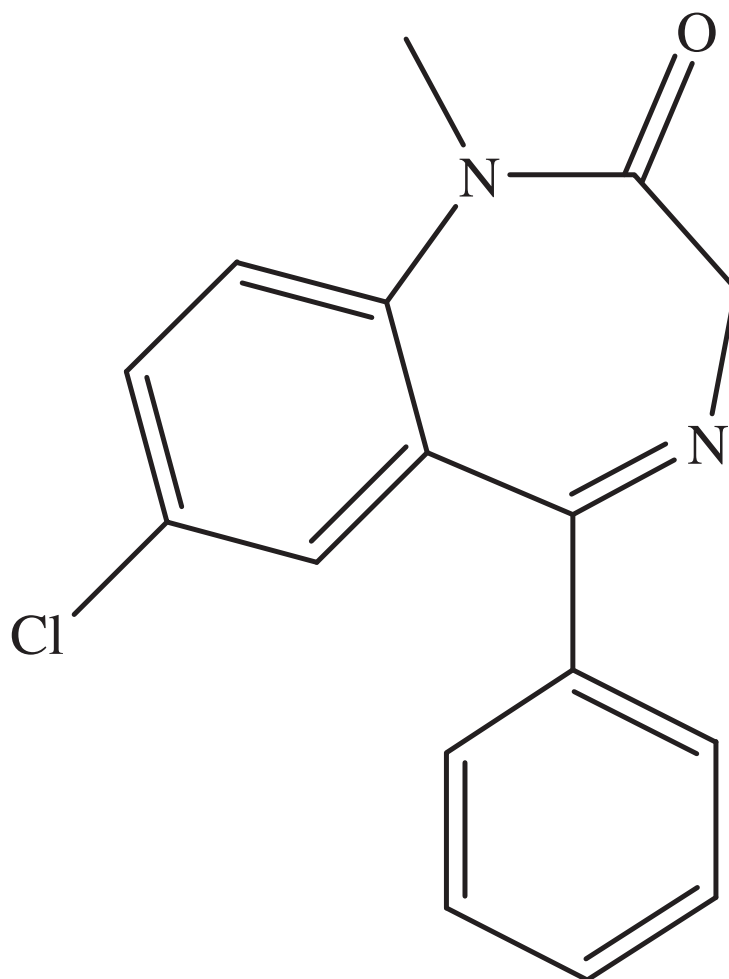


Figure 2.1. Chemical structure of diazepam (7-chloro-1,3-dihydro-1-methyl-5-phenyl-2H-1,4-benzodiazepin-2-one; molar mass: $284.74 \text{ g}\cdot\text{mol}^{-1}$).

The aim of this study is to provide experimental solubility values of diazepam in different water + *tert*-butyl alcohol solvent mixtures as well as density values of the diazepam-free and diazepam-saturated solvent mixtures in the temperature range from 293.15 to 313.15 K at atmospheric pressure. From these data, the thermodynamic quantities relative to the dissolution process of the drug in the different solvent mixtures under phase equilibrium condition were determined and the changes in the excess partial molar thermodynamic quantities of diazepam with the solvent composition were used to identify the forces driving the variation of the drug solubility in the different solvent mixtures. Special emphasis was paid to the methodology used to produce the data in order to minimize their possible contribution to error sources in solubility modeling as well as to the thermodynamic framework used for their interpretation.

2.2. Theory¹

2.2.1. Solid–liquid equilibrium

Consider, on the one hand, a non-reactive closed system containing a solvent defined as component 1, either neat or a blend, and a drug defined as component 2 and on the other hand, a solid–liquid equilibrium for which the solid phase is pure crystalline component 2 and the liquid phase is a mixture of components 1 and 2 saturated with respect to component 2. Complete thermodynamic equilibrium condition requires temperature and pressure uniformity throughout the system as well as equality of the chemical potential of component 2 in both solid and liquid phases. Thus:

$$\mu_2^*(\text{cr}, T, P) = \mu_2^{\text{sat}}(1, T, P, X) \quad (2.1)$$

where μ_2 is the chemical potential of component 2, the superscripts * and sat stand respectively for pure component and mixture saturation condition, cr and l indicate the state of aggregation of the phases as crystalline solid and liquid, respectively, and T, P and X are the system temperature, pressure and phase composition, respectively.

The dissolution process of the pure crystalline solid component 2 into the saturated liquid mixture at a given system temperature and pressure can be divided into two subsequent processes, namely fusion and mixing processes, so that from Eq. (2.1):

$$\begin{aligned} \Delta_{\text{sol}} G_{\text{m},2}^{\text{sat}}(T, P, X) &= \mu_2^{\text{sat}}(1, T, P, X) - \mu_2^*(\text{cr}, T, P) \\ &= [\mu_2^*(1, T, P) - \mu_2^*(\text{cr}, T, P)] + [\mu_2^{\text{sat}}(1, T, P, X) - \mu_2^*(1, T, P)] \\ &= \Delta_{\text{fus}} G_{\text{m},2}(T, P) + \Delta_{\text{mix}} G_{\text{m},2}^{\text{sat}}(T, P) \\ &= 0 \end{aligned} \quad (2.2)$$

where $G_{\text{m},2} = \mu_2$ is by definition the partial molar Gibbs energy of component 2, the Δ symbol denotes the change in an extensive thermodynamic quantity associated with a process and where the subscripts fus, mix and sol refer to the fusion, mixing and dissolution processes, respectively.

The fusion of the pure crystalline solid component 2 into a hypothetical pure supercooled liquid can be decomposed through the well-known isobaric three-step thermodynamic cycle [61] wherein pure component 2 in the solid state is first brought from the system temperature to its fusion temperature $T_{\text{fus},2}(P)$ at the system pressure, then converted from the solid state to the liquid state under

¹ In this work, the saturated liquid phase is considered as a mixture with attendant definitions of standard chemical potential and activity coefficient for components in a mixed condensed phase. For the sake of coherence and to prevent any confusion, the use of the terms solution, solvent and solute is avoided in this section. Nevertheless, they are used in other sections for convenience and clarity without implying any changes in the way the liquid phase is defined.

equilibrium conditions and finally brought back to the original system temperature so that the molar Gibbs energy change upon fusion at the system temperature and pressure is given by:

$$\begin{aligned}\Delta_{\text{fus}}G_{m,2}(T, P) &= \Delta_{\text{fus}}H_{m,2}(T, P) - T\Delta_{\text{fus}}S_{m,2}(T, P) \\ &= [\Delta_{\text{I}}H_{m,2} + \Delta_{\text{II}}H_{m,2} + \Delta_{\text{III}}H_{m,2}] - T[\Delta_{\text{I}}S_{m,2} + \Delta_{\text{II}}S_{m,2} + \Delta_{\text{III}}S_{m,2}]\end{aligned}\quad (2.3)$$

where subscripts I, II and III refer to the steps of the thermodynamic cycle above described. The first step involves heating of pure solid component 2 at constant pressure. Provided that no solid-solid phase transition occurs, the corresponding molar enthalpy and entropy changes are:

$$\Delta_{\text{I}}H_{m,2} = \int_T^{T_{\text{fus},2}} C_{p,m,2}^*(\text{cr}, T') \cdot dT' \quad (2.4)$$

$$\Delta_{\text{I}}S_{m,2} = \int_T^{T_{\text{fus},2}} C_{p,m,2}^*(\text{cr}, T') \cdot \frac{dT'}{T'} \quad (2.5)$$

where $C_{p,m,2}^*$ is the molar heat capacity at constant system pressure of pure component 2 in the defined state of aggregation. The second step implies phase change of pure component 2 at solid–liquid equilibrium for which the molar Gibbs energy change is:

$$\Delta_{\text{II}}G_{m,2}(T_{\text{fus},2}) = \Delta_{\text{II}}H_{m,2} - T_{\text{fus},2} \cdot \Delta_{\text{II}}S_{m,2} = 0 \quad (2.6)$$

where $\Delta_{\text{II}}H_{m,2} = \Delta_{\text{fus}}H_{m,2}(T_{\text{fus},2})$ is the molar fusion enthalpy of pure component 2 at its fusion point and $\Delta_{\text{II}}S_{m,2} = \Delta_{\text{fus}}S_{m,2}(T_{\text{fus},2})$ is the corresponding molar fusion entropy as given from Eq. (2.6) by:

$$\Delta_{\text{II}}S_{m,2}(T_{\text{fus},2}) = \frac{\Delta_{\text{fus}}H_{m,2}(T_{\text{fus},2})}{T_{\text{fus},2}} \quad (2.7)$$

The third step entails supercooling of pure liquid component 2 at constant pressure. The corresponding molar enthalpy and entropy changes are given by:

$$\Delta_{\text{III}}H_{m,2} = \int_{T_{\text{fus},2}}^T C_{p,m,2}^*(\text{l}, T') \cdot dT' \quad (2.8)$$

$$\Delta_{\text{III}}S_{m,2} = \int_{T_{\text{fus},2}}^T C_{p,m,2}^*(\text{l}, T') \cdot \frac{dT'}{T'} \quad (2.9)$$

From combination of Eqs. (2.3) to (2.9), the molar Gibbs energy change of component 2 upon fusion at the system temperature and pressure is rigorously expressed as:

$$\Delta_{\text{fus}} G_{\text{m},2}(T, P) = \Delta_{\text{fus}} H_{\text{m},2}(T_{\text{fus},2}) \cdot \left[1 - \frac{T}{T_{\text{fus},2}} \right] + \int_{T_{\text{fus},2}}^T \Delta C_{p,\text{m},2}(T') \cdot dT' - T \cdot \int_{T_{\text{fus},2}}^T \Delta C_{p,\text{m},2}(T') \cdot \frac{dT'}{T'} \quad (2.10)$$

with $T_{\text{fus},2} = T_{\text{fus},2}(P)$ and $\Delta C_{p,\text{m},2}(T') = C_{p,\text{m},2}^*(\text{l}, T') - C_{p,\text{m},2}^*(\text{cr}, T')$

The partial molar Gibbs energy change of component 2 upon mixing in the saturated liquid mixture at the system temperature and pressure is defined by the following equation:

$$\Delta_{\text{mix}} G_{\text{m},2}^{\text{sat}}(T, P, X) = RT \cdot \ln(x_2^{\text{sat}} \gamma_2^{\text{sat}}) \quad (2.11)$$

where R is the molar ideal gas constant and where $x_2^{\text{sat}} = x_2^{\text{sat}}(1, T, P, X)$ and $\gamma_2^{\text{sat}} = \gamma_2^{\text{sat}}(1, T, P, X)$ are the mole fraction solubility and the symmetrical activity coefficient of component 2 in the saturated liquid mixture at the temperature and pressure of the system, respectively.

Substitution of Eq. (2.10) and Eq. (2.11) into Eq. (2.2) and rearrangement lead to the following general expression for the solubility of crystalline solid component 2 in liquid component 1 at the system temperature and pressure:

$$\ln x_2^{\text{sat}} = -\frac{\Delta_{\text{fus}} H_{\text{m},2}(T_{\text{fus},2})}{R} \cdot \left[\frac{1}{T} - \frac{1}{T_{\text{fus},2}} \right] - \frac{1}{RT} \cdot \int_{T_{\text{fus},2}}^T \Delta C_{p,\text{m},2}(T') \cdot dT' + \frac{1}{R} \cdot \int_{T_{\text{fus},2}}^T \Delta C_{p,\text{m},2}(T') \cdot \frac{dT'}{T'} - \ln \gamma_2^{\text{sat}} \quad (2.12)$$

Provided that $\Delta_{\text{fus}} H_{\text{m},2}(T_{\text{fus},2})$ and $\Delta C_{p,\text{m},2}$ are known, this expression allows calculating γ_2^{sat} from experimental solubility data.

2.2.2. Solubility temperature dependence

An excess partial molar thermodynamic property of component 2 in the saturated mixture $Z_{\text{m},2}^{\text{sat,E}}$ is defined as the difference in the partial molar property of mixing over that for an ideal saturated mixture. That is:

$$Z_{\text{m},2}^{\text{sat,E}}(1, T, P, X) = \Delta_{\text{mix}} Z_{\text{m},2}^{\text{sat}}(T, P, X) - \Delta_{\text{mix}} Z_{\text{m},2}^{\text{sat,id}}(T, P, X) \quad (2.13)$$

where Z is the thermodynamic properties of interest and where the superscripts id and E stand for ideal and excess quantities, respectively. Since under ideal condition the activity coefficient is equal to unity, it appears from Eq. (2.11) and Eq. (2.13) that:

$$\Delta_{\text{mix}} G_{\text{m},2}^{\text{sat,id}}(T, P, X) = RT \cdot \ln x_2^{\text{sat}} \quad (2.14)$$

and therefore

$$G_{\text{m},2}^{\text{sat,E}}(1, T, P, X) = RT \cdot \ln \gamma_2^{\text{sat}} \quad (2.15)$$

Substitution of Eq. (2.14) and Eq. (2.15) into Eq. (2.2) and rearrangement lead to the following expression:

$$\ln x_2^{\text{sat}} = -\frac{1}{RT} \cdot [\Delta_{\text{fus}} G_{\text{m},2}(T, P) + G_{\text{m},2}^{\text{sat,E}}(1, T, P, X)] \quad (2.16)$$

with

$$G_{\text{m},2}^{\text{sat,E}}(1, T, P, X) = H_{\text{m},2}^{\text{sat,E}}(1, T, P, X) - TS_{\text{m},2}^{\text{sat,E}}(1, T, P, X) \quad (2.17)$$

Introduction of Eq. (2.3) and Eq. (2.17) into Eq. (2.16) yields:

$$\ln x_2^{\text{sat}} = -\frac{1}{RT} \cdot [\Delta_{\text{fus}} H_{\text{m},2}(T, P) + H_{\text{m},2}^{\text{sat,E}}(1, T, P, X)] + \frac{1}{R} \cdot [\Delta_{\text{fus}} S_{\text{m},2}(T, P) + S_{\text{m},2}^{\text{E}}(1, T, P, X)] \quad (2.18)$$

Since by definition $\Delta_{\text{mix}} H_{\text{m},2}^{\text{sat,id}}(T, P, X) = 0$ it follows that $H_{\text{m},2}^{\text{E}}(1, T, P, X) = \Delta_{\text{mix}} H_{\text{m},2}(T, P, X)$ so that $[\Delta_{\text{fus}} H_{\text{m},2}(T, P) + H_{\text{m},2}^{\text{sat,E}}(1, T, P, X)] = [\Delta_{\text{fus}} H_{\text{m},2}(T, P) + \Delta_{\text{mix}} H_{\text{m},2}^{\text{sat}}(T, P, X)] = \Delta_{\text{sol}} H_{\text{m},2}^{\text{sat}}(T, P, X)$ is the partial molar enthalpy change accompanying the transfer of component 2 molecules from the pure crystalline solid to the saturated liquid mixture at a given system temperature and pressure. Thus, Eq. (2.18) can be written as:

$$\ln x_2^{\text{sat}} = -\frac{1}{RT} \cdot [\Delta_{\text{sol}} H_{\text{m},2}^{\text{sat}}(T, P, X)] + \frac{1}{R} \cdot [\Delta_{\text{fus}} S_{\text{m},2}(T, P) + S_{\text{m},2}^{\text{E}}(1, T, P, X)] \quad (2.19)$$

Provided that at constant pressure the natural logarithm of the mole fraction experimental solubility of component 2 in component 1 exhibits a linear dependence on the reciprocal absolute temperature over the temperature range of interest, it can be described by an equation of the form:

$$\ln x_2^{\text{sat}} = \frac{1}{T} \cdot A + B \quad (2.20)$$

where A and B are the slope and intercept of the linear function, respectively, and are independent of both temperature and composition over the temperature and composition ranges of interest. It is clearly apparent from Eq. (2.19) and Eq. (2.20) that the coefficients of the so-called linear van't Hoff solubility plot are:

$$A = -\frac{1}{R} \cdot \Delta_{\text{sol}} H_{\text{m},2}^{\text{sat}}(P) \quad (2.21.a)$$

$$B = \frac{1}{R} \cdot [\Delta_{\text{fus}} S_{\text{m},2}(T, P) + S_{\text{m},2}^{\text{E}}(1, T, P, X)] \quad (2.21.b)$$

2.3. Material and methods

2.3.1. Chemicals

Bulk diazepam (7-chloro-1,3-dihydro-1-methyl-5-phenyl-2H-1,4-benzodiazepin-2-one, [CAS 439-14-5], purity: 0.998 in mass fraction, DZP) and corresponding analytical reference standard were purchased from Cooper (Melun, France) and from the European Directorate for the Quality of Medicines (EDQM, Strasbourg, France), respectively. *Tert*-butyl alcohol (2-methylpropan-2-ol, [CAS 75-65-0], purity: 0.99 in mass fraction, TBA), methanol (HPLC grade, [CAS 67-56-1], purity > 0.999 in mass fraction, MEOH), acetonitrile (HPLC grade, [CAS 75-05-8], purity > 0.999 in mass fraction, ACN) and tetrabutylammonium hydrogen sulfate ([CAS 32503-27-8], purity: 0.98 in mass fraction, TBAHS) were purchased from Fisher Scientific (Loughborough, United Kingdom). Ultra-pure water, otherwise known as type 1 water, ([CAS 7732-18-5], 18.2 MΩ·cm resistivity at 298.15 K, total organic carbon < 10 ppb, sodium < 1 ppb, chlorine < 1 ppb and silica < 3 ppb, W) was produced by a Synergy water purification system (Merck Millipore, Molsheim, France) and used in all experiments. All chemicals were used as received with no further purification. Overview of chemicals used in this study is summarized in Table 2.1.

2.3.2. Solvent mixtures preparation

Since pure TBA is in the solid state at room temperature, the original container was warmed in a water bath a few degrees above its fusion temperature until the entire was melted and was further homogenized prior to use. All W + TBA solvent mixtures were prepared by mass in quantities of 100 g using a Sartorius CP225D analytical balance (Goettingen, Germany) with an accuracy of ± 0.1 mg. The mass fraction of TBA in solvent mixture ranges from 0.10 to 0.90 with increments of 0.10 in order to study nine solvent binary mixtures and both neat solvents. The uncertainty in mixture composition was less than 0.5% of the nominal mass fraction for each solvent.

2.3.3. Solid–liquid equilibria

Equilibrium solubility experiments were performed at atmospheric pressure using the conventional saturation method at temperatures ranging from 293.15 to 313.15 K. For each solvent composition and each temperature investigated, five independent solubility samples were carried out in parallel and prepared according to the following procedure.

Table 2.1. Overview of chemicals used in this study.

Chemical	CAS RN	Formula	Molar mass (g·mol ⁻¹)	Source	Mass purity (%)	Analysis method
Acetonitrile	75-05-8	CH ₃ CN	41.05	Fisher Chemical	99.99	GC ^a
Diazepam CRS ^b	439-14-5	C ₁₆ H ₁₃ ClN ₂ O	284.74	EDQM ^b	99.9	HPLC ^c
Diazepam	439-14-5	C ₁₆ H ₁₃ ClN ₂ O	284.74	Cooper	99.8	HPLC ^c
Methanol	67-56-1	CH ₃ OH	32.04	Fisher Chemical	99.99	GC ^a
<i>Tert</i> -butyl alcohol	75-65-0	(CH ₃) ₃ COH	74.12	Fisher Chemical	> 99	GC ^a
Tetrabutylammonium hydrogen sulfate	32503-27-8	(CH ₃ CH ₂ CH ₂ CH ₂) ₄ N(HSO ₄)	339.53	Acros Organics	98	Titration Acid
Water Type I	7732-18-5	H ₂ O	18.02	In-house	Ultra-pure	Resistivity

^a GC: gas chromatography

^b CRS: chemical reference substance provided by EDQM: european directorate for the quality of medicines

^c HPLC: high performance liquid chromatography

At least a two-fold excess of solid was weighed into 10 mL volumetric amber glass flask. A PTFE-coated stirring magnet was introduced into the flask and closed ballast rings were placed around the flask neck. The solubility medium was then added to the mark of the flask which was immediately capped with a PTFE stopper to prevent any liquid phase modification due to solvent evaporation. All solid-liquid mixtures were placed on a Cimarec multi-position magnetic stirrer (Thermo Fisher Scientific, Villebon-sur-Yvette, France) immersed in a thermostatic water bath kept at the appropriate temperature using a Julabo ED heating immersion circulator (Seelbach, Germany) with an accuracy of ± 0.1 K. The solid-liquid mixtures were then stirred at 500 rpm for 96 h to reach the phase equilibrium. The temperature was monitored over the entire equilibration time using an YC-747UD data logger thermometer (YCT, Taipei, Taiwan) with an accuracy of ± 0.01 K connected to four type K thermocouples (TC Direct, Dardilly, France) disposed in the water bath. Recorded temperature data were processed with Temp Monitor S2 software. The uncertainty in the experimental temperatures was measured to be ± 0.03 K. The experimental set-up used in this study is depicted in Figure 2.2. Once the equilibrium achieved, excess of solid was separated from the saturated solution by filtration under isothermal conditions. The suspensions were transferred into 10 mL polypropylene syringe (Terumo, Leuven, Belgium) and filtered through 0.2 μm pore size regenerated cellulose membrane syringe filter (Fisher Scientific, Illkirch, France). Syringes and filter units were heated in oven at the equilibrium temperature for at least 24 h and kept at this temperature until use. Absence of colloidal particles in the saturated solutions was systematically checked by shining a laser beam through the filtered samples and assessed by absence of Tyndall light scattering. One milliliter of saturated solution intended for solubility measurement was immediately diluted with the same volume of MEOH to prevent DZP reprecipitation which could arise from difference between the room and equilibrium temperatures. For the same reason, the remaining saturated solution was maintained a few degrees above the experimental temperature until density measurement. To avoid preferential evaporation of TBA and consequential composition changes, both samples were kept in hermetically sealed vials and analysis were performed within a day.

2.3.4. Solubility measurements

Quantification of DZP in saturated solutions was performed by reverse-phase high-performance liquid chromatography with ultraviolet detection (HPLC-UV) using an external calibration.

2.3.4.1. Preparation of calibration standards and quality control samples

Accurately weighed 20.0 mg of DZP reference standard was transferred to 20 mL volumetric flask and dissolved with MEOH to prepare a stock solution at concentration of $1000 \mu\text{g}\cdot\text{mL}^{-1}$. Six calibration standard solutions at 1.0, 2.5, 5.0, 10, 25 and $50 \mu\text{g}\cdot\text{mL}^{-1}$ were prepared in 50 mL volumetric flasks by diluting required volumes of stock solution with the same solvent.

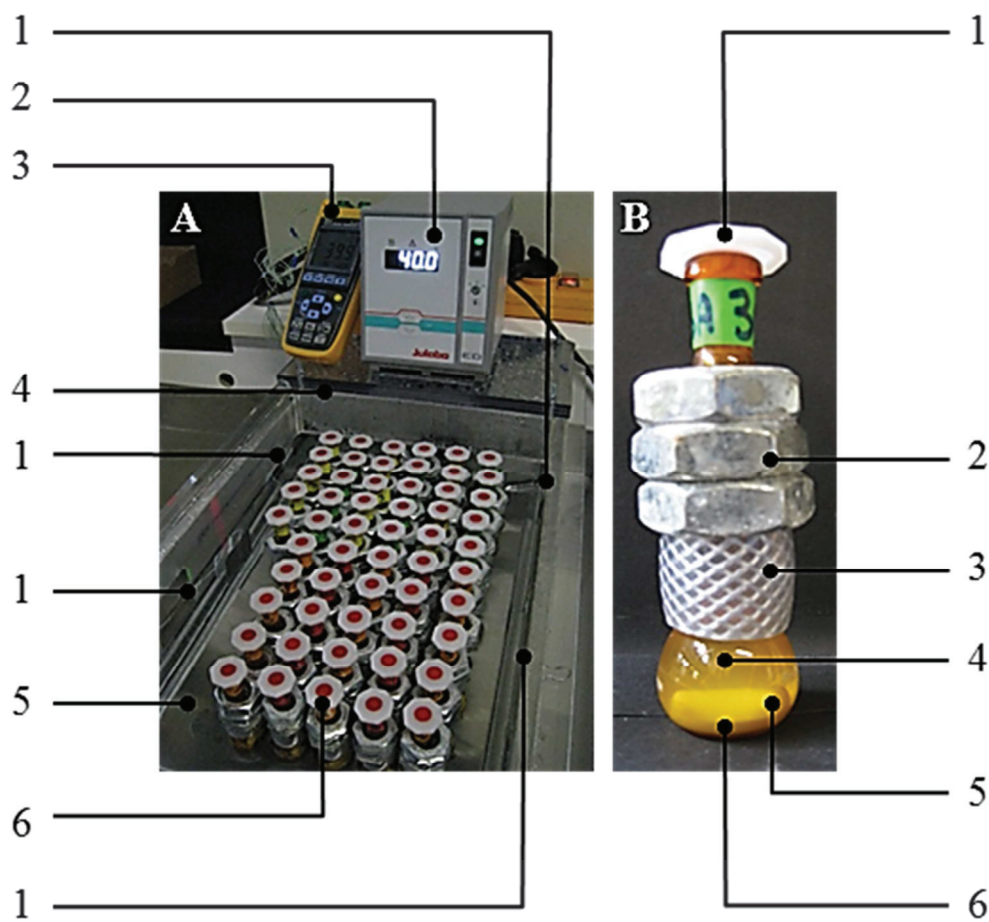


Figure 2.2. Experimental set-up used to carry out parallel solid–liquid equilibria experiments (A): General overview of the complete system: (1): Type K thermocouple; (2): Heating immersion circulator; (3): Data logger thermometer; (4): Plexiglass tank containing water as thermostating medium; (5): 60 positions magnetic stirrer connect to controller; (6): Immersed 10 mL volumetric amber glass flasks containing samples; (B): Detail view of sample-containing system: (1): PTFE stopper; (2): Ballast rings; (3): PE fiber-reinforced PVC tube; (4): Saturated liquid phase; (5): PTFE-coated magnetic stirring bar; (6): Excess solid phase (Note that the tank is normally covered by a plexiglass plate when experiments are in progress).

Quality control (QC) samples were prepared in the same way from a different stock solution at three representative concentration levels of the calibration curve, namely 1.75, 7.5 and 37.5 $\mu\text{g}\cdot\text{mL}^{-1}$. Stock solutions, calibration standards and QC samples were aliquoted in 1.5 mL polypropylene microcentrifuge tubes (Eppendorf, Sartrouville, France), stored at 193 K and used within a month. For each analytical batch, both in validation study and along with the solubility samples, calibration standards and QC samples were thawed and allowed to equilibrate at room temperature. The thawed samples were then vortexed to ensure complete mixing of the content and transferred into 2 mL HPLC autosampler amber glass vial before analysis.

2.3.4.2. Preparation of solubility samples

Half-diluted solubility samples were further diluted with MEOH to adjust concentration of DZP within the calibration range and resulting solutions were transferred into 2 mL HPLC amber glass vials. Total dilution factors range from 2 to 2000, depending on the equilibrium temperature and the solvent mixture composition.

2.3.4.3. Instrumentation and analytical conditions

The method was developed, validated and operated on a SpectraSystem chromatographic apparatus (Thermo Electron, Les Ulis, France) equipped with a P1000XR quaternary pump, a SCM1000 on-line degasser, an AS3000 autosampler fitted with a 100 μ L loop, a SN4000 system controller and an UV6000 photodiode array detector. Instrument control, data acquisition and data processing were achieved with ChromQuest software. Chromatographic separations were performed at 303 ± 0.5 K using a Kinetex C18 100 Å (150 mm \times 4.6 mm, 5 μ m) analytical column (Phenomenex, Torrance, USA). A 1:1 volumetric ratio mixture of ACN and 0.01 M TBAHS aqueous solution was used as the mobile phase and isocratically delivered at a flow rate of 1.0 mL \cdot min⁻¹. The autosampler was programmed with an injection volume of 10 μ L and a run time of 8 min. The UV-Vis spectra were obtained in the range 200-400 nm and diazepam was detected at 230 nm.

2.3.4.4. Method validation

To ensure correct determination of DZP concentration in saturated solutions, the method was validated according to International Conference on Harmonization guidelines for validation of analytical procedures [62] regarding to linearity, precision, accuracy, limit of detection (LOD), lower limit of quantification (LLOQ) and recovery. It was demonstrated that hydrolysis of DZP occurs only in strong acidic or alkaline media after exposure to higher temperatures than those used in this study and over a time-period much longer than those required to reach the equilibrium solubility [63, 64]. Thus, interferences from DZP degradation products were not expected so that method specificity was not investigated. In order to evaluate the linearity of the method, ten separate calibration curves, ranging from 1.0 to 50 μ g \cdot mL⁻¹, were constructed on ten consecutive days by plotting DZP peak area versus nominal concentration of six calibration standard solutions. Linearity over the concentration range investigated was assessed from squared correlation coefficient values of calibration curves fitted by least-squares linear regression. The precision, expressed as the relative standard deviation (RSD), and accuracy, expressed as the mean percentage deviation (MPD) of the calculated concentrations from the nominal concentrations, were evaluated by analysis of QC samples at low, medium and high concentration levels along with calibration standards. The intra-day precision was assessed by analyzing ten replicates of each QC samples in the same experiment whereas inter-day precision and

accuracy were determined from each QC samples by performing ten separate experiments on six consecutive days. The quantification parameters LOD and LLOQ were determined based on signal-to-noise ratio (S/N) by analyzing five replicates of samples with decreasing DZP concentrations. The LOD and LLOQ were defined as the lowest concentrations resulting in a peak signal to noise of baseline ratio equivalent to 3:1 and 10:1, respectively. In addition, analysis of ten replicates of QC samples with DZP concentration at the LLOQ was performed to ensure that these samples can be quantified with acceptable precision and accuracy. In order to evaluate potential filter sorption of DZP through the solid–liquid phases separation process, recovery was determined by comparing the mean peak area obtained from analysis of five replicates of QC samples at low and high concentration levels before and after filtration with syringe filter units previously described.

Under the used analytical conditions the retention time of DZP was 3.63 ± 0.03 min. A typical chromatogram is provided in Figure 2.3. The results of the validation procedure are summarized in Table 2.2. The HPLC-UV method showed a good linearity in the calibration concentration range as indicating by the average squared correlation coefficient value which exceeds 0.999. The LOD and LLOQ for DZP were found to be $0.25 \mu\text{g}\cdot\text{mL}^{-1}$ and $0.75 \mu\text{g}\cdot\text{mL}^{-1}$, respectively. Both accuracy and precision of the method evaluated at the low, medium and high concentration levels were found to be satisfactory. The MPD values for accuracy ranged from -4.7% to 2.8% whereas the RSD values of the intra-day and inter-day precisions were less than 2.0% and 1.0% , respectively. In addition, the recovery values for both low and high concentration levels were determined to be 100% within the measurement uncertainty indicating that DZP is not adsorbed onto the filters used for solid–liquid phase separation. These results testified that this chromatographic method is accurate and reliable for the quantification of DZP in saturated solutions.

2.3.4.5. Quantification of diazepam in solubility samples

For each analytical batch, calibration standards and QC samples were analyzed along with solubility samples. Solubility data were accepted if the QC samples analyzed in duplicate before and after solubility samples were quantitatively determined with an individual systematic error lower than 5% . Neither peak shape deformation nor presence of additional peaks were detected on the chromatograms of solubility samples so it can be ensure that DZP did not undergo any degradation over the time-period of equilibration.

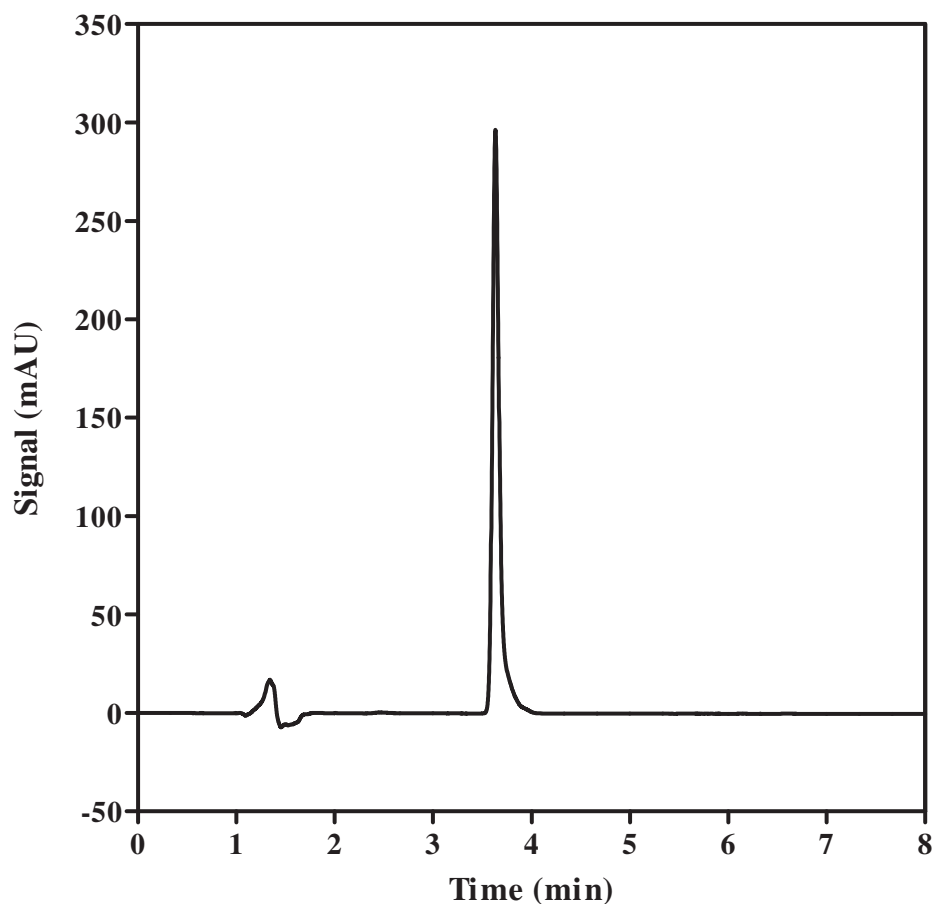


Figure 2.3. HPLC chromatogram of diazepam (sample concentration: $7.5 \mu\text{g}\cdot\text{mL}^{-1}$ in methanol; injection volume: $10 \mu\text{L}$; column: C18 100 Å, $150 \times 4.6 \text{ mm}$, $5 \mu\text{m}$; column temperature: 303 K ; mobile phase: acetonitrile/ tetrabutylammonium hydrogen sulfate 0.01 M in water $50:50 \text{ v/v}$; elution: isocratic; flow rate: $1 \text{ mL}\cdot\text{min}^{-1}$; detection: UV 230 nm).

2.3.5. Density measurements

In order to convert mass concentration solubility into mole fraction solubility, the densities of every saturated solution were measured with a DMA 4500 M vibrating-tube digital density meter (Anton Paar, Graz, Austria) with an accuracy of $\pm 1\cdot 10^{-5} \text{ g}\cdot\text{mL}^{-1}$. Apparatus was operated in the static mode at the relevant temperature. An incorporated Peltier system was used to control the temperature of the measuring cell with an accuracy of $\pm 0.01 \text{ K}$. Every measurement was preceded by density meter calibration with dry air and ultra-pure water. The uncertainty in density measurement and measuring cell temperature were found to be less than $5\cdot 10^{-5} \text{ g}\cdot\text{mL}^{-1}$ and 0.03 K , respectively. In addition, the densities of the solvent mixtures and neat solvents free of solute were measured in triplicate at each equilibrium temperature using the same experimental procedure.

Table 2.2. Validation results of the HPLC-UV method for quantification of diazepam in saturated solutions^a.

Linearity range ($\mu\text{g}\cdot\text{mL}^{-1}$)	Linear regression parameters of calibration curve				LOD (S/N = 3) ($\mu\text{g}\cdot\text{mL}^{-1}$)	LLOQ (S/N = 10) ($\mu\text{g}\cdot\text{mL}^{-1}$)
	Slope ($\text{mAU}\cdot\text{min}\cdot\text{mL}\cdot\mu\text{g}^{-1}$)	Intercept ($\text{mAU}\cdot\text{min}$)	r^2			
1.0 – 50.0	$262.656 (1.983) \cdot 10^3$	$- 65.309 (7.702) \cdot 10^3$	0.9996 (0.0001)		0.25	0.75
Quality Control Level	Nominal Concentration ($\mu\text{g}\cdot\text{mL}^{-1}$)	Intra-day Precision RSD (%)	Inter-day Precision RSD (%)	Accuracy MPD (%)	Recovery (%)	
High	37.5	0.3	0.3	2.8	100.3 (0.6)	
Medium	7.5	0.4	0.5	- 4.7	—	
Low	1.75	1.7	0.8	- 3.3	99.9 (0.6)	
LLOQ	0.75	1.8	—	—	—	

^a Values in parentheses are standard deviations. See material and methods section 2.3.4.4 for details of the validation procedure.

2.3.6. Differential scanning calorimetry measurements

Thermal properties of DZP original crystals were obtained by differential scanning calorimetry (DSC). Experiments were carried out on a DSC Q200 apparatus equipped with a refrigerated cooling system (TA Instruments, Guyancourt, France). Calibration for both temperature and heat flow was performed using certified indium as standard. The uncertainty in the calibration was estimated to be within 1 K and $2 \text{ J}\cdot\text{g}^{-1}$, respectively. Nitrogen was used as the purge gas at a flow rate of $50 \text{ mL}\cdot\text{min}^{-1}$. For the thermal analysis experiments, samples of 3-5 mg were accurately weighed in Tzero aluminium pans using the analytical balance previously described with an uncertainty of $\pm 0.01 \text{ mg}$. The powder was slightly pressed within the pan with a flat-end stainless steel device to avoid thermal gradient effects across the sample. The pans were then hermetically sealed with Tzero aluminium lids using a press. An identical empty aluminium pan was used as a reference. Analyzes were performed in standard DSC mode, which samples were equilibrated at 293 K for 2 min and then heated at $5 \text{ K}\cdot\text{min}^{-1}$ to 423 K. The data were processed using TA Universal Analysis software. In order to determine whether any solid-state form changes have occurred during equilibration process, the individual solid phases obtained after equilibration with the neat solvents and solvent mixtures at the lowest and highest experimental temperatures were also investigated. These samples were analyzed using the same experimental procedure, except that excess of solvent was left to evaporate to dryness at ambient conditions prior to DSC measurements. In all cases, experiments were performed in triplicate.

2.3.7. Calculations

As described in the theoretical section, equations related to the fusion process of the drug at the system temperature and pressure under isobaric condition involve the differential molar heat capacity of the pure liquid and crystalline solid forms of the drug over the temperature range $[T; T_{\text{fus},2}]$. Since the molar heat capacity of the pure liquid drug well below its fusion temperature cannot be determined experimentally, the differential molar heat capacity of DZP was assumed to be temperature independent over the temperature range of interest and that it can be empirically approximated by the molar entropy of fusion of DZP at its fusion temperature according to Hildebrand and Scott [65] and as detailed elsewhere [66]:

$$\Delta C_{p,m,2} \cong \Delta_{\text{fus}} S_{m,2}(T_{\text{fus},2}) = \frac{\Delta_{\text{fus}} H_{m,2}(T_{\text{fus},2})}{T_{\text{fus},2}} \quad (2.22)$$

With these assumptions and according to Eqs. (2.3) to (2.10) the molar thermodynamic quantities for the fusion process of DZP at the system temperature and pressure were calculated as:

$$\Delta_{\text{fus}} H_{m,2}(T, P) = \Delta_{\text{fus}} H_{m,2}(T_{\text{fus},2}) \cdot \frac{T}{T_{\text{fus},2}} \quad (2.23.a)$$

$$\Delta_{\text{fus}}S_{m,2}(T, P) = \frac{\Delta_{\text{fus}}H_{m,2}(T_{\text{fus},2})}{T_{\text{fus},2}} \cdot \left[1 + \ln \frac{T}{T_{\text{fus},2}} \right] \quad (2.23.b)$$

$$\Delta_{\text{fus}}G_{m,2}(T, P) = \Delta_{\text{fus}}H_{m,2}(T_{\text{fus},2}) \cdot \frac{T}{T_{\text{fus},2}} \cdot \ln \frac{T_{\text{fus},2}}{T} \quad (2.23.c)$$

whereas the partial molar enthalpy and entropy changes for the dissolution process of DZP in a given TBA + W solvent mixture were calculated respectively from temperature dependence of the experimental drug solubility according to Eq. (2.21) and from phase equilibrium condition Eq. (2.2) as:

$$\Delta_{\text{sol}}S_{m,2}^{\text{sat}}(T, P, X) = \frac{1}{T} \cdot \Delta_{\text{sol}}H_{m,2}^{\text{sat}}(T, P, X) \quad (2.24)$$

The partial molar thermodynamic quantities for the mixing process of DZP in the saturated liquid mixture at the system temperature and pressure were calculated according to their definition:

$$\Delta_{\text{mix}}H_{m,2}^{\text{sat}}(T, P, X) = \Delta_{\text{sol}}H_{m,2}^{\text{sat}}(T, P, X) - \Delta_{\text{fus}}H_{m,2}(T, P) \quad (2.25.a)$$

$$\Delta_{\text{mix}}S_{m,2}^{\text{sat}}(T, P, X) = \Delta_{\text{sol}}S_{m,2}^{\text{sat}}(T, P, X) - \Delta_{\text{fus}}S_{m,2}(T, P) \quad (2.25.b)$$

$$\Delta_{\text{mix}}G_{m,2}^{\text{sat}}(T, P, X) = -\Delta_{\text{fus}}G_{m,2}(T, P) \quad (2.25.c)$$

as well as the partial molar excess thermodynamic quantities:

$$H_{m,2}^{\text{sat,E}}(1, T, P, X) = \Delta_{\text{mix}}H_{m,2}^{\text{sat}}(T, P, X) \quad (2.26.a)$$

$$S_{m,2}^{\text{sat,E}}(1, T, P, X) = \Delta_{\text{mix}}S_{m,2}^{\text{sat}}(T, P, X) + R \cdot \ln x_2^{\text{sat}} \quad (2.26.b)$$

$$G_{m,2}^{\text{sat,E}}(1, T, P, X) = RT \cdot \ln \gamma_2^{\text{sat}} \quad (2.26.c)$$

Finally, the ideal mole fraction solubility of DZP at a given temperature was calculated from experimental values of fusion temperature and molar heat of fusion at the fusion temperature of the drug crystals according to the following equation derived from Eq. (2.12) along with assumptions related to the differential molar heat capacity term:

$$\ln x_2^{\text{sat,id}} = \frac{\Delta_{\text{fus}}H_{m,2}(T_{\text{fus},2})}{RT_{\text{fus},2}} \cdot \ln \frac{T}{T_{\text{fus},2}} \quad (2.27)$$

and accordingly, the activity coefficients of DZP in the different saturated solvent mixtures were calculated from ideal mole fraction solubility and experimental mole fraction solubility values at the temperature of the system as:

$$\ln \gamma_2^{\text{sat}} = \ln x_2^{\text{sat,id}} - \ln x_2^{\text{sat}} \quad (2.28)$$

2.3.8. Statistical analysis

Standard error propagation equations were used to estimate the standard deviations in values calculated from those obtained from experimental measurements [67]. Regression analyses were performed using ordinary least-squares method. Goodness-of-fit of regression equations was evaluated by the squared correlation coefficient and its statistical significance was assessed by one-tailed Fisher's *F*-test whereas statistical significance of estimated regression coefficients was determined by two-tailed Student's *t*-test. All calculations were carried out using Microsoft Excel 2010 software (Microsoft, Redmond, USA).

2.4. Results and discussion

2.4.1. Experimental data

2.4.1.1. Thermal analysis of original drug crystals and excess solid phases from solubility samples

The DSC thermograms of DZP original crystals displayed a single sharp melting endotherm upon heating and no other thermal events were detected in the temperature range studied, indicating that the raw material exists in a single crystal form. A typical thermogram of DZP original crystal is provided in Figure 2.4. The experimentally determined values of the DZP fusion temperature at atmospheric pressure $T_{\text{fus},2}$ and the corresponding molar heat of fusion $\Delta_{\text{fus}}H_{\text{m},2}(T_{\text{fus},2})$ were found to be equal to 404.12 ± 0.02 K and 26.17 ± 0.14 kJ·mol⁻¹, respectively. These values are in good agreement with those reported by Rubino ($\Delta_{\text{fus}}H_{\text{m},2}(T_{\text{fus},2}) = 25.3$ kJ·mol⁻¹, $T_{\text{fus},2} = 404.15$ K) [68], Wassvik *et al.* ($\Delta_{\text{fus}}H_{\text{m},2}(T_{\text{fus},2}) = 24.70$ kJ·mol⁻¹, $T_{\text{fus},2} = 404.75$ K) [69] and Verheyen *et al.* ($\Delta_{\text{fus}}H_{\text{m},2}(T_{\text{fus},2}) = 25.49$ kJ·mol⁻¹, $T_{\text{fus},2} = 403.55$ K) [70]. The heating scans of the solid phases obtained after equilibration with the neat solvents and W + TBA solvent mixtures did not reveal any additional thermal events in comparison with those of the original drug crystals. Additionally, the values of the fusion temperature and molar heat of fusion did not significantly differ from those measured for the original crystals with deviations being less than 0.2% and 3%, respectively. These results indicate that neither polymorphic conversion nor solvates formation occur during equilibration of the solid phase with the saturated solutions at the experimental temperature range. Therefore, the contribution of solid-state properties to the solubility of DZP could be considered as constant in all solvent compositions studied.

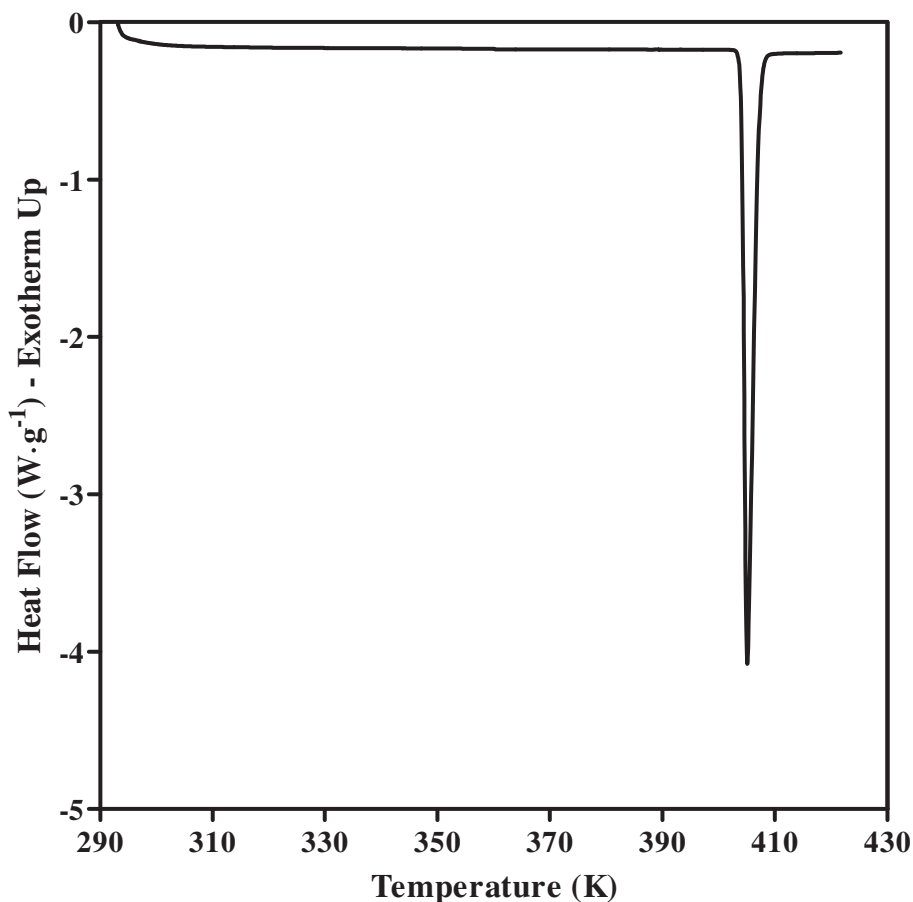


Figure 2.4. DSC thermogram of diazepam (sample size: 3.95 mg; pan: aluminium hermetically sealed; heating rate: $5 \text{ K}\cdot\text{min}^{-1}$; sample purge flow N_2 : $50 \text{ mL}\cdot\text{min}^{-1}$).

2.4.1.2. Density of diazepam-free and diazepam-saturated water + *tert*-butyl alcohol solvent mixtures

The experimental data for the density of the W + TBA solvent mixtures free of solute ρ_1 as well as those of the saturated solutions ρ^{sat} are given in Table 2.3 according to the phase composition expressed by the TBA mass fraction in solvent mixture free of solute w_{TBA} . In all cases, the relative standard deviations of the density values were less than 0.1%. Regarding to the density of the solvent binary mixtures free of solute, the experimental values presented in this work are in good agreement with those recently reported by Egorov and Makarov [71]. This is illustrated in Figure 2.5 where the values provided by these authors and those obtained in this study are compared at a temperature of 308.15 K. As expected from the respective density of neat solvents, it can be observed from Table 2.3 that for every isotherm, the density of the W + TBA solvent mixture decreases as the content of TBA in the mixture increases. Moreover, for a given solvent composition, it can be remarked that the density of the solvent binary mixture decreases as the temperature increases. Considering the density

of the W + TBA solvent mixtures saturated with DZP, it can be noticed that the relative increase in the mixture density value resulting from the presence of the solute is less than 0.5% for solvent mixtures containing a TBA mass fraction lower or equal to 0.30 and is at most of 3.6% for other solvent mixture compositions. Consequently, variation of the density of saturated solutions with respect the mass fraction of TBA in the solvent mixtures follows the same trends that those of the solvent binary mixtures free of solute for every isotherm. Additionally, it appears that as the temperature increases, the relative increase in density increases for every solvent composition but with a higher magnitude for the TBA-rich mixtures.

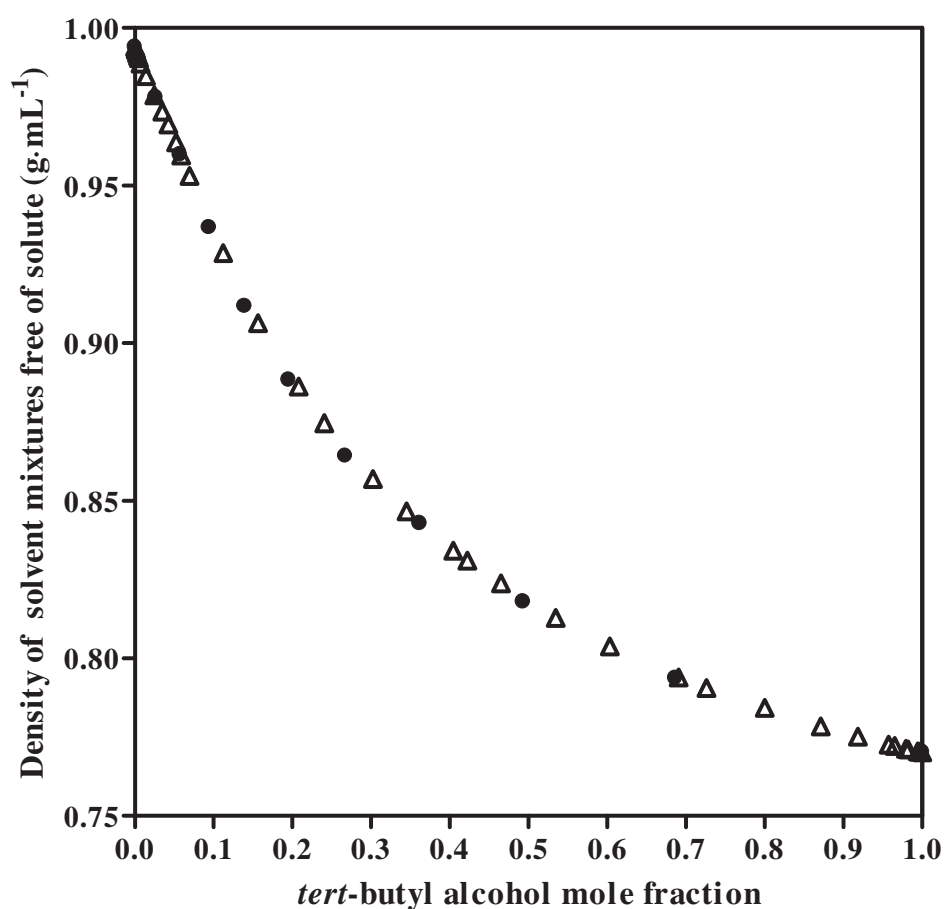


Figure 2.5. Comparison of the experimental density values of the water + *tert*-butyl alcohol solvent mixtures free of diazepam at 308.15 K from this work (●) and from Reference [71] (△) (error bars are omitted for readability).

Table 2.3. Density of diazepam-free and diazepam-saturated water + *tert*-butyl alcohol solvent mixtures ρ_1 and ρ^{sat} at system temperature T and pressure $P = 0.1$ MPa^a.

$w_{\text{TBA}}^{\text{b}}$	$T = 293.15$ K	$T = 299.15$ K	$T = 303.15$ K	$T = 308.15$ K	$T = 313.15$ K
ρ_1 (g·mL ⁻¹)					
0.00	9.9820 (0.0001) · 10 ⁻¹	9.9679 (0.0001) · 10 ⁻¹	9.9566 (0.0001) · 10 ⁻¹	9.9405 (0.0001) · 10 ⁻¹	9.9224 (0.0001) · 10 ⁻¹
0.10	9.8345 (0.0002) · 10 ⁻¹	9.8154 (0.0002) · 10 ⁻¹	9.8007 (0.0002) · 10 ⁻¹	9.7802 (0.0002) · 10 ⁻¹	9.7576 (0.0002) · 10 ⁻¹
0.20	9.6913 (0.0002) · 10 ⁻¹	9.6555 (0.0002) · 10 ⁻¹	9.6305 (0.0002) · 10 ⁻¹	9.5983 (0.0002) · 10 ⁻¹	9.5651 (0.0002) · 10 ⁻¹
0.30	9.4786 (0.0001) · 10 ⁻¹	9.4347 (0.0001) · 10 ⁻¹	9.4049 (0.0001) · 10 ⁻¹	9.3674 (0.0001) · 10 ⁻¹	9.3294 (0.0001) · 10 ⁻¹
0.40	9.2358 (0.0002) · 10 ⁻¹	9.1893 (0.0002) · 10 ⁻¹	9.1575 (0.0002) · 10 ⁻¹	9.1173 (0.0002) · 10 ⁻¹	9.0767 (0.0002) · 10 ⁻¹
0.50	9.0076 (0.0001) · 10 ⁻¹	8.9593 (0.0001) · 10 ⁻¹	8.9262 (0.0001) · 10 ⁻¹	8.8844 (0.0001) · 10 ⁻¹	8.8421 (0.0001) · 10 ⁻¹
0.60	8.7693 (0.0002) · 10 ⁻¹	8.7194 (0.0002) · 10 ⁻¹	8.6853 (0.0002) · 10 ⁻¹	8.6421 (0.0002) · 10 ⁻¹	8.5981 (0.0002) · 10 ⁻¹
0.70	8.5592 (0.0001) · 10 ⁻¹	8.5081 (0.0001) · 10 ⁻¹	8.4730 (0.0001) · 10 ⁻¹	8.4286 (0.0001) · 10 ⁻¹	8.3833 (0.0001) · 10 ⁻¹
0.80	8.3161 (0.0002) · 10 ⁻¹	8.2628 (0.0002) · 10 ⁻¹	8.2265 (0.0002) · 10 ⁻¹	8.1804 (0.0002) · 10 ⁻¹	8.1334 (0.0002) · 10 ⁻¹
0.90	8.0784 (0.0001) · 10 ⁻¹	8.0231 (0.0001) · 10 ⁻¹	7.9853 (0.0001) · 10 ⁻¹	7.9373 (0.0001) · 10 ⁻¹	7.8885 (0.0001) · 10 ⁻¹
1.00	—	7.7948 (0.0001) · 10 ⁻¹	7.7549 (0.0001) · 10 ⁻¹	7.7028 (0.0001) · 10 ⁻¹	7.6498 (0.0001) · 10 ⁻¹
ρ^{sat} (g·mL ⁻¹)					
0.00	9.9820 (0.0000) · 10 ⁻¹	9.9679 (0.0000) · 10 ⁻¹	9.9567 (0.0000) · 10 ⁻¹	9.9406 (0.0000) · 10 ⁻¹	9.9225 (0.0000) · 10 ⁻¹
0.10	9.8345 (0.0005) · 10 ⁻¹	9.8154 (0.0001) · 10 ⁻¹	9.8022 (0.0000) · 10 ⁻¹	9.7816 (0.0000) · 10 ⁻¹	9.7595 (0.0000) · 10 ⁻¹
0.20	9.6953 (0.0007) · 10 ⁻¹	9.6632 (0.0001) · 10 ⁻¹	9.6438 (0.0001) · 10 ⁻¹	9.6147 (0.0004) · 10 ⁻¹	9.5820 (0.0000) · 10 ⁻¹
0.30	9.5027 (0.0000) · 10 ⁻¹	9.4636 (0.0000) · 10 ⁻¹	9.4428 (0.0002) · 10 ⁻¹	9.4073 (0.0001) · 10 ⁻¹	9.3742 (0.0005) · 10 ⁻¹
0.40	9.2947 (0.0004) · 10 ⁻¹	9.2633 (0.0011) · 10 ⁻¹	9.2346 (0.0002) · 10 ⁻¹	9.2048 (0.0000) · 10 ⁻¹	9.1750 (0.0004) · 10 ⁻¹
0.50	9.0894 (0.0009) · 10 ⁻¹	9.0524 (0.0001) · 10 ⁻¹	9.0291 (0.0001) · 10 ⁻¹	9.0108 (0.0001) · 10 ⁻¹	8.9788 (0.0013) · 10 ⁻¹
0.60	8.8815 (0.0002) · 10 ⁻¹	8.8538 (0.0001) · 10 ⁻¹	8.8300 (0.0007) · 10 ⁻¹	8.8243 (0.0000) · 10 ⁻¹	8.8064 (0.0003) · 10 ⁻¹
0.70	8.6749 (0.0002) · 10 ⁻¹	8.6527 (0.0011) · 10 ⁻¹	8.6399 (0.0004) · 10 ⁻¹	8.6319 (0.0004) · 10 ⁻¹	8.6267 (0.0001) · 10 ⁻¹
0.80	8.4554 (0.0003) · 10 ⁻¹	8.4385 (0.0001) · 10 ⁻¹	8.4266 (0.0001) · 10 ⁻¹	8.4277 (0.0002) · 10 ⁻¹	8.4230 (0.0007) · 10 ⁻¹
0.90	8.2130 (0.0001) · 10 ⁻¹	8.1877 (0.0000) · 10 ⁻¹	8.1692 (0.0009) · 10 ⁻¹	8.1688 (0.0001) · 10 ⁻¹	8.1444 (0.0027) · 10 ⁻¹
1.00	—	7.8758 (0.0000) · 10 ⁻¹	7.8497 (0.0002) · 10 ⁻¹	7.8237 (0.0003) · 10 ⁻¹	7.7926 (0.0009) · 10 ⁻¹

^a Values in parentheses are standard deviations, $u(T) = 0.03$ K, $u_r(P) = 0.05$ and $u_r(w_{\text{TBA}}) = 0.005$.

^b Mass fraction of *tert*-butyl alcohol in the solvent mixture free of solute.

2.4.1.3. Solubility of diazepam in water + *tert*-butyl alcohol solvent mixtures

The experimental data for the mole fraction solubility of DZP x_2^{sat} in W + TBA solvent mixtures in the temperature range studied are reported in Table 2.4 according to the solvent mixtures composition expressed by the TBA mass fraction in solvent mixture free of solute. These data expressed in other units are also available in Appendix B (Table B.1) for convenience in application and use. Table 2.4 also includes the ideal mole fraction solubility of DZP $x_2^{\text{sat,id}}$ calculated from Eq. (2.27) using the experimental values of fusion temperature and molar enthalpy and entropy changes upon fusion at the fusion temperature. The relative standard deviations of solubility values ranged from 0.3% to 4.5% which was considered to be satisfactory considering the magnitude of DZP solubility in the solvents investigated. The aqueous solubility values in this work are in good agreement with those available in the literature. The solubility of DZP in neat water was measured to be $1.489 \cdot 10^{-4} \text{ mol} \cdot \text{L}^{-1}$ at 293.15 K which is close to the values of $1.413 \cdot 10^{-4} \text{ mol} \cdot \text{L}^{-1}$ and $1.479 \cdot 10^{-4} \text{ mol} \cdot \text{L}^{-1}$ reported at the same temperature by Wassvik *et al.* [69] and Du-Cuny *et al.* [72], respectively. The aqueous solubility values for DZP determined in this work are also consistent with those published by Jouyban and coworkers who presented molar solubility values of $1.5 \cdot 10^{-4} \text{ mol} \cdot \text{L}^{-1}$ and $2.0 \cdot 10^{-4} \text{ mol} \cdot \text{L}^{-1}$ at 298.15 K [49, 52, 53] and mole fraction solubility values of $3.0 \cdot 10^{-6}$ and $4.0 \cdot 10^{-6}$ at 303.15 K [45, 73]. In this study, the measured molar solubility value of $1.665 \cdot 10^{-4} \text{ mol} \cdot \text{L}^{-1}$ at 299.15 K and the mole fraction solubility value of $3.604 \cdot 10^{-6}$ at 303.15 K are in the solubility range reported by these authors. From the best of our knowledge, no solubility data for DZP in neat TBA or in W + TBA solvent mixtures are available in the literature making any other comparisons impossible.

The evolution of the mole fraction solubility of DZP according to temperatures and the mass fraction of TBA in the solvent mixtures free of solute is shown in Figure 2.6. Regarding the influence of the W + TBA mixture composition on the solubility of DZP, it can be observed that the solubility of the drug increases with addition of TBA to reach a maximum and then decreases with further increase in TBA concentration. At all the temperature studied, the maximum solubility values are obtained in the same solvent mixture but its composition depends on the unit in which solubility is expressed. It corresponds to a solvent mixture containing a TBA mass fraction of 0.90 for solubility expressed in mole fraction and to a solvent mixture containing a TBA mass fraction of 0.80 for solubility expressed in other units. In addition, considering a given solvent composition, it can be noted that the solubility of DZP increases with temperature, with no exception. Depending on the solvent mixture composition, substantial differences exist between experimental solubility values and those predicted assuming the model of an ideal solution, the former being less than the latter in all cases. According to Eq. (2.27), the theoretical solubility value that would be obtained in a perfect solvent depends only on the strength of solute-solute intermolecular interactions within the crystal lattice. The results obtained indicate that the contribution of solute-solute, solvent-solvent and solvent-solute intermolecular interactions in the liquid phase to the solubility of DZP in W + TBA solvent mixtures is significant.

Table 2.4. Mole fraction solubility of diazepam x_2^{sat} in water + *tert*-butyl alcohol solvent mixtures at system temperature T and pressure $P = 0.1 \text{ MPa}^{\text{a}}$.

$w_{\text{TBA}}^{\text{b}}$	$T = 293.15 \text{ K}$	$T = 299.15 \text{ K}$	$T = 303.15 \text{ K}$	$T = 308.15 \text{ K}$	$T = 313.15 \text{ K}$
x_2^{sat}					
0.00	2.688 (0.014) · 10 ⁻⁶	3.010 (0.033) · 10 ⁻⁶	3.604 (0.036) · 10 ⁻⁶	3.973 (0.012) · 10 ⁻⁶	4.860 (0.060) · 10 ⁻⁶
0.10	7.790 (0.354) · 10 ⁻⁶	1.033 (0.004) · 10 ⁻⁵	1.407 (0.010) · 10 ⁻⁵	1.708 (0.013) · 10 ⁻⁵	2.358 (0.070) · 10 ⁻⁵
0.20	5.755 (0.256) · 10 ⁻⁵	1.100 (0.022) · 10 ⁻⁴	1.643 (0.034) · 10 ⁻⁴	2.236 (0.023) · 10 ⁻⁴	2.914 (0.071) · 10 ⁻⁴
0.30	4.866 (0.169) · 10 ⁻⁴	6.271 (0.081) · 10 ⁻⁴	8.186 (0.179) · 10 ⁻⁴	9.889 (0.172) · 10 ⁻⁴	1.332 (0.047) · 10 ⁻³
0.40	1.217 (0.034) · 10 ⁻³	1.539 (0.009) · 10 ⁻³	1.873 (0.043) · 10 ⁻³	2.260 (0.027) · 10 ⁻³	2.860 (0.123) · 10 ⁻³
0.50	2.250 (0.057) · 10 ⁻³	2.863 (0.039) · 10 ⁻³	3.456 (0.070) · 10 ⁻³	4.088 (0.047) · 10 ⁻³	5.239 (0.104) · 10 ⁻³
0.60	3.497 (0.054) · 10 ⁻³	4.321 (0.127) · 10 ⁻³	5.531 (0.053) · 10 ⁻³	6.340 (0.075) · 10 ⁻³	8.172 (0.169) · 10 ⁻³
0.70	5.162 (0.165) · 10 ⁻³	6.187 (0.116) · 10 ⁻³	8.047 (0.124) · 10 ⁻³	9.220 (0.125) · 10 ⁻³	1.154 (0.020) · 10 ⁻²
0.80	6.820 (0.107) · 10 ⁻³	8.287 (0.120) · 10 ⁻³	1.075 (0.011) · 10 ⁻²	1.247 (0.043) · 10 ⁻²	1.519 (0.026) · 10 ⁻²
0.90	7.647 (0.108) · 10 ⁻³	9.179 (0.082) · 10 ⁻³	1.208 (0.024) · 10 ⁻²	1.385 (0.007) · 10 ⁻²	1.689 (0.069) · 10 ⁻²
1.00	—	6.342 (0.039) · 10 ⁻³	7.618 (0.217) · 10 ⁻³	9.277 (0.093) · 10 ⁻³	1.195 (0.034) · 10 ⁻²
Ideal	8.201 (0.153) · 10 ⁻²	9.603 (0.168) · 10 ⁻²	1.065 (0.018) · 10 ⁻¹	1.210 (0.019) · 10 ⁻¹	1.371 (0.021) · 10 ⁻¹

^a Values in parentheses are standard deviations, $u(T) = 0.03 \text{ K}$, $u_i(P) = 0.05$ and $u_i(w_{\text{TBA}}) = 0.005$.

^b Mass fraction of *tert*-butyl alcohol in the solvent mixture free of solute.

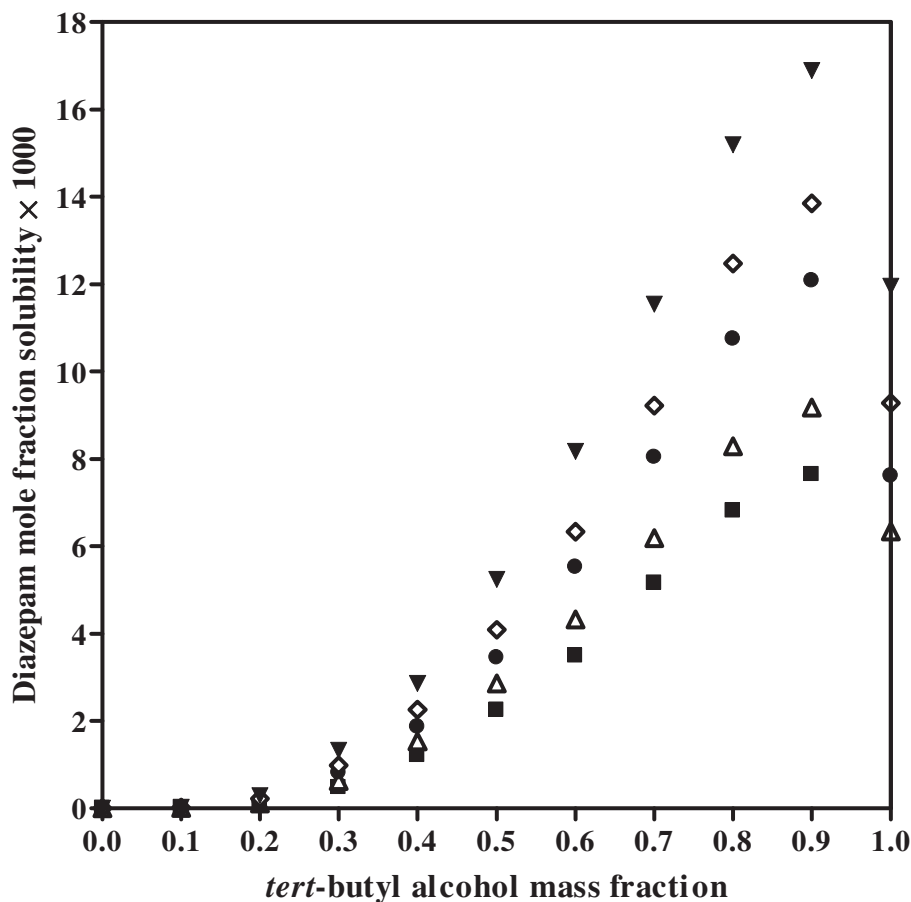


Figure 2.6. Experimental mole fraction solubility of diazepam in water + *tert*-butyl alcohol solvent mixtures as function of the *tert*-butyl alcohol mass fraction in solvent mixture free of solute (■): $T = 293.15$ K; (△): $T = 299.15$ K; (●): $T = 303.15$ K; (◇): $T = 308.15$ K; (▼): $T = 313.15$ K (error bars are omitted for readability).

2.4.1.4. Temperature dependence of the solubility of diazepam in water + *tert*-butyl alcohol solvent mixtures

The so-called van't Hoff solubility-temperature plots obtained from experimental data are shown in Figure 2.7. It can be observed that for every investigated solvent composition, the natural logarithm of the DZP mole fraction solubility exhibits a linear dependence to the reciprocal of the system temperature over the experimental temperature range and could be regressed into a straight line. The least-squares linear regression parameters for the van't Hoff curves are given in Table 2.5. The statistical significance of the estimated regression coefficients and squared correlation coefficients were assessed using Student's *t*-test and Fisher's *F*-test, respectively, and corresponding *p*-values as asterisks are also reported in Table 2.5. The complete statistical analysis results are provided in Appendix B (Table B.2). The obtained squared correlation coefficients values are very high and range

from 0.977 to 0.998 and their associated p -values were less than 0.01 in all cases, indicating a strong and significant goodness-of-fit between the dependent and independent variables of interest for every solvent composition. Regarding to the linear coefficient estimates, the values of the slopes are always negatives whereas those of the intercepts are always positive, with exception of neat water. For every solvent composition, the linear coefficient estimates are found to be statistically significant with p -values mostly lower than 0.01 and at least lower than 0.05 so that they can be appropriately used to calculate the partial molar enthalpy change of DZP upon dissolution $\Delta_{\text{sol}}H_{\text{m},2}^{\text{sat}}$ and the entropic term $[\Delta_{\text{fus}}S_{\text{m},2} + S_{\text{m},2}^{\text{sat,E}}]$ according to Eqs. (2.20) and (2.21). Their values are included in Table 2.5. Importantly, for a given solvent or solvent mixture, these two thermodynamic quantities can be considered to be independent of both temperature and composition within the temperature range investigated.

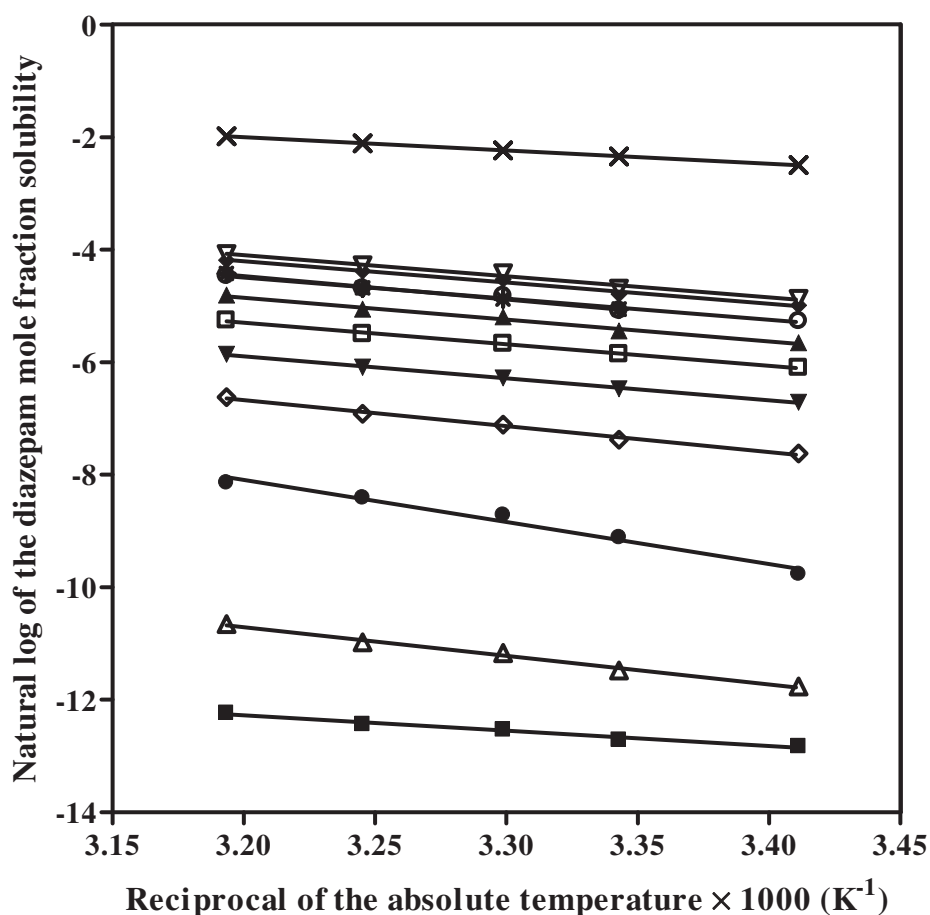


Figure 2.7. Natural logarithm of the experimental mole fraction solubility of diazepam in water + *tert*-butyl alcohol solvent mixtures as function of the reciprocal of the absolute temperature (■): $w_{\text{TBA}} = 0.00$; (△): $w_{\text{TBA}} = 0.10$; (●): $w_{\text{TBA}} = 0.20$; (◇): $w_{\text{TBA}} = 0.30$; (▼): $w_{\text{TBA}} = 0.40$; (□): $w_{\text{TBA}} = 0.50$; (▲): $w_{\text{TBA}} = 0.60$; (○): $w_{\text{TBA}} = 0.70$; (◆): $w_{\text{TBA}} = 0.80$; (▽): $w_{\text{TBA}} = 0.90$; (*): $w_{\text{TBA}} = 1.00$; (×): Ideal (the solid lines are model fits to experimental data as described in section 2.2.2; error bars are omitted for readability).

Table 2.5. Parameters of the linear regression of the natural logarithm of the diazepam mole fraction solubility x_2^{sat} on reciprocal of the absolute system temperature T for the different water + *tert*-butyl alcohol solvent mixtures and derived thermodynamic quantities at pressure $P = 0.1$ MPa^a.

w_{TBA}^b	n^c	Linear regression parameters of van't Hoff solubility curves			$\Delta_{\text{sol}}H_{\text{m},2}^{\text{sat}}$ (kJ·mol ⁻¹)	$\Delta_{\text{fus}}S_{\text{m},2} + S_{\text{m},2}^{\text{sat,E}}$ (J·K ⁻¹ ·mol ⁻¹)
		Slope (K)	Intercept	r^2		
0.00	5	-2.719 (0.239) · 10 ³ **	-3.579 (0.787) · 10 ⁰ *	0.9774 **	22.61 (1.98)	-29.76 (6.54)
0.10	5	-5.076 (0.263) · 10 ³ ***	5.532 (0.868) · 10 ⁰ **	0.9920 ***	42.20 (2.19)	46.00 (7.22)
0.20	5	-7.451 (0.631) · 10 ³ **	1.575 (0.208) · 10 ¹ **	0.9789 **	61.94 (5.25)	130.92 (17.31)
0.30	5	-4.611 (0.226) · 10 ³ ***	8.079 (0.747) · 10 ⁰ **	0.9928 ***	38.34 (1.88)	67.17 (6.21)
0.40	5	-3.914 (0.114) · 10 ³ ****	6.627 (0.376) · 10 ⁰ ****	0.9975 ****	32.54 (0.95)	55.10 (3.13)
0.50	5	-3.830 (0.135) · 10 ³ ****	6.959 (0.444) · 10 ⁰ ****	0.9963 ****	31.85 (1.12)	57.86 (3.69)
0.60	5	-3.885 (0.232) · 10 ³ ***	7.580 (0.765) · 10 ⁰ **	0.9894 ***	32.30 (1.93)	63.02 (6.36)
0.70	5	-3.742 (0.260) · 10 ³ ***	7.478 (0.858) · 10 ⁰ **	0.9857 ***	31.11 (2.16)	62.17 (7.13)
0.80	5	-3.751 (0.235) · 10 ³ ***	7.793 (0.774) · 10 ⁰ **	0.9883 ***	31.18 (1.95)	64.79 (6.43)
0.90	5	-3.721 (0.274) · 10 ³ ***	7.805 (0.903) · 10 ⁰ **	0.9840 ***	30.94 (2.28)	64.89 (7.51)
1.00	4	-4.182 (0.172) · 10 ³ **	8.912 (0.564) · 10 ⁰ **	0.9966 **	34.77 (1.43)	74.10 (4.69)
Ideal	5	-2.359 (0.013) · 10 ³ ****	5.545 (0.044) · 10 ⁰ ****	0.9999 ****	19.61 (0.11)	46.10 (0.37)

^a Values in parentheses are standard deviations, $u(T) = 0.03$ K, $u_r(P) = 0.05$ and $u_r(w_{\text{TBA}}) = 0.005$.

^b Mass fraction of *tert*-butyl alcohol in the solvent mixture free of solute.

^c Number of regressed data points.

**** $p \leq 0.0001$, *** $p \leq 0.001$, ** $p \leq 0.01$, * $p \leq 0.05$

2.4.2. Thermodynamics of the solubility of diazepam in water + *tert*-butyl alcohol solvent mixtures²

As described in the theoretical section, the overall dissolution process of DZP in the different W + TBA solvent mixtures under phase equilibrium conditions can be decomposed into fusion of pure solid drug crystals and mixing of the resultant hypothetical pure supercooled liquid form of the drug with the liquid solvent, both processes occurring at the same temperature as the saturated solution. Since the contribution of the solid-state properties of DZP to the dissolution process of the drug at a given system temperature is constant over the whole solvent composition range, variations in partial molar thermodynamic quantities of dissolution with the cosolvent content in the mixture depends only on those of the mixing process. Since the mixing process of the drug in actual solutions can be decomposed into those of the ideal solution corrected by excess quantities, only the latter are presented here since in addition to cancelling the constant molar thermodynamic quantities relative to the fusion process of DZP out, they also provide deviation of the system from ideality. Nevertheless, values of the changes in thermodynamic quantities of DZP upon fusion and mixing, as well as their relative contribution to the dissolution process of the drug for the different systems investigated are given in Appendix B along with those of the partial molar entropy of dissolution (Tables B.3 to B.6).

2.4.2.1. Activity coefficient of diazepam in water + *tert*-butyl alcohol solvent mixtures

The values of the activity coefficient of DZP in saturated solutions γ_2^{sat} are given in Table 2.6. They were calculated from Eqs. (2.27) and (2.28) using experimental solubility and calculated ideal solubility values displayed in Table 2.4. In all cases, the activity coefficient values are superior to the unity and the largest ones are obtained in neat water ($\gamma_2^{\text{sat}} \cong 30\,000$). As the mass fraction of TBA in the solvent mixture increases, the activity coefficient values decrease, indicating a more ideal behavior in presence of the cosolvent. The lowest activity coefficients are found in the mixtures with a TBA mass fraction of 0.90 ($\gamma_2^{\text{sat}} \cong 10$) which corresponds to the solvent composition of DZP maximum solubility. In addition, for all the studied solvent compositions with exception of neat water, the activity coefficient values decrease as the temperature increases, indicating lesser deviations from ideality at higher solution temperatures.

² By defining the standard pressure as the atmospheric pressure and by selecting the reference temperature as the system temperature, all thermodynamic quantities presented in this work become standard thermodynamic quantities.

Table 2.6. Activity coefficient of diazepam γ_2^{sat} in water + *tert*-butyl alcohol solvent mixtures at system temperature T and pressure $P = 0.1$ MPa.^a

$w_{\text{TBA}}^{\text{b}}$	$T = 293.15$ K	$T = 299.15$ K	$T = 303.15$ K	$T = 308.15$ K	$T = 313.15$ K
γ_2^{sat}					
0.00	$3.051 (0.059) \cdot 10^4$	$3.191 (0.066) \cdot 10^4$	$2.955 (0.057) \cdot 10^4$	$3.045 (0.049) \cdot 10^4$	$2.821 (0.055) \cdot 10^4$
0.10	$1.053 (0.052) \cdot 10^4$	$9.294 (0.166) \cdot 10^3$	$7.569 (0.137) \cdot 10^3$	$7.084 (0.124) \cdot 10^3$	$5.816 (0.193) \cdot 10^3$
0.20	$1.425 (0.228) \cdot 10^3$	$8.733 (0.230) \cdot 10^2$	$6.484 (0.171) \cdot 10^2$	$5.410 (0.103) \cdot 10^2$	$4.707 (0.135) \cdot 10^2$
0.30	$1.685 (0.066) \cdot 10^2$	$1.531 (0.033) \cdot 10^2$	$1.301 (0.036) \cdot 10^2$	$1.223 (0.029) \cdot 10^2$	$1.029 (0.039) \cdot 10^2$
0.40	$6.739 (0.227) \cdot 10^1$	$6.241 (0.115) \cdot 10^1$	$5.687 (0.161) \cdot 10^1$	$5.352 (0.107) \cdot 10^1$	$4.796 (0.218) \cdot 10^1$
0.50	$3.645 (0.115) \cdot 10^1$	$3.355 (0.074) \cdot 10^1$	$3.082 (0.081) \cdot 10^1$	$2.959 (0.058) \cdot 10^1$	$2.617 (0.065) \cdot 10^1$
0.60	$2.345 (0.057) \cdot 10^1$	$2.222 (0.076) \cdot 10^1$	$1.925 (0.037) \cdot 10^1$	$1.908 (0.038) \cdot 10^1$	$1.678 (0.043) \cdot 10^1$
0.70	$1.589 (0.059) \cdot 10^1$	$1.552 (0.040) \cdot 10^1$	$1.323 (0.030) \cdot 10^1$	$1.312 (0.027) \cdot 10^1$	$1.189 (0.027) \cdot 10^1$
0.80	$1.203 (0.029) \cdot 10^1$	$1.159 (0.026) \cdot 10^1$	$9.903 (0.195) \cdot 10^0$	$9.700 (0.367) \cdot 10^0$	$9.031 (0.204) \cdot 10^0$
0.90	$1.072 (0.025) \cdot 10^1$	$1.046 (0.021) \cdot 10^1$	$8.814 (0.227) \cdot 10^0$	$8.736 (0.145) \cdot 10^0$	$8.117 (0.353) \cdot 10^0$
1.00	—	$1.514 (0.028) \cdot 10^1$	$1.398 (0.046) \cdot 10^1$	$1.304 (0.025) \cdot 10^1$	$1.148 (0.037) \cdot 10^1$

^a Values in parentheses are standard deviations, $u(T) = 0.03$ K, $u_i(P) = 0.05$ and $u_i(w_{\text{TBA}}) = 0.005$.

^b Mass fraction of *tert*-butyl alcohol in the solvent mixture free of solute.

2.4.2.2. Excess partial molar thermodynamic quantities of diazepam in water + *tert*-butyl alcohol solvent mixtures

The values of the partial molar excess thermodynamic quantities of DZP in the different saturated solutions are given in Table 2.7 and depicted in Figure 2.8 as a function of the solvent mixture composition. Table 2.7 also includes the relative contribution of excess partial molar enthalpy and entropy to the excess partial molar Gibbs energy. Let us notice that the solute excess partial molar entropy can be calculated according to two methods. Firstly, one can use the intercept of the van't Hoff solubility plots according to Eqs. (2.20) and (2.21) (see Table 2.5). Secondly, one can use Eqs. (2.24), (2.25) and (2.26). The two methods give values that differ for less than $1 \text{ J}\cdot\text{K}^{-1}\cdot\text{mol}^{-1}$.

As can be seen from Table 2.7, the values of the solute excess partial Gibbs energy $G_{m,2}^{\text{sat,E}}$ are positive in all solvent mixtures over the temperature range investigated, indicating positive deviations of the systems of interest from ideal behavior, as expected from the values of the activity coefficient of DZP presented in Table 2.6. Considering the variation of this thermodynamic quantity with the solvent composition for a given system temperature, it can be observed from Figure 2.8.A that the value of the excess partial molar Gibbs energy of DZP presents a maximum in neat water ($G_{m,2}^{\text{sat,E}} \cong 26 \text{ kJ}\cdot\text{mol}^{-1}$) and decreases in a smooth and continuous manner as the mass fraction of TBA in the solvent increases down to a minimum in the solvent mixture with a TBA mass fraction of 0.90 ($G_{m,2}^{\text{sat,E}} \cong 5.6 \text{ kJ}\cdot\text{mol}^{-1}$) and then slightly increases in neat *tert*-butyl alcohol ($G_{m,2}^{\text{sat,E}} \cong 6.6 \text{ kJ}\cdot\text{mol}^{-1}$). It can be noticed that for all the solvent composition investigated, the excess partial molar Gibbs energy of DZP is not very temperature dependent, may be with exception of neat water and the solvent mixture containing a TBA mass fraction of 0.20 for which increasing the temperature results in an increase and a decrease in these thermodynamic quantities, respectively.

Regarding to the relative contribution (RC) of the excess partial molar enthalpy to the excess partial molar Gibbs energy of DZP in the different W + TBA solvent mixtures, one can observed from Table 2.7 and Figure 2.8.B that for every solvent compositions investigated, enthalpy is the main contributor to deviation of the systems from ideality, with noticeable exception of neat water. In this particular solvent, entropy contribution accounts for about 90% of the excess partial molar Gibbs energy of DZP. This is in good agreement with the thermodynamic features related to hydrophobic hydration phenomenon in which rearrangement of the H-bond network of water in the vicinity of hydrophobic solute molecules results in structural changes in the system accompanied by a large negative excess entropy [74, 75].

Table 2.7. Partial molar excess thermodynamic quantities of diazepam $G_{m,2}^{\text{sat,E}}$, $H_{m,2}^{\text{sat,E}}$, $TS_{m,2}^{\text{sat,E}}$ and $S_{m,2}^{\text{sat,E}}$ in water + *tert*-butyl alcohol solvent mixtures at system temperature T and pressure $P = 0.1 \text{ MPa}$ ^a.

$w_{\text{TBA}}^{\text{b}}$	$G_{m,2}^{\text{sat,E}}$ (kJ·mol ⁻¹)	$H_{m,2}^{\text{sat,E}}$ (kJ·mol ⁻¹)	$TS_{m,2}^{\text{sat,E}}$ (kJ·mol ⁻¹)	$S_{m,2}^{\text{sat,E}}$ (J·K ⁻¹ ·mol ⁻¹)	$H_{m,2}^{\text{sat,E}}$ (%RC) ^c	$TS_{m,2}^{\text{sat,E}}$ (%RC) ^d
$T = 293.15 \text{ K}$						
0.00	25.17 (2.81)	3.62 (1.99)	-21.54 (1.99)	-73.49 (6.77)	14.4	85.6
0.10	22.57 (3.10)	23.21 (2.19)	0.64 (2.19)	2.19 (7.48)	97.3	2.7
0.20	17.70 (7.42)	42.96 (5.25)	25.26 (5.25)	86.16 (17.90)	63.0	37.0
0.30	12.50 (2.67)	19.35 (1.89)	6.86 (1.89)	23.39 (6.44)	73.8	26.2
0.40	10.26 (1.35)	13.56 (0.96)	3.30 (0.96)	11.24 (3.26)	80.4	19.6
0.50	8.76 (1.60)	12.86 (1.13)	4.09 (1.13)	13.97 (3.84)	75.8	24.2
0.60	7.69 (2.73)	13.31 (1.93)	5.62 (1.93)	19.18 (6.59)	70.3	29.7
0.70	6.74 (3.06)	12.13 (2.17)	5.39 (2.17)	18.37 (7.39)	69.2	30.8
0.80	6.06 (2.76)	12.20 (1.96)	6.13 (1.95)	20.92 (6.66)	66.5	33.5
0.90	5.78 (3.23)	11.95 (2.28)	6.17 (2.28)	21.04 (7.78)	66.0	34.0
$T = 299.15 \text{ K}$						
0.00	25.79 (2.81)	3.23 (1.99)	-22.56 (1.99)	-75.41 (6.64)	12.5	87.5
0.10	22.73 (3.10)	22.83 (2.19)	0.10 (2.19)	0.34 (7.32)	99.6	0.4
0.20	16.84 (7.42)	42.57 (5.25)	25.73 (5.25)	86.00 (17.54)	62.3	37.7
0.30	12.51 (2.67)	18.96 (1.88)	6.45 (1.89)	21.56 (6.31)	74.6	25.4
0.40	10.28 (1.35)	13.17 (0.96)	2.89 (0.95)	9.66 (3.19)	82.0	18.0
0.50	8.74 (1.59)	12.47 (1.13)	3.73 (1.13)	12.48 (3.76)	77.0	23.0
0.60	7.71 (2.73)	12.92 (1.93)	5.21 (1.93)	17.42 (6.46)	71.3	28.7
0.70	6.82 (3.06)	11.74 (2.17)	4.92 (2.16)	16.44 (7.24)	70.5	29.5
0.80	6.09 (2.76)	11.81 (1.96)	5.71 (1.95)	19.10 (6.53)	67.4	32.6
0.90	5.84 (3.23)	11.56 (2.28)	5.72 (2.28)	19.13 (7.62)	66.9	33.1
1.00	6.76 (2.04)	15.39 (1.44)	8.63 (1.44)	28.85 (4.81)	64.1	35.9
$T = 303.15 \text{ K}$						
0.00	25.94 (2.81)	2.98 (1.99)	-22.97 (1.99)	-75.77 (6.55)	11.5	88.5
0.10	22.51 (3.10)	22.57 (2.19)	0.06 (2.19)	0.18 (7.23)	99.8	0.2
0.20	16.32 (7.42)	42.31 (5.25)	25.99 (5.25)	85.74 (17.31)	61.9	38.1
0.30	12.27 (2.67)	18.70 (1.89)	6.43 (1.89)	21.22 (6.22)	74.4	25.6
0.40	10.18 (1.35)	12.91 (0.96)	2.73 (0.96)	8.99 (3.16)	82.6	17.4

^a Values in parentheses are standard deviations, $u(T) = 0.03 \text{ K}$, $u_r(P) = 0.05$ and $u_r(w_{\text{TBA}}) = 0.005$.

^b Mass fraction of *tert*-butyl alcohol in the solvent mixture free of solute.

$$^c \text{RC}_{H_{m,2}^{\text{sat,E}}} = \left| H_{m,2}^{\text{sat,E}} \right| / \left[\left| H_{m,2}^{\text{sat,E}} \right| + \left| TS_{m,2}^{\text{sat,E}} \right| \right]$$

$$^d \text{RC}_{TS_{m,2}^{\text{sat,E}}} = \left| TS_{m,2}^{\text{sat,E}} \right| / \left[\left| H_{m,2}^{\text{sat,E}} \right| + \left| TS_{m,2}^{\text{sat,E}} \right| \right]$$

Table 2.7. Partial molar excess thermodynamic quantities of diazepam $G_{m,2}^{\text{sat,E}}$, $H_{m,2}^{\text{sat,E}}$, $TS_{m,2}^{\text{sat,E}}$ and $S_{m,2}^{\text{sat,E}}$ in water + *tert*-butyl alcohol solvent mixtures at system temperature T and pressure $P = 0.1$ MPa (*continued*)^a.

$w_{\text{TBA}}^{\text{b}}$	$G_{m,2}^{\text{sat,E}}$ (kJ·mol ⁻¹)	$H_{m,2}^{\text{sat,E}}$ (kJ·mol ⁻¹)	$TS_{m,2}^{\text{sat,E}}$ (kJ·mol ⁻¹)	$S_{m,2}^{\text{sat,E}}$ (J·K ⁻¹ ·mol ⁻¹)	$H_{m,2}^{\text{sat,E}}$ (%RC) ^c	$TS_{m,2}^{\text{sat,E}}$ (%RC) ^d
0.50	8.64 (1.59)	12.21 (1.13)	3.57 (1.13)	11.78 (3.72)	77.4	22.6
0.60	7.45 (2.73)	12.66 (1.93)	5.21 (1.93)	17.19 (6.37)	70.9	29.1
0.70	6.51 (3.06)	11.48 (2.17)	4.97 (2.16)	16.39 (7.14)	69.8	30.2
0.80	5.78 (2.76)	11.55 (1.96)	5.77 (1.95)	19.03 (6.44)	66.7	33.3
0.90	5.49 (3.23)	11.30 (2.28)	5.82 (2.28)	19.19 (7.52)	66.0	34.0
1.00	6.65 (2.04)	15.13 (1.44)	8.48 (1.44)	27.98 (4.75)	64.1	35.9
$T = 308.15$ K						
0.00	26.45 (2.81)	2.65 (1.99)	-23.80 (1.99)	-77.23 (6.44)	10.0	90.0
0.10	22.71 (3.10)	22.24 (2.19)	-0.47 (2.19)	-1.53 (7.11)	97.9	2.1
0.20	16.12 (7.42)	41.99 (5.25)	25.86 (5.25)	83.93 (17.03)	61.9	38.1
0.30	12.31 (2.67)	18.38 (1.89)	6.07 (1.89)	19.68 (6.12)	75.2	24.8
0.40	10.20 (1.35)	12.59 (0.96)	2.39 (0.96)	7.76 (3.10)	84.0	16.0
0.50	8.68 (1.59)	11.89 (1.13)	3.21 (1.13)	10.41 (3.65)	78.7	21.3
0.60	7.55 (2.73)	12.34 (1.93)	4.79 (1.93)	15.53 (6.27)	72.1	27.9
0.70	6.59 (3.06)	11.15 (2.17)	4.56 (2.16)	14.80 (7.02)	71.0	29.0
0.80	5.82 (2.77)	11.22 (1.96)	5.40 (1.96)	17.53 (6.35)	67.5	32.5
0.90	5.55 (3.23)	10.98 (2.28)	5.43 (2.28)	17.61 (7.40)	66.9	33.1
1.00	6.58 (2.04)	14.81 (1.44)	8.23 (1.44)	26.70 (4.67)	64.3	35.7
$T = 313.15$ K						
0.00	26.68 (2.81)	2.33 (1.99)	-24.35 (1.99)	-77.77 (6.34)	8.7	91.3
0.10	22.57 (3.10)	21.92 (2.19)	-0.65 (2.19)	-2.07 (7.00)	97.1	2.9
0.20	16.02 (7.42)	41.66 (5.25)	25.64 (5.25)	81.88 (16.76)	61.9	38.1
0.30	12.06 (2.67)	18.06 (1.89)	5.99 (1.89)	19.13 (6.03)	75.1	24.9
0.40	10.08 (1.36)	12.26 (0.96)	2.19 (0.96)	6.98 (3.07)	84.9	15.1
0.50	8.50 (1.59)	11.56 (1.13)	3.06 (1.13)	9.78 (3.60)	79.1	20.9
0.60	7.34 (2.73)	12.02 (1.93)	4.67 (1.93)	14.93 (6.17)	72.0	28.0
0.70	6.44 (3.06)	10.83 (2.17)	4.39 (2.16)	14.01 (6.91)	71.2	28.8
0.80	5.73 (2.76)	10.90 (1.96)	5.17 (1.95)	16.51 (6.24)	67.8	32.2
0.90	5.45 (3.23)	10.66 (2.28)	5.20 (2.28)	16.62 (7.29)	67.2	32.8
1.00	6.35 (2.04)	14.48 (1.44)	8.13 (1.44)	25.96 (4.60)	64.0	36.0

^a Values in parentheses are standard deviations, $u(T) = 0.03$ K, $u_r(P) = 0.05$ and $u_r(w_{\text{TBA}}) = 0.005$.

^b Mass fraction of *tert*-butyl alcohol in the solvent mixture free of solute.

$$^{\text{c}} \text{RC}_{H_{m,2}^{\text{sat,E}}} = \left| H_{m,2}^{\text{sat,E}} \right| / \left[\left| H_{m,2}^{\text{sat,E}} \right| + \left| TS_{m,2}^{\text{sat,E}} \right| \right]$$

$$^{\text{d}} \text{RC}_{TS_{m,2}^{\text{sat,E}}} = \left| TS_{m,2}^{\text{sat,E}} \right| / \left[\left| H_{m,2}^{\text{sat,E}} \right| + \left| TS_{m,2}^{\text{sat,E}} \right| \right]$$

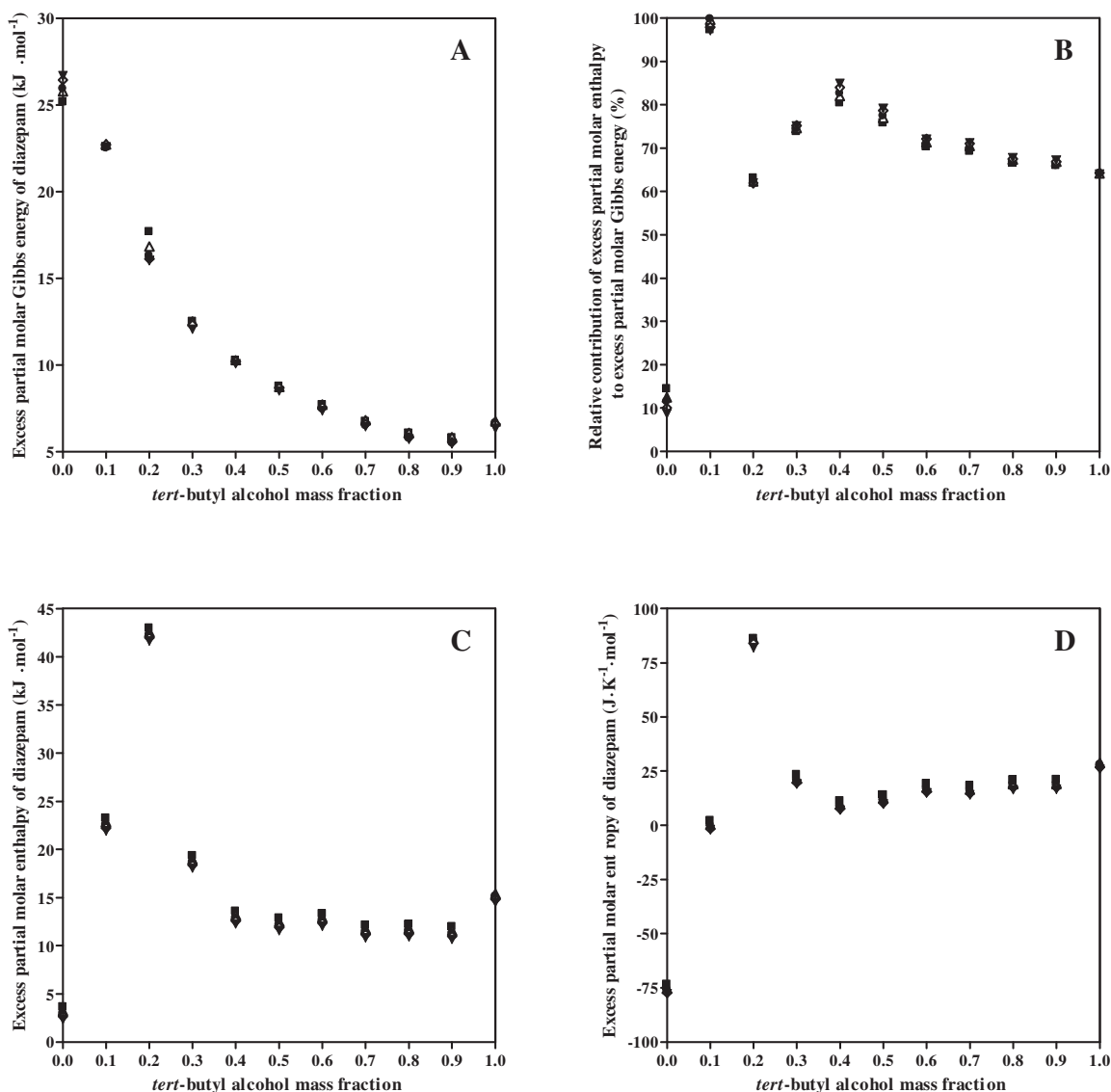


Figure 2.8. Excess partial thermodynamic quantities of diazepam in saturated water + *tert*-butyl alcohol solvent mixtures as function of the *tert*-butyl alcohol mass fraction in solvent mixture free of solute (A): Excess partial molar Gibbs energy; (B): Relative contribution of excess partial molar enthalpy to excess partial molar Gibbs energy; (C): Excess partial molar enthalpy; (D): Excess partial molar entropy; (■): $T = 293.15$ K; (△): $T = 299.15$ K; (●): $T = 303.15$ K; (◇): $T = 308.15$ K; (▼): $T = 313.15$ K (error bars are omitted for readability).

The transition from the entropic behavior in neat water to the enthalpic behavior in W + TBA solvent mixtures and in neat *tert*-butyl alcohol is linked to the simultaneous evolution of $H_{m,2}^{\text{sat,E}}(l, T, P, X)$ and $S_{m,2}^{\text{sat,E}}(l, T, P, X)$ according to Eq. (2.17). It can be observed from Figures 2.8.C and 2.8.D, respectively, that $H_{m,2}^{\text{sat,E}}$ globally increases from $3 \text{ kJ}\cdot\text{mol}^{-1}$ in neat water to approximately $13 \text{ kJ}\cdot\text{mol}^{-1}$ in the TBA-rich region while $S_{m,2}^{\text{sat,E}}$ globally increases from $-75 \text{ J}\cdot\text{mol}^{-1}\cdot\text{K}^{-1}$ in neat water to

approximately $20 \text{ J}\cdot\text{mol}^{-1}\cdot\text{K}^{-1}$ in the TBA-rich region. In between, these two quantities reach a maximum in the solvent mixture containing a TBA mass fraction of 0.20. This is no mere coincidence. Indeed, this particular W + TBA solvent mixture is an eutectic composition [28] where water and *tert*-butyl alcohol molecules interact preferentially with each other and are strongly associated through H-bonding [76]. The reverse V-shaped profile of the excess partial molar enthalpy and entropy of DZP in the water-rich region can be attributed to structuredness of the solvent as the TBA content in the solvent mixture increases up to the eutectic composition and to disruption of the solvent structure resulting from further increase in TBA content in the solvent mixture [76]. Finally, let us notice that the temperature has little influence on the excess partial molar enthalpy and entropy of DZP, especially in the water-rich region where it is almost insignificant. For every solvent composition, both these thermodynamic quantities decrease linearly with the temperature over the temperature range investigated with a constant slope of $-0.065 \text{ kJ}\cdot\text{mol}^{-1}\cdot\text{K}^{-1}$ and $-0.21 \text{ J}\cdot\text{K}^{-2}\cdot\text{mol}^{-1}$, respectively.

2.5. Conclusion and perspectives

The solubility of diazepam in water + *tert*-butyl alcohol solvent mixtures and the density of the diazepam-free and diazepam-saturated solvent mixtures were determined in the temperature range from 293.15 to 313.15 K at atmospheric pressure. The relative increase in the mixture density resulting from the presence of the drug increases with temperature and is at most of 3.6%. The solubility of diazepam depends on both solvent composition and temperature. The solubility of the drug increases as the temperature increases and as the *tert*-butyl alcohol content in the solvent mixture increases up to a mass fraction of 0.90. In this solvent mixture, the mole fraction solubility of diazepam is in the order of $1\cdot 10^{-2}$. The natural logarithm of the drug mole fraction solubility exhibits a linear dependence to the reciprocal of the system temperature over the experimental temperature range for every solvent mixture composition investigated. From the temperature dependence of the drug solubility and thermophysical properties of the drug crystals, the thermodynamic quantities related to the dissolution process of diazepam under saturation condition were calculated and the variations in the drug excess partial molar thermodynamic quantities with the solvent composition were used to identify the forces driving the variation of the drug solubility. The drug solubility enhancement resulting from the increase in the *tert*-butyl alcohol content in the solvent mixture is related to a decrease of the drug activity coefficient. In turn, this decrease is related to a simultaneous evolution of the drug excess partial molar enthalpy and entropy with respect with the solvent mixture composition.

The solubility data provided in this work were found to be reliable and accurate so that they can be used to train existing cosolvency models in their original or extended forms and to evaluate their capability and accuracy for correlating the solubility of diazepam in water + *tert*-butyl alcohol mixtures. This will be the subject of future works. However, solubility prediction of hydrophobic drugs in this cosolvent system, whatever the model retained, would require availability of a large

experimental solubility data set. Experimental determination of the solubility of non-structurally related hydrophobic drugs in water + *tert*-butyl alcohol mixtures are currently underway in our laboratory.

Nomenclature

Latin letters

A	parameter of the van't Hoff equation (K)
B	parameter of the van't Hoff equation
c	amount concentration ($\text{mol}\cdot\text{L}^{-1}$) or mass concentration ($\text{mg}\cdot\text{mL}^{-1}$)
$C_{p,m}$	molar heat capacity at constant pressure ($\text{J}\cdot\text{K}^{-1}\cdot\text{mol}^{-1}$)
cr	crystalline solid phase
F	Fisher statistic
G_m	partial molar Gibbs energy ($\text{kJ}\cdot\text{mol}^{-1}$)
H_m	partial molar enthalpy ($\text{kJ}\cdot\text{mol}^{-1}$)
l	liquid phase
M	molar mass ($\text{g}\cdot\text{mol}^{-1}$)
n	number of regressed data points
P	pressure (MPa)
p	statistical probability
R	molar ideal gas constant ($8.3145\text{ J}\cdot\text{K}^{-1}\cdot\text{mol}^{-1}$)
r^2	squared correlation coefficient
S_m	partial molar entropy ($\text{J}\cdot\text{K}^{-1}\cdot\text{mol}^{-1}$)
T	temperature (K)
t	Student statistic
u	standard uncertainty (varies)
u_r	relative standard uncertainty
w	mass fraction
X	phase composition
x	mole fraction
Z_m	partial molar quantity (varies)

Greek letters

γ	activity coefficient referenced to Raoult's law
Δ	change in quantity
μ	chemical potential ($\text{kJ}\cdot\text{mol}^{-1}$)
ρ	density ($\text{g}\cdot\text{mL}^{-1}$)

Superscripts

*	pure component
E	excess quantity
id	ideal quantity
sat	saturation condition

Subscripts

1	component 1
2	component 2
fus	fusion process

mix mixing process
sol dissolution process

Abbreviations

ACN acetonitrile
df statistical degree of freedom
CRS chemical reference substance
DSC differential scanning calorimetry
DZP diazepam
EDQM european directorate for the quality of medicines
GC gas chromatography
HPLC high performance liquid chromatography
LLOQ lower limit of quantification
LOD limit of detection
MEOH methanol
MPD mean percentage deviation
QC quality control
RC relative contribution
RSD relative standard deviation
S/N signal-to-noise ratio
TBA *tert*-butyl alcohol
TBAHS tetrabutylammonium hydrogen sulfate
UV ultraviolet
W water

References

- [1] C.A. Lipinski, Drug-like properties and the causes of poor solubility and poor permeability, *J Pharmacol Toxicol*, 44 (2000) 235-249.
- [2] G.M. Keseru, G.M. Makara, The influence of lead discovery strategies on the properties of drug candidates, *Nat Rev Drug Discov*, 8 (2009) 203-212.
- [3] C. Tyrchan, N. Blomberg, O. Engkvist, T. Kogej, S. Muresan, Physicochemical property profiles of marketed drugs, clinical candidates and bioactive compounds, *Bioorg Med Chem Lett*, 19 (2009) 6943-6947.
- [4] S. Stegemann, F. Leveiller, D. Franchi, H. de Jong, H. Lindén, When poor solubility becomes an issue: From early stage to proof of concept, *Eur J Pharm Sci*, 31 (2007) 249-261.
- [5] R. Liu, *Water-Insoluble Drug Formulation*, Second ed., CRC Press, 2008.
- [6] D. Douroumis, A. Fahr, *Drug Delivery Strategies for Poorly Water-Soluble Drugs*, John Wiley & Sons Ltd, 2013.
- [7] H.D. Williams, N.L. Trevaskis, S.A. Charman, R.M. Shanker, W.N. Charman, C.W. Pouton, C.J.H. Porter, Strategies to Address Low Drug Solubility in Discovery and Development, *Pharmacol Rev*, 65 (2013) 315-499.
- [8] J.A. Mollica, S. Ahuja, J. Cohen, Stability of pharmaceuticals, *J Pharm Sci*, 67 (1978) 443-465.
- [9] E. Fournier, M.-H. Dufresne, D. Smith, M. Ranger, J.-C. Leroux, A Novel One-Step Drug-Loading Procedure for Water-Soluble Amphiphilic Nanocarriers, *Pharm Res*, 21 (2004) 962-968.
- [10] D. Le Garrec, S. Gori, L. Luo, D. Lessard, D.C. Smith, M.A. Yessine, M. Ranger, J.C. Leroux, Poly(N-vinylpyrrolidone)-block-poly(d,l-lactide) as a new polymeric solubilizer for hydrophobic anticancer drugs: in vitro and in vivo evaluation, *J Control Release*, 99 (2004) 83-101.
- [11] C. Li, Y. Deng, A novel method for the preparation of liposomes: Freeze drying of monophasic solutions, *J Pharm Sci*, 93 (2004) 1403-1414.
- [12] D.J. Van Drooge, W.L.J. Hinrichs, H.W. Frijlink, Incorporation of lipophilic drugs in sugar glasses by lyophilization using a mixture of water and tertiary butyl alcohol as solvent, *J Pharm Sci*, 93 (2004) 713-725.
- [13] Z. Wang, Y. Deng, S. Sun, X. Zhang, Preparation of Hydrophobic Drugs Cyclodextrin Complex by Lyophilization Monophasic Solution, *Drug Dev Ind Pharm*, 32 (2006) 73-83.
- [14] Z. Wang, Y. Deng, X. Zhang, The novel application of tertiary butyl alcohol in the preparation of hydrophobic drug-HP β CD complex, *J Pharm Pharmacol*, 58 (2006) 409-414.
- [15] H. de Waard, W.L.J. Hinrichs, H.W. Frijlink, A novel bottom-up process to produce drug nanocrystals: Controlled crystallization during freeze-drying, *J Control Release*, 128 (2008) 179-183.
- [16] J. Moes, S. Koolen, A. Huitema, J. Schellens, J. Beijnen, B. Nuijen, Pharmaceutical development and preliminary clinical testing of an oral solid dispersion formulation of docetaxel (ModraDoc001), *Int J Pharm*, 420 (2011) 244-250.
- [17] M.D. Eddleston, B. Patel, G.M. Day, W. Jones, Cocrystallization by Freeze-Drying: Preparation of Novel Multicomponent Crystal Forms, *Cryst Growth Des*, 13 (2013) 4599-4606.
- [18] J. Moes, S. Koolen, A. Huitema, J. Schellens, J. Beijnen, B. Nuijen, Development of an oral solid dispersion formulation for use in low-dose metronomic chemotherapy of paclitaxel, *Eur J Pharm Biopharm*, 83 (2013) 87-94.
- [19] D.J. van Drooge, W.L.J. Hinrichs, K.A.M. Wegman, M.R. Visser, A.C. Eissens, H.W. Frijlink, Solid dispersions based on inulin for the stabilisation and formulation of Δ 9-tetrahydrocannabinol, *Eur J Pharm Sci*, 21 (2004) 511-518.
- [20] F. Franks, T. Auffret, *Freeze-drying of Pharmaceuticals and Biopharmaceuticals: Principles and Practice*, The Royal Society of Chemistry, 2007.
- [21] L. Rey, J.C. May, *Freeze Drying/Lyophilization of Pharmaceutical and Biological Products*, Third ed., Informa Healthcare, 2010.
- [22] D.L. Teagarden, D.S. Baker, Practical aspects of lyophilization using non-aqueous co-solvent systems, *Eur J Pharm Sci*, 15 (2002) 115-133.
- [23] Teagarden, D.L. Wei Wang, D.S. Baker, Practical Aspects of Freeze-Drying of Pharmaceutical and Biological Products Using Nonaqueous Cosolvent Systems, in: *Freeze Drying/Lyophilization of Pharmaceutical and Biological Products*, Third ed., Informa Healthcare, 2010, pp. 254-287.
- [24] S. Vessot, J. Andrieu, A Review on Freeze Drying of Drugs with tert-Butanol (TBA) + Water Systems: Characteristics, Advantages, Drawbacks, *Dry Technol* 30 (2012) 377-385.
- [25] S.T. Jay, Solubilization Using Cosolvent Approach, in: *Water-Insoluble Drug Formulation*, Second ed., CRC Press, 2008, pp. 161-194.

- [26] B. Nuijen, M. Bouma, R.E.C. Henrar, P. Floriano, J.M. Jimeno, H. Talsma, J.J. Kettenes-van den Bosch, A.J.R. Heck, A. Bult, J.H. Beijnen, Pharmaceutical Development of a Parenteral Lyophilized Formulation of the Novel Antitumor Agent Aplidine, *PDA J Pharm Sci Technol*, 54 (2000) 193-208.
- [27] S.C. van der Schoot, B. Nuijen, F.M. Flesch, A. Gore, D. Mirejovsky, L. Lenaz, J.H. Beijnen, Development of a bladder instillation of the indoloquinone anticancer agent EO-9 using tert-butyl alcohol as lyophilization vehicle, *AAPS PharmSciTech*, 8 (2007) E78-E87.
- [28] K. Kasraian, P.P. DeLuca, Thermal analysis of the tertiary butyl alcohol-water system and its implications on freeze-drying, *Pharm Res*, 12 (1995) 484-490.
- [29] K. Kasraian, P.P. DeLuca, The effect of tertiary butyl alcohol on the resistance of the dry product layer during primary drying, *Pharm Res*, 12 (1995) 491-495.
- [30] R. Daoussi, S. Vessot, J. Andrieu, O. Monnier, Sublimation kinetics and sublimation end-point times during freeze-drying of pharmaceutical active principle with organic co-solvent formulations, *Chem Eng Res Des*, 87 (2009) 899-907.
- [31] R. Daoussi, E. Bogdani, S. Vessot, J. Andrieu, O. Monnier, Freeze-Drying of an Active Principle Ingredient Using Organic Co-Solvent Formulations: Influence of Freezing Conditions and Formulation on Solvent Crystals Morphology, Thermodynamics Data, and Sublimation Kinetics, *Dry Technol*, 29 (2011) 1858-1867.
- [32] C.A. Lipinski, F. Lombardo, B.W. Dominy, P.J. Feeney, Experimental and computational approaches to estimate solubility and permeability in drug discovery and development settings, *Adv Drug Deliv Rev*, 64, Supplement (2012) 4-17.
- [33] B. Faller, P. Ertl, Computational approaches to determine drug solubility, *Adv Drug Deliv Rev*, 59 (2007) 533-545.
- [34] W.-Q. Tong, Practical Aspects of Solubility Determination in Pharmaceutical Preformulation, in: *Solvent Systems and Their Selection in Pharmaceutics and Biopharmaceutics*, Springer Science & Business Media, 2007, pp. 137-149.
- [35] A. Jouyban, Review of the cosolvency models for predicting solubility of drugs in water-cosolvent mixtures, *J Pharm Pharm Sci*, 11 (2008) 32-58.
- [36] A. Li, S.H. Yalkowsky, Predicting Cosolvency. 1. Solubility Ratio and Solute log Kow, *Ind Eng Chem Res*, 37 (1998) 4470-4475.
- [37] J. Millard, F. Alvarez-Nunez, S. Yalkowsky, Solubilization by cosolvents. Establishing useful constants for the log-linear model, *Int J Pharm*, 245 (2002) 153-166.
- [38] A. Jouyban, Solubility prediction of drugs in water-polyethylene glycol 400 mixtures using Jouyban-acree model, *Chem Pharm Bull* 54 (2006) 1561-1566.
- [39] A. Jouyban, W.E. Acree, Jr., In silico prediction of drug solubility in water-ethanol mixtures using Jouyban-Acree model, *J Pharm Pharm Sci*, 9 (2006) 262-269.
- [40] A. Jouyban, Prediction of drug solubility in water-propylene glycol mixtures using Jouyban-Acree model, *Pharmazie*, 62 (2007) 365-367.
- [41] A. Jouyban, In silico prediction of drug solubility in water-dioxane mixtures using the Jouyban-Acree model, *Pharmazie*, 62 (2007) 46-50.
- [42] C. Telang, R. Suryanarayanan, Crystallization of Cephalothin Sodium During Lyophilization from tert-Butyl Alcohol—Water Cosolvent System, *Pharm Res*, 22 (2005) 153-160.
- [43] B. Munjal, A.K. Bansal, Impact of Tert-Butyl Alcohol on Crystallization Kinetics of Gemcitabine Hydrochloride in Frozen Aqueous Solutions, *J Pharm Sci*, 104 (2015) 87-97.
- [44] N.E. Calcaterra, J.C. Barrow, Classics in Chemical Neuroscience: Diazepam (Valium), *ACS Chem Neurosci*, 5 (2014) 253-260.
- [45] A. Jouyban, J. Shokri, M. Barzegar-Jalali, D. Hassanzadeh, W.E. Acree, T. Ghafourian, A. Nokhodchi, Solubility of Chlordiazepoxide, Diazepam, and Lorazepam in Ethanol + Water Mixtures at 303.2 K, *J Chem Eng Data*, 54 (2009) 2142-2145.
- [46] A. Shayanfar, M.A.A. Fakhree, W.E. Acree, A. Jouyban, Solubility of Lamotrigine, Diazepam, and Clonazepam in Ethanol + Water Mixtures at 298.15 K, *J Chem Eng Data*, 54 (2009) 1107-1109.
- [47] S. Soltanpour, W.E. Acree, A. Jouyban, Solubility of 5-(2-Chlorophenyl)-7-nitro-1,3-dihydro-1,4-benzodiazepin-2-one, 7-Chloro-1-methyl-5-phenyl-3H-1,4-benzodiazepin-2-one, and 6-(2,3-Dichlorophenyl)-1,2,4-triazine-3,5-diamine in the Mixtures of Poly(ethylene glycol) 600, Ethanol, and Water at a Temperature of 298.2 K, *J Chem Eng Data*, 55 (2010) 1727-1731.
- [48] S. Soltanpour, Z. Bastami, S. Sadeghilar, M. Kouhestani, F. Pouya, A. Jouyban, Solubility of Clonazepam and Diazepam in Polyethylene Glycol 200, Propylene Glycol, N-Methyl Pyrrolidone, Ethanol, and Water at (298.2 to 318.2) K and in Binary and Ternary Mixtures of Polyethylene Glycol 200, Propylene Glycol, and Water at 298.2 K, *J Chem Eng Data*, 58 (2013) 307-314.

- [49] A. Shayanfar, W.E. Acree, A. Jouyban, Solubility of Lamotrigine, Diazepam, Clonazepam, and Phenobarbital in Propylene Glycol + Water Mixtures at 298.15 K, *J Chem Eng Data*, 54 (2009) 1153-1157.
- [50] A. Jouyban, J. Shokri, M. Barzegar-Jalali, D. Hassanzadeh, W.E. Acree, T. Ghafourian, A. Nokhodchi, Solubility of 7-Chloro-2-methylamino-5-phenyl-3H-1,4-benzodiazepine-4-oxide, 7-Chloro-1,3-dihydro-1-methyl-5-phenyl-2H-1,4-benzodiazepin-2-one, and 7-Chloro-5-(2-chlorophenyl)-3-hydroxy-1,3-dihydro-1,4-benzodiazepin-2-one in (Propane-1,2-diol + Water) at a Temperature of 303.2 K, *J Chem Eng Data*, 55 (2010) 539-542.
- [51] Z. Bastami, S. Soltanpour, V. Panahi-Azar, A. Jouyban, Solubility of clonazepam and diazepam in binary and ternary mixtures of polyethylene glycols 400 or 600, propylene glycol and water at 298.2 K – Experimental data and modeling, *J Serb Chem Soc*, 79 (2014) 445-456.
- [52] A. Shayanfar, W.E. Acree, A. Jouyban, Solubility of Clonazepam, Diazepam, Lamotrigine, and Phenobarbital in N-Methyl-2-pyrrolidone + Water Mixtures at 298.2 K, *J Chem Eng Data*, 54 (2009) 2964-2966.
- [53] S. Soltanpour, V. Panahi-Azar, A. Taheri, Z. Bastami, A. Jouyban, Solubility Data of Diazepam in Binary and Ternary Mixtures of PEGs 200 and 400 with N-Methyl Pyrrolidone and Water at 298.2 K: Experimental Data and Modeling, *J Sol Chem*, 42 (2013) 2281-2295.
- [54] A. Ramezani, A. Shayanfar, J.L. Manzoori, A. Jouyban, Solubility of some basic drugs in dioxane + water mixtures at 298.2 K, *Lat Am J Pharm*, 31 (2012) 1176-1181.
- [55] M. Škerget, Ž. Knez, M. Knez-Hrnčič, Solubility of Solids in Sub- and Supercritical Fluids: a Review, *J Chem Eng Data*, 56 (2011) 694-719.
- [56] K.N. Marsh, J.A. Boxall, R. Lichtenthaler, Room temperature ionic liquids and their mixtures—a review, *Fluid Phase Equilib*, 219 (2004) 93-98.
- [57] A. Forte, C.I. Melo, R. Bogel-Lukasik, E. Bogel-Lukasik, A favourable solubility of isoniazid, an antitubercular antibiotic drug, in alternative solvents, *Fluid Phase Equilib*, 318 (2012) 89-95.
- [58] A.D. dos Santos, A.R.C. Morais, C. Melo, R. Bogel-Lukasik, E. Bogel-Lukasik, Solubility of pharmaceutical compounds in ionic liquids, *Fluid Phase Equilib*, 356 (2013) 18-29.
- [59] R.A. Faria, E. Bogel-Lukasik, Solubilities of pharmaceutical and bioactive compounds in trihexyl(tetradecyl)phosphonium chloride ionic liquid, *Fluid Phase Equilib*, 397 (2015) 18-25.
- [60] Y. Yamini, J. Hassan, S. Haghgo, Solubilities of Some Nitrogen-Containing Drugs in Supercritical Carbon Dioxide, *J Chem Eng Data*, 46 (2001) 451-455.
- [61] S.I. Sandler, Phase Equilibrium in Mixtures, in: *Chemical and Engineering Thermodynamics*, Third ed., John Wiley & Sons Ltd, 1999, pp. 478-629.
- [62] ICH Harmonized Tripartite Guideline Q2 (R1), Validation of Analytical Procedures: Text and Methodology, International Conference on the Harmonization of Technical Requirements for the Registration of Pharmaceuticals for Human Use, 2005.
- [63] N.S. Nudelman, R.G. de Waisbaum, Acid hydrolysis of diazepam. Kinetic study of the reactions of 2-(N-methylamino)-5-chlorobenzophenone, with HCl in MeOH-H₂O, *J Pharm Sci*, 84 (1995) 998-1004.
- [64] S.K. Yang, Mechanism of Alkaline Hydrolysis of Diazepam, *J Chin Chem Soc*, 45 (1998) 277-284.
- [65] J.H. Hildebrand, R.L. Scott, Thermodynamic Relations, in: *Regular Solutions*, Prentice Hall, 1962, pp. 8-25.
- [66] S. Neau, S. Bhandarkar, E. Hellmuth, Differential Molar Heat Capacities to Test Ideal Solubility Estimations, *Pharm Res*, 14 (1997) 601-605.
- [67] P.R. Bevington, D.K. Robinson, *Data Reduction and Error Analysis for the Physical Sciences*, Third ed., McGraw-Hill, 2003.
- [68] J.T. Rubino, Solubilization of Some Poorly Soluble Drugs by Cosolvents, Ph.D. Thesis, University of Arizona, United States of America, 1984.
- [69] C.M. Wassvik, A.G. Holmén, C.A.S. Bergström, I. Zamora, P. Artursson, Contribution of solid-state properties to the aqueous solubility of drugs, *Eur J Pharm Sci*, 29 (2006) 294-305.
- [70] S. Verheyen, P. Augustijns, R. Kinget, G. Van den Mooter, Determination of partial solubility parameters of five benzodiazepines in individual solvents, *Int J Pharm*, 228 (2001) 199-207.
- [71] G.I. Egorov, D.M. Makarov, Densities and volume properties of (water + tert-butanol) over the temperature range of (274.15 to 348.15) K at pressure of 0.1 MPa, *J Chem Thermodyn*, 43 (2011) 430-441.
- [72] L. Du-Cuny, J. Huwyler, M. Wiese, M. Kansy, Computational aqueous solubility prediction for drug-like compounds in congeneric series, *Eur J Med Chem*, 43 (2008) 501-512.
- [73] A. Jouyban, J. Shokri, M. Barzegar-Jalali, D. Hassanzadeh, W.E. Acree, T. Ghafourian, A. Nokhodchi, Solubility of Benzodiazepines in Polyethylene Glycol 200 + Water Mixtures at 303.2 K, *J Chem Eng Data*, 55 (2010) 519-522.

- [74] V.V. Yaminsky, E.A. Vogler, Hydrophobic hydration, *Curr Opin Colloid Interface Sci*, 6 (2001) 342-349.
- [75] Y.A. Mikheev, L.N. Guseva, E.Y. Davydov, Y.A. Ershov, The hydration of hydrophobic substances, *Russ J Phys Chem A*, 81 (2007) 1897-1913.
- [76] D. Subramanian, J.B. Klauda, J. Leys, M.A. Anisimov, Thermodynamic anomalies and structural fluctuations in aqueous solutions of tertiary butyl alcohol, *Herald of St. Petersburg University*, 4 (2013) 139-153.

Chapter 3

Solubility of diazepam in water + *tert*-butyl alcohol solvent mixtures: Correlation using Scatchard-Hildebrand and combined Scatchard-Hildebrand/Flory-Huggins excess Gibbs energy models

Abstract

The aim of this work is to evaluate the performances of two excess Gibbs energy models, namely the Scatchard-Hildebrand model and the combined Scatchard-Hildebrand/Flory-Huggins model, in correlating the composition and temperature dependence of the solubility of diazepam in water + *tert*-butyl alcohol solvent mixtures. The dependence of the pure component properties required as input data to the models on temperature was considered as well as that of the adjustable binary interaction parameters. For this purpose, a set of twenty-seven model versions containing from three up to six adjustable parameters and differing from one another by the dependence of at least one binary interaction parameter on temperature was generated for the two excess Gibbs energy models investigated. To rank and weight among these different model versions, second-order Akaike's information criterion corrected for small sample size was used. The correlative performances of the most parsimonious versions of the Scatchard-Hildebrand and combined Scatchard-Hildebrand/Flory-Huggins models selected from this approach were then evaluated, compared and discussed.

This page is intentionally left blank.

3.1. Introduction

Solvent mixtures are of widespread use in the pharmaceutical industry as reaction, crystallization, extraction, separation or formulation media [1]. Over the past decades, water + *tert*-butyl alcohol solvent mixtures have been received an increasing interest from scientists in both academic and industrial settings as lyophilization vehicle for the preparation of freeze-dried pharmaceutical compositions [2-4]. In addition to be fully miscible with water under ambient temperature and pressure conditions, *tert*-butyl alcohol is a low toxicity [5] and environmentally friendly solvent relatively safe in use [6] which exhibits suitable physical properties with regard to the freeze-drying process including a high fusion temperature, a high solid vapor pressure and a low sublimation enthalpy [2-4]. Binary mixtures of this monohydric alcohol with water share these desirable properties as well so that, unlike other aqueous organic cosolvent systems, they can be frozen under operating conditions for conventional industrial-scale freeze-dryers [7-11] and, for identical process parameters, they sublime faster than neat water [12, 13]. Although to date this cosolvent system is used for the industrial production of a single marketed drug approved by the Food and Drug Administration [14, 15], it has been successfully investigated for the last fifteen years as freeze-drying medium for a wide variety of bulk or formulated small-molecule therapeutic agents including, among others, anti-inflammatories [16-21], antibiotics [22, 23], anticonvulsants [24-28], antidiabetics [29], antiemetics [20, 24, 30, 31], antihyperlipidemics [32-35], antihypertensives [17, 24, 28, 36], antineoplastics [31, 37-49], contraceptives [50] and immunosuppressants [24, 48, 51, 52]. Some of these drug formulations freeze-dried from water + *tert*-butyl alcohol solvent mixtures were evaluated for proof-of-concept in humans [41, 44, 47] and it can be expected that many others will enter clinical study in the near future.

The first step in the manufacturing process of most lyophilized pharmaceutical compositions consisting in preparing a homogeneous solution of the ingredients to be dried, the use of water + *tert*-butyl alcohol solvent mixtures is especially valuable when considering freeze-drying of high-dosage hydrophobic drugs, for which the concentration in the solution to be lyophilized must be high enough to make the whole process economically viable for a large-scale production [2-4]. Besides to enable to incorporate the intended amount of drug per unit dosage form in an acceptable volume of solvent, it can also decrease the hydrolytic degradation rate of water-labile drugs in solution [41, 53, 54]. This allows performing pre-lyophilization unit operations over an extended temperature range and/or time-period, thus adding flexibility in the manufacturing process as well as in the production scheduling of such freeze-dried pharmaceutical compositions [55, 56]. Rational design of such poorly water-soluble drug formulations intended to be freeze-dried obviously requires, among many others, knowledge of the solubility of the drug of interest in water + *tert*-butyl alcohol solvent mixtures. However, it is unlikely to be found in the literature, let alone under temperature conditions of interest, since at this

time, solubility data of drugs in this cosolvent system are very scarce and often limited to a narrow solvent composition range [41, 57, 58].

Even if experimental values are always desirable, experimental determination of drug solubility is a time-consuming and cost-effective procedure being mostly unworkable for drug candidates in the early stages of development [59-61]. Fortunately, a countless number of mathematical expressions have been developed and expanded in the past allowing modeling solid-liquid equilibrium data. Among thermodynamic models, the Scatchard-Hildebrand equation [62, 63], the Wilson equation [64], the non-random two liquids equation [65] and the universal quasi-chemical equation [66] have been widely used in their original or modified forms to describe solubility of a large variety of drugs in either pure or mixed solvents including, non-exhaustively, analgesic and antipyretic agents [67-84], anti-infective agents [68, 74, 77, 85-98], central system nervous agents [68, 72, 83, 99-105], antihistamine agents [77, 82, 100, 104, 106-111] as well as hormones and vitamins [74, 112-114]. Above and beyond their capabilities and limitations, one common feature of these excess Gibbs energy models is that they are all parameterized in terms of binary interaction parameters, characteristic of a given pair of unlike molecules. Hence, they can be employed not only to correlate the solubility of drugs in either pure or mixed solvents, but also to predict the solubility of drugs in mixed solvents from binary equilibrium data. Nevertheless, determination of the binary interaction parameters set for a given multicomponent system from global regression of multicomponent equilibrium data commonly yields a better representation of the phase equilibria under specified temperature and pressure conditions than from regression of binary equilibrium data for all possible contributing binary subsystems, as discussed elsewhere [115].

In the first part of this work [116], solubility data of the poorly water-soluble drug diazepam (7-chloro-1,3-dihydro-1-methyl-5-phenyl-2H-1,4-benzodiazepin-2-one) in water + *tert*-butyl alcohol solvent mixtures in the temperature range from 293.15 to 313.15 K were reported. From these, the changes in thermodynamic quantities of diazepam upon fusion and mixing as well as the excess thermodynamic quantities of the drug in the different saturated solvent compositions over the temperature range investigated were determined using classical thermodynamic approaches. As a direct continuation, the aim of the present study is to evaluate the correlative performance of the Scatchard-Hildebrand model, both corrected and uncorrected for relative difference in molar volume of individual components in the liquid phase, in correlating the dependence of the solubility of diazepam in water + *tert*-butyl alcohol solvent mixtures on solute-free binary solvent composition and system temperature. Unlike local composition theory-based excess Gibbs energy models, the Scatchard-Hildebrand equation, combined or not to the Flory-Huggins equation for the excess molar combinatorial entropy of mixing, contains only one adjustable binary interaction parameter per pair of unlike molecules but due to the assumptions underlying the model, its use in the chemical engineering

literature is traditionally restricted to liquid mixtures into which the only intermolecular interactions existing are instantaneous dipole-induced dipole forces [117-128]. In the pharmaceutical literature, however, a modified form of the Scatchard-Hildebrand model introduced by Martin and coworkers [85, 86, 99, 100, 106, 112, 129] is widely used to correlate the solubility of drugs in mixed solvents, included hydrogen-bonded cosolvent systems such as that presently investigated [67, 69, 78, 79, 81, 87, 88, 93, 95, 101, 102, 107, 108]. In this approach, the Scatchard-Hildebrand expression for the activity coefficient of a component in a binary mixture is used, irrespectively of the real number of components in the saturated liquid phase, and the cosolvent system is considered as a pure component so that the resulting equation does contain only one adjustable parameter, but this depends on both the qualitative and quantitative composition of the mixed solvent. In the present work, the use of this approach was avoided in order to preserve the capability of the model to predict multicomponent equilibrium data from binary equilibrium data only. Furthermore, it was considered that the capability of the excess Gibbs energy models investigated in correlating the solubility of diazepam in water + *tert*-butyl alcohol solvent mixtures over the temperature range under consideration could be enhanced by taking into account not only the temperature dependence of the pure component properties required to their use, but also that of the binary interaction parameters and for this purpose, an approach based on information-theoretic concepts was employed. The correlative performances of the most parsimonious versions of the Scatchard-Hildebrand and combined Scatchard-Hildebrand/Flory-Huggins models selected from this approach were evaluated, compared and discussed, before providing some practical recommendations for their use.

3.2. Theory

3.2.1. Solid-liquid equilibria

According to the International Union of Pure and Applied Chemistry (IUPAC) [130], solubility is defined as the analytical composition of a mixture saturated with respect to one of its components, expressed in terms of the proportion of the designated component in the designated mixture, and hence, it can be determined only from phase equilibria experiments. In the framework of solid-fluid equilibria, analytical expressions describing the solubility of a component in a fluid can be derived from complete thermodynamic equilibrium condition between phases and relevant thermodynamic cycle, as described elsewhere [131, 132]. Accordingly, provided that the solid phase is made of pure k and presents a single crystalline form, the solubility of component k in either a pure or a mixed homogeneous solvent at the system temperature and pressure is given by the following general expression:

$$\ln x_k^{\text{sat}} = - \left\{ \frac{\Delta_{\text{fus}} H_{m,k}(T_{\text{fus},k})}{RT} \left[1 - \frac{T}{T_{\text{fus},k}} \right] + \frac{1}{RT} \int_{T_{\text{fus},k}}^T \Delta C_{p,m,k}(T') dT' - \frac{1}{R} \int_{T_{\text{fus},k}}^T \Delta C_{p,m,k}(T') \frac{dT'}{T'} \right\} - \ln \gamma_k^{\text{sat}} \quad (3.1)$$

where $x_k^{\text{sat}} = x_k^{\text{sat}}(1, T, P, X)$ and $\gamma_k^{\text{sat}} = \gamma_k^{\text{sat}}(1, T, P, X)$ are respectively the mole fraction solubility and the symmetrical activity coefficient of component k in the saturated liquid phase of composition X at the system temperature T and pressure P , $\Delta_{\text{fus}} H_{m,k}(T_{\text{fus},k}) = H_{m,k}^*(1, T_{\text{fus},k}, P) - H_{m,k}^*(\text{cr}, T_{\text{fus},k}, P)$ is the molar fusion enthalpy of pure component k at its fusion temperature at the system pressure $T_{\text{fus},k} = T_{\text{fus},k}(P)$, $\Delta C_{p,m,k}(T') = C_{p,m,k}^*(1, T') - C_{p,m,k}^*(\text{cr}, T')$ is the differential molar heat capacity at constant system pressure between the hypothetical pure supercooled liquid and crystalline solid forms of component k at any temperature T' comprised in the range $[T; T_{\text{fus},k}]$, R is the molar ideal gas constant, the superscripts * and sat stand respectively for pure component and mixture saturation condition, the subscript fus refers to fusion process whereas cr and l indicate the state of aggregation of the phases as crystalline solid and liquid, respectively. In this equation, the braced term represents the contribution of component k to its own solubility whereas the activity coefficient term characterizes the deviation from the ideal solubility behavior due to the non-ideality of the saturated mixture, thermodynamically expressed by its excess Gibbs energy. While the first is inherently independent of the solvent nature, the second is obviously not. Hence, computation of the mole fraction solubility of component k in a solvent at a given system temperature and pressure from Eq. (3.1) requires, in addition to knowledge of its thermophysical properties in the pure state, a model allowing to appropriately describe the excess Gibbs energy of the mixture in order to compute its activity coefficient in the saturated liquid phase.

3.2.2. Excess Gibbs energy models

From basic thermodynamics [133, 134], the activity coefficient of any component k in a mixture containing m number of components $\gamma_k = \gamma_k(1, T, P, X)$ is related to the excess molar Gibbs energy of the mixture $G_m^{\text{E}} = G_m^{\text{E}}(1, T, P, X)$ through the following equation:

$$\ln \gamma_k = \frac{1}{RT} \left(\frac{\partial G_m^{\text{E}} \sum_i^m n_i}{\partial n_k} \right)_{T, P, n_{i \neq k}} \quad (3.2)$$

where n_i is the amount of the i -th mixture component and where other terms are as previously stated. Accordingly, for any mathematical expression satisfying the Euler theorem and describing the dependence of the excess Gibbs energy of a mixture at a given system temperature and pressure as a

function of the amount of components, the activity coefficients of each component in a mixture of defined composition can be obtained from appropriate partial differentiation.

3.2.2.1. Scatchard-Hildebrand model

Derived on the basis of the works of van der Waals [135] and van Laar [136-138] by assuming, on the one hand, ideal behavior with respect to entropy and volume changes upon mixing of pure liquid components under constant temperature and pressure conditions so that the excess internal energy of a mixture equals its excess enthalpy and that changes in the nature and strength of intermolecular interaction patterns arising upon mixing of the pure liquid components account for the entire deviation of the liquid mixture from Raoult's law, and on the other hand, that under isothermal conditions the internal energy change on going from a liquid mixture to an ideal gas of same composition can be expressed by a quadratic function of the volume fractions of individual components, the Scatchard-Hildebrand model [62, 63, 139, 140] for the excess molar Gibbs energy of a multicomponent mixture into which the only intermolecular interactions existing are instantaneous dipole-induced dipole forces is as follows:

$$G_m^E = \left(\sum_{i=1}^m x_i V_{m,i}^* \right) \left\{ \frac{1}{2} \sum_{i=1}^m \sum_{j=1}^m \phi_i \phi_j \left[(\delta_i^* - \delta_j^*)^2 + 2\delta_i^* \delta_j^* l_{i,j} \right] \right\} \quad (3.3.a)$$

with $l_{i,j} = l_{j,i}$ and $l_{i,i} = l_{j,j} = \dots = 0$, for which

$$\ln \gamma_k = \frac{V_{m,k}^*}{RT} \sum_i^m \sum_j^m \phi_i \phi_j \left\{ \left[(\delta_i^* - \delta_k^*)^2 + 2l_{i,k} \delta_i^* \delta_k^* \right] - \frac{1}{2} \left[(\delta_i^* - \delta_j^*)^2 + 2l_{i,j} \delta_i^* \delta_j^* \right] \right\} \quad (3.3.b)$$

where $x_i = x_i(1, T, P, X)$ and $V_{m,i}^* = V_{m,i}^*(1, T, P)$ are the mole fraction of the i -th mixture component and the molar volume of component i in the pure liquid state at the system temperature and pressure, where $\phi_j = \phi_j(1, T, P, X)$ is the volume fraction of the the j -th mixture component defined according to both the underlying model assumption of ideal mixing behavior with respect to volume change stated above and IUPAC statements [141], as:

$$\phi_j = \frac{x_j V_{m,j}^*}{\sum_i^m x_i V_{m,i}^*} \quad (3.4)$$

and where $\delta_i^* = \delta_i^*(T, P)$ is the solubility parameter of pure component i at the system temperature and pressure defined as the square root of its cohesive energy density [142-144]¹:

$$\delta_i^* = \left(\frac{\Delta_{\text{vap}} U_{m,i}}{V_{m,i}^*} \right)^{1/2} \quad (3.5)$$

where $\Delta_{\text{vap}} U_{m,i} = U_{m,i}^*(g, T, P=0) - U_{m,i}^*(l, T, P)$ is the molar internal energy change upon isothermal vaporization of the pure liquid to the ideal gas state with g denoting the state of aggregation of the phase as gas, whereas $l_{i,j} = l_{i,j}(T, P)$ is a dimensionless empirical binary interaction parameter characteristic of a given pair of unlike molecules which can be positive or negative but usually small compared to unity, introduced into the original equation to relax it from the geometric mean mixing rule for the cohesive energy densities of unlike non-polar molecular pairs² [145, 146]. Provided that, and only if, $l_{i,j} = l_{j,k} = \dots = 0$, these equations reduce to those given by the original regular solution theory and contains only pure component properties.

3.2.2.2. Combined Scatchard-Hildebrand/Flory-Huggins model

According to Hildebrand, Prausnitz and Scott [146], the Flory-Huggins equation [147-150] for the excess molar combinatorial entropy of mixing, derived from statistical mechanics analyses of flexible chain molecules in dilute solution by using a quasi-crystalline lattice model for the liquid state and by assuming, among others, ideal mixing behavior with respect to volume change under constant temperature and pressure conditions, can be introduced into Eq. (3.3.a) in order to account for the deviation from ideality due to the relative differences in molar volume between individual mixture components:

$$G_m^E = \left(\sum_{i=1}^m x_i V_{m,i}^* \right) \left\{ \frac{1}{2} \sum_{i=1}^m \sum_{j=1}^m \phi_i \phi_j \left[(\delta_i^* - \delta_j^*)^2 + 2\delta_i^* \delta_j^* l'_{i,j} \right] \right\} + RT \sum_{i=1}^m x_i \ln \left(\frac{\phi_i}{x_i} \right) \quad (3.6.a)$$

with $l'_{i,j} = l'_{j,i}$ and $l'_{i,i} = l'_{j,j} = \dots = 0$, for which

¹ As highlighted and fully detailed by Verdier and Andersen [144], it should be emphasized that several definitions of the cohesive energy density are in use in the literature as a result of differences in both the pressure at which the molar volume of the pure liquid component is taken and the thermodynamic path used to compute its cohesive energy. The definition herein adopted is the larger one, allowing considering the dependence of the solubility parameter not only on temperature but also on pressure.

² For liquid mixtures within which intermolecular interactions other than instantaneous dipole-induced dipole forces operate and molecules differ in size and shape such as the system presently under investigation, binary interaction parameters would account for overall deviations from regular behavior, provided that the model yields a perfect quantitative agreement with experimental data.

$$\ln \gamma_k = \frac{V_{m,k}^*}{RT} \sum_i^m \sum_j^m \phi_i \phi_j \left\{ \left[(\delta_i^* - \delta_k^*)^2 + 2l'_{i,k} \delta_i^* \delta_k^* \right] - \frac{1}{2} \left[(\delta_i^* - \delta_j^*)^2 + 2l'_{i,j} \delta_i^* \delta_j^* \right] \right\} + \ln \left(\frac{\phi_k}{x_k} \right) + 1 - \frac{\phi_k}{x_k} \quad (3.6.b)$$

where all terms are as previously defined. Provided that, and only if, $V_{m,i}^* = V_{m,j}^* = V_{m,k}^* \dots$ so that $x_i = \phi_i$, these equations reduce to those set out in the preceding section and $l'_{i,j} = l_{i,j}$.

3.3. Methods

3.3.1. Calculations

As described in the theoretical section, values of both molar volume in the pure liquid state and solubility parameter of each mixture component at the system temperature and pressure are required as input data to Scatchard-Hildebrand (SH) and combined Scatchard-Hildebrand/Flory-Huggins (SH/FH) models. A common and convenient practice, consistent with the thermodynamic development of the original regular solution theory, is to assume these two parameters to be temperature and pressure independent and to use values at $T = 298.15$ K and $P = 0.1$ MPa. Although for the system under investigation solid-liquid equilibria experiments were carried out at atmospheric pressure and over a narrow temperature range comprising the herein above mentioned customary reference temperature, the dependence of molar volumes and solubility parameters of individual mixture component on temperature was considered. This was done, in part, for consistency purposes since, at first glance, binary interaction parameters were not envisioned to be temperature independent, as explicated in the following section.

For pure liquid water (W, component 1) and either pure liquid or hypothetical pure supercooled liquid *tert*-butyl alcohol (TBA, component 2), molar volume values at temperatures corresponding those used for solubility measurements as well as at the reference temperature mentioned above were calculated from knowledge of components molar mass M_i and density $\rho_i^* = \rho_i^*(1, T, P)$ at the relevant temperature and atmospheric pressure according to:

$$V_{m,i}^* = \frac{M_i}{\rho_i^*} \quad (3.7)$$

The density values of the pure liquid components required for these calculations were taken from a previous work [151]. If not available at the appropriate temperature, experimental density data provided in were regressed against temperature by ordinary least-squares method in order to estimate the few missing values. In this process, linear extrapolation and second-order polynomial interpolation

were used to obtain the density of supercooled liquid TBA at 293.15 and 298.15 K and that of liquid W at 298.15 K, respectively. The values of $V_{m,1}^*$ and $V_{m,2}^*$ computed in this way for the five isotherms investigated are given in Table 3.1. In turn, these were used to further calculate solubility parameter values for pure liquid W and either pure liquid or hypothetical pure supercooled liquid TBA at the system temperature and pressure from those at $T = 298.15$ K and $P = 0.1$ MPa reported in reference handbook [152]. This was done by using the following expression given by Fedors [153] which relates the temperature dependence of the solubility parameter of a pure liquid component to that of its molar volume, provided that T and T' do not differ by more than 150 K and that both are at or below the normal boiling temperature of the pure liquid:

$$\delta_i^*(T', P) = \delta_i^*(T, P) \left[\frac{V_{m,i}^*(1, T, P)}{V_{m,i}^*(1, T', P)} \right]^{17/15} \quad (3.8)$$

The values of δ_1^* and δ_2^* calculated in this manner at system temperature and pressure are listed in Table 3.1. For hypothetical pure supercooled liquid diazepam (DZP, component 3), molar volume and solubility parameter values at $T = 298.15$ K and $P = 0.1$ MPa were estimated from its molecular structure using the group contribution method devised by Fedors [153], as detailed in Table 3.2. Since the density of the pure liquid drug well below its fusion temperature cannot be determined experimentally, the use of Eq. (3.7) and Eq. (3.8) to obtain values of the molar volume and solubility parameter of DZP at the different temperatures of interest from those thereby calculated by group contribution method at 298.15 K is prevented. This issue was overcome by considering the solubility parameter of the solute-free binary solvent mixture $\delta_{1,2}^0 = \delta_{1,2}^0(T, P, X)$. This quantity being defined as the volume fraction average of the solubility parameters of its components [117, 154, 155], the following expression was employed to compute that of the W + TBA solvent mixture from knowledge of its composition, expressed as the mole fraction of TBA in the solute-free binary solvent mixture x_2^0 , and pure component data at the required temperature:

$$\delta_{1,2}^0 = \frac{(1-x_2^0)V_{m,1}^*\delta_1^* + x_2^0V_{m,2}^*\delta_2^*}{(1-x_2^0)V_{m,1}^* + x_2^0V_{m,2}^*} \quad (3.9)$$

The original regular solution theory predicts that when the value of the solubility parameter of a solute lies between those of two solvents, its mole fraction solubility will be greater in certain binary solvent mixtures than in either pure solvents and will reach the ideal solubility when the solute-free binary solvent mixture composition yields equality between the solubility parameter of the solute and that of the mixed solvent [117, 154, 155].

Table 3.1. Molar volume $V_{m,i}^*$ and solubility parameter δ_i^* of water, *tert*-butyl alcohol and diazepam in their pure liquid or hypothetical pure supercooled liquid state at system temperature T and pressure $P = 0.1$ MPa^a.

T (K)	Water		<i>Tert</i> -butyl alcohol		Diazepam	
	$V_{m,1}^*$ (cm ³ ·mol ⁻¹)	δ_1^* (MPa ^{1/2})	$V_{m,2}^*$ (cm ³ ·mol ⁻¹)	δ_2^* (MPa ^{1/2})	$V_{m,3}^*$ (cm ³ ·mol ⁻¹)	δ_3^* (MPa ^{1/2})
293.15	18.05	47.86	94.30	21.92	194.53	25.31
299.15	18.08	47.79	95.09	21.71	195.96	25.10
303.15	18.10	47.72	95.59	21.58	196.88	24.97
308.15	18.13	47.64	96.24	21.42	198.07	24.80
313.15	18.16	47.54	96.91	21.25	199.30	24.63

^aSee methods section 3.3.1 for details of the calculation procedure.

Table 3.2. Calculation of diazepam molar volume $V_{m,3}^*$ and solubility parameter δ_3^* at $T = 298.15$ K and pressure $P = 0.1$ MPa from Fedors group contribution method [153]^a.

Atom or group	$v_{i,3}$	$V_{m,i}$ (cm ³ ·mol ⁻¹)	$\Delta_{\text{vap}}U_{m,i}$ (J·mol ⁻¹) ^b
-CH=	8	13.5	4309.52
>C=	5	-5.5	4309.52
-CH ₃	1	33.5	4707.00
>C=O	1	10.8	17363.60
-CH ₂	1	16.1	4937.12
-N<	1	-9.0	4184.00
-N=	1	5.0	11715.20
-Cl	1	24.0	11547.84
Ring closure ≥ 5 atoms	3	16.0	1046.00
Conjugated double bond in ring	6	-2.2	1673.60

$$V_{m,3}^* = \sum_i v_{i,3} V_{m,i} = 195.70 \text{ cm}^3 \cdot \text{mol}^{-1} \text{ and } \delta_3^* = \left(\frac{\sum_i v_{i,3} \Delta_{\text{vap}} U_{m,i}}{\sum_i v_{i,3} V_{m,i}} \right)^{1/2} = 25.14 \text{ MPa}^{1/2}$$

^a $v_{i,3}$: number of atoms or groups i in diazepam; $V_{m,i}$: molar volume of atom or group i ; $\Delta_{\text{vap}}U_{m,i}$: molar internal energy of vaporization of atom or group i .

^b Converted from original values expressed in cal_{th}·mol⁻¹ by using 1 cal_{th} = 4.184 J.

Hence, and even if the maximum mole fraction solubility of DZP in W + TBA solvent mixtures was found to fall short of the ideal solubility for the different isotherms investigated, it was assumed the temperature dependence of the solubility parameter of DZP to be identical to that of the solubility parameter of the solute-free binary solvent mixture of equal value. This was supported by the fact that among the W + TBA solvent mixtures investigated, the maximum in experimental solubility of DZP was always obtained for the same solute-free binary solvent composition with $w_2^0 = 0.90$, irrespective of the system temperature [116]. Furthermore, while the experimental solubility parameter value for drugs are commonly taken as the one corresponding to the solute-free solvent mixture composition into which maximum solubility enhancement is observed, that estimated from group contribution method was preferred. First, because this value was found to be convenient with the solubility profile of the DZP in W + TBA solvent mixtures, and second, because an accurate experimental determination would have required to obtained solubility data over much smaller solute-free binary solvent mixture composition intervals [99, 156], especially in the vicinity of the observed solubility maximum, as well as to ensure absence of chameleonic effect arising from the nature of the solvents investigated [86, 88, 157, 158]. From these statements, the above equation was first used to determine x_2^0 value for which $\delta_{1,2}^0 = \delta_3^*$ by using pure component data at $T = 298.15$ K and $P = 0.1$ MPa.

Introducing $V_{m,1}^* = 18.07 \text{ cm}^3 \cdot \text{mol}^{-1}$, $\delta_1^* = 47.80 \text{ MPa}^{1/2}$, $V_{m,2}^* = 94.94 \text{ cm}^3 \cdot \text{mol}^{-1}$ and $\delta_2^* = 21.75 \text{ MPa}^{1/2}$ into Eq. (3.9) and then solving it with respect to x_2^0 after setting $\delta_{1,2}^0 = \delta_3^* = 25.14 \text{ MPa}^{1/2}$ yielded $x_2^0 = 0.56$ corresponding to $w_2^0 = 0.84$ in agreement with experimental data [116]. The same equation with $x_2^0 = 0.56$ was then used again to compute values of the solubility parameter of hypothetical pure supercooled liquid DZP at the different system temperatures from those of molar volume and solubility parameter of pure liquid W and either pure liquid or hypothetical pure supercooled liquid TBA reported in Table 3.1. In turn, these values were introduced into Eq. (3.8) to calculate molar volume values of hypothetical pure supercooled liquid DZP at the different system temperatures from the pure component data estimated from group contribution method and displayed in Table 3.2. The values of $V_{m,3}^*$ and δ_3^* at system temperature and pressure computed in this way are listed in Table 3.1 together with those of the two other components.

3.3.2. Data reduction

Rather than assuming that over the temperature range investigated, the dependence of all binary interaction parameters of both the SH and SH/FH models on temperature can be neglected or represented by an identical function, it was judged to be more relevant to envision that the temperature dependence of each individual binary interaction parameter $A_{i,j}$, with $A_{i,j} = l_{i,j}$ or $A_{i,j} = l'_{i,j}$ depending on the excess Gibbs energy model considered, could be described independently from that of the others by one of these three equations:

$$A_{i,j} = b_{i,j} \quad (3.10.a)$$

$$A_{i,j} = a_{i,j}T \quad (3.10.b)$$

$$A_{i,j} = a_{i,j}T + b_{i,j} \quad (3.10.c)$$

Accordingly, by considering all possible combinations of the three types of temperature dependence relationships for each of the three binary interaction parameters, a set of twenty-seven model versions containing from three up to six adjustable parameters and differing from one another by the temperature dependence of at least one binary interaction parameter was generated for both the SH model and the SH/FH model, as summarized in Table 3.3.

Table 3.3. Overview of the different versions of the Scatchard-Hildebrand and combined Scatchard-Hildebrand/Flory-Huggins models investigated in this study^a.

Model	$A_{1,2}$	$A_{1,3}$	$A_{2,3}$	k^b
Scatchard-Hildebrand model: Eq. (3.3) with $A_{i,j} = l_{i,j}$				
Combined Scatchard-Hildebrand/Flory-Huggins model: Eq. (3.6) with $A_{i,j} = l'_{i,j}$				
1	□	□	□	3
2	◻	□	□	3
3	□	◻	□	3
4	□	□	◻	3
5	◻	◻	□	3
6	◻	□	◻	3
7	□	◻	◻	3
8	◻	◻	◻	3
9	■	□	□	4
10	□	■	□	4
11	□	□	■	4
12	■	◻	◻	4
13	◻	■	◻	4
14	◻	◻	■	4
15	□	◻	■	4
16	□	■	◻	4
17	◻	□	■	4
18	■	□	◻	4
19	◻	■	□	4
20	■	◻	□	4
21	■	■	□	5
22	■	□	■	5
23	□	■	■	5
24	■	■	◻	5
25	■	◻	■	5
26	◻	■	■	5
27	■	■	■	6

^a (□): $A_{i,j} = b_{i,j}$; (◻): $A_{i,j} = a_{i,j}T$; (■): $A_{i,j} = a_{i,j}T + b_{i,j}$

^b k : number of adjustable model parameters.

Estimates of adjustable parameters $a_{i,j}$ and/or $b_{i,j}$ were determined simultaneously for the three pairs of unlike molecules from ordinary non-linear least-squares analysis of the whole experimental data set by minimizing the following objective function (OF):

$$\text{OF} = \sum_{i=1}^N \left(\ln \gamma_{3,\text{expt}}^{\text{sat}} - \ln \gamma_{3,\text{calc}}^{\text{sat}} \right)_i^2 \quad (3.11)$$

where $\gamma_{3,\text{expt}}^{\text{sat}}$ and $\gamma_{3,\text{calc}}^{\text{sat}}$ are the experimental and model-calculated activity coefficients of DZP in saturated mixtures, respectively, and N is the number of data points. Minimization of the objective function was performed by generalized reduced gradient nonlinear solving method [159] using the solver function within Microsoft Excel 2010 software (Microsoft, Redmond, USA). The experimental values of the activity coefficient of DZP in W + TBA solvent mixtures were provided in the first part of this work [116]. They were computed from Eq. (3.1) by assuming the differential molar heat capacity of the pure liquid and crystalline solid forms of DZP to be temperature independent and equal to the molar entropy of the drug at its fusion temperature [160-162]:

$$\ln \gamma_3^{\text{sat}} = \left[\frac{\Delta_{\text{fus}} H_{\text{m},3}(T_{\text{fus},3})}{RT_{\text{fus},3}} \ln \left(\frac{T}{T_{\text{fus},3}} \right) \right] - \ln x_3^{\text{sat}} \quad (3.12)$$

The values of the model-calculated activity coefficient of DZP in W + TBA solvent mixtures under saturation condition were computed from Eq. (3.3.b) for the SH model and from Eq. (3.6.b) for the SH/FH model, which for the ternary system investigated take the form of Eq. (3.13.a) and Eq. (3.13.b), respectively:

$$\begin{aligned} \ln \gamma_3^{\text{sat}} = & \frac{V_{\text{m},3}^*}{RT} \left\{ (\phi_1^{\text{sat}})^2 \left[(\delta_1^* - \delta_3^*)^2 + 2l_{1,3} \delta_1^* \delta_3^* \right] + (\phi_2^{\text{sat}})^2 \left[(\delta_2^* - \delta_3^*)^2 + 2l_{2,3} \delta_2^* \delta_3^* \right] \right. \\ & \left. + 2\phi_1^{\text{sat}} \phi_2^{\text{sat}} \left[(\delta_3^*)^2 + \delta_1^* \delta_3^* (l_{1,3} - 1) + \delta_2^* \delta_3^* (l_{2,3} - 1) - \delta_1^* \delta_2^* (l_{1,2} - 1) \right] \right\} \end{aligned} \quad (3.13.a)$$

$$\begin{aligned} \ln \gamma_3^{\text{sat}} = & \frac{V_{\text{m},3}^*}{RT} \left\{ (\phi_1^{\text{sat}})^2 \left[(\delta_1^* - \delta_3^*)^2 + 2l'_{1,3} \delta_1^* \delta_3^* \right] + (\phi_2^{\text{sat}})^2 \left[(\delta_2^* - \delta_3^*)^2 + 2l'_{2,3} \delta_2^* \delta_3^* \right] \right. \\ & \left. + 2\phi_1^{\text{sat}} \phi_2^{\text{sat}} \left[(\delta_3^*)^2 + \delta_1^* \delta_3^* (l'_{1,3} - 1) + \delta_2^* \delta_3^* (l'_{2,3} - 1) - \delta_1^* \delta_2^* (l'_{1,2} - 1) \right] \right\} \\ & + \ln \left(\frac{\phi_3^{\text{sat}}}{x_3^{\text{sat}}} \right) + 1 - \frac{\phi_3^{\text{sat}}}{x_3^{\text{sat}}} \end{aligned} \quad (3.13.b)$$

These equations were used by setting $x_1^{\text{sat}} = (1 - x_2^0)(1 - x_3^{\text{sat}})$ and $x_2^{\text{sat}} = x_2^0(1 - x_3^{\text{sat}})$ to ensure summation of the mole fractions of each component in the saturated liquid phase to be equal to unity during iteration steps as well as to be more convenient for practical application in the field.

3.3.3. Models comparison and selection

For both model sets herein above defined, second-order Akaike's information criterion corrected for small sample size (AIC_c) [163-165] was used as model selection method to rank and weight among the different versions of the SH and SH/FH models according to the parsimony principle. Full explanation of this approach based on information-theoretic concepts and mathematical statistics can be found in the comprehensive book by Burnham and Anderson [166]. Assuming that the requirements of residuals normality and homoscedasticity were met for all models included in the sets under consideration, AIC_c scores were computed from ordinary least-squares regression statistics as:

$$\text{AIC}_c = N \ln \left[\frac{\text{SS}(e)}{N} \right] + 2(k+1) + \frac{2(k+1)(k+2)}{N-k-2} \quad (3.14)$$

where $\text{SS}(e) = \sum_i^N e_i^2$ is the sum-of-squares of the residuals from regression, k is the number of adjustable model parameters and N is the number of data points as previously stated. According to this model selection method, the candidate model presenting the lowest AIC_c score was estimated to be the most parsimonious model given the data and the model set. The so-called Akaike weights w_A , which are the weights of evidence in favor of each candidate model in the set being the actual best model in the sense of minimum Kullback-Leibler information loss [167] normalized to sum up to unity so that they may be interpreted as probabilities, were calculated from differences in AIC_c score between a particular model and the estimated best model according to:

$$w_{A,j} = \frac{\exp\left(-\frac{1}{2}\Delta\text{AIC}_{c,j}\right)}{\sum_{i=1}^r \exp\left(-\frac{1}{2}\Delta\text{AIC}_{c,i}\right)} \quad (3.15)$$

where $\Delta\text{AIC}_{c,i} = \text{AIC}_{c,i} - \min \text{AIC}_c$ with the min being over all the models in the set and where r is the number of candidate models constituting it.

3.3.4. Statistical analysis

Standard error propagation equations were used to estimate the standard deviations in values calculated from those obtained from experimental measurements as well as to compute standard deviations in model-calculated values from relevant variance-covariance matrix of estimated model coefficients [168]. Goodness-of-fit of regression equations was evaluated by the adjusted squared correlation coefficient and its statistical significance was assessed by one-tailed Fisher's F -test whereas statistical significance of estimated regression coefficients was determined by two-tailed Student's t -test. Accuracy and precision of regression equations were appraised from standard deviation of the residuals and range of relative standard deviation of the dependent variable estimates, respectively. All calculations were carried out using Microsoft Excel 2010 software (Microsoft, Redmond, USA).

3.4. Results and discussion

3.4.1. Correlation of the temperature and composition dependence of the activity coefficient of diazepam in water + *tert*-butyl alcohol solvent mixtures

In order to avoid underfitting or overfitting by arbitrary selecting the same function to describe the temperature dependence of binary interaction parameters of the SH and SH/FH models, performances of the different model versions investigated in the framework of this study in balancing the decrease in the residual sum-of-squares against the number of adjustable coefficients were evaluated using an information-theoretic approach, as described in section 3.3.3. The results are presented in Tables C.1 and C.2 for the SH and SH/FH models, respectively. For convenience, alternative model versions are ranked in ascending order with respect to their AIC_c scores, recalling that the lower the AIC_c score, the better the tradeoff between model fit and complexity. In addition to AIC_c scores, are also presented in Tables C.1 and C.2 the values of the residual sum-of-squares $SS(e)$, the adjusted squared correlation coefficient r_{adj}^2 and the Akaike weights w_A for the different model versions tested. From these tables, one can see that among candidate models, model number thirteen for the SH model set and model number five for the SH/FH model set emerge as the most parsimonious models for these data. However, although clearly in both model sets many of the candidate models represent a poor approximation to the data at hand, considerable uncertainty in the selection of the best approximating models remains. Indeed, based on the Akaike weight values, the first-ranked SH model and SH/FH model versions are, respectively, only 1.3 to 2.5 times and 1.2 to 2.8 times more likely to be the best approximating model in their respective model set than the four next best-ranked candidate models. Nevertheless, it can also be stated that they are, respectively, more than 9.5 times and 26.1 times more likely to be the best approximating model than the model number twenty-seven, where the dependence

of each binary interaction parameter on temperature is described by a linear relationship, and more than a million times more likely than the model number one, where all binary interaction parameters are assumed to be temperature independent. Hence, and despite the level of empirical support being substantial for some of other candidate models in both model sets, these two model versions were selected as the optimal final models. For convenience and sake of conciseness, from this point and for the remainder of the present paper, selected most parsimonious versions of the SH and SH/FH models will be shortly referred to as SH and SH/FH models, respectively.

The corresponding least-squares regression parameters are presented in Table 3.4, including p -values of regression coefficient estimates and adjusted squared correlation coefficients reported as asterisks. Full statistical analysis results are summarized in Tables C.3, C.4 and C.5, including the respective variance-covariance matrices. It can be observed from Table 3.4 that for the two excess Gibbs models under consideration, the coefficient estimates are all found to be statistically significant at the 95 percent level of confidence with p -values mostly lower than $1 \cdot 10^{-4}$. Additionally, the values of the adjusted squared determination r_{adj}^2 are higher than 0.99 with associated p -values of less than $1 \cdot 10^{-4}$ in both cases, indicating that almost all of the total variation in the dependent variable is accounted for by the SH and SH/FH models. In Figure 3.1.A and Figure 3.1.B are displayed the scatter plots of calculated against experimental $\ln \gamma_3^{\text{sat}}$ values for the SH and SH/FH models, respectively. The first striking observation from these figures is that both plots exhibits an exact identical pattern where the data points in the lower extreme of the plot fall along the identity line whereas those in the center and the upper extreme of the plot are slightly scattered around. In addition, these figures do not reveal any systematic shift or strongly marked differences in the trends in the calculated values with respect to the experimental ones so that agreement between experimental and model-calculated values can be considered satisfactory overall.

Regarding to the to the accuracy of the two excess Gibbs energy model under consideration, the value of the standard deviation of the residuals from regression was found to be only about 0.25 natural log unit for both the SH and SH/FH models, which seems reasonable but remains from 1.5- to more than 15-fold higher than the uncertainty in experimental data used for models parameterization. Analyses of residuals from the two regression models investigated were graphically performed to ensure that assumptions underlying the least-squares method were satisfied as well as to further investigate their performances in correlating the dependence of the activity coefficient of DZP in W + TBA solvent mixtures on composition and temperature under saturation condition. For both models, the mean of the residuals from regression is found to be close to zero with a value of less than $3 \cdot 10^{-4}$ natural log unit.

Table 3.4. Results of the non-linear least-squares regressions of the natural logarithm of the activity coefficient of diazepam γ_3^{sat} in water + *tert*-butyl alcohol solvent mixtures at system temperature T and pressure $P = 0.1$ MPa to the selected most parsimonious versions of the Scatchard-Hildebrand and combined Scatchard-Hildebrand/Flory-Huggins models^a.

Parameters ^b	SH model	SH/FH model
N	54	54
$a_{1,2}$ (K^{-1})	$-8.764 (0.087) \cdot 10^{-4}$ ****	$-8.541 (0.087) \cdot 10^{-4}$ ****
$b_{1,2}$	0	0
$a_{1,3}$ (K^{-1})	$-6.469 (0.498) \cdot 10^{-4}$ ****	$-3.961 (0.017) \cdot 10^{-4}$ ****
$b_{1,3}$	$3.564 (1.510) \cdot 10^{-2}$ *	0
$a_{2,3}$ (K^{-1})	$7.000 (0.371) \cdot 10^{-5}$ ****	0
$b_{2,3}$	0	$2.456 (0.112) \cdot 10^{-2}$ ****
r_{adj}^2	0.9905 ****	0.9907 ****
$s(e)$	0.265	0.262
$s_r(\ln \gamma_{3,\text{calc}})$ (%) ^c	0.52 – 3.54	0.70 – 3.59

**** $p \leq 0.0001$, *** $p \leq 0.001$, ** $p \leq 0.01$, * $p \leq 0.05$.

^a Values in parentheses are standard deviations.

^b N : number of regressed data points; $a_{i,j}$ and $b_{i,j}$: adjustable model parameters; r_{adj}^2 : adjusted squared determination coefficients; $s(e)$: standard deviations of the residuals from regression; $s_r(\ln \gamma_{3,\text{calc}})$: relative standard deviations of the estimates of the natural logarithm of diazepam activity coefficient.

^c Over the ranges $T = 293.15 - 313.15$ K, $x_2^0 = 0 - 1$ and $x_3 = 0 - 0.02$.

To assess whether or not residual errors from the two excess Gibbs energy models are approximately normally distributed, the standardized residuals were plotted against theoretical z -scores derived from the Gaussian distribution. The resulting normal probability plots are depicted in Figure 3.2.A and 3.2.B for the SH and SH/FH models, respectively. From these, one can note that for both models, the probability plots exhibit a reasonably straight-line pattern of the data but that the first and last points in the lower and upper extremes of the plots show departure from the reference fitted line. It can also be seen in these figures that both the lower and upper tails of the distribution show departure from linearity above the fitted line, neither characteristic of a short-tailed nor of a long-tailed distribution with respect to the normal one, and also that the lower tails of the distributions appeared to be noticeably shorter than the upper ones. The values of the squared correlation coefficient associated with the linear least-squared fit to the data are found to be equal to 0.9549 and 0.9418 for the SH and

SH/FH models, respectively, indicating that deviation from an ideal Gaussian distribution is slightly less important for the former model than for latter one.

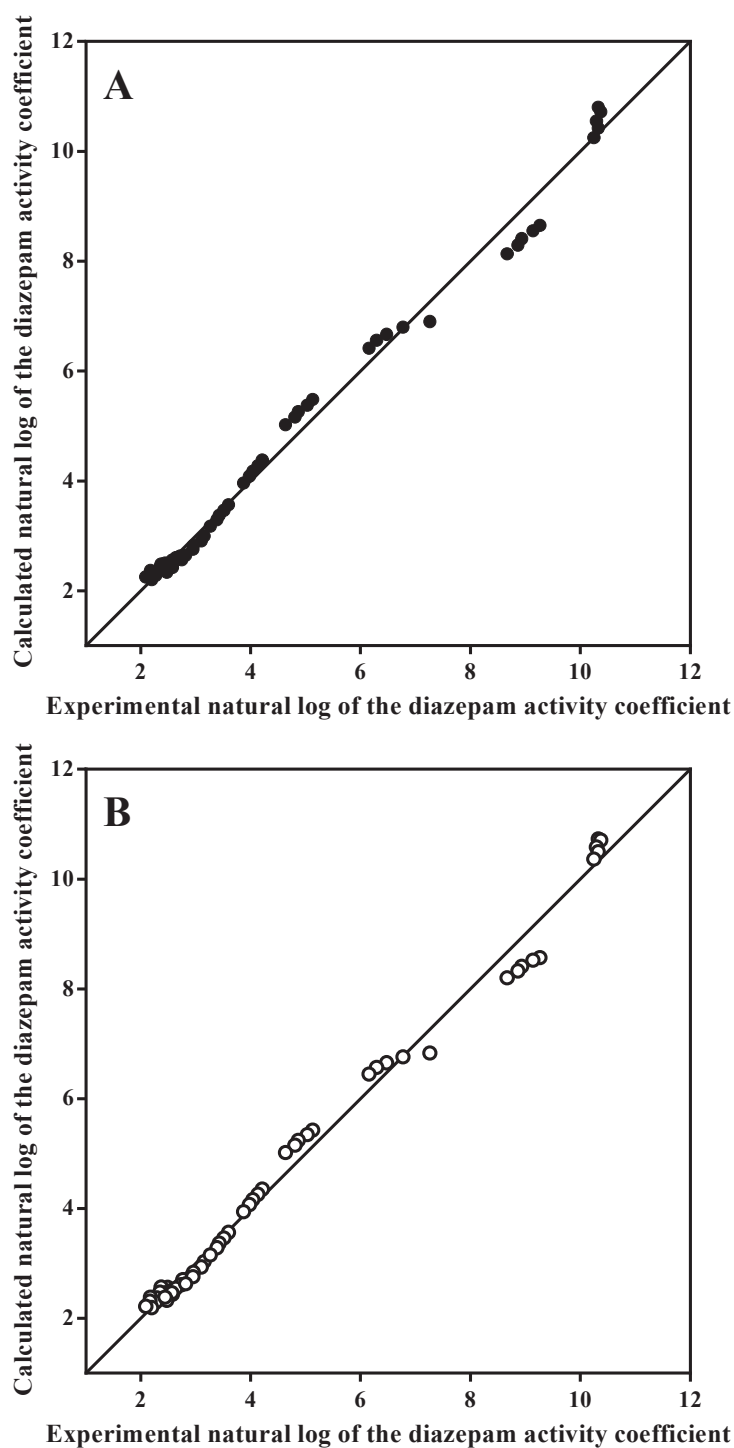


Figure 3.1. Scatter plots of the values of the natural logarithm of the diazepam activity coefficient calculated from the selected most parsimonious versions of (A): Scatchard-Hildebrand model and (B): combined Scatchard-Hildebrand/Flory-Huggins model (B) against the experimental values (the solid line is the identity line).

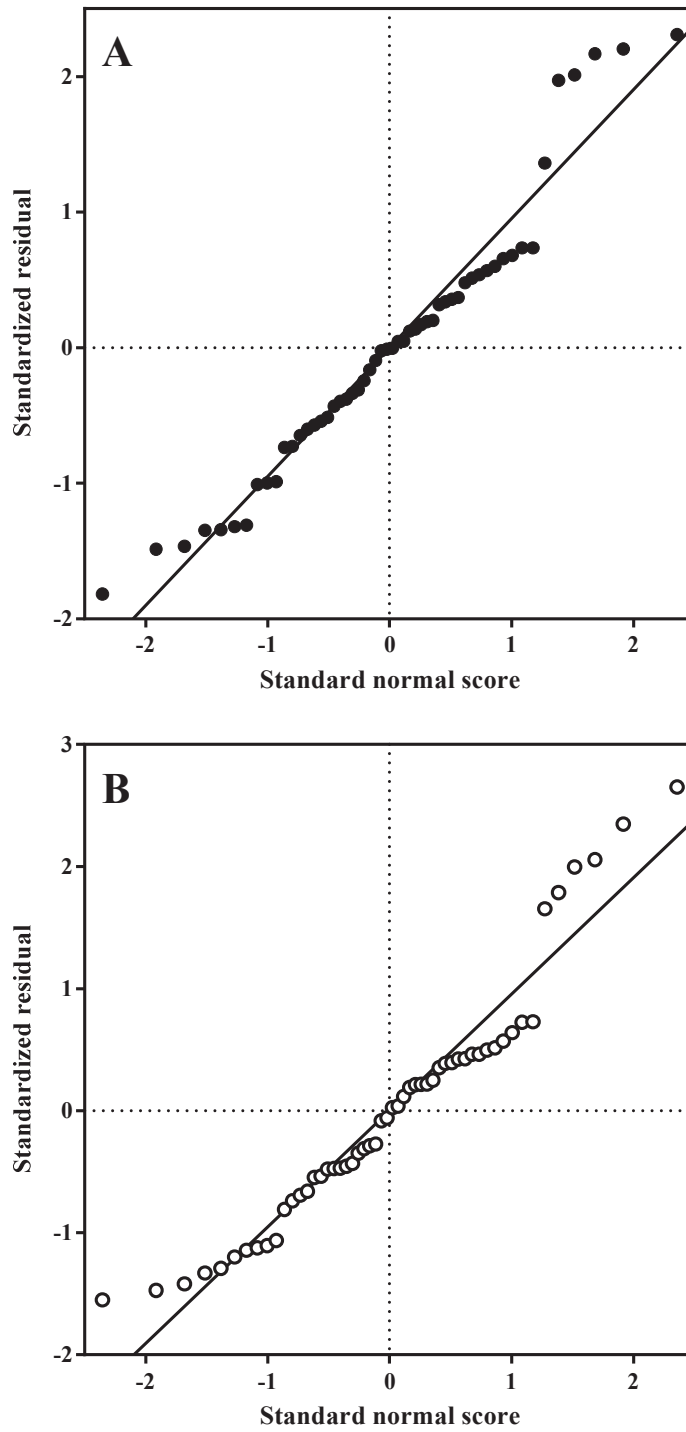


Figure 3.2. Normal probability plots of the residuals from the selected most parsimonious versions of (A): Scatchard-Hildebrand model and (B): combined Scatchard-Hildebrand/Flory-Huggins model (residuals are standardized with respect to mean and standard deviation; the solid lines are linear fits to data).

To ensure that the distribution of the residuals from regressions cannot be better approximated by another symmetric distribution with same means and variances, Tukey lambda probability plot correlation coefficient plots were constructed for the two excess Gibbs energy models under consideration in the usual way by plotting the correlation coefficient values computed for the probability plot associated with a given value of the shape parameter λ against their corresponding shape parameter values, ranging in the present study from minus one to one as displayed in Figure 3.3.

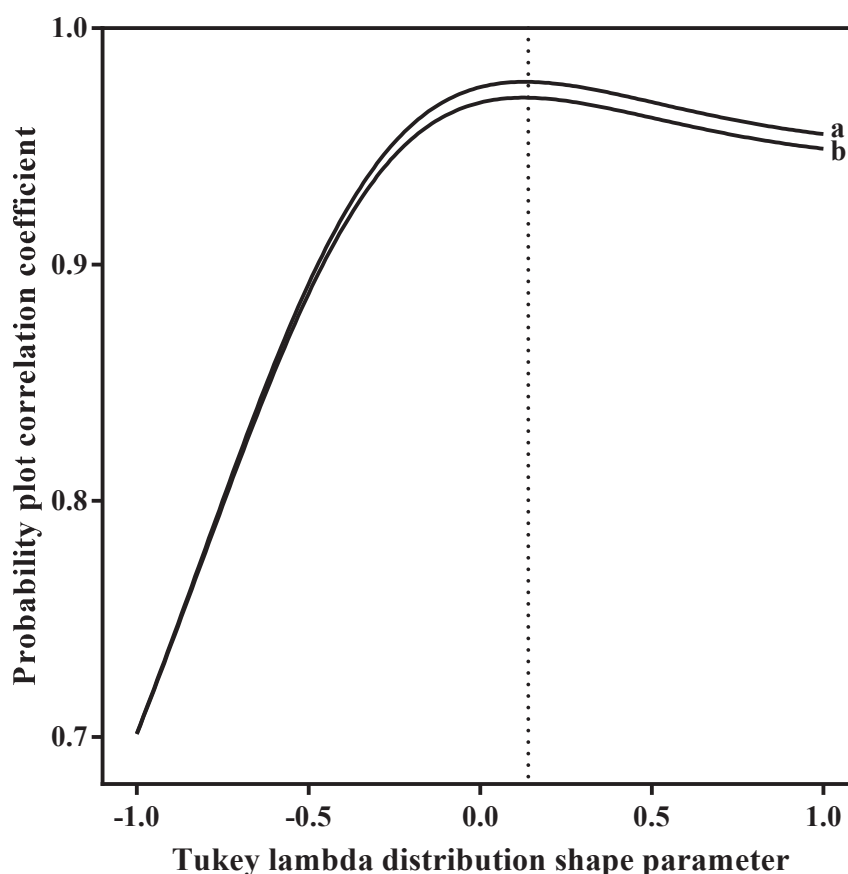


Figure 3.3. Tukey lambda probability plot correlation coefficient plot of the residuals from the selected most parsimonious versions of (a): Scatchard-Hildebrand model and (b): combined Scatchard-Hildebrand/Flory-Huggins model (the dashed line indicates the shape parameter value corresponding to an approximately normal distribution).

For both the SH and SH/FH models, it can be observed from this figure that the maximum correlation occurs for a value of λ very close to 0.14 and hence it can be reasonably concluded that the distribution of residuals from regression are better described by a Gaussian distribution than by any of other commonly used symmetric distribution. Scatter plots of the residuals from regression against model response and predictor variables for the SH and SH/FH models are displayed in Figures 3.4.A

and 3.4.B, respectively. For the two excess Gibbs energy models under consideration, the exact same comments can be made.

Considering the plots of the residuals against the model-calculated values displayed in Figures 3.4.A.1 and 3.4.B.1, it appears that the residuals are clustered on either one side or the other of the zero line over most of the model response range. The magnitude of the deviation around the zero line being not constant with respect to the model response, this translates into a sinusoidal wave-shaped distribution pattern of increasing amplitude toward larger model-calculated values. Turning to Figures 3.4.A.2 and 3.4.B.2 where the residuals are plotted against the TBA mass fraction in the solute-free binary solvent mixtures, it can be observed that the distribution of the residuals also displays a sinusoidal wave-shaped pattern due to the clustering of the residuals on one side of the zero line or the other. In a less obvious manner, heteroscedasticity of errors is also demonstrated from the plots of the residuals against the mole fraction solubility of DZP in W + TBA solvent mixtures as depicted in Figures 3.4.A.3 and 3.4.B.3. When one examines these figures, one first remarks that in the lower extreme and middle of the mole fraction solubility range, residuals are satisfactory well scattered on both sides of the zero line but nevertheless with a large difference in the magnitude of deviation around the said line. However, the magnitude of the deviation around the zero line becomes nearly constant as the mole fraction solubility of DZP in W + TBA solvent mixtures increases but residuals adjacent to one another tend to have similar sign. Nevertheless, such clustering does not translate into a sinusoidal wave-shaped distribution pattern as observed in the top plots of Figure 3.4. Looking to Figures 3.4.A.4 and 3.4.B.4 where the residuals are plotted against the system temperature, it is striking to see that for both excess Gibbs energy models under investigation, the individual data points are almost perfectly randomly distributed from either sides of the zero line and that requirement of homoscedasticity of errors is quite fully met with respect to this variable. Finally, serial independence of residuals from regression was checked by plotting for the two excess Gibbs energy models investigated each i -th residual value against the corresponding $(i - 1)$ -th one, as depicted in Figures 3.5. It can be seen from the top plots of this figure that by ranking residual values in an increasing order first with respect to TBA mass fraction in the solute-free binary solvent mixture, that for the two excess Gibbs energy models investigated, the data are clustered along the lag plot diagonals, similar to those coming from an autoregressive model with moderate positive autocorrelation, which highlight some degree of dependence between successive residual values when considering these ranking criteria. Unlikely, it can also be observed from both the middle and bottom plots of Figure 3.5 that when residual values are ranked in an increasing order first with respect of either mole fraction solubility of DZP or temperature, the lag plots no more exhibit any identifiable pattern assessing of the independence of residuals from both the SH and the SH/FH models with respect to these ranking criteria.

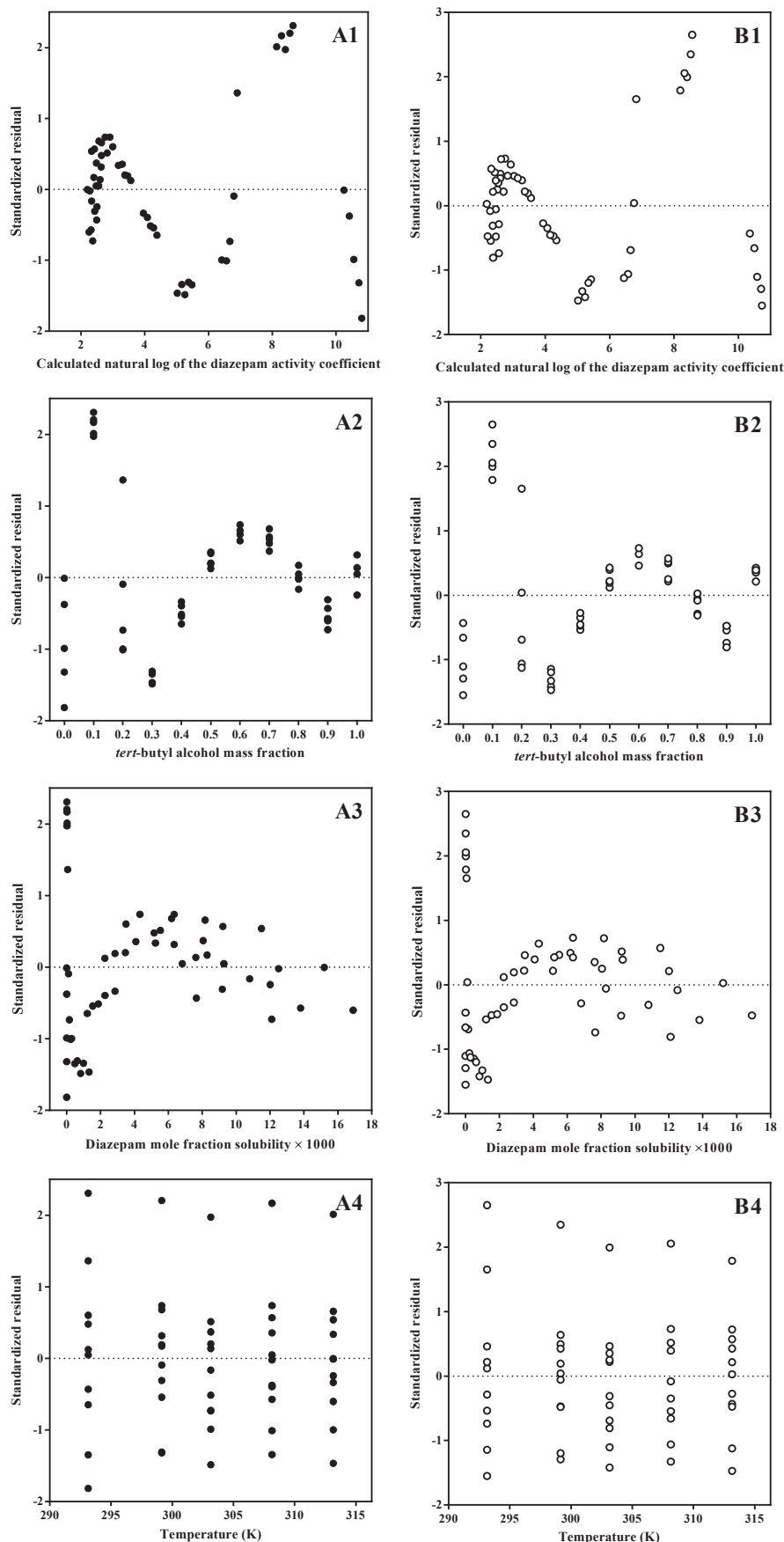


Figure 3.4. Scatter plots of the residuals from the selected most parsimonious versions of (A): Scatchard-Hildebrand model and (B): combined Scatchard-Hildebrand/Flory-Huggins model, against (1): calculated natural logarithm of diazepam activity coefficient; (2): *tert*-butyl alcohol mole fraction in solvent mixture free of solute; (3): diazepam mole fraction solubility and (4): absolute temperature (residuals are standardized with respect to mean and standard deviation).

From these results, one can emphasize first that the selected most parsimonious versions of the two excess Gibbs energy models under investigation perform almost equally well in least-squares fitting the experimental data and provide an overall good representation of the phenomenon under study. Second, and despite the residual distributions being found to be close to a normal one, assumptions underlying the regression method are only partially satisfied. Whereas both the SH and SH/FH models appeared to be adequate and complete to account for the temperature dependence of the natural logarithm of the activity coefficient of DZP over the whole range of solute-free binary solvent mixture composition, the detected structural relationships between residuals from regression and mixture composition variables clearly evidence that they perform less well in describing the composition dependence of the deviation of the liquid phase from ideal mixing behavior under isothermal conditions. This can be ascribed, on the one hand, to the methodology used to best describe the dependence of individual binary interaction parameters on temperature, and on the other hand, to the model structures themselves since they have been originally developed for mixtures within which instantaneous dipole-induced dipole forces are the only intermolecular interactions operating, remembering that, in addition to any other specific intermolecular interaction, both water and *tert*-butyl alcohol are associated liquids able to interact through hydrogen-bonding not only with each other, but also with diazepam.

Although by using the values of adjustable parameters provided in Table 3.4 one could compute from the SH and SH/FH model the activity coefficients of individual mixture components over the whole composition range and temperature range within the framework of this study, in practice, occurrence of the condition of saturation depending on both solute-free binary solvent mixture composition and system temperature sets an upper limit to the mole fraction of DZP that is very low. Hence, evaluation of the precision of the two excess Gibbs energy models under consideration was limited to mixture compositions with x_3 in the range from 0 up to $2 \cdot 10^{-2}$, which encompass the mole fraction solubility of DZP in W + TBA solvent mixtures over the temperature range investigated. From Table 3.4, it can be observed that within these limits, the relative standard deviation in values of $\ln \gamma_{3,\text{calc}}$ computed from the SH and SH/FH models are found to range from 0.52 to 3.54% and from 0.70 to 3.59%, respectively, which can be considered satisfactory in regard to the relative standard deviation in corresponding experimental data, found to range from 0.19 to 2.20%.

In Figure 3.6 are depicted, for x_3 values corresponding to the upper and lower limits of the range just stated above, the uncertainty in $\ln \gamma_{3,\text{calc}}$ computed from the SH and SH/FH models as a function of the composition of the solute-free binary solvent mixtures for temperatures corresponding to the mean temperature of the range currently under discussion and at this temperature plus and minus 5 and 10 K.

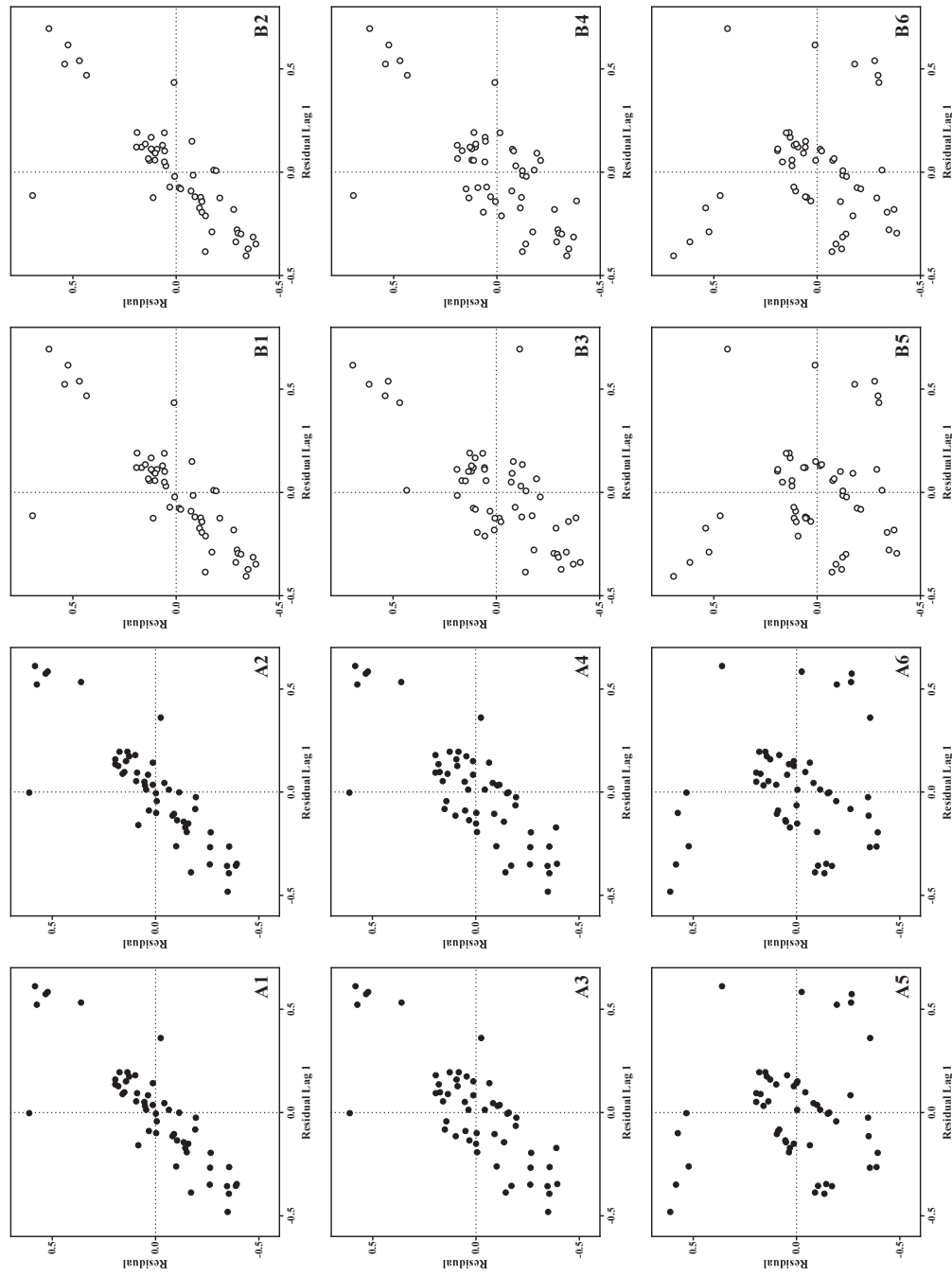


Figure 3.5. Lag plots of the residuals from the selected most parsimonious versions of (A): Scatchard-Hildebrand model and (B): combined Scatchard-Hildebrand/Flory-Huggins model, with residuals ranked in an increasing value order (1): first with respect to the *tert*-butyl alcohol mass fraction in solvent mixture free of solute, second with respect to the diazepam mole fraction solubility and third with respect to the absolute temperature, (2): first with respect to the *tert*-butyl alcohol mass fraction in solvent mixture free of solute, second with respect to the absolute temperature and third with respect to the diazepam mole fraction solubility, (3): first with respect to the diazepam mole fraction solubility, second with respect to the *tert*-butyl alcohol mass fraction in solvent mixture free of solute and third with respect to the absolute temperature, (4): first with respect to the absolute temperature, second with respect to the diazepam mole fraction solubility, second with respect to the *tert*-butyl alcohol mass fraction in solvent mixture free of solute and third with respect to the absolute temperature, (5): first with respect to the absolute temperature and third with respect to the diazepam mole fraction solubility and (6): first with respect to the absolute temperature, second with respect to the diazepam mole fraction solubility and third with respect to the *tert*-butyl alcohol mass fraction in solvent mixture free of solute.

It can be seen from this figure that, within the restricted mixture composition range, uncertainty values in $\ln \gamma_{3,\text{calc}}$ never exceed 0.10 natural log unit for the SH model and 0.15 natural log unit for the SH/FH model. Regarding to the composition and temperature dependence of the uncertainty of $\ln \gamma_{3,\text{calc}}$, it appears that for both the SH and SH/FH models, the uncertainty in $\ln \gamma_{3,\text{calc}}$ increases going away from the mean temperature of the range in the water-rich region of the solute-free binary solvent mixture composition range whereas in the remaining part the uncertainty in $\ln \gamma_{3,\text{calc}}$ increases with temperature. For the SH model, the uncertainty in $\ln \gamma_{3,\text{calc}}$ is almost insensitive to temperature except in the water-rich region of the solute-free binary solvent mixture composition range but the opposite is observed for the SH/FH model. Considering the influence of x_3 on the precision of model estimates, it can be remarked from Figure 3.6 that for both the SH and SH/FH models, the uncertainty in $\ln \gamma_{3,\text{calc}}$ decreases as x_3 increases, irrespective of the solute-free binary solvent mixture composition and temperature. However, the magnitude of this decrease is found to be larger in the water-rich region than in the remaining part of the solute-free binary solvent mixture composition range.

In the light of these results, it can be concluded that the selected most parsimonious versions of the SH and SH/FH model performed equally well in correlating the temperature and composition dependence of the activity coefficient of DZP in W + TBA solvent mixtures. One may be tempted to claim that it evidences that for the system under consideration, the relative difference in molar volumes of components is not large enough to require the FH expression for the excess molar combinatorial entropy of mixing to be combined with the SH model. However, it must also be pointed out that fitting the selected most parsimonious versions of the SH and SH/FH models to the data yields approximately the same sum-of-squares of the residuals. The former model containing one more adjustable parameter than the latter one, it is obvious that it is less parsimonious. This can be numerically appreciated by pairwise comparison of two excess Gibbs energy models under consideration using the same information-theoretic approach that leads to their selection. The value of w_A corresponding to the SH/FH model is now calculated to be equal to 0.86 indicating that it is more than 6 times more likely to be the best model for the data at hand than the SH model. Nevertheless, one can also argue that such comparison does not provide compelling support that incorporation of the FH expression for the excess molar combinatorial entropy of mixing into the SH model is not worthless since the temperature dependence of their respective binary interaction parameters is not the same. When the two excess Gibbs energy models are compared pairwise for each of the twenty-seven model versions investigated in this work, it appears that in exactly two-thirds of the cases, the SH/FH model emerges as being the actual Kullback-Leibler best model.

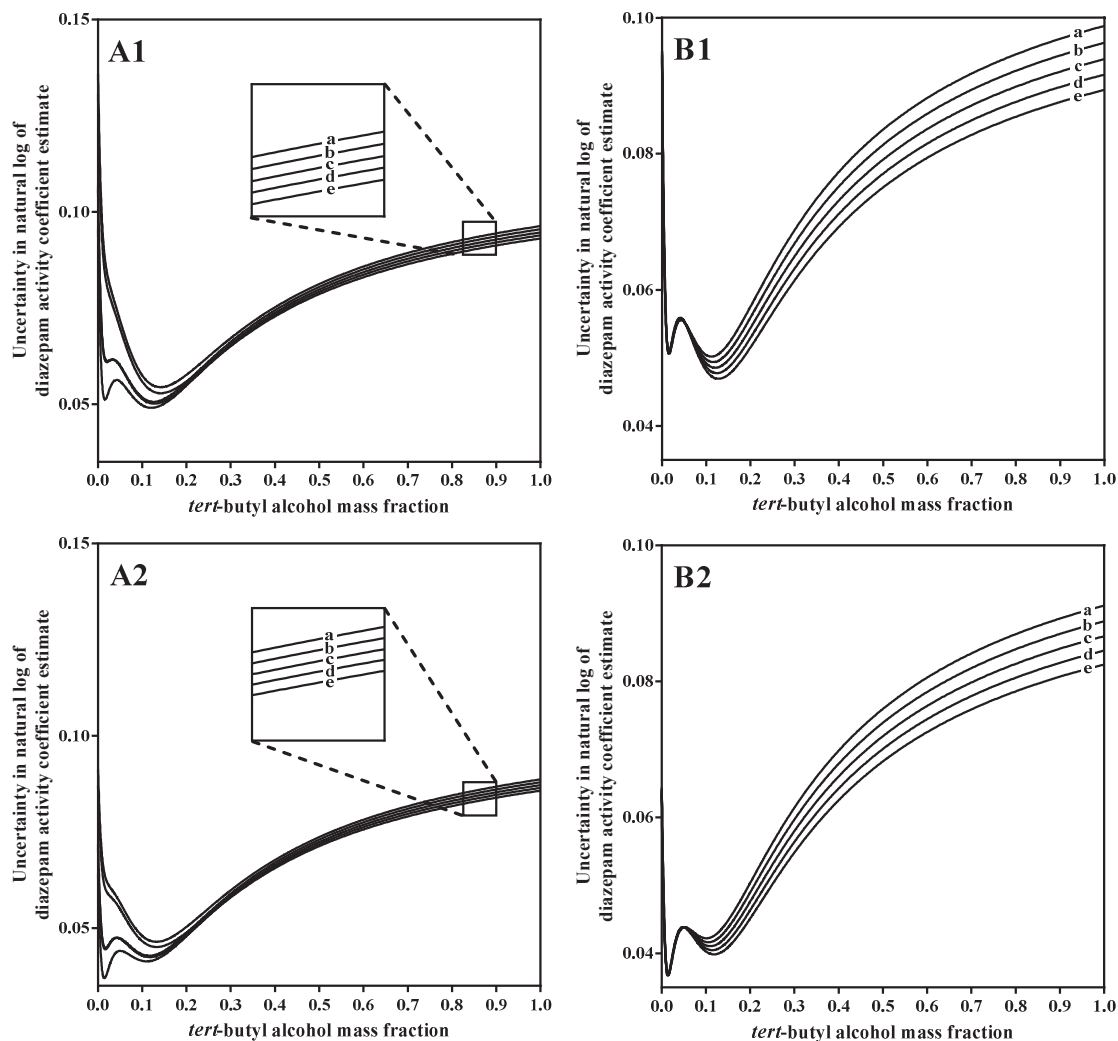


Figure 3.6. Uncertainty in natural logarithm of diazepam activity coefficient estimates calculated from the selected most parsimonious versions of (A): Scatchard-Hildebrand model and (B): combined Scatchard-Hildebrand/Flory-Huggins model by setting (1): $x_3 = 0$ and (2): $x_3 = 2 \cdot 10^{-2}$ as a function of the *tert*-butyl alcohol mass fraction in solvent mixture free of solute; (a): $T = 293.15$ K; (b): $T = 298.15$ K; (c): $T = 303.15$ K; (d): $T = 308.15$ K; (e): $T = 313.15$ K.

3.4.2. Accuracy and precision of calculated solubility of diazepam in water + *tert*-butyl alcohol solvent mixtures

Computation of the mole fraction solubility of DZP in W + TBA solvent mixtures from Eq. (3.1) along with assumptions related to the differential molar heat capacity term by using either the SH or SH/FH model to express the temperature and composition dependence of the activity coefficient of the

drug in the saturated liquid phases requires an iterative procedure which, irrespective of the solute-free binary solvent mixture composition or system temperature, was found to rapidly converge to an optimum solution, provided that the value for the variable is initially set equal to zero and imposed to be lower than $2 \cdot 10^{-2}$. The values of $x_{3,\text{calc}}^{\text{sat}}$ computed this way for our experimental compositions and temperature are provided in Table C.6 together with their standard deviations. For convenience in comparison, in this table are also included experimental data reported in the first part of this work [116]. In Figure 3.7 are displayed the model-calculated mole fraction solubility of DZP in W + TBA computed over the whole solute-free binary solvent mixture composition range for temperatures corresponding to the experimental isotherms together with experimental solubility data. In agreement with the results from analysis of residuals from regressions, it can be observed from this figure that, in spite of their simplicity, both excess Gibbs energy models under consideration provide an overall reasonably good representation of the phenomenon under study, but fail in perfectly modeling the experimental data at hand. The accuracy and precision in $x_{3,\text{calc}}^{\text{sat}}$ were evaluated by considering the absolute relative deviation (ARD) between model-calculated values and the experimental ones and relative standard deviation in model-calculated values $s_r(x_{3,\text{calc}}^{\text{sat}})$, respectively.

The distributions of ARD in $x_{3,\text{calc}}^{\text{sat}}$ calculated from Eq. (3.1) using the SH and SH/FH models are graphically presented as scatter and box-and-whiskers plots in Figure 3.8.A and Figure 3.8.B, respectively. Looking to Figure 3.8.A, where ARD values of individual data points are plotted against the solute-free binary solvent mixture composition, one can see that for both excess Gibbs energy models under consideration the ARD values does not exhibit a particular trend with respect to the TBA mass fraction in the solute-free binary solvent mixtures and are about dozens of percent over the whole composition range. Turning to Figure 3.8.B to examine the respective distributions of the ARD values, it can be observed that they range from less than 0.1% to 85% for the SH model and from about 1% up to 100% for the SH/FH model whereas the values of the 25th, 50th and 75th percentiles are found to be equal to 8.39, 17.26 and 27.94% for the former model and to 10.08, 16.29 and 28.42% for the latter one, respectively.

Although various criteria are in used in the literature, the mean ARD in model-calculated values is the one more widely used to express the overall accuracy of a model in correlating and/or predicting the solubility of drugs in mixed solvents [169]. In the present study, the mean ARD values in mole fraction solubility of DZP in the W + TBA solvent mixtures computed from the SH and SH/FH models are 21.87% and 22.77% which must be judged with respect to, on the one hand, the wide mole fraction solubility range of DZP in W + TBA solvent mixtures, and on the other hand, the nevertheless low mole fraction solubility of this drug in this cosolvent system. For practical applications in liquid formulation design, a model enabling to estimate the solubility of a drug with an ARD value lower

than that of the relative standard deviation in corresponding experimental data obtained from measurements of independent replicate samples is of an ideal nature but such degree of accuracy is hardly ever reached.

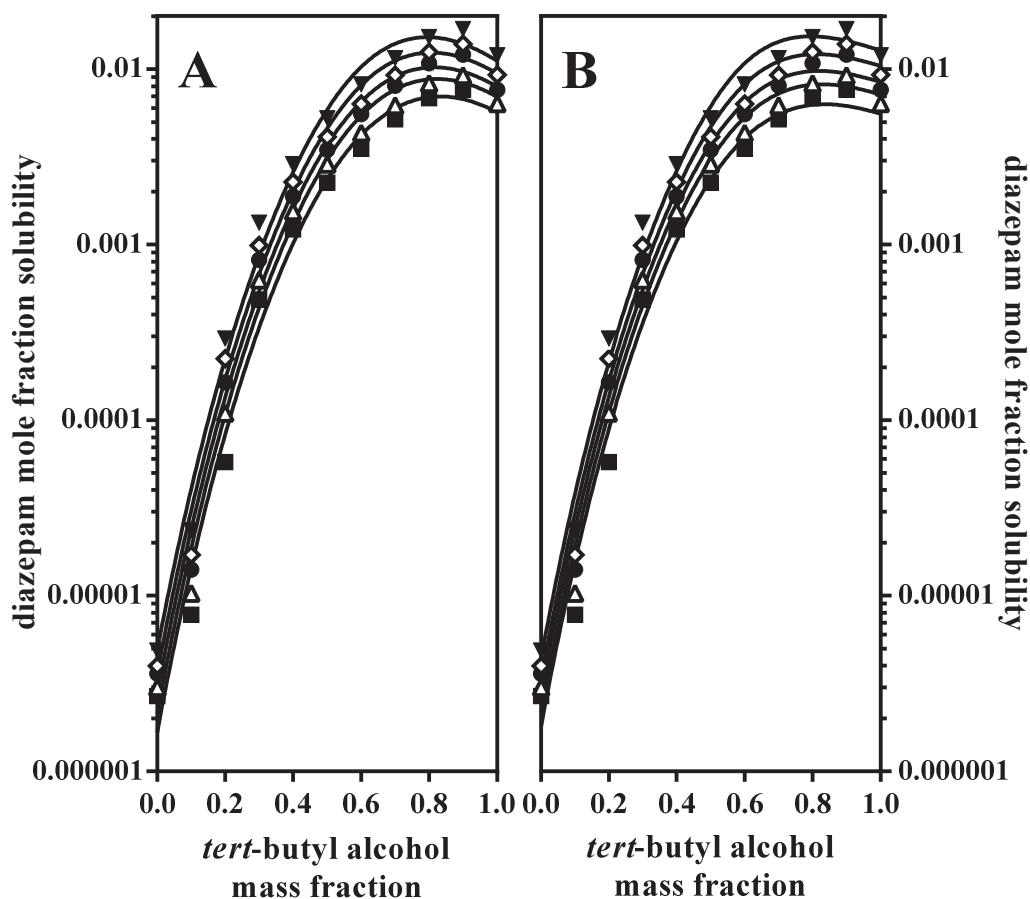


Figure 3.7. Mole fraction solubility of diazepam in water + *tert*-butyl alcohol solvent mixtures as function of the *tert*-butyl alcohol mass fraction in solvent mixture free of solute. Symbols are experimental values from Reference [116] (■): $T = 293.15$ K; (Δ): $T = 299.15$ K; (●): $T = 303.15$ K; (\diamond): $T = 308.15$ K; (\blacktriangledown): $T = 313.15$ K and solid lines are calculated from the selected most parsimonious versions of (A): Scatchard-Hildebrand model and (B): combined Scatchard-Hildebrand/Flory-Huggins model (error bars for experimental data and lines for model-calculated data corresponding to plus and minus one standard deviation are omitted for readability).

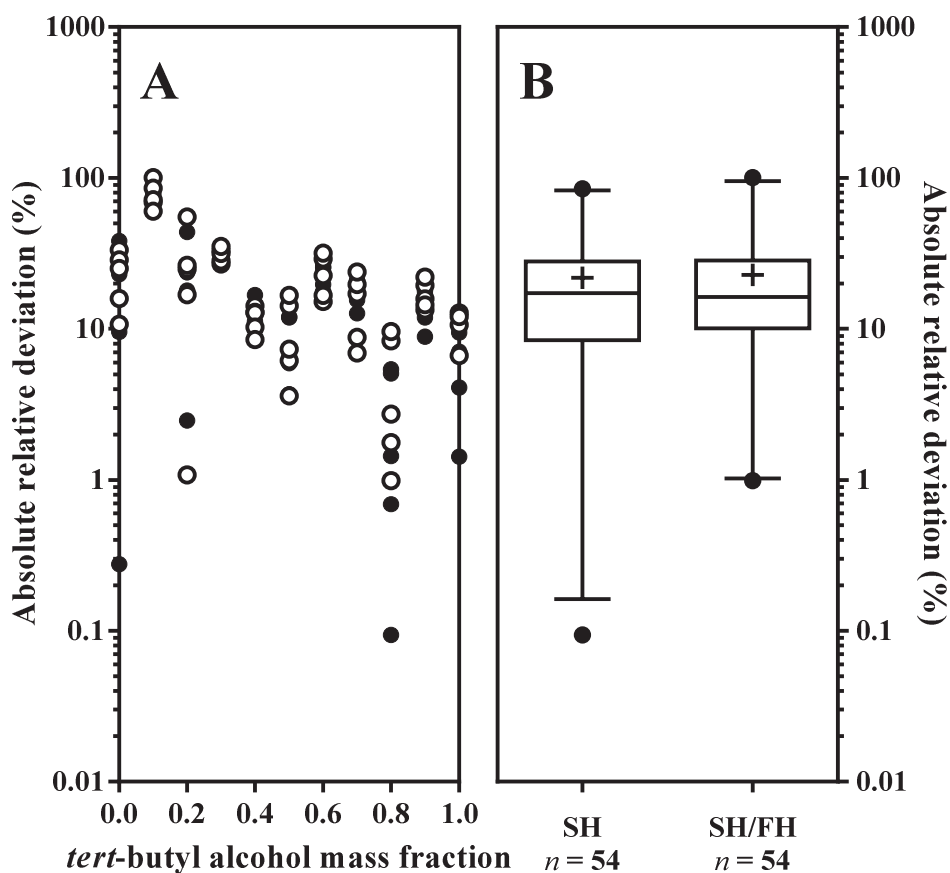


Figure 3.8. Absolute relative deviation in model-calculated values of the mole fraction solubility of diazepam in water + *tert*-butyl alcohol solvent mixtures from experimental values from Reference [116] displays as (A): scatter plot against *tert*-butyl alcohol mass fraction in the solute-free binary solvent mixtures (●): selected most parsimonious version of the Scatchard-Hildebrand model; (○): selected most parsimonious version of the combined Scatchard-Hildebrand/Flory-Huggins model and (B): box-and-whiskers plots (the upper and lower hinges of the boxes indicate the 25th and 75th percentiles, respectively, the lines within the boxes represent the 50th percentiles, the whiskers extend from the 2.5th to the 97.5th percentiles, the crosses denote the means and the dots correspond to individual values which are outside the range delimited by whiskers).

Due to the special emphasis paid to the methodology used to minimize the possible contribution of experimental data to error sources in solubility modeling, the relative standard deviations in experimental solubility values ranged only from 0.3 to 4.5%. Hence, this accuracy requirement is found to be met for only 7.4% and 5.6% of the values computed from the SH and the SH/FH models, respectively. However, it is commonly admitted in the literature that for correlation of the solubility of drug in mixed solvent, a model can be considered as accurate enough for practical applications on the field provided that its mean ARD in mole fraction solubility estimates is less than 30% [129, 169-171].

From this more reasonable requirement level, the accuracy of the two excess Gibbs energy models under investigation appears to be satisfactory.

Considering now the precision of the mole fraction solubility of DZP in W + TBA solvent mixtures calculated from the SH and SH/FH models, it can be observed from Figure 3.9.A that the two excess Gibbs energy models under consideration clearly do not perform equally well with this respect. Indeed, one can remark that over the whole solute-free binary solvent mixture composition range the values of $s_r(x_{3,\text{calc}}^{\text{sat}})$ are higher for the SH/FH model than for the SH model and that for both models the scatter plots exhibit, regarding to the sensitivity of this parameter to temperature as a function the mass fraction of TBA in the solute-free binary solvent mixtures, the same features than those described in the preceding section for the uncertainty in $\ln \gamma_{3,\text{calc}}$ computed from their respective variance-covariance matrices. Regarding to the distribution of the $s_r(x_{3,\text{calc}}^{\text{sat}})$ values, it can be seen from Figure 3.9.B that they range from 4.84% to 13.72% for the SH model and from 20.47% to 30.91% for the SH/FH model, the values of the 25th, 50th and 75th percentiles being equal to 5.55, 6.39 and 8.41% for the former model and to 22.49, 23.01, 24.94% for the latter one, respectively. Unlike accuracy, precision in model-calculated values is rarely evaluated and, from the best of our knowledge, criteria and associated cut-off values allowing stating whether or not the overall precision of a model in correlating and/or predicting the solubility of drugs in mixed solvents is adequate enough to be use for liquid formulation design are still not be defined. One can always argue that the lower the mean $s_r(x_{3,\text{calc}}^{\text{sat}})$ value, the better the model and with this respect, the SH model would perform better than the SH/FH model, the mean $s_r(x_{3,\text{calc}}^{\text{sat}})$ value being equal to 7.10 for the former model and to 24.29 for the latter one. However, keeping in mind that both excess Gibbs energy models do not perfectly describe the experimental solubility data, this must be balanced by considering the proportion of experimental values falling into the confidence interval of the model output for a given probability level since the greater the model precision, the narrower the model confidence interval. In Figures 3.10.A and 3.10.B are shown for the two excess Gibbs energy models under consideration the coverage rates of the 99% model confidence interval based on a Student's distribution, over the solute-free binary solvent mixture composition and temperature ranges partitioned into discrete classes. It can be immediately observed that whereas 100% of the experimental solubility data are within the confidence interval limits of the SH model, only about 48% of them are within those of the SH model. It is also striking to note that for this latter model, the coverage rate values increase as the mass fraction of TBA in the solute-free binary solvent mixtures increases and as the temperature departs from the mean temperature of the range. These obviously result from the variations of the width of the 99% model confidence interval with respect to both solute-free binary solvent mixture composition and temperature.

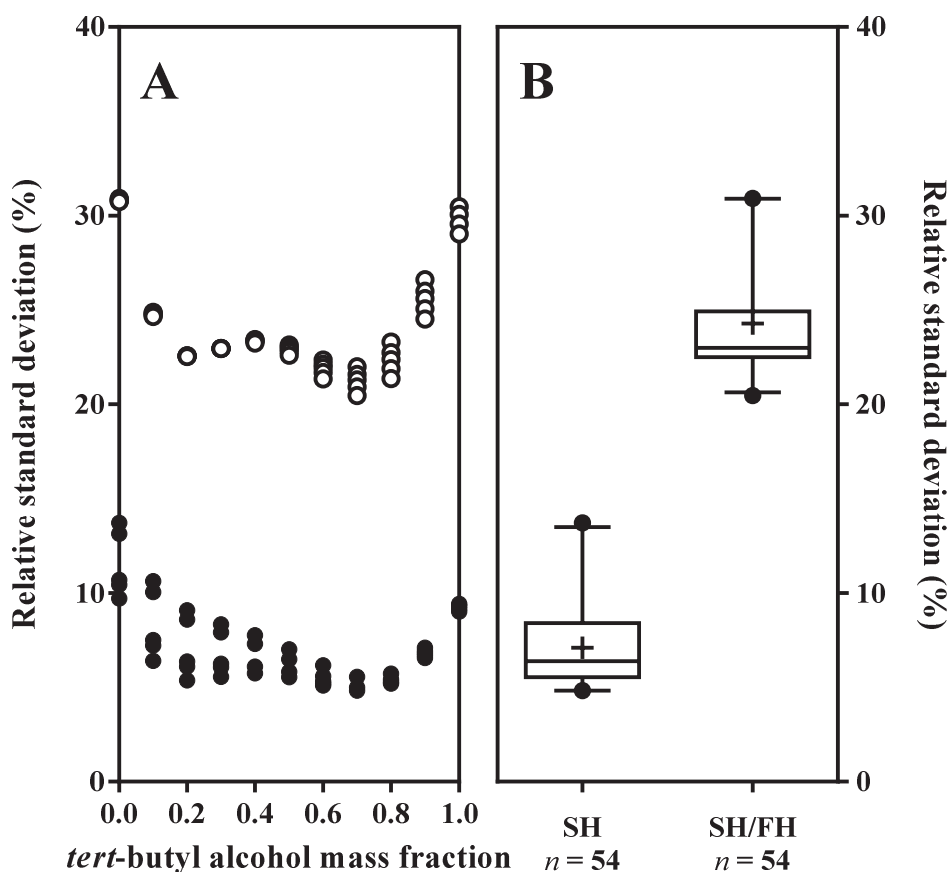


Figure 3.9. Relative standard deviation in model-calculated values of the mole fraction solubility of diazepam in water + *tert*-butyl alcohol solvent mixtures displays as (A): scatter plot against *tert*-butyl alcohol mass fraction in the solute-free binary solvent mixtures (●): selected most parsimonious version of the Scatchard-Hildebrand model; (○): selected most parsimonious version of the combined Scatchard-Hildebrand/Flory-Huggins model and (B): box-and-whiskers plots (the upper and lower hinges of the boxes indicate the 25th and 75th percentiles, respectively, the lines within the boxes represent the 50th percentiles, the whiskers extend from the 2.5th to the 97.5th percentiles, the crosses denote the means and the dots correspond to individual values which are outside the range delimited by whiskers).

For the two excess Gibbs energy models under consideration, the width of the 99% confidence interval was found to be extremely narrow in the water-rich end of the solute-free binary solvent mixture composition range with values in the order of $1 \cdot 10^{-6}$ mole fraction units for both the SH and SH/FH models and widens as the mass fraction of TBA in the solute-free binary solvent mixtures and the temperature increase, without exceeding $6 \cdot 10^{-3}$ mole fraction units for the SH model and $2 \cdot 10^{-2}$ mole fraction units for the SH/FH model. The difference in the coverage values between the two excess Gibbs energy models under consideration is fully attributable to that in the width of the 99% model confidence interval which, depending on the solute-free binary solvent mixture composition and temperature considered, is from 2 to 4 times wider for the SH/FH model than for the SH model.

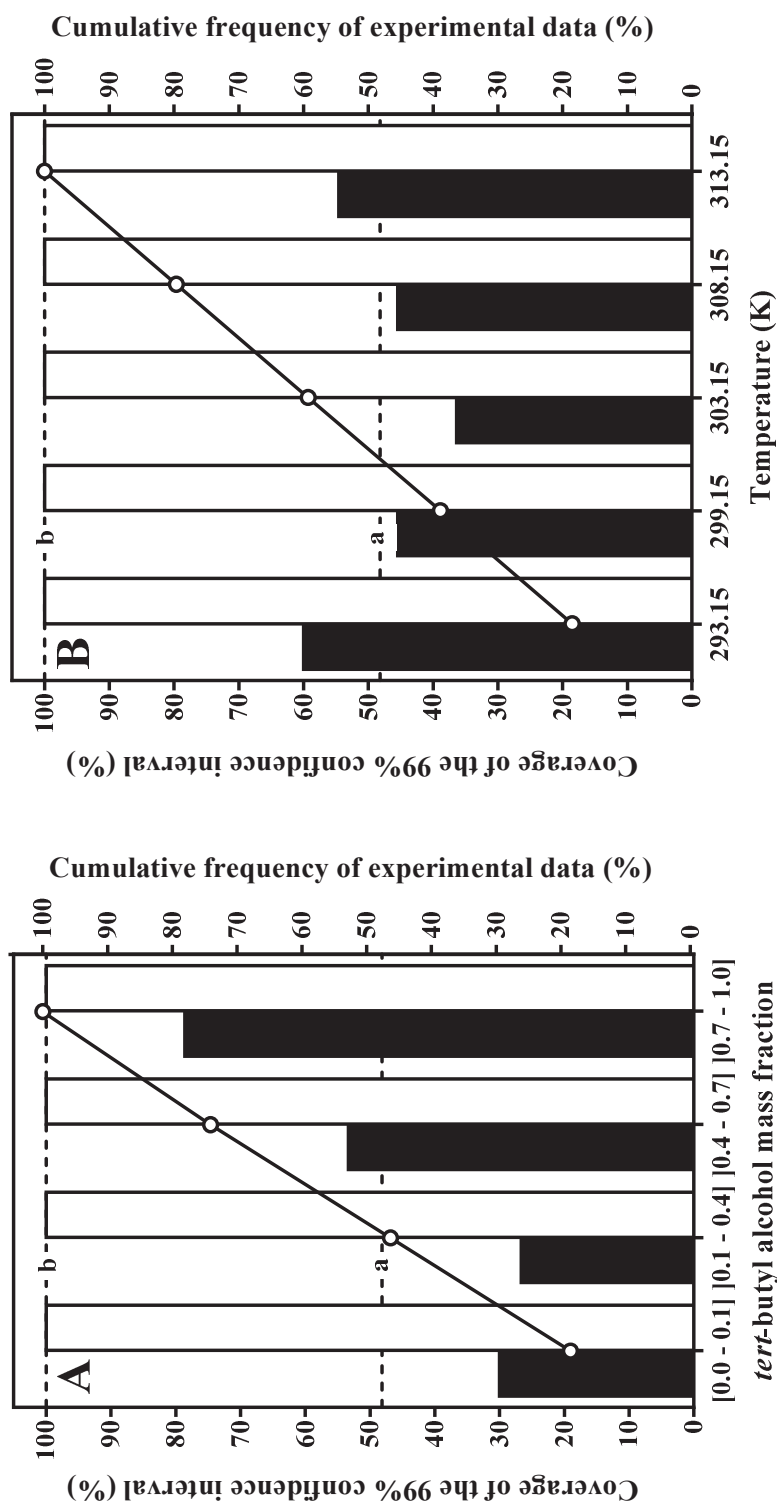


Figure 3.10. Relative frequency distributions of the coverage rate by experimental values Reference [116] of the 99% confidence interval mole fraction solubility of diazepam in water + *tert*-butyl alcohol solvent mixtures calculated from the selected most parsimonious versions of (black bars): Scatchard-Hildebrand model and (white bars): combined Scatchard-Hildebrand/Flory-Huggins model and corresponding cumulative relative frequency distributions of experimental data (dots), per class of solute-free binary solvent mixture composition (A) and temperature (B) (the dashed lines a and b are the coverage rate for the whole composition and temperature ranges of the Scatchard-Hildebrand and combined Scatchard-Hildebrand/Flory-Huggins models, respectively).

3.4.3. Practical considerations

Since the mole fraction solubility of DZP in W + TBA solvent mixtures was never found to exceed 2% over the temperature range investigated in the framework of this study, the accuracy and precision of the model-calculated drug solubility were also evaluated under the assumption of infinite dilution. From this hypothesis, computation of the mole fraction solubility of DZP in W + TBA solvent mixtures from Eq. (3.1), still along with assumptions related to the differential molar heat capacity term, by using either the SH or SH/FH model to express the temperature and composition dependence of the activity coefficient of the drug in the saturated liquid phases does not require an iterative procedure anymore. It was found that in comparison to those obtained under finite dilution conditions, the distributions and hence the mean values of both the ARD in $x_{3,\text{calc}}^{\text{sat}}$ and the $s_r(x_{3,\text{calc}}^{\text{sat}})$ remained almost unchanged upon setting $x_{3,\text{calc}}^{\text{sat}} = 0$ into the SH and SH/FH equations for the dependence of the drug activity coefficient on composition and temperature. Accordingly, the two excess Gibbs energy models under consideration can be used assuming infinite dilution of DZP in W + TBA solvent mixtures without dramatically impairing their performances, which allows saving computation time.

For practical purposes in the field, mass fraction or mass concentration units would be preferred over molar units to express the solubility of the drug in the binary solvent mixtures. Conversion from mole fractions to mass fractions is straightforward and requires only knowledge of the molar mass of the individual mixture components. However, pharmaceutical scientists might prefer to express diazepam solubility as the mass of drug per unit volume of solute-free binary solvent mixture. This can be readily achieved from knowledge of the mass fraction solubility of DZP in the solute-free binary solvent mixture of defined mass fraction composition, but it also requires knowledge of the specific volume of the W + TBA binary solvent mixture of interest at the considered temperature. For this purpose, experimental volumetric data on the W + TBA binary solvent mixtures provided in a previous work [151] can be used. If not available for the composition and/or for the temperature of interest, the specific volume of the W + TBA binary solvent mixture can be estimated with a good accuracy and precision by using the model equation reported in which covers the whole composition range and the exact same temperature range than that encompassed in the present study.

3.5. Conclusion and perspectives

In the present investigation, the performances of the Scatchard-Hildebrand and combined Scatchard-Hildebrand/Flory-Huggins models in correlating the composition and temperature dependence of the solubility of diazepam in water + *tert*-butyl alcohol solvent mixtures were evaluated and compared. Notwithstanding their relative simplicity, the two excess Gibbs energy models enable a reasonable description of the data at hand, provided the temperature dependencies of the pure components

properties required as input data is taken into account and those of the adjustable binary interaction parameter is selected among the ones investigated with respect to the parsimony principle. The selected most parsimonious versions of the Scatchard-Hildebrand and combined Scatchard-Hildebrand/Flory-Huggins models achieve essentially the same accuracy with a mean absolute relative deviation between estimated and experimental values of 21.87 and 22.77%, respectively, but do not provide the same precision, the mean relative standard deviation in solubility estimates being of 7.10% for the former model and of 24.29% for the latter one. Whether or not correcting the Scatchard-Hildebrand model for the relative differences in molar volume between components by using the Flory-Huggins model for the excess molar combinatorial entropy mixing is justified for the present system remains difficult to be stated categorically based on these accuracy and precision criteria alone, especially because the selected most parsimonious version of the each of the two models compared does not contain the same number of adjustable parameters. From pairwise comparison of the two excess Gibbs energy models under consideration for each of the investigated model versions, the combined Scatchard-Hildebrand/Flory-Huggins model emerges as the one that performs best in balancing the decrease in the residual sum-of-squares against the number of adjustable parameters in two-thirds of the cases. Still based on information-theoretic considerations, the selected most parsimonious version of the combined Scatchard-Hildebrand/Flory-Huggins model appears to be more than 6 times more likely to be the best model for the data at hand than the one of the Scatchard-Hildebrand model. In addition to be more parsimonious and as a counterpart of its worse precision, the selected version of the combined Scatchard-Hildebrand/Flory Huggins model has the advantage over that of the Scatchard-Hildebrand model of encompassing all experimental solubility data within the limits of its 99% confidence interval, without this being outrageously wide. For these reasons, it is left to the end-user to choose which model to adopt depending on its own requirements. In the framework of developing solid dosage forms of poorly water-soluble drugs by freeze-drying from water + *tert*-butyl alcohol solvent mixtures, selected most parsimonious versions of the two excess Gibbs energy models investigated are accurate and precise enough for preformulation studies at early development stages. However, one should not expect that models with such as simple structure might allow describing the dependence of the solubility of drugs in this cosolvent system on composition and temperature with the level of accuracy and precision required at latter development stages. It is quite likely that, due to their more complex structures, excess Gibbs energy models based on local composition theory would perform better than the two excess Gibbs energy models presently investigated in correlating experimental solubility data, but this should obviously be evaluated. This will be the subject of future works. Nevertheless, it is possible even now to highlight that by considering the exact same three functions to describe the possible dependence of binary interaction parameters on temperature before selecting the best combination with respect to the parsimony principle using second-order Akaike's information criterion corrected for small sample size as presently done, the number of model versions generated for local composition theory-based excess

Gibbs energy models to be compared is substantially higher than that for the two excess Gibbs energy models investigated in this work. For a ternary system such as the one studied here, the number of model versions reaches up to 729 for excess Gibbs energy models containing two binary interaction parameters per pair of unlike molecules, and up to 19 683 for those containing three. With this respect, it might be wiser to evaluate directly the predictive performances of these models by determining binary interaction parameters from regression of binary equilibrium data while keeping the same approach to best select their respective dependencies on temperature. As a result, the number of model versions does reduce to either 9 or 27 per each of the three contributing binary subsystems, depending on the number of binary interaction parameters per pair of unlike molecules contained in the excess Gibbs energy model considered. Although this would allow saving computational efforts, it would be nevertheless interesting to compare the performances of the local composition theory-based excess Gibbs energy models as well as those investigated in the present work in both correlating and predicting the composition and temperature dependence of the solubility of diazepam in water + *tert*-butyl alcohol mixtures. Efforts towards such computations are currently underway in our laboratory.

This page is intentionally left blank.

Nomenclature

Latin letters

A	interaction parameter of any excess Gibbs energy model
a	adjustable parameter of any excess Gibbs energy model (K^{-1})
b	adjustable parameter of any excess Gibbs energy model
$C_{p,m}$	molar heat capacity at constant pressure ($\text{J}\cdot\text{K}^{-1}\cdot\text{mol}^{-1}$)
cr	crystalline solid phase
e	residual from least-squares regression (varies)
F	Fisher statistic
g	gas phase
G_m	molar Gibbs energy ($\text{J}\cdot\text{mol}^{-1}$)
H_m	molar enthalpy ($\text{J}\cdot\text{mol}^{-1}$)
k	number of adjustable model parameters
l	liquid phase
l	interaction parameter of the Scatchard-Hildebrand model
l'	interaction parameter of the combined Scatchard-Hildebrand/Flory-Huggins model
M	molar mass ($\text{g}\cdot\text{mol}^{-1}$)
m	number of mixture components
N	number of regressed data points
n	amount of substance (mol)
P	pressure (MPa)
p	statistical probability
R	molar ideal gas constant ($8.3145 \text{ J}\cdot\text{K}^{-1}\cdot\text{mol}^{-1}$)
r	number of models
r_{adj}^2	adjusted squared correlation coefficient
s	standard deviation (varies)
s_r	relative standard deviation
T	temperature (K)
t	Student statistic
U_m	molar internal energy ($\text{J}\cdot\text{mol}^{-1}$)
V_m	molar volume ($\text{cm}^3\cdot\text{mol}^{-1}$)
v	number of atoms or groups
w_A	Akaike weight
w	mass fraction
X	phase composition
x	mole fraction
z	normal statistic

Greek letters

γ	activity coefficient referenced to Raoult's law
Δ	change in quantity
δ	solubility parameter ($\text{MPa}^{1/2}$)
λ	shape parameter of Tukey lambda distribution
ν	number of atoms or groups
ρ	density ($\text{g}\cdot\text{cm}^{-3}$)
ϕ	volume fraction

Superscripts

*	pure component
0	solute-free
sat	saturation condition

Subscripts

1	component 1
2	component 2
3	component 3
expt	experimental
calc	back-calculated from a model equation
fus	fusion process
vap	vaporization process

Abbreviations

AIC _c	second-order Akaike's information criterion
df	statistical degree of freedom
DZP	diazepam
FH	Flory-Huggins
IUPAC	international union of pure and applied chemistry
OF	objective function
SH	Scatchard-Hildebrand
SS	sum-of-squares
TBA	<i>tert</i> -butyl alcohol
W	water

References

- [1] P. Kolář, J.-W. Shen, A. Tsuboi, T. Ishikawa, Solvent selection for pharmaceuticals, *Fluid Phase Equilibria*, 194–197 (2002) 771-782.
- [2] D.L. Teagarden, D.S. Baker, Practical aspects of lyophilization using non-aqueous co-solvent systems, *European Journal of Pharmaceutical Sciences*, 15 (2002) 115-133.
- [3] D.L. Teagarden, W. Wang, D.S. Baker, Practical aspects of freeze-drying of pharmaceutical and biological products using nonaqueous cosolvent systems, in: *Freeze Drying/Lyophilization of Pharmaceutical and Biological Products*, third ed., Informa Healthcare, 2010, pp. 254-287.
- [4] S. Vessot, J. Andrieu, A review on freeze drying of drugs with tert-butanol (TBA) + water systems: Characteristics, advantages, drawbacks, *Drying Technology*, 30 (2012) 377-385.
- [5] ICH harmonized tripartite guideline Q3C (R5), Impurities: guideline for residual solvents, in: *International Conference on the Harmonization of Technical Requirements for the Registration of Pharmaceuticals for Human Use*, 2011.
- [6] D. Prat, O. Pardigon, H.-W. Flemming, S. Letestu, V. Ducandas, P. Isnard, E. Guntrum, T. Senac, S. Ruisseau, P. Cruciani, P. Hosek, Sanofi's solvent selection guide: A step toward more sustainable processes, *Organic Process Research & Development*, 17 (2013) 1517-1525.
- [7] K. Kasraian, P.P. DeLuca, Thermal analysis of the tertiary butyl alcohol-water system and its implications on freeze-drying, *Pharmaceutical Research*, 12 (1995) 484-490.
- [8] D.L. Teagarden, W.J. Petre, P.M. Gold, Stabilized prostaglandin E1, US Patent No. 5,741,523, (1998).
- [9] R. Daoussi, E. Bogdani, S. Vessot, J. Andrieu, O. Monnier, Freeze-drying of an active principle ingredient using organic co-solvent formulations: Influence of freezing conditions and formulation on solvent crystals morphology, thermodynamics data, and sublimation kinetics, *Drying Technology*, 29 (2011) 1858-1867.
- [10] E. Bogdani, S. Vessot, J. Andrieu, Experimental and modeling study during freeze drying of aqueous tert-butanol-based formulations in vials, *Drying Technology*, 31 (2013) 1772-1779.
- [11] E. Bogdani, S. Vessot, G. Do, J. Andrieu, G. Degobert, Optimization of freeze-drying cycle for tert-butanol-based formulations of ibuprofen, *Drying Technology*, 31 (2013) 308-313.
- [12] K. Kasraian, P.P. DeLuca, The effect of tertiary butyl alcohol on the resistance of the dry product layer during primary drying, *Pharmaceutical Research*, 12 (1995) 491-495.
- [13] R. Daoussi, S. Vessot, J. Andrieu, O. Monnier, Sublimation kinetics and sublimation end-point times during freeze-drying of pharmaceutical active principle with organic co-solvent formulations, *Chemical Engineering Research and Design*, 87 (2009) 899-907.
- [14] D.L. Teagarden, W.J. Petre, P.M. Gold, Stabilized prostaglandin E1, United States Patent No. 5,741,523, (1998).
- [15] D.L. Teagarden, W.J. Petre, P.M. Gold, Method for preparing stabilized prostaglandin E1, United States Patent No. 5,770,230, in, 1998.
- [16] C. Li, Y. Deng, A novel method for the preparation of liposomes: Freeze drying of monophasic solutions, *Journal of Pharmaceutical Sciences*, 93 (2004) 1403-1414.
- [17] Z. Wang, Y. Deng, X. Zhang, The novel application of tertiary butyl alcohol in the preparation of hydrophobic drug-HP β CD complex, *Journal of Pharmacy and Pharmacology*, 58 (2006) 409-414.
- [18] Z. Wang, Y. Deng, S. Sun, X. Zhang, Preparation of hydrophobic drugs cyclodextrin complex by lyophilization monophasic solution, *Drug Development and Industrial Pharmacy*, 32 (2006) 73-83.
- [19] E. Bogdani, S. Vessot, J. Andrieu, Optimization of freeze-drying cycles of pharmaceutical organic co-solvent-based formulations using the design space methodology, *Drying Technology*, 30 (2012) 1297-1306.
- [20] M.D. Eddleston, B. Patel, G.M. Day, W. Jones, Cocrystallization by freeze-drying: Preparation of novel multicomponent crystal forms, *Crystal Growth & Design*, 13 (2013) 4599-4606.
- [21] S.Y.K. Fong, A. Ibisogly, A. Bauer-Brandl, Solubility enhancement of BCS Class II drug by solid phospholipid dispersions: Spray drying versus freeze-drying, *International Journal of Pharmaceutics*, 496 (2015) 382-391.
- [22] S. Wittaya-Areekul, G.F. Needham, N. Milton, M.L. Roy, S.L. Nail, Freeze-drying of tert-butanol/water cosolvent systems: A case report on formation of a friable freeze-dried powder of tobramycin sulfate, *Journal of Pharmaceutical Sciences*, 91 (2002) 1147-1155.
- [23] C. Telang, R. Suryanarayanan, Crystallization of cephalothin sodium during lyophilization from tert-butyl alcohol-water cosolvent system, *Pharmaceutical Research*, 22 (2005) 153-160.
- [24] D.J. Van Drooge, W.L.J. Hinrichs, H.W. Frijlink, Incorporation of lipophilic drugs in sugar glasses by lyophilization using a mixture of water and tertiary butyl alcohol as solvent, *Journal of Pharmaceutical Sciences*, 93 (2004) 713-725.

- [25] D.J. van Drooge, W.L.J. Hinrichs, H.W. Frijlink, Anomalous dissolution behaviour of tablets prepared from sugar glass-based solid dispersions, *Journal of Controlled Release*, 97 (2004) 441-452.
- [26] D.J. van Drooge, W.L.J. Hinrichs, M.R. Visser, H.W. Frijlink, Characterization of the molecular distribution of drugs in glassy solid dispersions at the nano-meter scale, using differential scanning calorimetry and gravimetric water vapour sorption techniques, *International Journal of Pharmaceutics*, 310 (2006) 220-229.
- [27] H. de Waard, W.L.J. Hinrichs, M.R. Visser, C. Bologna, H.W. Frijlink, Unexpected differences in dissolution behavior of tablets prepared from solid dispersions with a surfactant physically mixed or incorporated, *International Journal of Pharmaceutics*, 349 (2008) 66-73.
- [28] P. Srinarong, S. Kouwen, M.R. Visser, W.L.J. Hinrichs, H.W. Frijlink, Effect of drug-carrier interaction on the dissolution behavior of solid dispersion tablets, *Pharmaceutical Development and Technology*, 15 (2010) 460-468.
- [29] H.F. Mansour, U. F. Aly, In vitro evaluation and in vivo performance of lyophilized gliclazide, *Drug Development and Industrial Pharmacy*, 41 (2015) 650-657.
- [30] D.J. van Drooge, W.L.J. Hinrichs, K.A.M. Wegman, M.R. Visser, A.C. Eissens, H.W. Frijlink, Solid dispersions based on inulin for the stabilisation and formulation of Δ^9 -tetrahydrocannabinol, *European Journal of Pharmaceutical Sciences*, 21 (2004) 511-518.
- [31] T. Wang, N. Wang, Y. Zhang, W. Shen, X. Gao, T. Li, Solvent injection-lyophilization of tert-butyl alcohol/water cosolvent systems for the preparation of drug-loaded solid lipid nanoparticles, *Colloids and Surfaces B: Biointerfaces*, 79 (2010) 254-261.
- [32] H. de Waard, W.L.J. Hinrichs, H.W. Frijlink, A novel bottom-up process to produce drug nanocrystals: Controlled crystallization during freeze-drying, *Journal of Controlled Release*, 128 (2008) 179-183.
- [33] P. Srinarong, J.H. Faber, M.R. Visser, W.L.J. Hinrichs, H.W. Frijlink, Strongly enhanced dissolution rate of fenofibrate solid dispersion tablets by incorporation of superdisintegrants, *European Journal of Pharmaceutics and Biopharmaceutics*, 73 (2009) 154-161.
- [34] H. de Waard, T. De Beer, W.L.J. Hinrichs, C. Vervaet, J.-P. Remon, H.W. Frijlink, Controlled crystallization of the lipophilic drug fenofibrate during freeze-drying: Elucidation of the mechanism by in-line Raman spectroscopy, *The AAPS Journal*, 12 (2010) 569-575.
- [35] J.G. Rosas, H. de Waard, T. De Beer, C. Vervaet, J.P. Remon, W.L.J. Hinrichs, H.W. Frijlink, M. Blanco, NIR spectroscopy for the in-line monitoring of a multicomponent formulation during the entire freeze-drying process, *Journal of Pharmaceutical and Biomedical Analysis*, 97 (2014) 39-46.
- [36] A. Alqurshi, K.L.A. Chan, P.G. Royall, In-situ freeze-drying - forming amorphous solids directly within capsules: An investigation of dissolution enhancement for a poorly soluble drug, *Scientific Reports*, 7 (2017) 2910.
- [37] B. Nuijen, M. Bouma, R.E.C. Henrar, P. Floriano, J.M. Jimeno, H. Talsma, J.J. Kettenes-van den Bosch, A.J.R. Heck, A. Bult, J.H. Beijnen, Pharmaceutical development of a parenteral lyophilized formulation of the novel antitumor agent aplidine, *PDA Journal of Pharmaceutical Science and Technology*, 54 (2000) 193-208.
- [38] N. Ni, M. Tesconi, S.E. Tabibi, S. Gupta, S.H. Yalkowsky, Use of pure t-butanol as a solvent for freeze-drying: a case study, *International Journal of Pharmaceutics*, 226 (2001) 39-46.
- [39] E. Fournier, M.-H. Dufresne, D.C. Smith, M. Ranger, J.-C. Leroux, A novel one-step drug-loading procedure for water-soluble amphiphilic nanocarriers, *Pharmaceutical Research*, 21 (2004) 962-968.
- [40] D. Le Garrec, S. Gori, L. Luo, D. Lessard, D.C. Smith, M.A. Yessine, M. Ranger, J.C. Leroux, Poly(N-vinylpyrrolidone)-block-poly(d,l-lactide) as a new polymeric solubilizer for hydrophobic anticancer drugs: in vitro and in vivo evaluation, *Journal of Controlled Release*, 99 (2004) 83-101.
- [41] S.C. van der Schoot, B. Nuijen, F.M. Flesch, A. Gore, D. Mirejovsky, L. Lenaz, J.H. Beijnen, Development of a bladder instillation of the indoloquinone anticancer agent EO-9 using tert-butyl alcohol as lyophilization vehicle, *AAPS PharmSciTech*, 8 (2007) E78-E87.
- [42] S.C. van der Schoot, L.D. Vainchtein, J.H. Beijnen, A. Gore, D. Mirejovsky, L. Lenaz, B. Nuijen, EO-9 bladder instillations: Formulation selection based on stability characteristics and in vitro simulation studies, *International Journal of Pharmaceutics*, 329 (2007) 135-141.
- [43] N. Elgindy, K. Elkhodairy, A. Molokhia, A. Elzoghby, Lyophilization monophasic solution technique for improvement of the physicochemical properties of an anticancer drug, flutamide, *European Journal of Pharmaceutics and Biopharmaceutics*, 74 (2010) 397-405.
- [44] J.J. Moes, S.L.W. Koolen, A.D.R. Huitema, J.H.M. Schellens, J.H. Beijnen, B. Nuijen, Pharmaceutical development and preliminary clinical testing of an oral solid dispersion formulation of docetaxel (ModraDoc001), *International Journal of Pharmaceutics*, 420 (2011) 244-250.
- [45] N. Elgindy, K. Elkhodairy, A. Molokhia, A. Elzoghby, Lyophilization monophasic solution technique for preparation of amorphous flutamide dispersions, *Drug Development and Industrial Pharmacy*, 37 (2011) 754-764.

- [46] N. Elgindy, K. Elkhodairy, A. Molokhia, A. Elzoghby, Lyophilized flutamide dispersions with polyols and amino acids: preparation and in vitro evaluation, *Drug Development and Industrial Pharmacy*, 37 (2011) 446-455.
- [47] J. Moes, S. Koolen, A. Huitema, J. Schellens, J. Beijnen, B. Nuijen, Development of an oral solid dispersion formulation for use in low-dose metronomic chemotherapy of paclitaxel, *European Journal of Pharmaceutics and Biopharmaceutics*, 83 (2013) 87-94.
- [48] K. Tomoda, Y.T. Tam, H. Cho, D. Buehler, K.R. Kozak, G.S. Kwon, Triolimus: A Multi-Drug Loaded Polymeric Micelle Containing Paclitaxel, 17-AAG, and Rapamycin as a Novel Radiosensitizer, *Macromolecular Bioscience*, 17 (2017) 1600194-n/a.
- [49] T.A. Debele, S.L. Mekuria, H.-C. Tsai, A pH-sensitive micelle composed of heparin, phospholipids, and histidine as the carrier of photosensitizers: Application to enhance photodynamic therapy of cancer, *International Journal of Biological Macromolecules*, 98 (2017) 125-138.
- [50] P.T. Fowler, G.F. Doncel, P.M. Bummer, G.A. Digenis, Coprecipitation of nonoxynol-9 with polyvinylpyrrolidone to decrease vaginal irritation potential while maintaining spermicidal potency, *AAPS PharmSciTech*, 4 (2003) 10-17.
- [51] P. Srinarong, B.T. Pham, M. Holen, A. van der Plas, R.C.A. Schellekens, W.L.J. Hinrichs, H.W. Frijlink, Preparation and physicochemical evaluation of a new tacrolimus tablet formulation for sublingual administration, *Drug Development and Industrial Pharmacy*, 38 (2012) 490-500.
- [52] C. Liu, C. Kong, G. Wu, J. Zhu, B. Javid, F. Qian, Uniform and amorphous rifampicin microspheres obtained by freezing induced LLPS during lyophilization, *International Journal of Pharmaceutics*, 495 (2015) 500-507.
- [53] B. Nuijen, M. Bouma, R.E.C. Henrar, P. Floriano, J.M. Jimeno, H. Talsma, J.J. Kettenes-van den Bosch, A.J.R. Heck, A. Bult, J.H. Beijnen, Pharmaceutical Development of a Parenteral Lyophilized Formulation of the Novel Antitumor Agent Aplidine, *PDA J Pharm Sci Technol*, 54 (2000) 193-208.
- [54] S.T. Jay, Solubilization Using Cosolvent Approach, in: *Water-Insoluble Drug Formulation*, Second ed., CRC Press, 2008, pp. 161-194.
- [55] F. Franks, T. Auffret, *Freeze-drying of Pharmaceuticals and Biopharmaceuticals: Principles and Practice*, The Royal Society of Chemistry, 2007.
- [56] L. Rey, J.C. May, *Freeze Drying/Lyophilization of Pharmaceutical and Biological Products*, Third ed., Informa Healthcare, 2010.
- [57] C. Telang, R. Suryanarayanan, Crystallization of Cephalothin Sodium During Lyophilization from tert-Butyl Alcohol—Water Cosolvent System, *Pharm Res*, 22 (2005) 153-160.
- [58] B. Munjal, A.K. Bansal, Impact of Tert-Butyl Alcohol on Crystallization Kinetics of Gemcitabine Hydrochloride in Frozen Aqueous Solutions, *J Pharm Sci*, 104 (2015) 87-97.
- [59] B. Faller, P. Ertl, Computational approaches to determine drug solubility, *Adv Drug Deliv Rev*, 59 (2007) 533-545.
- [60] W.-Q. Tong, Practical Aspects of Solubility Determination in Pharmaceutical Preformulation, in: *Solvent Systems and Their Selection in Pharmaceutics and Biopharmaceutics*, Springer Science & Business Media, 2007, pp. 137-149.
- [61] C.A. Lipinski, F. Lombardo, B.W. Dominy, P.J. Feeney, Experimental and computational approaches to estimate solubility and permeability in drug discovery and development settings, *Adv Drug Deliv Rev*, 64, Supplement (2012) 4-17.
- [62] G. Scatchard, Equilibria in non-electrolyte solutions in relation to the vapor pressures and densities of the components, *Chemical Reviews*, 8 (1931) 321-333.
- [63] J.H. Hildebrand, S.E. Wood, The derivation of equations for regular solutions, *The Journal of Chemical Physics*, 1 (1933) 817-822.
- [64] G.M. Wilson, Vapor-liquid equilibrium. XI. A new expression for the excess free energy of mixing, *Journal of the American Chemical Society*, 86 (1964) 127-130.
- [65] H. Renon, J.M. Prausnitz, Local compositions in thermodynamic excess functions for liquid mixtures, *AIChE Journal*, 14 (1968) 135-144.
- [66] D.S. Abrams, J.M. Prausnitz, Statistical thermodynamics of liquid mixtures: A new expression for the excess Gibbs energy of partly or completely miscible systems, *AIChE Journal*, 21 (1975) 116-128.
- [67] C.V.S. Subrahmanyam, M. Sreenivasa Reddy, J. Venkata Rao, P. Gundu Rao, Irregular solution behaviour of paracetamol in binary solvents, *International Journal of Pharmaceutics*, 78 (1992) 17-24.
- [68] A. Jouyban-Gharamaleki, The modified Wilson model and predicting drug solubility in water-cosolvent mixtures, *Chemical and Pharmaceutical Bulletin*, 46 (1998) 1058-1061.
- [69] S. Romero, B. Escalera, P. Bustamante, Solubility behavior of polymorphs I and II of mefenamic acid in solvent mixtures, *International Journal of Pharmaceutics*, 178 (1999) 193-202.

- [70] H. Hojjati, S. Rohani, Measurement and prediction of solubility of paracetamol in water–isopropanol solution. Part 1. Measurement and data analysis, *Organic Process Research & Development*, 10 (2006) 1101-1109.
- [71] H. Hojjati, S. Rohani, Measurement and prediction of solubility of paracetamol in water–isopropanol solution. Part 2. Prediction, *Organic Process Research & Development*, 10 (2006) 1110-1118.
- [72] U. Domańska, A. Pobudkowska, A. Pelczarska, P. Gierycz, pKa and solubility of drugs in water, ethanol, and 1-octanol, *The Journal of Physical Chemistry B*, 113 (2009) 8941-8947.
- [73] H. Matsuda, K. Kaburagi, S. Matsumoto, K. Kurihara, K. Tochigi, K. Tomono, Solubilities of salicylic acid in pure solvents and binary mixtures containing cosolvent, *Journal of Chemical & Engineering Data*, 54 (2009) 480-484.
- [74] U. Domańska, A. Pobudkowska, A. Pelczarska, M. Winiarska-Tusznio, P. Gierycz, Solubility and pKa of select pharmaceuticals in water, ethanol, and 1-octanol, *The Journal of Chemical Thermodynamics*, 42 (2010) 1465-1472.
- [75] H. Matsuda, K. Kaburagi, K. Kurihara, K. Tochigi, K. Tomono, Prediction of solubilities of pharmaceutical compounds in water+co-solvent systems using an activity coefficient model, *Fluid Phase Equilibria*, 290 (2010) 153-157.
- [76] U. Domańska, A. Pobudkowska, A. Pelczarska, Solubility of sparingly soluble drug derivatives of anthranilic acid, *The Journal of Physical Chemistry B*, 115 (2011) 2547-2554.
- [77] U. Domańska, A. Pobudkowska, A. Pelczarska, Ł. Żukowski, Modelling, solubility and pKa of five sparingly soluble drugs, *International Journal of Pharmaceutics*, 403 (2011) 115-122.
- [78] M. Kharwade, G. Achyuta, C.V.S. Subrahmanyam, P.R. Sathesh Babu, Solubility behavior of lornoxicam in binary solvents of pharmaceutical interest, *Journal of Solution Chemistry*, 41 (2012) 1364-1374.
- [79] D.M. Cristancho, D.R. Delgado, F. Martínez, Meloxicam solubility in ethanol+water mixtures according to the extended Hildebrand solubility approach, *Journal of Solution Chemistry*, 42 (2013) 1706-1716.
- [80] R.G. Sotomayor, A.R. Holguín, D.M. Cristancho, D.R. Delgado, F. Martínez, Extended Hildebrand solubility approach applied to piroxicam in ethanol+water mixtures, *Journal of Molecular Liquids*, 180 (2013) 34-38.
- [81] P.B. Rathi, K.V. Deshpande, Extended Hildebrand approach: An empirical model for solubility prediction of etodolac in 1,4-Dioxane and water mixtures, *Journal of Solution Chemistry*, 43 (2014) 1886-1903.
- [82] H. Matsuda, K. Mori, M. Tomioka, N. Kariyasu, T. Fukami, K. Kurihara, K. Tochigi, K. Tomono, Determination and prediction of solubilities of active pharmaceutical ingredients in selected organic solvents, *Fluid Phase Equilibria*, 406 (2015) 116-123.
- [83] A. Pobudkowska, U. Domańska, B.A. Jurkowska, K. Dymczuk, Solubility of pharmaceuticals in water and alcohols, *Fluid Phase Equilibria*, 392 (2015) 56-64.
- [84] S. Nozohouri, A. Shayanfar, E. Kenndler, A. Jouyban, Solubility of celecoxib in N-methyl-2-pyrrolidone + 2-propanol mixtures at various temperatures, *Journal of Molecular Liquids*, 241 (2017) 1032-1037.
- [85] A. Martin, M.J. Miralles, Extended Hildebrand solubility approach: Solubility of tolbutamide, acetohexamide, and sulfisomidine in binary solvent mixtures, *Journal of Pharmaceutical Sciences*, 71 (1982) 439-442.
- [86] A. Martin, P.L. Wu, Z. Liron, S. Cohen, Dependence of solute solubility parameters on solvent polarity, *Journal of Pharmaceutical Sciences*, 74 (1985) 638-642.
- [87] A. Regosz, T. Pelplińska, P. Kowalski, Z. Thiel, Prediction of solubility of sulfonamides in water and organic solvents based on the extended regular solution theory, *International Journal of Pharmaceutics*, 88 (1992) 437-442.
- [88] J.B. Escalera, P. Bustamante, A. Martin, Predicting the solubility of drugs in solvent mixtures: Multiple solubility maxima and the chameleonic effect, *Journal of Pharmacy and Pharmacology*, 46 (1994) 172-176.
- [89] C.V.S. Subrahmanyam, K.R. Prakash, P.G. Rao, Estimation of the solubility parameter of trimethoprim by current methods, *Pharmaceutica Acta Helveticae*, 71 (1996) 175-183.
- [90] F. Varanda, M.J. Pratas de Melo, A.I. Caço, R. Dohrn, F.A. Makrydaki, E. Voutsas, D. Tassios, I.M. Marrucho, Solubility of antibiotics in different Solvents. 1. Hydrochloride forms of tetracycline, moxifloxacin, and ciprofloxacin, *Industrial & Engineering Chemistry Research*, 45 (2006) 6368-6374.
- [91] A.I. Caço, F. Varanda, M.J. Pratas de Melo, A.M.A. Dias, R. Dohrn, I.M. Marrucho, Solubility of antibiotics in different solvents. Part II. Non-hydrochloride forms of tetracycline and ciprofloxacin, *Industrial & Engineering Chemistry Research*, 47 (2008) 8083-8089.
- [92] X. Wang, Y. Qin, T. Zhang, W. Tang, B. Ma, J. Gong, Measurement and correlation of solubility of azithromycin monohydrate in five pure solvents, *Journal of Chemical & Engineering Data*, 59 (2014) 784-791.

- [93] Z.J. Cárdenas, D.M. Jiménez, D.R. Delgado, M.Á. Peña, F. Martínez, Extended Hildebrand solubility approach applied to some sulphonamides in propylene glycol + water mixtures, *Physics and Chemistry of Liquids*, 53 (2015) 763-775.
- [94] M. Sun, K. Li, S. Du, Y. Liu, D. Han, X. Li, P. Yang, S. Liu, J. Gong, Correlation and thermodynamic analysis of solubility of cefmetazole acid in three (alcohol + water) binary solvents at temperatures from 278.15 K to 303.15 K, *The Journal of Chemical Thermodynamics*, 103 (2016) 355-365.
- [95] D.R. Delgado, M.Á. Peña, F. Martínez, Extended Hildebrand solubility approach applied to some sulphapyrimidines in some {methanol (1) + water (2)} mixtures, *Physics and Chemistry of Liquids*, (2017) 1-13.
- [96] H. Shen, S. Wu, Y. Liu, K. Li, S. Xu, J. Gong, Determination and correlation of Avermectin B1a solubility in different binary solvent mixtures at temperatures from (283.15 to 313.15) K, *The Journal of Chemical Thermodynamics*, 105 (2017) 253-266.
- [97] H. Zhang, Y. Yang, M. Zhu, S. Jiang, S. Xu, S. Du, B. Yu, J. Gong, Solid-liquid phase equilibrium and thermodynamic analysis of prothioconazole in mono-solvents and binary solvents from 283.15 K to 313.15 K, *Journal of Molecular Liquids*, 240 (2017) 162-171.
- [98] K. Zhang, H. Shen, S. Xu, H. Zhang, M. Zhu, P. Shi, X. Fu, Y. Yang, J. Gong, Thermodynamic study of solubility for pyrazinamide in ten solvents from T=(283.15 to 323.15) K, *The Journal of Chemical Thermodynamics*, 112 (2017) 204-212.
- [99] A. Adjei, J. Newburger, A. Martin, Extended Hildebrand approach: Solubility of caffeine in dioxane-water mixtures, *Journal of Pharmaceutical Sciences*, 69 (1980) 659-661.
- [100] A. Martin, A.N. Paruta, A. Adjei, Extended Hildebrand solubility approach: Methylxanthines in mixed solvents, *Journal of Pharmaceutical Sciences*, 70 (1981) 1115-1120.
- [101] M.A. Herrador, A.G. González, Solubility prediction of caffeine in aqueous N,N-dimethylformamide mixtures using the extended Hildebrand solubility approach, *International Journal of Pharmaceutics*, 156 (1997) 239-244.
- [102] A. Nokhodchi, J. Shokri, M. Barzegar-Jalali, T. Ghafourian, Prediction of benzodiazepines solubility using different cosolvency models, *Il Farmaco*, 57 (2002) 555-557.
- [103] U. Domańska, A. Pelczarska, A. Pobudkowska, Solubility and pKa determination of six structurally related phenothiazines, *International Journal of Pharmaceutics*, 421 (2011) 135-144.
- [104] S. Du, Y. Wang, J. Li, S. Wu, W. Dun, X. Song, J. Wang, J. Gong, Correlation and thermodynamic analysis of solubility of diphenhydramine hydrochloride in pure and binary solvents, *The Journal of Chemical Thermodynamics*, 93 (2016) 132-142.
- [105] S. Liu, S. Xu, S. Du, B. Yu, J. Gong, Determination and correlation of solubility and thermodynamic properties of eszopiclone in pure and mixed solvents, *Journal of Molecular Liquids*, 221 (2016) 1035-1044.
- [106] A. Martin, J. Newburger, A. Adjei, Extended Hildebrand solubility approach: Solubility of theophylline in polar binary solvents, *Journal of Pharmaceutical Sciences*, 69 (1980) 487-491.
- [107] J.G. Fokkens, J.G.M. van Amelsfoort, C.J. de Blaey, C.G. de Kruif, J. Wilting, A thermodynamic study of the solubility of theophylline and its hydrate, *International Journal of Pharmaceutics*, 14 (1983) 79-93.
- [108] A.G. González, M.A. Herrador, A.G. Asuero, Solubility of theophylline in aqueous N,N-dimethylformamide mixtures, *International Journal of Pharmaceutics*, 108 (1994) 149-154.
- [109] M. Mirmehrabi, S. Rohani, K.S.K. Murthy, B. Radatus, Solubility, dissolution rate and phase transition studies of ranitidine hydrochloride tautomeric forms, *International Journal of Pharmaceutics*, 282 (2004) 73-85.
- [110] H. Matsuda, S. Matsumoto, K. Kaguragi, K. Kurihara, K. Tochigi, K. Tomono, Determination and correlation of solubilities of famotidine in water + co-solvent mixed solvents, *Fluid Phase Equilibria*, 302 (2011) 115-122.
- [111] A. Pobudkowska, U. Domańska, J.A. Kryśka, The physicochemical properties and solubility of pharmaceuticals – Methyl xanthines, *The Journal of Chemical Thermodynamics*, 79 (2014) 41-48.
- [112] A. Martin, P.L. Wu, A. Adjei, M. Mehdizadeh, K.C. James, C. Metzler, Extended Hildebrand solubility approach: Testosterone and testosterone propionate in binary solvents, *Journal of Pharmaceutical Sciences*, 71 (1982) 1334-1340.
- [113] J. Fang, M. Zhang, P. Zhu, J. Ouyang, J. Gong, W. Chen, F. Xu, Solubility and solution thermodynamics of sorbic acid in eight pure organic solvents, *The Journal of Chemical Thermodynamics*, 85 (2015) 202-209.
- [114] X. Li, D. Han, Y. Wang, S. Du, Y. Liu, J. Zhang, B. Yu, B. Hou, J. Gong, Measurement of solubility of thiamine hydrochloride hemihydrate in three binary solvents and mixing properties of solutions, *Journal of Chemical & Engineering Data*, 61 (2016) 3665-3678.
- [115] S.M. Walas, Activity Coefficients, in: *Phase Equilibria in Chemical Engineering*, Butterworth-Heinemann, 1985, pp. 165-244.

- [116] F. Aman-Pommier, G. Degobert, C. Jallut, Solubility of diazepam in water + tert-butyl alcohol solvent mixtures: Part 1. Experimental data and thermodynamic analysis, *Fluid Phase Equilibria*, 408 (2016) 284-298.
- [117] L.J. Gordon, R.L. Scott, Enhanced solubility in solvent mixtures. I. The system phenanthrene-cyclohexane-methylene iodide, *Journal of the American Chemical Society*, 74 (1952) 4138-4140.
- [118] A.L. Myers, J.M. Prausnitz, Thermodynamics of solid carbon dioxide solubility in liquid solvents at low temperatures, *Industrial & Engineering Chemistry Fundamentals*, 4 (1965) 209-212.
- [119] Y. Arai, S. Saito, S. Maeda, Prediction of solvent selectivity in extractive distillation and of vapor-liquid equilibria of hydrocarbons, *Journal of Chemical Engineering of Japan*, 2 (1969) 8-13.
- [120] M. Vitoria, J. Walkley, Studies in regular solution theory. Part 1. Solubility studies of tetraphenyltin in simple non-polar solvents, *Transactions of the Faraday Society*, 65 (1969) 57-61.
- [121] M. Vitoria, J. Walkley, Studies in regular solution theory. Part 2. Entropy of solution of tetraphenyltin in simple non-polar solvents, *Transactions of the Faraday Society*, 65 (1969) 62-69.
- [122] E.W. Funk, J.M. Prausnitz, Thermodynamic properties of liquid mixtures: Aromatic-saturated hydrocarbon systems, *Industrial & Engineering Chemistry*, 62 (1970) 8-15.
- [123] G.T. Preston, J.M. Prausnitz, Thermodynamics of solid solubility in cryogenic solvents, *Industrial & Engineering Chemistry Process Design and Development*, 9 (1970) 264-271.
- [124] E.R. Bazúa, J.M. Prausnitz, Vapour-liquid equilibria for cryogenic mixtures, *Cryogenics*, 11 (1971) 114-119.
- [125] G.T. Preston, E.W. Funk, J.M. Prausnitz, Solubilities of hydrocarbons and carbon dioxide in liquid methane and in liquid argon, *The Journal of Physical Chemistry*, 75 (1971) 2345-2352.
- [126] G. Maffiolo, J. Vidal, L. Asselineau, Coefficients d'équilibre liquide vapeur dans les mélanges d'hydrocarbures a pression modérée, *Chemical Engineering Science*, 30 (1975) 625-630.
- [127] Y.B. Tewari, M.M. Miller, S.P. Wasik, D. Cronin, D.H. Blackburn, W.K. Haller, J. Wegstein, D. Martire, J. Purnell, A.K. Gaigalas, Calculation of aqueous solubility of organic compounds, *Journal of Research of the National Bureau of Standards*, 87 (1982).
- [128] D.S. Mishra, S.H. Yalkowsky, Solubility of organic compounds in non-aqueous systems: Polycyclic aromatic hydrocarbons in benzene, *Industrial & Engineering Chemistry Research*, 29 (1990) 2278-2283.
- [129] A. Beerbower, P.L. Wu, A. Martin, Expanded solubility parameter approach I: Naphthalene and benzoic acid in individual solvents, *Journal of Pharmaceutical Sciences*, 73 (1984) 179-188.
- [130] H. Gamsjäger, J.W. Lorimer, P. Scharlin, D.G. Shaw, Glossary of terms related to solubility (IUPAC Recommendations 2008), *Pure and Applied Chemistry*, 80 (2008) 233-276.
- [131] S.I. Sandler, Mixture phase equilibria involving solids, in: *Chemical, Biochemical, and Engineering Thermodynamics*, fourth ed., John Wiley & Sons Inc., 2006, pp. 658-702.
- [132] J. Vidal, Fluid-solid equilibria. Crystallization. Hydrates, in: *Thermodynamics: Applications in Chemical Engineering and the Petroleum Industry*, Institut Français du Pétrole Publications, 2003, pp. 355-373.
- [133] S.I. Sandler, Estimation of the Gibbs energy and fugacity of a component in a mixture, in: *Chemical, Biochemical, and Engineering Thermodynamics*, fourth ed., John Wiley & Sons Inc., 2006, pp. 399-488.
- [134] J. Vidal, Characterization of mixtures, in: *Thermodynamics: Applications in Chemical Engineering and the Petroleum Industry*, Institut Français du Pétrole Publications, 2003, pp. 143-166.
- [135] J.D. van der Waals, Molekulartheorie eines Körpers, der aus zwei verschiedenen Stoffen besteht, *Zeitschrift für Physikalische Chemie*, 5 (1890) 133-173.
- [136] J.J. van Laar, Über Dampfspannungen von binären Gemischen, *Zeitschrift für Physikalische Chemie*, 72 (1910) 723-751.
- [137] J.J. van Laar, Zur Theorie der Dampfspannungen von binären Gemischen, *Zeitschrift für Physikalische Chemie*, 83 (1913) 599-608.
- [138] J.J. van Laar, R. Lorenz, Berechnung von Mischungswärmen kondensierter Systeme, *Zeitschrift für anorganische und allgemeine Chemie*, 146 (1925) 42-44.
- [139] J.H. Hildebrand, R.L. Scott, Heat of Mixing, in: *Regular Solutions*, Prentice-Hall Inc., 1962, pp. 88-103.
- [140] J.H. Hildebrand, J.M. Prausnitz, R.L. Scott, Heat of Mixing, in: *Regular and Related Solutions: The Solubility of Gases, Liquids, and Solids*, Van Nostrand Reinhold Co., 1970, pp. 82-91.
- [141] E.R. Cohen, T. Cvitas, J.G. Frey, B. Holmström, K. Kuchitsu, R. Marquardt, I. Mills, F. Pavese, M. Quack, J. Stohner, H.L. Strauss, M. Takami, A.J. Thor, Quantities, Units, and Symbols in Physical Chemistry, third ed., The Royal Society of Chemistry, 2007.
- [142] J.H. Hildebrand, R.L. Scott, Solubility Parameters, in: *Regular Solutions*, Prentice-Hall Inc., 1962, pp. 166-170.
- [143] J.H. Hildebrand, J.M. Prausnitz, R.L. Scott, Solubility Parameters, in: *Regular and Related Solutions: The Solubility of Gases, Liquids, and Solids*, Van Nostrand Reinhold Co., 1970, pp. 207-215.

- [144] S. Verdier, S.I. Andersen, Internal pressure and solubility parameter as a function of pressure, *Fluid Phase Equilibria*, 231 (2005) 125-137.
- [145] C.A. Eckert, H. Renon, J.M. Prausnitz, Molecular thermodynamics of simple liquids. Mixtures, *Industrial & Engineering Chemistry Fundamentals*, 6 (1967) 58-67.
- [146] J.H. Hildebrand, J.M. Prausnitz, R.L. Scott, Gibbs Free Energies of Liquid Mixtures, in: *Regular and Related Solutions: The Solubility of Gases, Liquids, and Solids*, Van Nostrand Reinhold Co., 1970, pp. 92-110.
- [147] P.J. Flory, Thermodynamics of high polymer solutions, *The Journal of Chemical Physics*, 9 (1941) 660-660.
- [148] M.L. Huggins, Solutions of long chain compounds, *The Journal of Chemical Physics*, 9 (1941) 440-440.
- [149] P.J. Flory, Thermodynamics of high polymer solutions, *The Journal of Chemical Physics*, 10 (1942) 51-61.
- [150] M.L. Huggins, Thermodynamic properties of solutions of long-chain compounds, *Annals of the New York Academy of Sciences*, 43 (1942) 1-32.
- [151] F. Aman-Pommier, C. Jallut, Excess specific volume of water + tert-butyl alcohol solvent mixtures: Experimental data, modeling and derived excess partial specific quantities., *Fluid Phase Equilibria*, 439 (2017) 43-66.
- [152] C.M. Hansen, *Hansen Solubility Parameters: A User's Handbook*, second ed., CRC Press, 2007.
- [153] R.F. Fedors, A method for estimating both the solubility parameters and molar volumes of liquids, *Polymer Engineering and Science*, 14 (1974) 147-154.
- [154] J.H. Hildebrand, R.L. Scott, *Regular Solutions of Solids*, in: *Regular Solutions*, Prentice-Hall Inc., 1962, pp. 116-132.
- [155] J.H. Hildebrand, J.M. Prausnitz, R.L. Scott, *Solutions of Solids*, in: *Regular and Related Solutions: The Solubility of Gases, Liquids and Solids*, Van Nostrand Reinhold Co., 1970, pp. 142-165.
- [156] K.C. James, C.T. Ng, P.R. Noyce, Solubilities of testosterone propionate and related esters in organic solvents, *Journal of Pharmaceutical Sciences*, 65 (1976) 656-659.
- [157] M.J. Chertkoff, A.N. Martin, The solubility of benzoic acid in mixed solvents, *Journal of the American Pharmaceutical Association*, 49 (1960) 444-447.
- [158] H.-M. Lin, R.A. Nash, An experimental method for determining the Hildebrand solubility parameter of organic nonelectrolytes, *Journal of Pharmaceutical Sciences*, 82 (1993) 1018-1026.
- [159] L.S. Lasdon, A.D. Waren, A. Jain, M. Ratner, Design and testing of a generalized reduced gradient code for nonlinear programming, *ACM Transactions on Mathematical Software*, 4 (1978) 34-50.
- [160] J.H. Hildebrand, R.L. Scott, *Thermodynamic Relations*, in: *Regular Solutions*, Prentice-Hall Inc., 1962, pp. 8-25.
- [161] J.H. Hildebrand, J.M. Prausnitz, R.L. Scott, *Thermodynamic Relations*, in: *Regular and Related Solutions: The Solubility of Gases, Liquids and Solids*, Van Nostrand Reinhold Co., 1970, pp. 8-27.
- [162] S.H. Neau, S.V. Bhandarkar, E.W. Hellmuth, Differential molar heat capacities to test ideal solubility estimations, *Pharmaceutical Research*, 14 (1997) 601-605.
- [163] H. Akaike, Information theory as an extension of the maximum likelihood principle, in: B.N. Petrov, F. Csaki (Eds.) *Second International Symposium on Information Theory*, Akademiai Kiado, Budapest, Hungary, 1973, pp. 267-281.
- [164] N. Sugiura, Further analysis of the data by Akaike's information criterion and the finite corrections, *Communications in Statistics - Theory and Methods*, 7 (1978) 13-26.
- [165] C.M. Hurvich, C.-L. Tsai, Regression and time series model selection in small samples, *Biometrika*, 76 (1989) 297-307.
- [166] K.P. Burnham, D.R. Anderson, *Model Selection and Multimodel Inference: A Practical Information-Theoretic Approach*, second ed., Springer-Verlag New York, Inc., 2002.
- [167] S. Kullback, R.A. Leibler, On information and sufficiency, *The Annals of Mathematical Statistics*, 22 (1951) 79-86.
- [168] P.R. Bevington, D.K. Robinson, *Data Reduction and Error Analysis for the Physical Sciences*, third ed., McGraw-Hill, 2003.
- [169] J. Jouyban, Review of the cosolvency models for predicting solubility of drugs in water-cosolvent mixtures, *Journal of Pharmacy & Pharmaceutical Sciences*, 11 (2008) 32-58.
- [170] R.M. Dickhut, D.E. Armstrong, A.W. Andren, The solubility of hydrophobic aromatic chemicals in organic solvent/water mixtures: Evaluation of four mixed solvent solubility estimation methods, *Environmental Toxicology and Chemistry*, 10 (1991) 881-889.
- [171] A. Reillo, M. Cordoba, B. Escalera, E. Selles, M. Cordoba Jr, Prediction of sulfamethizole solubility in dioxane-water mixtures, *Pharmazie*, 50 (1995) 472-475.

This page is intentionally left blank.

Appendix A

Supplementary materials related to Chapter 1

This page is intentionally left blank.

Table A.1. Excess specific isobaric expansivity of water + *tert*-butyl alcohol mixtures e_p^E over the temperature range $T = 293.15\text{-}323.15$ K at pressure $P = 0.1$ MPa as calculated from Eq. (2.2) and Eq. (2.5)^a.

w_2	Eq. (2.2)	Eq. (2.5)	w_2	Eq. (2.2)	Eq. (2.5)
e_p^E (cm ³ ·g ⁻¹ ·K ⁻¹)			e_p^E (cm ³ ·g ⁻¹ ·K ⁻¹)		
0.025	-2.63 (0.13) · 10 ⁻⁵	-4.25 (0.41) · 10 ⁻⁵	0.525	-1.24 (3.93) · 10 ⁻⁶	-1.51 (0.05) · 10 ⁻⁵
0.050	-4.24 (0.23) · 10 ⁻⁵	-5.47 (0.50) · 10 ⁻⁵	0.550	-1.51 (0.41) · 10 ⁻⁵	-2.93 (0.11) · 10 ⁻⁵
0.075	-5.02 (0.26) · 10 ⁻⁵	-4.72 (0.48) · 10 ⁻⁵	0.575	-2.73 (0.45) · 10 ⁻⁵	-4.23 (0.17) · 10 ⁻⁵
0.100	-4.48 (0.30) · 10 ⁻⁵	-2.82 (0.45) · 10 ⁻⁵	0.600	-3.46 (0.49) · 10 ⁻⁵	-5.41 (0.23) · 10 ⁻⁵
0.125	-2.56 (0.33) · 10 ⁻⁵	-3.78 (4.47) · 10 ⁻⁶	0.625	-5.02 (0.53) · 10 ⁻⁵	-6.46 (0.29) · 10 ⁻⁵
0.150	9.04 (2.65) · 10 ⁻⁶	2.19 (0.44) · 10 ⁻⁵	0.650	-6.29 (0.58) · 10 ⁻⁵	-7.40 (0.33) · 10 ⁻⁵
0.175	4.99 (0.17) · 10 ⁻⁵	4.58 (0.41) · 10 ⁻⁵	0.675	-7.49 (0.63) · 10 ⁻⁵	-8.24 (0.35) · 10 ⁻⁵
0.200	8.33 (0.41) · 10 ⁻⁵	6.61 (0.37) · 10 ⁻⁵	0.700	-8.41 (0.70) · 10 ⁻⁵	-9.01 (0.36) · 10 ⁻⁵
0.225	1.06 (0.06) · 10 ⁻⁴	8.17 (0.35) · 10 ⁻⁵	0.725	-9.28 (0.76) · 10 ⁻⁵	-9.75 (0.34) · 10 ⁻⁵
0.250	1.13 (0.07) · 10 ⁻⁴	9.21 (0.34) · 10 ⁻⁵	0.750	-1.01 (0.08) · 10 ⁻⁴	-1.05 (0.03) · 10 ⁻⁴
0.275	1.11 (0.08) · 10 ⁻⁴	9.73 (0.36) · 10 ⁻⁵	0.775	-1.07 (0.09) · 10 ⁻⁴	-1.12 (0.03) · 10 ⁻⁴
0.300	1.06 (0.08) · 10 ⁻⁴	9.76 (0.37) · 10 ⁻⁵	0.800	-1.12 (0.10) · 10 ⁻⁴	-1.19 (0.03) · 10 ⁻⁴
0.325	9.70 (0.69) · 10 ⁻⁵	9.36 (0.36) · 10 ⁻⁵	0.825	-1.16 (0.10) · 10 ⁻⁴	-1.27 (0.04) · 10 ⁻⁴
0.350	8.79 (0.65) · 10 ⁻⁵	8.58 (0.33) · 10 ⁻⁵	0.850	-1.18 (0.11) · 10 ⁻⁴	-1.33 (0.04) · 10 ⁻⁴
0.375	7.69 (0.56) · 10 ⁻⁵	7.50 (0.29) · 10 ⁻⁵	0.875	-1.18 (0.12) · 10 ⁻⁴	-1.37 (0.04) · 10 ⁻⁴
0.400	6.45 (0.53) · 10 ⁻⁵	6.19 (0.23) · 10 ⁻⁵	0.900	-1.17 (0.13) · 10 ⁻⁴	-1.37 (0.04) · 10 ⁻⁴
0.425	5.38 (0.48) · 10 ⁻⁵	4.73 (0.17) · 10 ⁻⁵	0.925	-1.14 (0.13) · 10 ⁻⁴	-1.29 (0.05) · 10 ⁻⁴
0.450	3.90 (0.44) · 10 ⁻⁵	3.17 (0.11) · 10 ⁻⁵	0.950	-1.05 (0.14) · 10 ⁻⁴	-1.08 (0.05) · 10 ⁻⁴
0.475	3.63 (0.40) · 10 ⁻⁵	1.57 (0.05) · 10 ⁻⁵	0.975	-8.63 (1.56) · 10 ⁻⁵	-6.82 (0.41) · 10 ⁻⁵
0.500	1.25 (0.40) · 10 ⁻⁵	0.00 (0.00) · 10 ⁰			

^a Values in parentheses are standard deviations. Those corresponding to e_p^E computed from Eq. (2.5) are calculated from the variance-covariance matrix of the outlier-free training set according to the general error propagation equation.

Table A.2. Variance-covariance matrices of coefficients from Eq. (2.3)^{a,b}.

	A_0	A_1	A_2	A_3	A_4	A_5	A_6
$T = 293.15 \text{ K}$							
A_0	$1.16 \cdot 10^{-7}$	— ^c	$-1.51 \cdot 10^{-6}$	— ^c	$4.55 \cdot 10^{-6}$	— ^c	$-3.69 \cdot 10^{-6}$
A_1	— ^c	$2.33 \cdot 10^{-6}$	— ^c	$-1.21 \cdot 10^{-5}$	— ^c	$1.30 \cdot 10^{-5}$	— ^c
A_2	$-1.51 \cdot 10^{-6}$	— ^c	$3.79 \cdot 10^{-5}$	— ^c	$-1.37 \cdot 10^{-4}$	— ^c	$1.22 \cdot 10^{-4}$
A_3	— ^c	$-1.21 \cdot 10^{-5}$	— ^c	$7.96 \cdot 10^{-5}$	— ^c	$-9.52 \cdot 10^{-5}$	— ^c
A_4	$4.55 \cdot 10^{-6}$	— ^c	$-1.37 \cdot 10^{-4}$	— ^c	$5.56 \cdot 10^{-4}$	— ^c	$-5.28 \cdot 10^{-4}$
A_5	— ^c	$1.30 \cdot 10^{-5}$	— ^c	$-9.52 \cdot 10^{-5}$	— ^c	$1.24 \cdot 10^{-4}$	— ^c
A_6	$-3.69 \cdot 10^{-6}$	— ^c	$1.22 \cdot 10^{-4}$	— ^c	$-5.28 \cdot 10^{-4}$	— ^c	$5.28 \cdot 10^{-4}$
$T = 299.15 \text{ K}$							
A_0	$4.86 \cdot 10^{-8}$	— ^c	$-6.32 \cdot 10^{-7}$	— ^c	$1.90 \cdot 10^{-6}$	— ^c	$-1.54 \cdot 10^{-6}$
A_1	— ^c	$9.71 \cdot 10^{-7}$	— ^c	$-5.05 \cdot 10^{-6}$	— ^c	$5.42 \cdot 10^{-6}$	— ^c
A_2	$-6.32 \cdot 10^{-7}$	— ^c	$1.58 \cdot 10^{-5}$	— ^c	$-5.73 \cdot 10^{-5}$	— ^c	$5.08 \cdot 10^{-5}$
A_3	— ^c	$-5.05 \cdot 10^{-6}$	— ^c	$3.32 \cdot 10^{-5}$	— ^c	$-3.97 \cdot 10^{-5}$	— ^c
A_4	$1.90 \cdot 10^{-6}$	— ^c	$-5.73 \cdot 10^{-5}$	— ^c	$2.32 \cdot 10^{-4}$	— ^c	$-2.20 \cdot 10^{-4}$
A_5	— ^c	$5.42 \cdot 10^{-6}$	— ^c	$-3.97 \cdot 10^{-5}$	— ^c	$5.17 \cdot 10^{-5}$	— ^c
A_6	$-1.54 \cdot 10^{-6}$	— ^c	$5.08 \cdot 10^{-5}$	— ^c	$-2.20 \cdot 10^{-4}$	— ^c	$2.20 \cdot 10^{-4}$
$T = 303.15 \text{ K}$							
A_0	$3.20 \cdot 10^{-8}$	— ^c	$-4.17 \cdot 10^{-7}$	— ^c	$1.25 \cdot 10^{-6}$	— ^c	$-1.01 \cdot 10^{-6}$
A_1	— ^c	$6.40 \cdot 10^{-7}$	— ^c	$-3.33 \cdot 10^{-6}$	— ^c	$3.57 \cdot 10^{-6}$	— ^c
A_2	$-4.17 \cdot 10^{-7}$	— ^c	$1.04 \cdot 10^{-5}$	— ^c	$-3.77 \cdot 10^{-5}$	— ^c	$3.35 \cdot 10^{-5}$
A_3	— ^c	$-3.33 \cdot 10^{-6}$	— ^c	$2.19 \cdot 10^{-5}$	— ^c	$-2.62 \cdot 10^{-5}$	— ^c
A_4	$1.25 \cdot 10^{-6}$	— ^c	$-3.77 \cdot 10^{-5}$	— ^c	$1.53 \cdot 10^{-4}$	— ^c	$-1.45 \cdot 10^{-4}$
A_5	— ^c	$3.57 \cdot 10^{-6}$	— ^c	$-2.62 \cdot 10^{-5}$	— ^c	$3.41 \cdot 10^{-5}$	— ^c
A_6	$-1.01 \cdot 10^{-6}$	— ^c	$3.35 \cdot 10^{-5}$	— ^c	$-1.45 \cdot 10^{-4}$	— ^c	$1.45 \cdot 10^{-4}$
$T = 308.15 \text{ K}$							
A_0	$2.06 \cdot 10^{-8}$	— ^c	$-2.68 \cdot 10^{-7}$	— ^c	$8.04 \cdot 10^{-7}$	— ^c	$-6.52 \cdot 10^{-7}$
A_1	— ^c	$4.11 \cdot 10^{-7}$	— ^c	$-2.14 \cdot 10^{-6}$	— ^c	$2.29 \cdot 10^{-6}$	— ^c
A_2	$-2.68 \cdot 10^{-7}$	— ^c	$6.70 \cdot 10^{-6}$	— ^c	$-2.43 \cdot 10^{-5}$	— ^c	$2.15 \cdot 10^{-5}$
A_3	— ^c	$-2.14 \cdot 10^{-6}$	— ^c	$1.41 \cdot 10^{-5}$	— ^c	$-1.68 \cdot 10^{-5}$	— ^c
A_4	$8.04 \cdot 10^{-7}$	— ^c	$-2.43 \cdot 10^{-5}$	— ^c	$9.83 \cdot 10^{-5}$	— ^c	$-9.33 \cdot 10^{-5}$
A_5	— ^c	$2.29 \cdot 10^{-6}$	— ^c	$-1.68 \cdot 10^{-5}$	— ^c	$2.19 \cdot 10^{-5}$	— ^c
A_6	$-6.52 \cdot 10^{-7}$	— ^c	$2.15 \cdot 10^{-5}$	— ^c	$-9.33 \cdot 10^{-5}$	— ^c	$9.34 \cdot 10^{-5}$

^a Uncertainty in the experimental excess specific volume was considered to be uniform and set equal to the standard deviation of the regression residuals for the calculation of the curvature matrix elements.

^b Units of $s^2(A_i A_j)$ and $s^2(A_i A_j)$ are $\text{cm}^6 \cdot \text{g}^{-2}$.

^c Absolute value of $s^2(A_i A_j)$ is less than $1 \cdot 10^{-15} \text{ cm}^6 \cdot \text{g}^{-2}$ and was set equal to zero for subsequent calculations.

Table A.2. Variance-covariance matrices of coefficients from Eq. (2.3) (*continued*)^{a,b}.

	A_0	A_1	A_2	A_3	A_4	A_5	A_6
$T = 313.15 \text{ K}$							
A_0	$1.75 \cdot 10^{-8}$	— ^c	$-2.28 \cdot 10^{-7}$	— ^c	$6.85 \cdot 10^{-7}$	— ^c	$-5.55 \cdot 10^{-7}$
A_1	— ^c	$3.50 \cdot 10^{-7}$	— ^c	$-1.82 \cdot 10^{-6}$	— ^c	$1.95 \cdot 10^{-6}$	— ^c
A_2	$-2.28 \cdot 10^{-7}$	— ^c	$5.70 \cdot 10^{-6}$	— ^c	$-2.07 \cdot 10^{-5}$	— ^c	$1.83 \cdot 10^{-5}$
A_3	— ^c	$-1.82 \cdot 10^{-6}$	— ^c	$1.20 \cdot 10^{-5}$	— ^c	$-1.43 \cdot 10^{-5}$	— ^c
A_4	$6.85 \cdot 10^{-7}$	— ^c	$-2.07 \cdot 10^{-5}$	— ^c	$8.37 \cdot 10^{-5}$	— ^c	$-7.94 \cdot 10^{-5}$
A_5	— ^c	$1.95 \cdot 10^{-6}$	— ^c	$-1.43 \cdot 10^{-5}$	— ^c	$1.86 \cdot 10^{-5}$	— ^c
A_6	$-5.55 \cdot 10^{-7}$	— ^c	$1.83 \cdot 10^{-5}$	— ^c	$-7.94 \cdot 10^{-5}$	— ^c	$7.95 \cdot 10^{-5}$

^a Uncertainty in the experimental excess specific volume was considered to be uniform and set equal to the standard deviation of the regression residuals for the calculation of the curvature matrix elements.

^b Units of $s^2(A_i A_i)$ and $s^2(A_i A_j)$ are $\text{cm}^6 \cdot \text{g}^{-2}$.

^c Absolute value of $s^2(A_i A_j)$ is less than $1 \cdot 10^{-15} \text{ cm}^6 \cdot \text{g}^{-2}$ and was set equal to zero for subsequent calculations.

Table A.3. Statistical analysis results for the multiple linear least-squares regressions of the excess specific volume of the water + *tert*-butyl alcohol mixtures v^E on *tert*-butyl alcohol mass fraction w_2 at system temperature T and pressure $P = 0.1$ MPa^a.

Parameters	$T = 293.15$ K	$T = 299.15$ K	$T = 303.15$ K	$T = 308.15$ K	$T = 313.15$ K
n^b	41	41	41	41	41
A_0	$t(n-7)$ 338.93	524.55	642.86	799.99	868.31
	p < 0.000001	< 0.000001	< 0.000001	< 0.000001	< 0.000001
A_1	$t(n-7)$ 22.29	24.07	23.75	21.27	14.91
	p < 0.000001	< 0.000001	< 0.000001	< 0.000001	< 0.000001
A_2	$t(n-7)$ 8.45	12.43	14.30	16.86	17.82
	p < 0.000001	< 0.000001	< 0.000001	< 0.000001	< 0.000001
A_3	$t(n-7)$ 4.23	8.57	11.01	14.22	15.59
	p 0.00017	< 0.000001	< 0.000001	< 0.000001	< 0.000001
A_4	$t(n-7)$ 0.091	1.00	2.31	4.00	4.90
	p 0.93	0.32	0.027	0.00033	0.000023
A_5	$t(n-7)$ 6.44	11.34	13.28	15.71	16.14
	p < 0.000001	< 0.000001	< 0.000001	< 0.000001	< 0.000001
A_6	$t(n-7)$ 5.73	7.66	9.48	11.51	11.62
	p 0.0000019	< 0.000001	< 0.000001	< 0.000001	< 0.000001
r_{adj}^2	$F(7, n-7)$ 56 966.65	137 238.03	206 431.42	320 464.10	378 681.49
	p < 0.000001	< 0.000001	< 0.000001	< 0.000001	< 0.000001

^a $t(\text{df})$, p : t -score (degree of freedom), two-tailed Student's t -test p -value

$F(\text{df}_1, \text{df}_2)$, p : F -score (degree of freedom 1, degree of freedom 2), one-tailed Fisher's F -test p -value

^b Number of regressed data points.

Table A.4. Statistical analysis results for the least-squares linear regressions of equation coefficients A_i from Eq. (2.3) on system temperature T at pressure $P = 0.1$ MPa^a.

i	n^b	B_i		C_i		r_{adj}^2	
		$t(n-2)$	p	$t(n-2)$	p	$F(1, n-2)$	p
0	5	3.04	0.056	28.22	0.000098	9.24	0.056
1	5	12.97	0.00099	13.65	0.00085	168.30	0.00099
2	5	9.95	0.0022	13.01	0.00098	99.07	0.0022
3	5	3.26	0.047	2.56	0.083	10.60	0.047
4	5	11.08	0.0016	10.65	0.0018	122.69	0.0016
5	5	0.67	0.55	1.41	0.25	0.45	0.55
6	5	4.10	0.026	5.36	0.013	16.81	0.026

^a $t(\text{df})$, p : t -score (degree of freedom), two-tailed Student's t -test p -value

$F(\text{df}_1, \text{df}_2)$, p : F -score (degree of freedom 1, degree of freedom 2), one-tailed Fisher's F -test p -value

^b Number of regressed data points.

Table A.5. Variance-covariance matrix of coefficients from Eq. (2.4)^{a,b}.

C_0	C_1	C_2	C_3	C_4	C_5	C_6	B_1	B_2	B_3	B_4	B_6
Training set – Full											
C_0	$1.47 \cdot 10^{-8}$	$-1.91 \cdot 10^{-7}$	$-$ ^c	$5.73 \cdot 10^{-7}$	$-$ ^c	$-4.64 \cdot 10^{-7}$	$-$ ^c				
C_1	$-$ ^c	$2.33 \cdot 10^{-4}$	$4.00 \cdot 10^{-15}$	$-5.13 \cdot 10^{-4}$	$1.64 \cdot 10^{-6}$	$1.80 \cdot 10^{-14}$	$-7.67 \cdot 10^{-7}$	$-$ ^c	$1.69 \cdot 10^{-6}$	$-$ ^c	$-$ ^c
C_2	$-1.91 \cdot 10^{-7}$	$4.00 \cdot 10^{-15}$	$4.38 \cdot 10^{-3}$	$-9.00 \cdot 10^{-15}$	$-$ ^c	$1.78 \cdot 10^{-2}$	$-$ ^c	$-1.44 \cdot 10^{-5}$	$-$ ^c	$6.19 \cdot 10^{-5}$	$-5.85 \cdot 10^{-5}$
C_3	$-$ ^c	$-5.13 \cdot 10^{-4}$	$-9.00 \cdot 10^{-15}$	$1.55 \cdot 10^{-3}$	$4.40 \cdot 10^{-14}$	$-4.40 \cdot 10^{-14}$	$1.69 \cdot 10^{-6}$	$-$ ^c	$-5.06 \cdot 10^{-6}$	$-$ ^c	$-$ ^c
C_4	$5.73 \cdot 10^{-7}$	$-1.90 \cdot 10^{-14}$	$4.40 \cdot 10^{-14}$	$9.11 \cdot 10^{-2}$	$-$ ^c	$-9.24 \cdot 10^{-2}$	$-$ ^c	$6.19 \cdot 10^{-5}$	$-$ ^c	$-3.00 \cdot 10^{-4}$	$3.04 \cdot 10^{-4}$
C_5	$-$ ^c	$1.64 \cdot 10^{-6}$	$-1.20 \cdot 10^{-5}$	$-1.20 \cdot 10^{-5}$	$1.56 \cdot 10^{-5}$	$-$ ^c	$-$ ^c	$-$ ^c	$-$ ^c	$-$ ^c	$-$ ^c
C_6	$-4.64 \cdot 10^{-7}$	$1.80 \cdot 10^{-14}$	$1.78 \cdot 10^{-2}$	$-4.40 \cdot 10^{-14}$	$-$ ^c	$9.91 \cdot 10^{-2}$	$-$ ^c	$-5.85 \cdot 10^{-5}$	$-$ ^c	$3.04 \cdot 10^{-4}$	$-3.26 \cdot 10^{-4}$
B_1	$-$ ^c	$-7.67 \cdot 10^{-7}$	$-$ ^c	$1.69 \cdot 10^{-6}$	$-$ ^c	$-$ ^c	$2.53 \cdot 10^{-9}$	$-$ ^c	$-5.56 \cdot 10^{-9}$	$-$ ^c	$-$ ^c
B_2	$-$ ^c	$-$ ^c	$-1.44 \cdot 10^{-5}$	$-$ ^c	$6.19 \cdot 10^{-5}$	$-5.85 \cdot 10^{-5}$	$-$ ^c	$4.76 \cdot 10^{-8}$	$-$ ^c	$-2.04 \cdot 10^{-7}$	$1.93 \cdot 10^{-7}$
B_3	$-$ ^c	$1.69 \cdot 10^{-6}$	$-$ ^c	$-5.06 \cdot 10^{-6}$	$-$ ^c	$-$ ^c	$-$ ^c	$-$ ^c	$1.67 \cdot 10^{-8}$	$-$ ^c	$-$ ^c
B_4	$-$ ^c	$-$ ^c	$6.19 \cdot 10^{-5}$	$-$ ^c	$-3.00 \cdot 10^{-4}$	$3.04 \cdot 10^{-4}$	$-$ ^c	$-2.04 \cdot 10^{-7}$	$-$ ^c	$9.89 \cdot 10^{-7}$	$-1.00 \cdot 10^{-6}$
B_6	$-$ ^c	$-$ ^c	$-5.85 \cdot 10^{-5}$	$-$ ^c	$3.04 \cdot 10^{-4}$	$-3.26 \cdot 10^{-4}$	$-$ ^c	$1.93 \cdot 10^{-7}$	$-$ ^c	$-1.00 \cdot 10^{-6}$	$1.08 \cdot 10^{-6}$

^a Uncertainty in the experimental excess specific volume was considered to be uniform and set equal to the standard deviation of the regression residuals for the calculation of the curvature matrix elements.

^b Units of $s^2(C_i C_j)$ and $s^2(C_i B_j)$ are $\text{cm}^6 \cdot \text{g}^{-2}$, units of $s^2(B_i B_j)$ and $s^2(B_i B_j)$ are K^{-2} , units of $s^2(C_i B_i)$ and $s^2(C_i B_j)$ are $\text{cm}^3 \cdot \text{g}^{-1} \cdot \text{K}^{-1}$.

^c Absolute value of $s^2(C_i C_j)$, $s^2(B_i B_j)$, $s^2(C_i B_i)$ or $s^2(C_i B_j)$ is less than $1 \cdot 10^{-15}$ unit and was set equal to zero for subsequent calculations.

Table A.5. Variance-covariance matrix of coefficients from Eq. (2.4) (continued)^{a,b}.

C_0	C_1	C_2	C_3	C_4	C_5	C_6	B_1	B_2	B_3	B_4	B_6	
Training set – Outliers excluded												
C_0	$9.57 \cdot 10^{-9}$	$-4.45 \cdot 10^{-9}$	$-2.42 \cdot 10^{-7}$	$1.21 \cdot 10^{-8}$	$1.02 \cdot 10^{-6}$	$-2.59 \cdot 10^{-9}$	$-1.01 \cdot 10^{-6}$	$1.40 \cdot 10^{-11}$	$3.78 \cdot 10^{-10}$	$-3.48 \cdot 10^{-11}$	$-2.07 \cdot 10^{-9}$	$2.27 \cdot 10^{-9}$
C_1	$-4.45 \cdot 10^{-9}$	$1.57 \cdot 10^{-4}$	$8.04 \cdot 10^{-6}$	$-3.52 \cdot 10^{-4}$	$-8.21 \cdot 10^{-6}$	$-7.54 \cdot 10^{-7}$	$-1.71 \cdot 10^{-5}$	$-5.17 \cdot 10^{-7}$	$-2.62 \cdot 10^{-8}$	$1.16 \cdot 10^{-6}$	$2.74 \cdot 10^{-8}$	$5.49 \cdot 10^{-8}$
C_2	$-2.42 \cdot 10^{-7}$	$8.04 \cdot 10^{-6}$	$3.01 \cdot 10^{-3}$	$-4.58 \cdot 10^{-5}$	$-1.32 \cdot 10^{-2}$	$1.42 \cdot 10^{-6}$	$1.27 \cdot 10^{-2}$	$-2.58 \cdot 10^{-8}$	$-9.91 \cdot 10^{-6}$	$1.46 \cdot 10^{-7}$	$4.35 \cdot 10^{-5}$	$-4.17 \cdot 10^{-5}$
C_3	$1.21 \cdot 10^{-8}$	$-3.52 \cdot 10^{-4}$	$-4.58 \cdot 10^{-5}$	$1.11 \cdot 10^{-3}$	$2.63 \cdot 10^{-4}$	$-3.43 \cdot 10^{-6}$	$-2.12 \cdot 10^{-4}$	$1.16 \cdot 10^{-6}$	$1.49 \cdot 10^{-7}$	$-3.63 \cdot 10^{-6}$	$-8.57 \cdot 10^{-7}$	$6.90 \cdot 10^{-7}$
C_4	$1.02 \cdot 10^{-6}$	$-8.21 \cdot 10^{-6}$	$-1.32 \cdot 10^{-2}$	$2.63 \cdot 10^{-4}$	$6.59 \cdot 10^{-2}$	$-1.96 \cdot 10^{-5}$	$-6.80 \cdot 10^{-2}$	$2.10 \cdot 10^{-8}$	$4.35 \cdot 10^{-5}$	$-8.09 \cdot 10^{-7}$	$-2.17 \cdot 10^{-4}$	$2.24 \cdot 10^{-4}$
C_5	$-2.59 \cdot 10^{-9}$	$-7.54 \cdot 10^{-7}$	$1.42 \cdot 10^{-6}$	$-3.43 \cdot 10^{-6}$	$-1.96 \cdot 10^{-5}$	$1.11 \cdot 10^{-5}$	$2.62 \cdot 10^{-5}$	$6.17 \cdot 10^{-9}$	$-4.27 \cdot 10^{-9}$	$-1.63 \cdot 10^{-8}$	$6.17 \cdot 10^{-8}$	$-8.32 \cdot 10^{-8}$
C_6	$-1.01 \cdot 10^{-6}$	$-1.71 \cdot 10^{-5}$	$1.27 \cdot 10^{-2}$	$-2.12 \cdot 10^{-4}$	$-6.80 \cdot 10^{-2}$	$2.62 \cdot 10^{-5}$	$7.42 \cdot 10^{-2}$	$6.37 \cdot 10^{-8}$	$-4.17 \cdot 10^{-5}$	$6.26 \cdot 10^{-7}$	$2.24 \cdot 10^{-4}$	$-2.44 \cdot 10^{-4}$
B_1	$1.40 \cdot 10^{-11}$	$-5.17 \cdot 10^{-7}$	$-2.58 \cdot 10^{-8}$	$1.16 \cdot 10^{-6}$	$2.10 \cdot 10^{-8}$	$6.17 \cdot 10^{-9}$	$6.37 \cdot 10^{-8}$	$1.70 \cdot 10^{-9}$	$8.40 \cdot 10^{-11}$	$-3.83 \cdot 10^{-9}$	$-7.09 \cdot 10^{-11}$	$-2.04 \cdot 10^{-10}$
B_2	$3.78 \cdot 10^{-10}$	$-2.62 \cdot 10^{-8}$	$-9.91 \cdot 10^{-6}$	$1.49 \cdot 10^{-7}$	$4.35 \cdot 10^{-5}$	$-4.27 \cdot 10^{-9}$	$-4.17 \cdot 10^{-5}$	$8.40 \cdot 10^{-11}$	$3.26 \cdot 10^{-8}$	$-4.76 \cdot 10^{-10}$	$-1.43 \cdot 10^{-7}$	$1.37 \cdot 10^{-7}$
B_3	$-3.48 \cdot 10^{-11}$	$1.16 \cdot 10^{-6}$	$1.46 \cdot 10^{-7}$	$-3.63 \cdot 10^{-6}$	$-8.09 \cdot 10^{-7}$	$-1.63 \cdot 10^{-8}$	$6.26 \cdot 10^{-7}$	$-3.83 \cdot 10^{-9}$	$1.20 \cdot 10^{-8}$	$2.64 \cdot 10^{-9}$	$2.64 \cdot 10^{-9}$	$-2.04 \cdot 10^{-9}$
B_4	$-2.07 \cdot 10^{-9}$	$2.74 \cdot 10^{-8}$	$4.35 \cdot 10^{-5}$	$-8.57 \cdot 10^{-7}$	$-2.17 \cdot 10^{-4}$	$6.17 \cdot 10^{-8}$	$2.24 \cdot 10^{-4}$	$-7.09 \cdot 10^{-11}$	$-1.43 \cdot 10^{-7}$	$2.64 \cdot 10^{-9}$	$7.13 \cdot 10^{-7}$	$-7.35 \cdot 10^{-7}$
B_6	$2.27 \cdot 10^{-9}$	$5.49 \cdot 10^{-8}$	$-4.17 \cdot 10^{-5}$	$6.90 \cdot 10^{-7}$	$2.24 \cdot 10^{-4}$	$-8.32 \cdot 10^{-8}$	$-2.44 \cdot 10^{-4}$	$-2.04 \cdot 10^{-10}$	$1.37 \cdot 10^{-7}$	$-2.04 \cdot 10^{-9}$	$-7.35 \cdot 10^{-7}$	$8.01 \cdot 10^{-7}$

^a Uncertainty in the experimental excess specific volume was considered to be uniform and set equal to the standard deviation of the regression residuals for the calculation of the curvature matrix elements.

^b Units of $s^2(C_i C_j)$ and $s^2(C_i B_j)$ are $\text{cm}^6 \cdot \text{g}^{-2}$, units of $s^2(B_i B_j)$ and $s^2(B_i B_j)$ are K^{-2} , units of $s^2(C_i B_i)$ and $s^2(C_i B_j)$ are $\text{cm}^3 \cdot \text{g}^{-1} \cdot \text{K}^{-1}$.

Table A.5. Variance-covariance matrix of coefficients from Eq. (2.4) (*continued*)^{ab}.

C_0	C_1	C_2	C_3	C_4	C_5	C_6	B_1	B_2	B_3	B_4	B_6
Testing set – Full											
C_0	$9.42 \cdot 10^{-8}$	$-4.81 \cdot 10^{-8}$	$-3.39 \cdot 10^{-7}$	$1.53 \cdot 10^{-6}$	$4.93 \cdot 10^{-8}$	$-1.34 \cdot 10^{-6}$	$-1.69 \cdot 10^{-12}$	$-1.84 \cdot 10^{-9}$	$9.01 \cdot 10^{-10}$	$4.28 \cdot 10^{-9}$	$-2.60 \cdot 10^{-9}$
C_1	$1.83 \cdot 10^{-8}$	$1.67 \cdot 10^{-3}$	$-3.38 \cdot 10^{-3}$	$8.37 \cdot 10^{-4}$	$-3.57 \cdot 10^{-6}$	$7.52 \cdot 10^{-4}$	$-5.51 \cdot 10^{-6}$	$2.08 \cdot 10^{-6}$	$1.12 \cdot 10^{-5}$	$-2.64 \cdot 10^{-6}$	$-2.56 \cdot 10^{-6}$
C_2	$-4.81 \cdot 10^{-7}$	$-6.42 \cdot 10^{-4}$	$1.67 \cdot 10^{-3}$	$-1.12 \cdot 10^{-1}$	$-8.30 \cdot 10^{-5}$	$9.87 \cdot 10^{-2}$	$2.04 \cdot 10^{-6}$	$-9.39 \cdot 10^{-5}$	$-5.20 \cdot 10^{-6}$	$3.71 \cdot 10^{-4}$	$-3.26 \cdot 10^{-4}$
C_3	$-3.39 \cdot 10^{-7}$	$-3.38 \cdot 10^{-3}$	$8.94 \cdot 10^{-3}$	$-5.39 \cdot 10^{-3}$	$-3.42 \cdot 10^{-5}$	$1.36 \cdot 10^{-3}$	$1.11 \cdot 10^{-5}$	$-5.42 \cdot 10^{-6}$	$-2.94 \cdot 10^{-5}$	$1.73 \cdot 10^{-5}$	$-4.14 \cdot 10^{-6}$
C_4	$1.53 \cdot 10^{-6}$	$8.37 \cdot 10^{-4}$	$-1.12 \cdot 10^{-1}$	$4.88 \cdot 10^{-1}$	$4.87 \cdot 10^{-4}$	$-4.56 \cdot 10^{-1}$	$-2.41 \cdot 10^{-6}$	$3.71 \cdot 10^{-4}$	$1.60 \cdot 10^{-5}$	$-1.61 \cdot 10^{-3}$	$1.51 \cdot 10^{-3}$
C_5	$4.93 \cdot 10^{-8}$	$-3.57 \cdot 10^{-6}$	$-8.30 \cdot 10^{-5}$	$4.87 \cdot 10^{-4}$	$6.18 \cdot 10^{-5}$	$-5.33 \cdot 10^{-4}$	$3.97 \cdot 10^{-8}$	$2.64 \cdot 10^{-7}$	$-6.12 \cdot 10^{-8}$	$-1.54 \cdot 10^{-6}$	$1.68 \cdot 10^{-6}$
C_6	$-1.34 \cdot 10^{-6}$	$7.52 \cdot 10^{-4}$	$1.36 \cdot 10^{-3}$	$-4.56 \cdot 10^{-1}$	$-5.33 \cdot 10^{-4}$	$4.47 \cdot 10^{-1}$	$-2.81 \cdot 10^{-6}$	$-3.26 \cdot 10^{-4}$	$-2.70 \cdot 10^{-6}$	$1.51 \cdot 10^{-3}$	$-1.48 \cdot 10^{-3}$
B_1	$-1.69 \cdot 10^{-12}$	$-5.51 \cdot 10^{-6}$	$1.11 \cdot 10^{-5}$	$-2.41 \cdot 10^{-6}$	$3.97 \cdot 10^{-8}$	$-2.81 \cdot 10^{-6}$	$1.82 \cdot 10^{-8}$	$-6.63 \cdot 10^{-9}$	$-3.70 \cdot 10^{-8}$	$7.59 \cdot 10^{-9}$	$9.52 \cdot 10^{-9}$
B_2	$-1.84 \cdot 10^{-9}$	$2.08 \cdot 10^{-6}$	$-9.39 \cdot 10^{-5}$	$3.71 \cdot 10^{-4}$	$2.64 \cdot 10^{-7}$	$-3.26 \cdot 10^{-4}$	$-6.63 \cdot 10^{-9}$	$3.11 \cdot 10^{-7}$	$1.68 \cdot 10^{-8}$	$-1.23 \cdot 10^{-6}$	$1.08 \cdot 10^{-6}$
B_3	$9.01 \cdot 10^{-10}$	$1.12 \cdot 10^{-5}$	$-2.94 \cdot 10^{-5}$	$1.60 \cdot 10^{-5}$	$-6.12 \cdot 10^{-8}$	$-2.70 \cdot 10^{-6}$	$-3.70 \cdot 10^{-8}$	$1.68 \cdot 10^{-8}$	$9.72 \cdot 10^{-8}$	$-5.15 \cdot 10^{-8}$	$7.99 \cdot 10^{-9}$
B_4	$4.28 \cdot 10^{-9}$	$-2.64 \cdot 10^{-6}$	$1.73 \cdot 10^{-5}$	$-1.61 \cdot 10^{-3}$	$-1.54 \cdot 10^{-6}$	$1.51 \cdot 10^{-3}$	$7.59 \cdot 10^{-9}$	$-1.23 \cdot 10^{-6}$	$-5.15 \cdot 10^{-8}$	$5.34 \cdot 10^{-6}$	$-4.99 \cdot 10^{-6}$
B_6	$-2.60 \cdot 10^{-9}$	$-2.56 \cdot 10^{-6}$	$-4.14 \cdot 10^{-6}$	$1.51 \cdot 10^{-3}$	$1.68 \cdot 10^{-6}$	$-1.48 \cdot 10^{-3}$	$9.52 \cdot 10^{-9}$	$1.08 \cdot 10^{-6}$	$7.99 \cdot 10^{-9}$	$-4.99 \cdot 10^{-6}$	$4.89 \cdot 10^{-6}$

^a Uncertainty in the experimental excess specific volume was considered to be uniform and set equal to the standard deviation of the regression residuals for the calculation of the curvature matrix elements.

^b Units of $s^2(C_i C_j)$ and $s^2(C_i B_j)$ are $\text{cm}^6 \cdot \text{g}^{-2}$, units of $s^2(B_i B_j)$ and $s^2(C_i B_j)$ are K^{-2} , units of $s^2(C_i B_j)$ and $s^2(C_i B_j)$ are $\text{cm}^3 \cdot \text{g}^{-1} \cdot \text{K}^{-1}$.

Table A.5. Variance-covariance matrix of coefficients from Eq. (2.4) (*continued*)^{a,b}.

C_0	C_1	C_2	C_3	C_4	C_5	C_6	B_1	B_2	B_3	B_4	B_6	
Testing set – Outliers excluded												
C_0	$5.44 \cdot 10^{-8}$	$8.18 \cdot 10^{-8}$	$-3.63 \cdot 10^{-7}$	$-3.19 \cdot 10^{-7}$	$7.42 \cdot 10^{-7}$	$5.81 \cdot 10^{-8}$	$-3.64 \cdot 10^{-7}$	$-2.10 \cdot 10^{-10}$	$-7.47 \cdot 10^{-10}$	$8.20 \cdot 10^{-10}$	$2.81 \cdot 10^{-9}$	$-2.74 \cdot 10^{-9}$
C_1	$8.18 \cdot 10^{-8}$	$1.02 \cdot 10^{-3}$	$-4.21 \cdot 10^{-4}$	$-2.06 \cdot 10^{-3}$	$4.95 \cdot 10^{-4}$	$-3.03 \cdot 10^{-6}$	$5.64 \cdot 10^{-4}$	$-3.38 \cdot 10^{-6}$	$1.36 \cdot 10^{-6}$	$6.79 \cdot 10^{-6}$	$-1.55 \cdot 10^{-6}$	$-1.91 \cdot 10^{-6}$
C_2	$-3.63 \cdot 10^{-7}$	$-4.21 \cdot 10^{-4}$	$1.71 \cdot 10^{-2}$	$1.04 \cdot 10^{-3}$	$-6.63 \cdot 10^{-2}$	$-4.96 \cdot 10^{-5}$	$5.79 \cdot 10^{-2}$	$1.34 \cdot 10^{-6}$	$-5.63 \cdot 10^{-5}$	$-3.24 \cdot 10^{-6}$	$2.19 \cdot 10^{-4}$	$-1.91 \cdot 10^{-4}$
C_3	$-3.19 \cdot 10^{-7}$	$-2.06 \cdot 10^{-3}$	$1.04 \cdot 10^{-3}$	$5.31 \cdot 10^{-3}$	$-3.10 \cdot 10^{-3}$	$-1.75 \cdot 10^{-5}$	$4.82 \cdot 10^{-4}$	$6.77 \cdot 10^{-6}$	$-3.36 \cdot 10^{-6}$	$-1.75 \cdot 10^{-5}$	$9.96 \cdot 10^{-6}$	$-1.41 \cdot 10^{-6}$
C_4	$7.42 \cdot 10^{-7}$	$4.95 \cdot 10^{-4}$	$-6.63 \cdot 10^{-2}$	$-3.10 \cdot 10^{-3}$	$2.84 \cdot 10^{-1}$	$3.09 \cdot 10^{-4}$	$-2.63 \cdot 10^{-1}$	$-1.41 \cdot 10^{-6}$	$2.19 \cdot 10^{-4}$	$9.13 \cdot 10^{-6}$	$-9.37 \cdot 10^{-4}$	$8.68 \cdot 10^{-4}$
C_5	$5.81 \cdot 10^{-8}$	$-3.03 \cdot 10^{-6}$	$-4.96 \cdot 10^{-5}$	$-1.75 \cdot 10^{-5}$	$3.09 \cdot 10^{-4}$	$3.56 \cdot 10^{-5}$	$-3.55 \cdot 10^{-4}$	$2.62 \cdot 10^{-8}$	$1.58 \cdot 10^{-7}$	$-4.23 \cdot 10^{-8}$	$-9.81 \cdot 10^{-7}$	$1.12 \cdot 10^{-6}$
C_6	$-3.64 \cdot 10^{-7}$	$5.64 \cdot 10^{-4}$	$5.79 \cdot 10^{-2}$	$4.82 \cdot 10^{-4}$	$-2.63 \cdot 10^{-1}$	$-3.55 \cdot 10^{-4}$	$2.56 \cdot 10^{-1}$	$-2.07 \cdot 10^{-6}$	$-1.91 \cdot 10^{-4}$	$-4.51 \cdot 10^{-7}$	$8.69 \cdot 10^{-4}$	$-8.46 \cdot 10^{-4}$
B_1	$-2.10 \cdot 10^{-10}$	$-3.38 \cdot 10^{-6}$	$1.34 \cdot 10^{-6}$	$6.77 \cdot 10^{-6}$	$-1.41 \cdot 10^{-6}$	$2.62 \cdot 10^{-8}$	$-2.07 \cdot 10^{-6}$	$1.12 \cdot 10^{-8}$	$-4.34 \cdot 10^{-9}$	$-2.24 \cdot 10^{-8}$	$4.41 \cdot 10^{-9}$	$6.96 \cdot 10^{-9}$
B_2	$-7.47 \cdot 10^{-10}$	$1.36 \cdot 10^{-6}$	$-5.63 \cdot 10^{-5}$	$-3.36 \cdot 10^{-6}$	$2.19 \cdot 10^{-4}$	$1.58 \cdot 10^{-7}$	$-1.91 \cdot 10^{-4}$	$-4.34 \cdot 10^{-9}$	$1.86 \cdot 10^{-7}$	$1.05 \cdot 10^{-8}$	$-7.24 \cdot 10^{-7}$	$6.32 \cdot 10^{-7}$
B_3	$8.20 \cdot 10^{-10}$	$6.79 \cdot 10^{-6}$	$-3.24 \cdot 10^{-6}$	$-1.75 \cdot 10^{-5}$	$9.13 \cdot 10^{-6}$	$-4.23 \cdot 10^{-8}$	$-4.51 \cdot 10^{-7}$	$-2.24 \cdot 10^{-8}$	$1.05 \cdot 10^{-8}$	$5.77 \cdot 10^{-8}$	$-2.93 \cdot 10^{-8}$	$1.04 \cdot 10^{-9}$
B_4	$2.81 \cdot 10^{-9}$	$-1.55 \cdot 10^{-6}$	$2.19 \cdot 10^{-4}$	$9.96 \cdot 10^{-6}$	$-9.37 \cdot 10^{-4}$	$-9.81 \cdot 10^{-7}$	$8.69 \cdot 10^{-4}$	$4.41 \cdot 10^{-9}$	$-7.24 \cdot 10^{-7}$	$-2.93 \cdot 10^{-8}$	$3.10 \cdot 10^{-6}$	$-2.87 \cdot 10^{-6}$
B_6	$-2.74 \cdot 10^{-9}$	$-1.91 \cdot 10^{-6}$	$-1.91 \cdot 10^{-4}$	$-1.41 \cdot 10^{-6}$	$8.68 \cdot 10^{-4}$	$1.12 \cdot 10^{-6}$	$-8.46 \cdot 10^{-4}$	$6.96 \cdot 10^{-9}$	$6.32 \cdot 10^{-7}$	$1.04 \cdot 10^{-9}$	$-2.87 \cdot 10^{-6}$	$2.80 \cdot 10^{-6}$

^a Uncertainty in the experimental excess specific volume was considered to be uniform and set equal to the standard deviation of the regression residuals for the calculation of the curvature matrix elements.

^b Units of $s^2(C_i C_j)$ and $s^2(C_i B_j)$ are $\text{cm}^6 \cdot \text{g}^{-2}$, units of $s^2(B_i B_j)$ and $s^2(C_i B_j)$ are K^{-2} , units of $s^2(C_i B_j)$ and $s^2(C_i B_j)$ are $\text{cm}^3 \cdot \text{g}^{-1} \cdot \text{K}^{-1}$.

Table A.6. Statistical analysis results for the least-squares comparison of Eq. (2.4) with fixed coefficient values to the excess specific volume of the water + *tert*-butyl alcohol mixtures v^E data from this work (training set) and from literature (testing set)^a.

Parameters	Training set		Testing set		
	Full	Outliers excluded	Full	Outliers excluded	
n^b	195	184	393	368	
C_0	$t(n-12)$	951.35	1 177.35	375.32	493.93
	p	< 0.000001	< 0.000001	< 0.000001	< 0.000001
C_1	$t(n-12)$	25.93	31.60	9.69	12.36
	p	< 0.000001	< 0.000001	< 0.000001	< 0.000001
C_2	$t(n-12)$	3.00	3.62	1.18	1.52
	p	0.0031	0.00039	0.24	0.13
C_3	$t(n-12)$	4.60	5.44	1.91	2.48
	p	0.0000079	< 0.000001	0.057	0.014
C_4	$t(n-12)$	2.16	2.54	0.93	1.22
	p	0.032	0.012	0.35	0.22
C_5	$t(n-12)$	18.93	22.47	9.51	12.54
	p	< 0.000001	< 0.000001	< 0.000001	< 0.000001
C_6	$t(n-12)$	1.55	1.79	0.73	0.96
	p	0.12	0.075	0.47	0.33
B_1	$t(n-12)$	24.64	30.02	9.18	11.72
	p	< 0.000001	< 0.000001	< 0.000001	< 0.000001
B_2	$t(n-12)$	2.30	2.77	0.90	1.16
	p	0.023	0.0062	0.37	0.25
B_3	$t(n-12)$	5.87	6.93	2.43	3.16
	p	< 0.000001	< 0.000001	0.016	0.0017
B_4	$t(n-12)$	2.25	2.65	0.97	1.27
	p	0.025	0.0089	0.33	0.20
B_6	$t(n-12)$	1.18	1.37	0.56	0.73
	p	0.24	0.17	0.58	0.46
r_{adj}^2	$F(12, n-12)$	263 672.15	399 929.07	53 286.01	93 261.28
	p	< 0.000001	< 0.000001	< 0.000001	< 0.000001

^a $t(df)$, p : t -score (degree of freedom), two-tailed Student's t -test p -value

$F(df_1, df_2)$, p : F -score (degree of freedom 1, degree of freedom 2), one-tailed Fisher's F -test p -value

^b Number of regressed data points.

Table A.7. Excess partial specific volume water v_1^E in water + *tert*-butyl alcohol mixtures at system temperature T and pressure $P = 0.1$ MPa as calculated from Eq. (2.7.a)^a.

w_2	$T = 293.15$ K	$T = 298.15$ K	$T = 303.15$ K	$T = 308.15$ K	$T = 313.15$ K
v_1^E (cm ³ ·g ⁻¹)					
0.025	7.32 (0.31) · 10 ⁻⁴	6.46 (0.23) · 10 ⁻⁴	5.60 (0.19) · 10 ⁻⁴	4.74 (0.20) · 10 ⁻⁴	3.88 (0.27) · 10 ⁻⁴
0.050	1.92 (0.08) · 10 ⁻³	1.65 (0.06) · 10 ⁻³	1.39 (0.05) · 10 ⁻³	1.12 (0.05) · 10 ⁻³	8.59 (0.69) · 10 ⁻⁴
0.075	2.58 (0.11) · 10 ⁻³	2.12 (0.09) · 10 ⁻³	1.67 (0.07) · 10 ⁻³	1.22 (0.07) · 10 ⁻³	7.70 (0.97) · 10 ⁻⁴
0.100	2.24 (0.12) · 10 ⁻³	1.65 (0.09) · 10 ⁻³	1.06 (0.07) · 10 ⁻³	4.66 (0.79) · 10 ⁻⁴	-1.26 (1.03) · 10 ⁻⁴
0.125	8.21 (1.15) · 10 ⁻⁴	1.61 (0.85) · 10 ⁻⁴	-4.99 (0.68) · 10 ⁻⁴	-1.16 (0.07) · 10 ⁻³	-1.82 (0.10) · 10 ⁻³
0.150	-1.57 (0.11) · 10 ⁻³	-2.21 (0.08) · 10 ⁻³	-2.86 (0.06) · 10 ⁻³	-3.51 (0.07) · 10 ⁻³	-4.15 (0.10) · 10 ⁻³
0.175	-4.68 (0.13) · 10 ⁻³	-5.24 (0.09) · 10 ⁻³	-5.79 (0.07) · 10 ⁻³	-6.34 (0.08) · 10 ⁻³	-6.89 (0.11) · 10 ⁻³
0.200	-8.24 (0.15) · 10 ⁻³	-8.63 (0.10) · 10 ⁻³	-9.03 (0.08) · 10 ⁻³	-9.42 (0.09) · 10 ⁻³	-9.81 (0.13) · 10 ⁻³
0.225	-1.20 (0.02) · 10 ⁻²	-1.21 (0.01) · 10 ⁻²	-1.23 (0.01) · 10 ⁻²	-1.25 (0.01) · 10 ⁻²	-1.27 (0.01) · 10 ⁻²
0.250	-1.56 (0.02) · 10 ⁻²	-1.56 (0.01) · 10 ⁻²	-1.55 (0.01) · 10 ⁻²	-1.54 (0.01) · 10 ⁻²	-1.54 (0.01) · 10 ⁻²
0.275	-1.91 (0.01) · 10 ⁻²	-1.87 (0.01) · 10 ⁻²	-1.84 (0.01) · 10 ⁻²	-1.81 (0.01) · 10 ⁻²	-1.77 (0.01) · 10 ⁻²
0.300	-2.22 (0.01) · 10 ⁻²	-2.15 (0.01) · 10 ⁻²	-2.09 (0.01) · 10 ⁻²	-2.03 (0.01) · 10 ⁻²	-1.97 (0.01) · 10 ⁻²
0.325	-2.49 (0.01) · 10 ⁻²	-2.40 (0.01) · 10 ⁻²	-2.31 (0.01) · 10 ⁻²	-2.23 (0.01) · 10 ⁻²	-2.14 (0.01) · 10 ⁻²
0.350	-2.72 (0.01) · 10 ⁻²	-2.61 (0.01) · 10 ⁻²	-2.50 (0.01) · 10 ⁻²	-2.39 (0.01) · 10 ⁻²	-2.28 (0.01) · 10 ⁻²
0.375	-2.92 (0.02) · 10 ⁻²	-2.79 (0.01) · 10 ⁻²	-2.66 (0.01) · 10 ⁻²	-2.53 (0.01) · 10 ⁻²	-2.40 (0.01) · 10 ⁻²
0.400	-3.09 (0.02) · 10 ⁻²	-2.94 (0.01) · 10 ⁻²	-2.80 (0.01) · 10 ⁻²	-2.66 (0.01) · 10 ⁻²	-2.52 (0.02) · 10 ⁻²
0.425	-3.24 (0.02) · 10 ⁻²	-3.09 (0.01) · 10 ⁻²	-2.94 (0.01) · 10 ⁻²	-2.78 (0.01) · 10 ⁻²	-2.63 (0.02) · 10 ⁻²
0.450	-3.39 (0.02) · 10 ⁻²	-3.23 (0.01) · 10 ⁻²	-3.07 (0.01) · 10 ⁻²	-2.91 (0.01) · 10 ⁻²	-2.76 (0.02) · 10 ⁻²
0.475	-3.54 (0.02) · 10 ⁻²	-3.38 (0.01) · 10 ⁻²	-3.22 (0.01) · 10 ⁻²	-3.06 (0.01) · 10 ⁻²	-2.90 (0.02) · 10 ⁻²
0.500	-3.69 (0.02) · 10 ⁻²	-3.54 (0.01) · 10 ⁻²	-3.38 (0.01) · 10 ⁻²	-3.23 (0.01) · 10 ⁻²	-3.07 (0.02) · 10 ⁻²

^a Values in parentheses are standard deviations calculated from the variance-covariance matrix of the outlier-free training set according to the general error propagation equation.

Table A.7. Excess partial specific volume water v_1^E in water + *tert*-butyl alcohol mixtures at system temperature T and pressure $P = 0.1$ MPa as calculated from Eq. (2.7.a) (*continued*)^a.

w_2	$T = 293.15$ K	$T = 298.15$ K	$T = 303.15$ K	$T = 308.15$ K	$T = 313.15$ K
v_1^E (cm ³ ·g ⁻¹)					
0.525	-3.86 (0.02) · 10 ⁻²	-3.71 (0.01) · 10 ⁻²	-3.56 (0.01) · 10 ⁻²	-3.42 (0.01) · 10 ⁻²	-3.27 (0.02) · 10 ⁻²
0.550	-4.03 (0.02) · 10 ⁻²	-3.90 (0.02) · 10 ⁻²	-3.76 (0.01) · 10 ⁻²	-3.63 (0.02) · 10 ⁻²	-3.49 (0.02) · 10 ⁻²
0.575	-4.23 (0.02) · 10 ⁻²	-4.11 (0.02) · 10 ⁻²	-3.99 (0.02) · 10 ⁻²	-3.87 (0.02) · 10 ⁻²	-3.74 (0.02) · 10 ⁻²
0.600	-4.44 (0.02) · 10 ⁻²	-4.34 (0.02) · 10 ⁻²	-4.23 (0.02) · 10 ⁻²	-4.12 (0.02) · 10 ⁻²	-4.02 (0.02) · 10 ⁻²
0.625	-4.68 (0.02) · 10 ⁻²	-4.59 (0.02) · 10 ⁻²	-4.49 (0.02) · 10 ⁻²	-4.40 (0.02) · 10 ⁻²	-4.31 (0.02) · 10 ⁻²
0.650	-4.93 (0.02) · 10 ⁻²	-4.86 (0.02) · 10 ⁻²	-4.78 (0.02) · 10 ⁻²	-4.70 (0.02) · 10 ⁻²	-4.62 (0.02) · 10 ⁻²
0.675	-5.22 (0.02) · 10 ⁻²	-5.15 (0.02) · 10 ⁻²	-5.09 (0.02) · 10 ⁻²	-5.02 (0.02) · 10 ⁻²	-4.95 (0.02) · 10 ⁻²
0.700	-5.54 (0.03) · 10 ⁻²	-5.48 (0.02) · 10 ⁻²	-5.42 (0.02) · 10 ⁻²	-5.36 (0.02) · 10 ⁻²	-5.30 (0.02) · 10 ⁻²
0.725	-5.91 (0.03) · 10 ⁻²	-5.85 (0.03) · 10 ⁻²	-5.80 (0.02) · 10 ⁻²	-5.74 (0.02) · 10 ⁻²	-5.68 (0.03) · 10 ⁻²
0.750	-6.33 (0.04) · 10 ⁻²	-6.27 (0.03) · 10 ⁻²	-6.22 (0.02) · 10 ⁻²	-6.16 (0.03) · 10 ⁻²	-6.11 (0.04) · 10 ⁻²
0.775	-6.81 (0.05) · 10 ⁻²	-6.75 (0.03) · 10 ⁻²	-6.70 (0.03) · 10 ⁻²	-6.64 (0.03) · 10 ⁻²	-6.58 (0.04) · 10 ⁻²
0.800	-7.36 (0.05) · 10 ⁻²	-7.30 (0.03) · 10 ⁻²	-7.24 (0.03) · 10 ⁻²	-7.18 (0.03) · 10 ⁻²	-7.12 (0.04) · 10 ⁻²
0.825	-7.95 (0.04) · 10 ⁻²	-7.90 (0.03) · 10 ⁻²	-7.85 (0.03) · 10 ⁻²	-7.80 (0.03) · 10 ⁻²	-7.75 (0.04) · 10 ⁻²
0.850	-8.56 (0.05) · 10 ⁻²	-8.53 (0.04) · 10 ⁻²	-8.51 (0.03) · 10 ⁻²	-8.48 (0.03) · 10 ⁻²	-8.45 (0.04) · 10 ⁻²
0.875	-9.12 (0.07) · 10 ⁻²	-9.15 (0.05) · 10 ⁻²	-9.18 (0.04) · 10 ⁻²	-9.20 (0.04) · 10 ⁻²	-9.23 (0.06) · 10 ⁻²
0.900	-9.52 (0.08) · 10 ⁻²	-9.65 (0.06) · 10 ⁻²	-9.78 (0.05) · 10 ⁻²	-9.92 (0.06) · 10 ⁻²	-1.00 (0.01) · 10 ⁻¹
0.925	-9.58 (0.09) · 10 ⁻²	-9.89 (0.07) · 10 ⁻²	-1.02 (0.01) · 10 ⁻¹	-1.05 (0.01) · 10 ⁻¹	-1.08 (0.01) · 10 ⁻¹
0.950	-9.02 (0.07) · 10 ⁻²	-9.63 (0.05) · 10 ⁻²	-1.02 (0.01) · 10 ⁻¹	-1.08 (0.01) · 10 ⁻¹	-1.14 (0.01) · 10 ⁻¹
0.975	-7.47 (0.12) · 10 ⁻²	-8.52 (0.09) · 10 ⁻²	-9.58 (0.07) · 10 ⁻²	-1.06 (0.01) · 10 ⁻¹	-1.17 (0.01) · 10 ⁻¹
1.000	-4.37 (0.37) · 10 ⁻²	-6.10 (0.27) · 10 ⁻²	-7.82 (0.22) · 10 ⁻²	-9.54 (0.24) · 10 ⁻²	-1.13 (0.03) · 10 ⁻¹

^a Values in parentheses are standard deviations calculated from the variance-covariance matrix of the outlier-free training set according to the general error propagation equation.

Table A.8. Excess partial specific volume v_2^E in water + *tert*-butyl alcohol mixtures at system temperature T and pressure $P = 0.1$ MPa as calculated from Eq. (2.7.b)^a.

w_2	$T = 293.15$ K	$T = 299.15$ K	$T = 303.15$ K	$T = 308.15$ K	$T = 313.15$ K
v_2^E (cm ³ ·g ⁻¹)					
0.000	-4.21 (0.38) · 10 ⁻²	-5.45 (0.28) · 10 ⁻²	-6.69 (0.23) · 10 ⁻²	-7.93 (0.24) · 10 ⁻²	-9.17 (0.32) · 10 ⁻²
0.025	-1.06 (0.01) · 10 ⁻¹	-1.11 (0.01) · 10 ⁻¹	-1.16 (0.01) · 10 ⁻¹	-1.22 (0.01) · 10 ⁻¹	-1.27 (0.01) · 10 ⁻¹
0.050	-1.38 (0.01) · 10 ⁻¹	-1.38 (0.01) · 10 ⁻¹	-1.39 (0.01) · 10 ⁻¹	-1.39 (0.01) · 10 ⁻¹	-1.40 (0.01) · 10 ⁻¹
0.075	-1.48 (0.01) · 10 ⁻¹	-1.46 (0.01) · 10 ⁻¹	-1.44 (0.01) · 10 ⁻¹	-1.41 (0.01) · 10 ⁻¹	-1.39 (0.01) · 10 ⁻¹
0.100	-1.45 (0.01) · 10 ⁻¹	-1.41 (0.01) · 10 ⁻¹	-1.37 (0.01) · 10 ⁻¹	-1.34 (0.01) · 10 ⁻¹	-1.30 (0.01) · 10 ⁻¹
0.125	-1.34 (0.01) · 10 ⁻¹	-1.30 (0.01) · 10 ⁻¹	-1.25 (0.01) · 10 ⁻¹	-1.21 (0.01) · 10 ⁻¹	-1.16 (0.01) · 10 ⁻¹
0.150	-1.19 (0.01) · 10 ⁻¹	-1.15 (0.01) · 10 ⁻¹	-1.10 (0.01) · 10 ⁻¹	-1.06 (0.01) · 10 ⁻¹	-1.02 (0.01) · 10 ⁻¹
0.175	-1.03 (0.01) · 10 ⁻¹	-9.93 (0.03) · 10 ⁻²	-9.54 (0.03) · 10 ⁻²	-9.15 (0.03) · 10 ⁻²	-8.76 (0.04) · 10 ⁻²
0.200	-8.78 (0.05) · 10 ⁻²	-8.46 (0.03) · 10 ⁻²	-8.14 (0.03) · 10 ⁻²	-7.81 (0.03) · 10 ⁻²	-7.49 (0.04) · 10 ⁻²
0.225	-7.40 (0.05) · 10 ⁻²	-7.15 (0.03) · 10 ⁻²	-6.91 (0.03) · 10 ⁻²	-6.67 (0.03) · 10 ⁻²	-6.42 (0.04) · 10 ⁻²
0.250	-6.22 (0.04) · 10 ⁻²	-6.05 (0.03) · 10 ⁻²	-5.89 (0.03) · 10 ⁻²	-5.73 (0.03) · 10 ⁻²	-5.56 (0.04) · 10 ⁻²
0.275	-5.25 (0.04) · 10 ⁻²	-5.16 (0.03) · 10 ⁻²	-5.08 (0.02) · 10 ⁻²	-4.99 (0.02) · 10 ⁻²	-4.90 (0.03) · 10 ⁻²
0.300	-4.48 (0.03) · 10 ⁻²	-4.46 (0.02) · 10 ⁻²	-4.44 (0.02) · 10 ⁻²	-4.42 (0.02) · 10 ⁻²	-4.40 (0.02) · 10 ⁻²
0.325	-3.89 (0.02) · 10 ⁻²	-3.92 (0.02) · 10 ⁻²	-3.96 (0.02) · 10 ⁻²	-3.99 (0.02) · 10 ⁻²	-4.03 (0.02) · 10 ⁻²
0.350	-3.43 (0.02) · 10 ⁻²	-3.51 (0.02) · 10 ⁻²	-3.59 (0.02) · 10 ⁻²	-3.67 (0.02) · 10 ⁻²	-3.75 (0.02) · 10 ⁻²
0.375	-3.08 (0.02) · 10 ⁻²	-3.20 (0.02) · 10 ⁻²	-3.31 (0.02) · 10 ⁻²	-3.42 (0.02) · 10 ⁻²	-3.54 (0.02) · 10 ⁻²
0.400	-2.81 (0.02) · 10 ⁻²	-2.95 (0.02) · 10 ⁻²	-3.08 (0.02) · 10 ⁻²	-3.22 (0.02) · 10 ⁻²	-3.36 (0.02) · 10 ⁻²
0.425	-2.59 (0.02) · 10 ⁻²	-2.74 (0.02) · 10 ⁻²	-2.89 (0.02) · 10 ⁻²	-3.04 (0.02) · 10 ⁻²	-3.20 (0.02) · 10 ⁻²
0.450	-2.40 (0.02) · 10 ⁻²	-2.56 (0.02) · 10 ⁻²	-2.72 (0.01) · 10 ⁻²	-2.88 (0.02) · 10 ⁻²	-3.03 (0.02) · 10 ⁻²
0.475	-2.23 (0.02) · 10 ⁻²	-2.39 (0.01) · 10 ⁻²	-2.55 (0.01) · 10 ⁻²	-2.71 (0.01) · 10 ⁻²	-2.87 (0.02) · 10 ⁻²
0.500	-2.07 (0.02) · 10 ⁻²	-2.22 (0.01) · 10 ⁻²	-2.38 (0.01) · 10 ⁻²	-2.53 (0.01) · 10 ⁻²	-2.69 (0.02) · 10 ⁻²

^a Values in parentheses are standard deviations calculated from the variance-covariance matrix of the outlier-free training set according to the general error propagation equation.

Table A.8. Excess partial specific volume v_2^E in water + *tert*-butyl alcohol mixtures at system temperature T and pressure $P = 0.1$ MPa as calculated from Eq. (2.7.b) (*continued*)^a.

w_2	$T = 293.15$ K	$T = 299.15$ K	$T = 303.15$ K	$T = 308.15$ K	$T = 313.15$ K
v_2^E ($\text{cm}^3 \cdot \text{g}^{-1}$)					
0.525	-1.91 (0.02) · 10 ⁻²	-2.06 (0.01) · 10 ⁻²	-2.21 (0.01) · 10 ⁻²	-2.35 (0.01) · 10 ⁻²	-2.50 (0.02) · 10 ⁻²
0.550	-1.76 (0.02) · 10 ⁻²	-1.89 (0.01) · 10 ⁻²	-2.03 (0.01) · 10 ⁻²	-2.17 (0.01) · 10 ⁻²	-2.31 (0.02) · 10 ⁻²
0.575	-1.60 (0.02) · 10 ⁻²	-1.73 (0.01) · 10 ⁻²	-1.86 (0.01) · 10 ⁻²	-1.98 (0.01) · 10 ⁻²	-2.11 (0.02) · 10 ⁻²
0.600	-1.46 (0.02) · 10 ⁻²	-1.57 (0.01) · 10 ⁻²	-1.69 (0.01) · 10 ⁻²	-1.80 (0.01) · 10 ⁻²	-1.92 (0.02) · 10 ⁻²
0.625	-1.31 (0.02) · 10 ⁻²	-1.41 (0.01) · 10 ⁻²	-1.52 (0.01) · 10 ⁻²	-1.63 (0.01) · 10 ⁻²	-1.73 (0.01) · 10 ⁻²
0.650	-1.16 (0.01) · 10 ⁻²	-1.26 (0.01) · 10 ⁻²	-1.36 (0.01) · 10 ⁻²	-1.46 (0.01) · 10 ⁻²	-1.56 (0.01) · 10 ⁻²
0.675	-1.02 (0.01) · 10 ⁻²	-1.11 (0.01) · 10 ⁻²	-1.20 (0.01) · 10 ⁻²	-1.30 (0.01) · 10 ⁻²	-1.39 (0.01) · 10 ⁻²
0.700	-8.69 (0.11) · 10 ⁻³	-9.59 (0.08) · 10 ⁻³	-1.05 (0.01) · 10 ⁻²	-1.14 (0.01) · 10 ⁻²	-1.23 (0.01) · 10 ⁻²
0.725	-7.21 (0.12) · 10 ⁻³	-8.09 (0.10) · 10 ⁻³	-8.98 (0.08) · 10 ⁻³	-9.87 (0.09) · 10 ⁻³	-1.08 (0.01) · 10 ⁻²
0.750	-5.71 (0.14) · 10 ⁻³	-6.60 (0.10) · 10 ⁻³	-7.48 (0.09) · 10 ⁻³	-8.37 (0.10) · 10 ⁻³	-9.26 (0.13) · 10 ⁻³
0.775	-4.21 (0.14) · 10 ⁻³	-5.10 (0.11) · 10 ⁻³	-6.00 (0.09) · 10 ⁻³	-6.89 (0.10) · 10 ⁻³	-7.78 (0.13) · 10 ⁻³
0.800	-2.75 (0.14) · 10 ⁻³	-3.64 (0.10) · 10 ⁻³	-4.53 (0.08) · 10 ⁻³	-5.42 (0.09) · 10 ⁻³	-6.32 (0.12) · 10 ⁻³
0.825	-1.38 (0.12) · 10 ⁻³	-2.25 (0.08) · 10 ⁻³	-3.13 (0.07) · 10 ⁻³	-4.00 (0.08) · 10 ⁻³	-4.88 (0.11) · 10 ⁻³
0.850	-1.90 (1.06) · 10 ⁻⁴	-1.02 (0.08) · 10 ⁻³	-1.85 (0.06) · 10 ⁻³	-2.68 (0.07) · 10 ⁻³	-3.51 (0.10) · 10 ⁻³
0.875	7.07 (1.10) · 10 ⁻⁴	-3.71 (8.12) · 10 ⁻⁵	-7.82 (0.66) · 10 ⁻⁴	-1.53 (0.07) · 10 ⁻³	-2.27 (0.10) · 10 ⁻³
0.900	1.22 (0.12) · 10 ⁻³	6.05 (0.87) · 10 ⁻⁴	-0.82 (7.11) · 10 ⁻⁵	-6.22 (0.78) · 10 ⁻⁴	-1.24 (0.10) · 10 ⁻³
0.925	1.28 (0.11) · 10 ⁻³	8.42 (0.82) · 10 ⁻⁴	3.99 (0.67) · 10 ⁻⁴	-4.35 (7.28) · 10 ⁻⁵	-4.86 (0.97) · 10 ⁻⁴
0.950	9.32 (0.79) · 10 ⁻⁴	6.81 (0.58) · 10 ⁻⁴	4.30 (0.47) · 10 ⁻⁴	1.80 (0.52) · 10 ⁻⁴	-7.12 (6.91) · 10 ⁻⁵
0.975	3.53 (0.30) · 10 ⁻⁴	2.74 (0.22) · 10 ⁻⁴	1.94 (0.18) · 10 ⁻⁴	1.15 (0.20) · 10 ⁻⁴	3.56 (2.66) · 10 ⁻⁵

^a Values in parentheses are standard deviations calculated from the variance-covariance matrix of the outlier-free training set according to the general error propagation equation.

Table A.9. Excess partial specific isobaric expansivity of water $e_{p,1}^E$ and *tert*-butyl alcohol $e_{p,2}^E$ in water + *tert*-butyl alcohol mixtures over the temperature range $T = 293.15$ - 323.15 K at pressure $P = 0.1$ MPa as calculated from Eq. (2.8.a) and Eq. (2.8.b)^a.

w_2	$e_{p,1}^E$ ($\text{cm}^3 \cdot \text{g}^{-1} \cdot \text{K}^{-1}$)	$e_{p,2}^E$ ($\text{cm}^3 \cdot \text{g}^{-1} \cdot \text{K}^{-1}$)	w_2	$e_{p,1}^E$ ($\text{cm}^3 \cdot \text{g}^{-1} \cdot \text{K}^{-1}$)	$e_{p,2}^E$ ($\text{cm}^3 \cdot \text{g}^{-1} \cdot \text{K}^{-1}$)
0.025	-1.72 (0.22) $\cdot 10^{-5}$	-1.03 (0.09) $\cdot 10^{-3}$	0.525	2.93 (0.11) $\cdot 10^{-4}$	-2.94 (0.11) $\cdot 10^{-4}$
0.050	-5.31 (0.57) $\cdot 10^{-5}$	-8.48 (5.74) $\cdot 10^{-5}$	0.550	2.71 (0.13) $\cdot 10^{-4}$	-2.75 (0.12) $\cdot 10^{-4}$
0.075	-9.03 (0.80) $\cdot 10^{-5}$	4.85 (0.69) $\cdot 10^{-4}$	0.575	2.43 (0.14) $\cdot 10^{-4}$	-2.53 (0.13) $\cdot 10^{-4}$
0.100	-1.18 (0.09) $\cdot 10^{-4}$	7.84 (0.62) $\cdot 10^{-4}$	0.600	2.13 (0.14) $\cdot 10^{-4}$	-2.32 (0.13) $\cdot 10^{-4}$
0.125	-1.32 (0.08) $\cdot 10^{-4}$	8.94 (0.47) $\cdot 10^{-4}$	0.625	1.83 (0.12) $\cdot 10^{-4}$	-2.13 (0.11) $\cdot 10^{-4}$
0.150	-1.29 (0.08) $\cdot 10^{-4}$	8.78 (0.36) $\cdot 10^{-4}$	0.650	1.56 (0.09) $\cdot 10^{-4}$	-1.98 (0.09) $\cdot 10^{-4}$
0.175	-1.11 (0.10) $\cdot 10^{-4}$	7.83 (0.35) $\cdot 10^{-4}$	0.675	1.34 (0.11) $\cdot 10^{-4}$	-1.87 (0.07) $\cdot 10^{-4}$
0.200	-7.84 (1.10) $\cdot 10^{-5}$	6.44 (0.36) $\cdot 10^{-4}$	0.700	1.20 (0.17) $\cdot 10^{-4}$	-1.80 (0.07) $\cdot 10^{-4}$
0.225	-3.56 (1.16) $\cdot 10^{-5}$	4.86 (0.36) $\cdot 10^{-4}$	0.725	1.13 (0.24) $\cdot 10^{-4}$	-1.77 (0.09) $\cdot 10^{-4}$
0.250	1.41 (1.09) $\cdot 10^{-5}$	3.26 (0.32) $\cdot 10^{-4}$	0.750	1.13 (0.31) $\cdot 10^{-4}$	-1.77 (0.10) $\cdot 10^{-4}$
0.275	6.75 (0.94) $\cdot 10^{-5}$	1.76 (0.25) $\cdot 10^{-4}$	0.775	1.16 (0.35) $\cdot 10^{-4}$	-1.78 (0.11) $\cdot 10^{-4}$
0.300	1.21 (0.08) $\cdot 10^{-4}$	4.32 (1.74) $\cdot 10^{-5}$	0.800	1.17 (0.35) $\cdot 10^{-4}$	-1.79 (0.10) $\cdot 10^{-4}$
0.325	1.72 (0.08) $\cdot 10^{-4}$	-6.89 (1.11) $\cdot 10^{-5}$	0.825	1.03 (0.33) $\cdot 10^{-4}$	-1.75 (0.09) $\cdot 10^{-4}$
0.350	2.17 (0.09) $\cdot 10^{-4}$	-1.59 (0.10) $\cdot 10^{-4}$	0.850	5.46 (3.54) $\cdot 10^{-5}$	-1.66 (0.08) $\cdot 10^{-4}$
0.375	2.56 (0.11) $\cdot 10^{-4}$	-2.27 (0.12) $\cdot 10^{-4}$	0.875	-5.46 (4.67) $\cdot 10^{-5}$	-1.49 (0.08) $\cdot 10^{-4}$
0.400	2.86 (0.13) $\cdot 10^{-4}$	-2.74 (0.14) $\cdot 10^{-4}$	0.900	-2.63 (0.61) $\cdot 10^{-4}$	-1.23 (0.08) $\cdot 10^{-4}$
0.425	3.06 (0.13) $\cdot 10^{-4}$	-3.03 (0.14) $\cdot 10^{-4}$	0.925	-6.25 (0.67) $\cdot 10^{-4}$	-8.85 (0.80) $\cdot 10^{-5}$
0.450	3.17 (0.12) $\cdot 10^{-4}$	-3.17 (0.13) $\cdot 10^{-4}$	0.950	-1.21 (0.05) $\cdot 10^{-3}$	-5.02 (0.57) $\cdot 10^{-5}$
0.475	3.18 (0.11) $\cdot 10^{-4}$	-3.18 (0.11) $\cdot 10^{-4}$	0.975	-2.11 (0.09) $\cdot 10^{-3}$	-1.59 (0.22) $\cdot 10^{-5}$

^a Values in parentheses are standard deviations calculated from the variance-covariance matrix of the outlier-free training set according to the general error propagation equation.

This page is intentionally left blank.

Appendix B

Supplementary materials related to Chapter 2

This page is intentionally left blank.

Table B.1. Solubility of diazepam in water + *tert*-butyl alcohol solvent mixtures expressed in concentration c_2^{sat} and mass fraction w_2^{sat} at system temperature T and pressure $P = 0.1 \text{ MPa}^{\text{a}}$.

$w_{\text{TBA}}^{\text{b}}$	$T = 293.15 \text{ K}$	$T = 299.15 \text{ K}$	$T = 303.15 \text{ K}$	$T = 308.15 \text{ K}$	$T = 313.15 \text{ K}$
$c_2^{\text{sat}} \text{ (mg}\cdot\text{mL}^{-1}\text{)}$					
0.00	$4.240 (0.022) \cdot 10^{-2}$	$4.740 (0.052) \cdot 10^{-2}$	$5.670 (0.056) \cdot 10^{-2}$	$6.240 (0.019) \cdot 10^{-2}$	$7.620 (0.094) \cdot 10^{-2}$
0.10	$1.119 (0.051) \cdot 10^{-1}$	$1.481 (0.005) \cdot 10^{-1}$	$2.014 (0.014) \cdot 10^{-1}$	$2.439 (0.018) \cdot 10^{-1}$	$3.360 (0.099) \cdot 10^{-1}$
0.20	$7.485 (1.188) \cdot 10^{-1}$	$1.423 (0.028) \cdot 10^0$	$2.120 (0.043) \cdot 10^0$	$2.875 (0.030) \cdot 10^0$	$3.730 (0.091) \cdot 10^0$
0.30	$5.617 (0.195) \cdot 10^0$	$7.197 (0.093) \cdot 10^0$	$9.355 (0.204) \cdot 10^0$	$1.124 (0.020) \cdot 10^1$	$1.503 (0.053) \cdot 10^1$
0.40	$1.231 (0.035) \cdot 10^1$	$1.547 (0.009) \cdot 10^1$	$1.870 (0.043) \cdot 10^1$	$2.242 (0.027) \cdot 10^1$	$2.810 (0.120) \cdot 10^1$
0.50	$1.969 (0.050) \cdot 10^1$	$2.482 (0.034) \cdot 10^1$	$2.974 (0.060) \cdot 10^1$	$3.492 (0.040) \cdot 10^1$	$4.416 (0.087) \cdot 10^1$
0.60	$2.610 (0.040) \cdot 10^1$	$3.195 (0.094) \cdot 10^1$	$4.042 (0.039) \cdot 10^1$	$4.603 (0.055) \cdot 10^1$	$5.843 (0.121) \cdot 10^1$
0.70	$3.220 (0.103) \cdot 10^1$	$3.825 (0.072) \cdot 10^1$	$4.911 (0.076) \cdot 10^1$	$5.582 (0.075) \cdot 10^1$	$6.884 (0.117) \cdot 10^1$
0.80	$3.471 (0.055) \cdot 10^1$	$4.178 (0.061) \cdot 10^1$	$5.348 (0.055) \cdot 10^1$	$6.151 (0.210) \cdot 10^1$	$7.386 (0.124) \cdot 10^1$
0.90	$3.069 (0.043) \cdot 10^1$	$3.651 (0.032) \cdot 10^1$	$4.741 (0.092) \cdot 10^1$	$5.396 (0.026) \cdot 10^1$	$6.435 (0.261) \cdot 10^1$
1.00	—	$1.885 (0.012) \cdot 10^1$	$2.249 (0.064) \cdot 10^1$	$2.717 (0.027) \cdot 10^1$	$3.460 (0.099) \cdot 10^1$
$c_2^{\text{sat}} \text{ (mol}\cdot\text{L}^{-1}\text{)}$					
0.00	$1.489 (0.008) \cdot 10^{-4}$	$1.665 (0.018) \cdot 10^{-4}$	$1.991 (0.020) \cdot 10^{-4}$	$2.191 (0.006) \cdot 10^{-4}$	$2.676 (0.033) \cdot 10^{-4}$
0.10	$3.930 (0.178) \cdot 10^{-4}$	$5.201 (0.018) \cdot 10^{-4}$	$7.073 (0.049) \cdot 10^{-4}$	$8.566 (0.064) \cdot 10^{-4}$	$1.180 (0.035) \cdot 10^{-3}$
0.20	$2.629 (0.117) \cdot 10^{-3}$	$4.997 (0.098) \cdot 10^{-3}$	$7.445 (0.152) \cdot 10^{-3}$	$1.010 (0.010) \cdot 10^{-2}$	$1.310 (0.032) \cdot 10^{-2}$
0.30	$1.973 (0.069) \cdot 10^{-2}$	$2.528 (0.033) \cdot 10^{-2}$	$3.285 (0.072) \cdot 10^{-2}$	$3.946 (0.069) \cdot 10^{-2}$	$5.279 (0.184) \cdot 10^{-2}$
0.40	$4.324 (0.121) \cdot 10^{-2}$	$5.431 (0.030) \cdot 10^{-2}$	$6.568 (0.150) \cdot 10^{-2}$	$7.872 (0.095) \cdot 10^{-2}$	$9.869 (0.423) \cdot 10^{-2}$
0.50	$6.916 (0.176) \cdot 10^{-2}$	$8.718 (0.118) \cdot 10^{-2}$	$1.044 (0.021) \cdot 10^{-1}$	$1.226 (0.014) \cdot 10^{-1}$	$1.551 (0.031) \cdot 10^{-1}$
0.60	$9.165 (0.141) \cdot 10^{-2}$	$1.122 (0.033) \cdot 10^{-1}$	$1.420 (0.014) \cdot 10^{-1}$	$1.617 (0.019) \cdot 10^{-1}$	$2.052 (0.042) \cdot 10^{-1}$
0.70	$1.131 (0.036) \cdot 10^{-1}$	$1.343 (0.025) \cdot 10^{-1}$	$1.725 (0.027) \cdot 10^{-1}$	$1.960 (0.027) \cdot 10^{-1}$	$2.418 (0.041) \cdot 10^{-1}$
0.80	$1.219 (0.019) \cdot 10^{-1}$	$1.467 (0.021) \cdot 10^{-1}$	$1.878 (0.019) \cdot 10^{-1}$	$2.160 (0.074) \cdot 10^{-1}$	$2.594 (0.044) \cdot 10^{-1}$
0.90	$1.078 (0.015) \cdot 10^{-1}$	$1.282 (0.011) \cdot 10^{-1}$	$1.665 (0.032) \cdot 10^{-1}$	$1.895 (0.009) \cdot 10^{-1}$	$2.260 (0.092) \cdot 10^{-1}$
1.00	—	$6.620 (0.041) \cdot 10^{-2}$	$7.897 (0.225) \cdot 10^{-2}$	$9.541 (0.096) \cdot 10^{-2}$	$1.215 (0.035) \cdot 10^{-1}$
$100 w_2^{\text{sat}}$					
0.00	$4.248 (0.022) \cdot 10^{-3}$	$4.756 (0.053) \cdot 10^{-3}$	$5.695 (0.056) \cdot 10^{-3}$	$6.277 (0.019) \cdot 10^{-3}$	$7.680 (0.095) \cdot 10^{-3}$
0.10	$1.138 (0.052) \cdot 10^{-2}$	$1.509 (0.005) \cdot 10^{-2}$	$2.055 (0.014) \cdot 10^{-2}$	$2.494 (0.019) \cdot 10^{-2}$	$3.443 (0.102) \cdot 10^{-2}$
0.20	$7.711 (1.224) \cdot 10^{-2}$	$1.473 (0.029) \cdot 10^{-1}$	$2.198 (0.045) \cdot 10^{-1}$	$2.990 (0.031) \cdot 10^{-1}$	$3.893 (0.095) \cdot 10^{-1}$
0.30	$5.911 (0.205) \cdot 10^{-1}$	$7.605 (0.099) \cdot 10^{-1}$	$9.907 (0.216) \cdot 10^{-1}$	$1.195 (0.021) \cdot 10^0$	$1.603 (0.056) \cdot 10^0$
0.40	$1.325 (0.037) \cdot 10^0$	$1.670 (0.010) \cdot 10^0$	$2.025 (0.046) \cdot 10^0$	$2.435 (0.030) \cdot 10^0$	$3.063 (0.131) \cdot 10^0$
0.50	$2.167 (0.055) \cdot 10^0$	$2.742 (0.037) \cdot 10^0$	$3.294 (0.067) \cdot 10^0$	$3.876 (0.044) \cdot 10^0$	$4.918 (0.097) \cdot 10^0$
0.60	$2.938 (0.045) \cdot 10^0$	$3.608 (0.106) \cdot 10^0$	$4.578 (0.044) \cdot 10^0$	$5.216 (0.062) \cdot 10^0$	$6.635 (0.137) \cdot 10^0$
0.70	$3.712 (0.119) \cdot 10^0$	$4.421 (0.083) \cdot 10^0$	$5.685 (0.087) \cdot 10^0$	$6.467 (0.087) \cdot 10^0$	$7.980 (0.136) \cdot 10^0$
0.80	$4.105 (0.065) \cdot 10^0$	$4.951 (0.072) \cdot 10^0$	$6.346 (0.065) \cdot 10^0$	$7.298 (0.250) \cdot 10^0$	$8.769 (0.148) \cdot 10^0$
0.90	$3.737 (0.053) \cdot 10^0$	$4.459 (0.040) \cdot 10^0$	$5.803 (0.113) \cdot 10^0$	$6.606 (0.031) \cdot 10^0$	$7.967 (0.324) \cdot 10^0$
1.00	—	$2.393 (0.015) \cdot 10^0$	$2.864 (0.072) \cdot 10^0$	$3.472 (0.035) \cdot 10^0$	$4.440 (0.127) \cdot 10^0$

^a Values in parentheses are standard deviations, $u(T) = 0.03 \text{ K}$, $u_r(P) = 0.05$ and $u_r(w_{\text{TBA}}) = 0.005$.

^b Mass fraction of *tert*-butyl alcohol in the solvent mixture free of solute.

Table B.2. Statistical analysis results for the least-squares linear regression of the natural logarithm of the diazepam mole fraction solubility x_2^{sat} on reciprocal of the absolute system temperature T for the different water + *tert*-butyl alcohol solvent mixtures investigated at pressure $P = 0.1$ MPa^a.

$w_{\text{TBA}}^{\text{b}}$	n^{c}	Slope		Intercept		r^2	
		$t(n-2)$	p	$t(n-2)$	p	$F(1, n-2)$	p
0.00	5	11.40	0.0014	4.55	0.020	130.03	0.0014
0.10	5	19.29	0.00030	6.37	0.0078	372.21	0.00030
0.20	5	11.81	0.0013	7.56	0.0048	139.43	0.0013
0.30	5	20.36	0.00026	10.82	0.0017	414.70	0.00026
0.40	5	34.33	0.000054	17.62	0.00040	1 178.38	0.000054
0.50	5	28.44	0.000095	15.66	0.00057	809.01	0.000095
0.60	5	16.75	0.00046	9.91	0.0022	280.47	0.00046
0.70	5	14.40	0.00073	8.72	0.0032	207.27	0.00073
0.80	5	15.99	0.00053	10.07	0.0021	255.61	0.00053
0.90	5	13.59	0.00086	8.64	0.0033	184.65	0.00086
1.00	4	24.25	0.0017	15.80	0.0040	587.97	0.0017
Ideal	5	176.46	0.00000040	125.71	0.0000011	31 137.77	0.00000040

^a $t(\text{df})$, p : t -score (degree of freedom), two-tailed Student's t -test p -value

$F(\text{df}_1, \text{df}_2)$, p : F -score (degree of freedom 1, degree of freedom 2), one-tailed Fisher's F -test p -value

^b Mass fraction of *tert*-butyl alcohol in the solvent mixture free of solute.

^c Number of regressed data points.

Table B.3. Partial molar entropy changes of diazepam upon dissolution $\Delta_{\text{sol}}S_{\text{m},2}^{\text{sat}}$ in water + *tert*-butyl alcohol solvent mixtures at system temperature T and pressure $P = 0.1 \text{ MPa}^{\text{a}}$.

$w_{\text{TBA}}^{\text{b}}$	$T = 293.15 \text{ K}$	$T = 299.15 \text{ K}$	$T = 303.15 \text{ K}$	$T = 308.15 \text{ K}$	$T = 313.15 \text{ K}$
$\Delta_{\text{sol}}S_{\text{m},2}^{\text{sat}} (\text{J}\cdot\text{K}^{-1}\cdot\text{mol}^{-1})$					
0.00	77.13 (6.76)	75.58 (6.63)	74.58 (6.54)	73.37 (6.43)	72.20 (6.33)
0.10	143.96 (7.46)	141.07 (7.31)	139.21 (7.22)	136.95 (7.10)	134.76 (6.99)
0.20	211.31 (17.90)	207.07 (17.54)	204.34 (17.31)	201.02 (17.02)	197.81 (16.75)
0.30	130.78 (6.42)	128.16 (6.29)	126.47 (6.21)	124.41 (6.11)	122.43 (6.01)
0.40	111.02 (3.23)	108.79 (3.17)	107.36 (3.13)	105.61 (3.08)	103.93 (3.03)
0.50	108.63 (3.82)	106.45 (3.74)	105.05 (3.69)	103.34 (3.63)	101.69 (3.58)
0.60	110.18 (6.58)	107.97 (6.45)	106.55 (6.36)	104.82 (6.26)	103.14 (6.16)
0.70	106.13 (7.37)	104.00 (7.22)	102.63 (7.13)	100.97 (7.01)	99.35 (6.90)
0.80	106.37 (6.65)	104.23 (6.52)	102.86 (6.43)	101.19 (6.33)	99.57 (6.23)
0.90	105.54 (7.77)	103.42 (7.61)	102.05 (7.51)	100.40 (7.39)	98.80 (7.27)
1.00	—	116.21 (4.79)	114.68 (4.73)	112.82 (4.65)	111.02 (4.58)
Ideal	64.77 (0.50)	64.77 (0.49)	64.77 (0.48)	64.77 (0.47)	64.77 (0.46)

^a Values in parentheses are standard deviations, $u(T) = 0.03 \text{ K}$, $u_r(P) = 0.05$ and $u_r(w_{\text{TBA}}) = 0.005$.

^b Mass fraction of *tert*-butyl alcohol in the solvent mixture free of solute.

Table B.4. Molar thermodynamic quantities for the fusion process of diazepam $\Delta_{\text{fus}}G_{\text{m},2}$, $\Delta_{\text{fus}}H_{\text{m},2}$, $T\Delta_{\text{fus}}S_{\text{m},2}$ and $\Delta_{\text{fus}}S_{\text{m},2}$ at system temperature T and pressure $P = 0.1 \text{ MPa}$ ^a.

T (K)	$\Delta_{\text{fus}}G_{\text{m},2}$ (kJ·mol ⁻¹)	$\Delta_{\text{fus}}H_{\text{m},2}$ (kJ·mol ⁻¹)	$T\Delta_{\text{fus}}S_{\text{m},2}$ (kJ·mol ⁻¹)	$\Delta_{\text{fus}}S_{\text{m},2}$ (J·K ⁻¹ ·mol ⁻¹)	$\Delta_{\text{fus}}H_{\text{m},2}$ (%RC) ^b	$T\Delta_{\text{fus}}S_{\text{m},2}$ (%RC) ^c
293.15	6.10 (0.18)	18.99 (0.15)	12.89 (0.11)	43.98 (0.37)	59.6	40.4
299.15	5.83 (0.18)	19.38 (0.14)	13.55 (0.11)	45.29 (0.37)	58.9	41.1
303.15	5.64 (0.18)	19.63 (0.14)	13.99 (0.11)	46.15 (0.37)	58.4	41.6
308.15	5.41 (0.18)	19.96 (0.14)	14.55 (0.11)	47.21 (0.36)	57.8	42.2
313.15	5.17 (0.18)	20.28 (0.14)	15.11 (0.11)	48.25 (0.36)	57.3	42.7

^a Values in parentheses are standard deviations, $u(T) = 0.03 \text{ K}$, $u_r(P) = 0.05$ and $u_r(w_{\text{TBA}}) = 0.005$.

$$^b \text{RC}_{\Delta_{\text{fus}}H_{\text{m},2}} = |\Delta_{\text{fus}}H_{\text{m},2}| / [|\Delta_{\text{fus}}H_{\text{m},2}| + |T\Delta_{\text{fus}}S_{\text{m},2}|]$$

$$^c \text{RC}_{T\Delta_{\text{fus}}S_{\text{m},2}} = |T\Delta_{\text{fus}}S_{\text{m},2}| / [|\Delta_{\text{fus}}H_{\text{m},2}| + |T\Delta_{\text{fus}}S_{\text{m},2}|]$$

Table B.5. Partial molar thermodynamic quantities for the mixing process of diazepam $\Delta_{\text{mix}}G_{\text{m},2}^{\text{sat}}$, $\Delta_{\text{mix}}H_{\text{m},2}^{\text{sat}}$, $T\Delta_{\text{mix}}S_{\text{m},2}^{\text{sat}}$ and $\Delta_{\text{mix}}S_{\text{m},2}^{\text{sat}}$ in water + *tert*-butyl alcohol solvent mixtures at system temperature T and pressure $P = 0.1 \text{ MPa}$ ^a.

$w_{\text{TBA}}^{\text{b}}$	$\Delta_{\text{mix}}H_{\text{m},2}^{\text{sat}}$ (kJ·mol ⁻¹)	$T\Delta_{\text{mix}}S_{\text{m},2}^{\text{sat}}$ (kJ·mol ⁻¹)	$\Delta_{\text{mix}}S_{\text{m},2}^{\text{sat}}$ (J·K ⁻¹ ·mol ⁻¹)	$\Delta_{\text{mix}}H_{\text{m},2}^{\text{sat}}$ (%RC) ^c	$T\Delta_{\text{mix}}S_{\text{m},2}^{\text{sat}}$ (%RC) ^d
$T = 293.15 \text{ K}$ $\Delta_{\text{mix}}G_{\text{m},2}^{\text{sat}} = -6.10 (0.18) \text{ kJ}\cdot\text{mol}^{-1}$					
0.00	3.62 (1.99)	9.72 (1.99)	33.15 (6.77)	27.2	72.8
0.10	23.21 (2.19)	29.31 (2.19)	99.98 (7.47)	44.2	55.8
0.20	42.96 (5.25)	49.05 (5.25)	167.33 (17.90)	46.7	53.3
0.30	19.35 (1.89)	25.45 (1.89)	86.80 (6.43)	43.2	56.8
0.40	13.56 (0.96)	19.65 (0.95)	67.04 (3.26)	40.8	59.2
0.50	12.86 (1.13)	18.95 (1.13)	64.66 (3.84)	40.4	59.6
0.60	13.31 (1.93)	19.41 (1.93)	66.20 (6.59)	40.7	59.3
0.70	12.13 (2.17)	18.22 (2.16)	62.16 (7.38)	40.0	60.0
0.80	12.20 (1.96)	18.29 (1.95)	62.39 (6.66)	40.0	60.0
0.90	11.95 (2.28)	18.05 (2.28)	61.56 (7.78)	39.8	60.2
Ideal	0.00 (–)	6.10 (0.18)	20.79 (0.62)	0.0	100.0
$T = 299.15 \text{ K}$ $\Delta_{\text{mix}}G_{\text{m},2}^{\text{sat}} = -5.83 (0.18) \text{ kJ}\cdot\text{mol}^{-1}$					
0.00	3.23 (1.99)	9.06 (1.99)	30.29 (6.64)	26.3	73.7
0.10	22.83 (2.19)	28.65 (2.19)	95.78 (7.32)	44.3	55.7
0.20	42.57 (5.25)	48.40 (5.25)	161.78 (17.54)	46.8	53.2
0.30	18.96 (1.88)	24.79 (1.88)	82.87 (6.30)	43.3	56.7
0.40	13.17 (0.96)	19.00 (0.95)	63.50 (3.19)	40.9	59.1
0.50	12.47 (1.13)	18.30 (1.13)	61.17 (3.76)	40.5	59.5
0.60	12.92 (1.93)	18.75 (1.93)	62.68 (6.46)	40.8	59.2
0.70	11.74 (2.17)	17.56 (2.16)	58.72 (7.23)	40.1	59.9
0.80	11.81 (1.96)	17.63 (1.95)	58.95 (6.53)	40.1	59.9
0.90	11.56 (2.28)	17.39 (2.28)	58.13 (7.62)	39.9	60.1
1.00	15.39 (1.44)	21.22 (1.44)	70.93 (4.81)	42.0	58.0
Ideal	0.00 (–)	5.83 (1.82)	19.48 (0.61)	0.0	100.0
$T = 303.15 \text{ K}$ $\Delta_{\text{mix}}G_{\text{m},2}^{\text{sat}} = -5.64 (0.18) \text{ kJ}\cdot\text{mol}^{-1}$					
0.00	2.98 (1.99)	8.62 (1.99)	28.43 (6.55)	25.7	74.3
0.10	22.57 (2.19)	28.21 (2.19)	93.06 (7.23)	44.4	55.6
0.20	42.31 (5.25)	47.96 (5.25)	158.19 (17.31)	46.9	53.1
0.30	18.70 (1.89)	24.35 (1.89)	80.32 (6.22)	43.4	56.6
0.40	12.91 (0.96)	18.56 (0.95)	61.21 (3.15)	41.0	59.0
0.50	12.21 (1.13)	17.86 (1.13)	58.90 (3.71)	40.6	59.4

^a Values in parentheses are standard deviations, $u(T) = 0.03 \text{ K}$, $u_t(P) = 0.05$ and $u_t(w_{\text{TBA}}) = 0.005$.

^b Mass fraction of *tert*-butyl alcohol in the solvent mixture free of solute.

$$^{\text{c}}\text{RC}_{\Delta_{\text{mix}}H_{\text{m},2}^{\text{sat}}} = |\Delta_{\text{mix}}H_{\text{m},2}^{\text{sat}}| / [|\Delta_{\text{mix}}H_{\text{m},2}^{\text{sat}}| + |T\Delta_{\text{mix}}S_{\text{m},2}^{\text{sat}}|]$$

$$^{\text{d}}\text{RC}_{T\Delta_{\text{mix}}S_{\text{m},2}^{\text{sat}}} = |T\Delta_{\text{mix}}S_{\text{m},2}^{\text{sat}}| / [|\Delta_{\text{mix}}H_{\text{m},2}^{\text{sat}}| + |T\Delta_{\text{mix}}S_{\text{m},2}^{\text{sat}}|]$$

Table B.5. Partial molar thermodynamic quantities for the mixing process of diazepam $\Delta_{\text{mix}}G_{\text{m},2}^{\text{sat}}$, $\Delta_{\text{mix}}H_{\text{m},2}^{\text{sat}}$, $T\Delta_{\text{mix}}S_{\text{m},2}^{\text{sat}}$ and $\Delta_{\text{mix}}S_{\text{m},2}^{\text{sat}}$ in water + *tert*-butyl alcohol solvent mixtures at system temperature T and pressure $P = 0.1$ MPa (*continued*)^a.

$w_{\text{TBA}}^{\text{b}}$	$\Delta_{\text{mix}}H_{\text{m},2}^{\text{sat}}$ (kJ·mol ⁻¹)	$T\Delta_{\text{mix}}S_{\text{m},2}^{\text{sat}}$ (kJ·mol ⁻¹)	$\Delta_{\text{mix}}S_{\text{m},2}^{\text{sat}}$ (J·K ⁻¹ ·mol ⁻¹)	$\Delta_{\text{mix}}H_{\text{m},2}^{\text{sat}}$ (%RC) ^c	$T\Delta_{\text{mix}}S_{\text{m},2}^{\text{sat}}$ (%RC) ^d
0.60	12.66 (1.93)	18.31 (1.93)	60.40 (6.37)	40.9	59.1
0.70	11.48 (2.17)	17.12 (2.16)	56.48 (7.14)	40.1	59.9
0.80	11.55 (1.96)	17.19 (1.95)	56.71 (6.44)	40.2	59.8
0.90	11.30 (2.28)	16.95 (2.28)	55.91 (7.52)	40.0	60.0
1.00	15.13 (1.44)	20.78 (1.44)	68.53 (4.74)	42.1	57.9
Ideal	0.00 (–)	5.64 (0.18)	18.62 (0.60)	0.0	100.0
$T = 308.15$ K $\Delta_{\text{mix}}G_{\text{m},2}^{\text{sat}} = -5.41$ (0.18) kJ·mol ⁻¹					
0.00	2.65 (1.99)	8.06 (1.99)	26.17 (6.44)	24.7	75.3
0.10	22.24 (2.19)	27.65 (2.19)	89.74 (7.11)	44.6	55.4
0.20	41.99 (5.25)	47.40 (5.25)	153.81 (17.03)	47.0	53.0
0.30	18.38 (1.89)	23.79 (1.89)	77.21 (6.12)	43.6	56.4
0.40	12.59 (0.96)	18.00 (0.95)	58.41 (3.10)	41.2	58.8
0.50	11.89 (1.13)	17.30 (1.13)	56.14 (3.65)	40.7	59.3
0.60	12.34 (1.93)	17.75 (1.93)	57.61 (6.27)	41.0	59.0
0.70	11.15 (2.17)	16.57 (2.16)	53.76 (7.02)	40.2	59.8
0.80	11.22 (1.96)	16.63 (1.95)	53.98 (6.34)	40.3	59.7
0.90	10.98 (2.28)	16.39 (2.28)	53.19 (7.40)	40.1	59.9
1.00	14.81 (1.44)	20.22 (1.44)	65.61 (4.67)	42.3	57.7
Ideal	0.00 (–)	5.41 (0.18)	17.56 (0.59)	0.0	100.0
$T = 313.15$ K $\Delta_{\text{mix}}G_{\text{m},2}^{\text{sat}} = -5.17$ (0.18) kJ·mol ⁻¹					
0.00	2.33 (1.99)	7.50 (1.99)	23.95 (6.34)	23.7	76.3
0.10	21.92 (2.19)	27.09 (2.19)	86.51 (7.00)	44.7	55.3
0.20	41.66 (5.25)	46.84 (5.25)	149.56 (16.76)	47.1	52.9
0.30	18.06 (1.89)	23.23 (1.89)	74.18 (6.02)	43.7	56.3
0.40	12.26 (0.96)	17.43 (0.96)	55.68 (3.05)	41.3	58.7
0.50	11.56 (1.13)	16.74 (1.13)	53.44 (3.59)	40.9	59.1
0.60	12.02 (1.93)	17.19 (1.93)	54.89 (6.17)	41.1	58.9
0.70	10.83 (2.17)	16.00 (2.16)	51.10 (6.91)	40.4	59.6
0.80	10.90 (1.96)	16.07 (1.95)	51.32 (6.24)	40.4	59.6
0.90	10.66 (2.28)	15.83 (2.28)	50.55 (7.28)	40.2	59.8
1.00	14.48 (1.44)	19.66 (1.44)	62.77 (4.59)	42.4	57.6
Ideal	0.00 (–)	5.17 (0.18)	16.52 (0.59)	0.0	100.0

^a Values in parentheses are standard deviations, $u(T) = 0.03$ K, $u_r(P) = 0.05$ and $u_r(w_{\text{TBA}}) = 0.005$.

^b Mass fraction of *tert*-butyl alcohol in the solvent mixture free of solute.

$$^{\text{c}} \text{RC}_{\Delta_{\text{mix}}H_{\text{m},2}^{\text{sat}}} = |\Delta_{\text{mix}}H_{\text{m},2}^{\text{sat}}| / [|\Delta_{\text{mix}}H_{\text{m},2}^{\text{sat}}| + |T\Delta_{\text{mix}}S_{\text{m},2}^{\text{sat}}|]$$

$$^{\text{d}} \text{RC}_{T\Delta_{\text{mix}}S_{\text{m},2}^{\text{sat}}} = |T\Delta_{\text{mix}}S_{\text{m},2}^{\text{sat}}| / [|\Delta_{\text{mix}}H_{\text{m},2}^{\text{sat}}| + |T\Delta_{\text{mix}}S_{\text{m},2}^{\text{sat}}|]$$

Table B.6. Relative contribution RC of the fusion and mixing processes thermodynamic quantities to the dissolution process of diazepam in water + *tert*-butyl alcohol solvent mixtures at system temperature T and pressure $P = 0.1$ MPa^{a,b}.

w_{TBA}^c	$\Delta_{\text{fus}}H_{\text{m},2}$	$\Delta_{\text{mix}}H_{\text{m},2}^{\text{sat}}$	$T\Delta_{\text{fus}}S_{\text{m},2}$	$T\Delta_{\text{mix}}S_{\text{m},2}^{\text{sat}}$
$T = 293.15$ K				
0.00	42.0%	8.0%	28.5%	22.5%
0.10	22.5%	27.5%	15.3%	34.7%
0.20	15.3%	34.7%	10.4%	39.6%
0.30	24.8%	25.2%	16.8%	33.2%
0.40	29.2%	20.8%	19.8%	30.2%
0.50	29.8%	20.2%	20.2%	29.8%
0.60	29.4%	20.6%	20.0%	30.0%
0.70	30.5%	19.5%	20.7%	29.3%
0.80	30.4%	19.6%	20.7%	29.3%
0.90	30.7%	19.3%	20.8%	29.2%
1.00	—	—	—	—
Ideal	50.0%	0.0%	34.0%	16.0%
$T = 299.15$ K				
0.00	42.9%	7.1%	30.0%	20.0%
0.10	23.0%	27.0%	16.0%	34.0%
0.20	15.6%	34.4%	10.9%	39.1%
0.30	25.3%	24.7%	17.7%	32.3%
0.40	29.8%	20.2%	20.8%	29.2%
0.50	30.4%	19.6%	21.3%	28.7%
0.60	30.0%	20.0%	21.0%	29.0%
0.70	31.1%	18.9%	21.8%	28.2%
0.80	31.0%	18.9%	21.7%	28.3%
0.90	31.3%	18.7%	21.9%	28.1%
1.00	27.9%	22.1%	19.5%	30.5%
Ideal	50.0%	0.0%	35.0%	15.0%
$T = 303.15$ K				
0.00	43.4%	6.6%	30.9%	19.1%
0.10	23.3%	26.7%	16.6%	33.4%
0.20	15.9%	34.1%	11.3%	38.7%
0.30	25.6%	24.4%	18.2%	31.8%
0.40	30.2%	19.8%	21.5%	28.5%
0.50	30.8%	19.2%	22.0%	28.0%

^a $u(T) = 0.03$ K, $u_r(P) = 0.05$ and $u_r(w_{\text{TBA}}) = 0.005$.

^b $\text{RC}_{\Delta_r H_{\text{m},2}} = |\Delta_r H_{\text{m},2}| / [|\Delta_{\text{sol}} H_{\text{m},2}^{\text{sat}}| + |T\Delta_{\text{sol}} S_{\text{m},2}^{\text{sat}}|]$ and $\text{RC}_{T\Delta_r S_{\text{m},2}} = |T\Delta_r S_{\text{m},2}| / [|\Delta_{\text{sol}} H_{\text{m},2}^{\text{sat}}| + |T\Delta_{\text{sol}} S_{\text{m},2}^{\text{sat}}|]$.

^c Mass fraction of *tert*-butyl alcohol in the solvent mixture free of solute.

Table B.6. Relative contribution RC of the fusion and mixing processes thermodynamic quantities to the dissolution process of diazepam in water + *tert*-butyl alcohol solvent mixtures at system temperature T and pressure $P = 0.1$ MPa (*continued*)^{a,b}.

w_{TBA}^c	$\Delta_{\text{fus}}H_{\text{m},2}$	$\Delta_{\text{mix}}H_{\text{m},2}^{\text{sat}}$	$T\Delta_{\text{fus}}S_{\text{m},2}$	$T\Delta_{\text{mix}}S_{\text{m},2}^{\text{sat}}$
0.60	30.4%	19.6%	21.7%	28.3%
0.70	31.6%	18.4%	22.5%	27.5%
0.80	31.5%	18.5%	22.4%	27.6%
0.90	31.7%	18.3%	22.6%	27.4%
1.00	28.2%	21.8%	20.1%	29.9%
Ideal	50.0%	0.0%	35.6%	14.4%
$T = 308.15$ K				
0.00	44.1%	5.9%	32.2%	17.8%
0.10	23.7%	26.3%	17.2%	32.8%
0.20	16.1%	33.9%	11.7%	38.3%
0.30	26.0%	24.0%	19.0%	31.0%
0.40	30.7%	19.3%	22.3%	27.7%
0.50	31.3%	18.7%	22.8%	27.2%
0.60	30.9%	19.1%	22.5%	27.5%
0.70	32.1%	17.9%	23.4%	26.6%
0.80	32.0%	18.0%	23.3%	26.7%
0.90	32.3%	17.7%	23.5%	26.5%
1.00	28.7%	21.3%	20.9%	29.1%
Ideal	50.0%	0.0%	36.4%	13.6%
$T = 313.15$ K				
0.00	44.9%	5.1%	33.4%	16.6%
0.10	24.0%	26.0%	17.9%	32.1%
0.20	16.4%	33.6%	12.2%	37.8%
0.30	26.5%	23.5%	19.7%	30.3%
0.40	31.2%	18.8%	23.2%	26.8%
0.50	31.8%	18.2%	23.7%	26.3%
0.60	31.4%	18.6%	23.4%	26.6%
0.70	32.6%	17.4%	24.3%	25.7%
0.80	32.5%	17.5%	24.2%	25.8%
0.90	32.8%	17.2%	24.4%	25.6%
1.00	29.2%	20.8%	21.7%	28.3%
Ideal	50.0%	0.0%	37.3%	12.8%

^a $u(T) = 0.03$ K, $u_r(P) = 0.05$ and $u_r(w_{\text{TBA}}) = 0.005$.

^b $\text{RC}_{\Delta_r H_{\text{m},2}} = |\Delta_r H_{\text{m},2}| / [|\Delta_{\text{sol}} H_{\text{m},2}^{\text{sat}}| + |T\Delta_{\text{sol}} S_{\text{m},2}^{\text{sat}}|]$ and $\text{RC}_{T\Delta_r S_{\text{m},2}} = |T\Delta_r S_{\text{m},2}| / [|\Delta_{\text{sol}} H_{\text{m},2}^{\text{sat}}| + |T\Delta_{\text{sol}} S_{\text{m},2}^{\text{sat}}|]$.

^c Mass fraction of *tert*-butyl alcohol in the solvent mixture free of solute.

Appendix C

Supplementary materials related to Chapter 3

This page is intentionally left blank.

Table C.1. Results of Akaike's information criterion analysis for comparison of the different versions of the Scatchard-Hildebrand model in fitting the natural logarithm of the activity coefficient of diazepam γ_3^{sat} in water + *tert*-butyl alcohol solvent mixtures at system temperature T and pressure $P = 0.1 \text{ MPa}^{\text{a}}$.

Rank	Model ^b	N	$SS(e)$	r_{adj}^2	AIC_c	w_A
1	13	54	3.503	0.9905	-136.46	0.1805
2	12	54	3.541	0.9904	-135.88	0.1354
3	20	54	3.577	0.9903	-135.33	0.1027
4	5	54	3.788	0.9899	-134.67	0.0741
5	15	54	3.623	0.9902	-134.64	0.0727
6	24	54	3.462	0.9904	-134.56	0.0699
7	19	54	3.633	0.9901	-134.50	0.0677
8	26	54	3.490	0.9903	-134.12	0.0560
9	21	54	3.514	0.9903	-133.76	0.0469
10	25	54	3.527	0.9902	-133.55	0.0422
11	8	54	3.888	0.9897	-133.26	0.0366
12	14	54	3.743	0.9898	-132.88	0.0302
13	7	54	3.931	0.9895	-132.67	0.0273
14	23	54	3.623	0.9900	-132.10	0.0205
15	27	54	3.460	0.9902	-131.95	0.0190
16	16	54	3.864	0.9895	-131.16	0.0128
17	10	54	4.035	0.9891	-128.83	0.0040
18	3	54	4.364	0.9884	-127.03	0.0016
19	18	54	8.396	0.9772	-89.26	< 0.0001
20	22	54	8.051	0.9777	-88.99	< 0.0001
21	9	54	8.534	0.9768	-88.38	< 0.0001
22	1	54	10.173	0.9729	-81.32	< 0.0001
23	11	54	9.879	0.9732	-80.47	< 0.0001
24	4	54	10.384	0.9724	-80.22	< 0.0001
25	17	54	12.554	0.9659	-67.53	< 0.0001
26	2	54	14.740	0.9608	-61.30	< 0.0001
27	6	54	15.276	0.9594	-59.37	< 0.0001

^a N : number of regressed data points; $SS(e)$: residual sum-of-squares; r_{adj}^2 : adjusted squared correlation coefficient; AIC_c : second-order Akaike's information criterion; w_A : Akaike weight.

^b See Table 3.3 for alternative model versions investigated in this study.

Table C.2. Results of Akaike’s information criterion analysis for comparison of the different versions of the combined Scatchard-Hildebrand/Flory-Huggins model in fitting the natural logarithm of the activity coefficient of diazepam γ_3^{sat} in water + *tert*-butyl alcohol solvent mixtures at system temperature T and pressure $P = 0.1 \text{ MPa}^{\text{a}}$.

Rank	Model ^b	N	SS(e)	r_{adj}^2	AIC _c	w_{A}
1	5	54	3.500	0.9907	-138.95	0.2288
2	8	54	3.523	0.9906	-138.59	0.1912
3	12	54	3.440	0.9907	-137.44	0.1076
4	13	54	3.466	0.9906	-137.04	0.0880
5	19	54	3.477	0.9906	-136.87	0.0808
6	20	54	3.481	0.9906	-136.80	0.0784
7	14	54	3.498	0.9905	-136.53	0.0685
8	25	54	3.430	0.9905	-135.06	0.0328
9	24	54	3.438	0.9905	-134.93	0.0307
10	26	54	3.463	0.9904	-134.55	0.0254
11	21	54	3.475	0.9904	-134.35	0.0230
12	15	54	3.674	0.9900	-133.89	0.0182
13	23	54	3.577	0.9901	-132.80	0.0106
14	27	54	3.430	0.9903	-132.42	0.0088
15	16	54	3.861	0.9895	-131.20	0.0048
16	7	54	4.242	0.9887	-128.56	0.0013
17	10	54	4.077	0.9889	-128.27	0.0011
18	3	54	4.573	0.9878	-124.50	0.0002
19	18	54	5.679	0.9846	-110.37	< 0.0001
20	22	54	5.473	0.9848	-109.83	< 0.0001
21	1	54	6.035	0.9839	-109.52	< 0.0001
22	4	54	6.072	0.9838	-109.19	< 0.0001
23	9	54	5.807	0.9842	-109.16	< 0.0001
24	11	54	6.035	0.9836	-107.08	< 0.0001
25	17	54	7.729	0.9790	-93.73	< 0.0001
26	2	54	8.558	0.9772	-90.66	< 0.0001
27	6	54	8.955	0.9762	-88.21	< 0.0001

^a N : number of regressed data points; SS(e): residual sum-of-squares; r_{adj}^2 : adjusted squared correlation coefficient; AIC_c: second-order Akaike’s information criterion; w_{A} : Akaike weight.

^b See Table 3.3 for alternative model versions investigated in this study.

Table C.3. Statistical analysis results for the non-linear least-squares regressions of the natural logarithm of the activity coefficient of diazepam γ_3^{sat} in water + *tert*-butyl alcohol solvent mixtures at system temperature T and pressure $P = 0.1$ MPa to the selected most parsimonious versions of the Scatchard-Hildebrand and combined Scatchard-Hildebrand/Flory-Huggins models^a.

Parameters ^b		SH model	SH/FH model
N		54	54
k		4	3
$a_{1,2}$	$t(N-k)$	100.34	98.66
	p	< 0.000001	< 0.000001
$a_{1,3}$	$t(N-k)$	12.98	235.88
	p	< 0.000001	< 0.000001
$b_{1,3}$	$t(N-k)$	2.36	—
	p	0.022	—
$a_{2,3}$	$t(N-k)$	18.87	—
	p	< 0.000001	—
$b_{2,3}$	$t(N-k)$	—	22.02
	p	—	< 0.000001
r_{adj}^2	$F(k, N-k)$	1381.08	1880.25
	p	< 0.000001	< 0.000001

^a $t(\text{df})$, p : t -score (degree of freedom), two-tailed Student's t -test p -value.

$F(\text{df}_1, \text{df}_2)$, p : F -score (degree of freedom 1, degree of freedom 2), one-tailed Fisher's F -test p -value.

^b N : number of regressed data points, k : number of adjustable model parameters.

Table C.4. Variance-covariance matrix of regression coefficient estimates of the selected most parsimonious version of the Scatchard-Hildebrand model^{a,b}.

Coefficients	$b_{1,3}$	$a_{1,2}$	$a_{1,3}$	$a_{2,3}$
$b_{1,3}$	$2.28 \cdot 10^{-4}$	$4.05 \cdot 10^{-10}$	$-7.52 \cdot 10^{-7}$	$-2.68 \cdot 10^{-10}$
$a_{1,2}$	$4.05 \cdot 10^{-10}$	$7.63 \cdot 10^{-11}$	$8.52 \cdot 10^{-12}$	$2.23 \cdot 10^{-11}$
$a_{1,3}$	$-7.52 \cdot 10^{-7}$	$8.52 \cdot 10^{-12}$	$2.48 \cdot 10^{-9}$	$2.28 \cdot 10^{-12}$
$a_{2,3}$	$-2.68 \cdot 10^{-10}$	$2.23 \cdot 10^{-11}$	$2.28 \cdot 10^{-12}$	$1.38 \cdot 10^{-11}$

^a Uncertainty in the natural logarithm of the experimental activity coefficient of diazepam was considered to be uniform and set equal to the standard deviation of the regression residuals for the calculation of the curvature matrix elements.

^b Units of $s^2(aa)$ are K^{-2} and $s^2(ab)$ are K^{-1} .

Table C.5. Variance-covariance matrix of regression coefficient estimates of the selected most parsimonious version of the combined Scatchard-Hildebrand/Flory-Huggins model^{a,b}.

Coefficients	$b_{2,3}$	$a_{1,2}$	$a_{1,3}$
$b_{2,3}$	$1.24 \cdot 10^{-6}$	$6.65 \cdot 10^{-9}$	$4.18 \cdot 10^{-10}$
$a_{1,2}$	$6.65 \cdot 10^{-9}$	$7.50 \cdot 10^{-11}$	$9.67 \cdot 10^{-12}$
$a_{1,3}$	$4.18 \cdot 10^{-10}$	$9.67 \cdot 10^{-12}$	$2.82 \cdot 10^{-12}$

^a Uncertainty in the natural logarithm of the experimental activity coefficient of diazepam was considered to be uniform and set equal to the standard deviation of the regression residuals for the calculation of the curvature matrix elements.

^b Units of $s^2(aa)$ are K^{-2} and $s^2(ab)$ are K^{-1} .

Table C.6. Comparison between values of the mole fraction solubility of diazepam x_3^{sat} in water + *tert*-butyl alcohol solvent mixtures at system temperature T and pressure $P = 0.1$ MPa determined experimentally and calculated from the selected most parsimonious version of the combined Scatchard-Hildebrand/Flory-Huggins models^a.

w_2^0	x_3^{sat}		
	Experimental [116]	SH model	SH/FH model
$T = 293.15$ K			
0.00	$2.688 (0.014) \cdot 10^{-6}$	$1.661 (0.228) \cdot 10^{-6}$	$1.791 (0.554) \cdot 10^{-6}$
0.10	$7.790 (0.354) \cdot 10^{-6}$	$1.437 (0.153) \cdot 10^{-5}$	$1.563 (0.389) \cdot 10^{-5}$
0.20	$5.755 (0.256) \cdot 10^{-5}$	$8.277 (0.752) \cdot 10^{-5}$	$8.921 (2.015) \cdot 10^{-5}$
0.30	$4.866 (0.169) \cdot 10^{-4}$	$3.365 (0.281) \cdot 10^{-4}$	$3.556 (0.817) \cdot 10^{-4}$
0.40	$1.217 (0.034) \cdot 10^{-3}$	$1.013 (0.079) \cdot 10^{-3}$	$1.044 (0.245) \cdot 10^{-3}$
0.50	$2.250 (0.057) \cdot 10^{-3}$	$2.333 (0.164) \cdot 10^{-3}$	$2.331 (0.540) \cdot 10^{-3}$
0.60	$3.497 (0.054) \cdot 10^{-3}$	$4.188 (0.259) \cdot 10^{-3}$	$4.028 (0.901) \cdot 10^{-3}$
0.70	$5.162 (0.165) \cdot 10^{-3}$	$5.965 (0.331) \cdot 10^{-3}$	$5.520 (1.214) \cdot 10^{-3}$
0.80	$6.820 (0.107) \cdot 10^{-3}$	$6.918 (0.396) \cdot 10^{-3}$	$6.253 (1.457) \cdot 10^{-3}$
0.90	$7.647 (0.108) \cdot 10^{-3}$	$6.737 (0.479) \cdot 10^{-3}$	$6.162 (1.640) \cdot 10^{-3}$
$T = 299.15$ K			
0.00	$3.010 (0.033) \cdot 10^{-6}$	$2.122 (0.222) \cdot 10^{-6}$	$2.146 (0.662) \cdot 10^{-6}$
0.10	$1.033 (0.004) \cdot 10^{-5}$	$1.855 (0.134) \cdot 10^{-5}$	$1.916 (0.476) \cdot 10^{-5}$
0.20	$1.100 (0.022) \cdot 10^{-4}$	$1.072 (0.065) \cdot 10^{-4}$	$1.111 (0.251) \cdot 10^{-4}$
0.30	$6.271 (0.081) \cdot 10^{-4}$	$4.366 (0.265) \cdot 10^{-4}$	$4.495 (1.033) \cdot 10^{-4}$
0.40	$1.539 (0.009) \cdot 10^{-3}$	$1.316 (0.080) \cdot 10^{-3}$	$1.340 (0.314) \cdot 10^{-3}$
0.50	$2.863 (0.039) \cdot 10^{-3}$	$3.032 (0.177) \cdot 10^{-3}$	$3.039 (0.700) \cdot 10^{-3}$
0.60	$4.321 (0.127) \cdot 10^{-3}$	$5.422 (0.289) \cdot 10^{-3}$	$5.297 (1.172) \cdot 10^{-3}$
0.70	$6.187 (0.116) \cdot 10^{-3}$	$7.645 (0.383) \cdot 10^{-3}$	$7.245 (1.564) \cdot 10^{-3}$
0.80	$8.287 (0.120) \cdot 10^{-3}$	$8.734 (0.474) \cdot 10^{-3}$	$8.141 (1.852) \cdot 10^{-3}$
0.90	$9.179 (0.082) \cdot 10^{-3}$	$8.367 (0.580) \cdot 10^{-3}$	$7.956 (2.069) \cdot 10^{-3}$
1.00	$6.342 (0.039) \cdot 10^{-3}$	$6.942 (0.654) \cdot 10^{-3}$	$7.152 (2.179) \cdot 10^{-3}$
$T = 303.15$ K			
0.00	$3.604 (0.036) \cdot 10^{-6}$	$2.774 (0.270) \cdot 10^{-6}$	$2.698 (0.832) \cdot 10^{-6}$
0.10	$1.407 (0.010) \cdot 10^{-5}$	$2.375 (0.152) \cdot 10^{-5}$	$2.379 (0.590) \cdot 10^{-5}$
0.20	$1.643 (0.034) \cdot 10^{-4}$	$1.348 (0.073) \cdot 10^{-4}$	$1.365 (0.308) \cdot 10^{-4}$
0.30	$8.186 (0.179) \cdot 10^{-4}$	$5.402 (0.300) \cdot 10^{-4}$	$5.483 (1.260) \cdot 10^{-4}$
0.40	$1.873 (0.043) \cdot 10^{-3}$	$1.610 (0.092) \cdot 10^{-3}$	$1.633 (0.382) \cdot 10^{-3}$

^a Values in parentheses are standard deviations. Those of model-calculated values are computed from the relevant variance-covariance matrix according to the general error propagation equation.

Table C.6. Comparison between values of the mole fraction solubility of diazepam x_3^{sat} in water + *tert*-butyl alcohol solvent mixtures at system temperature T and pressure $P = 0.1$ MPa determined experimentally and calculated from the selected most parsimonious version of the combined Scatchard-Hildebrand/Flory-Huggins models (*continued*)^a.

w_2^0	x_3^{sat}		
	Experimental [116]	SH model	SH/FH model
0.50	$3.456 (0.070) \cdot 10^{-3}$	$3.678 (0.204) \cdot 10^{-3}$	$3.709 (0.851) \cdot 10^{-3}$
0.60	$5.531 (0.053) \cdot 10^{-3}$	$6.513 (0.333) \cdot 10^{-3}$	$6.455 (1.416) \cdot 10^{-3}$
0.70	$8.047 (0.124) \cdot 10^{-3}$	$9.066 (0.439) \cdot 10^{-3}$	$8.752 (1.864) \cdot 10^{-3}$
0.80	$1.075 (0.011) \cdot 10^{-2}$	$1.021 (0.054) \cdot 10^{-2}$	$9.724 (2.176) \cdot 10^{-3}$
0.90	$1.208 (0.024) \cdot 10^{-2}$	$9.654 (0.659) \cdot 10^{-3}$	$9.419 (2.412) \cdot 10^{-3}$
1.00	$7.618 (0.217) \cdot 10^{-3}$	$7.928 (0.739) \cdot 10^{-3}$	$8.429 (2.535) \cdot 10^{-3}$
$T = 308.15$ K			
0.00	$3.973 (0.012) \cdot 10^{-6}$	$3.595 (0.385) \cdot 10^{-6}$	$3.342 (1.029) \cdot 10^{-6}$
0.10	$1.708 (0.013) \cdot 10^{-5}$	$3.038 (0.228) \cdot 10^{-5}$	$2.935 (0.726) \cdot 10^{-5}$
0.20	$2.236 (0.023) \cdot 10^{-4}$	$1.702 (0.109) \cdot 10^{-4}$	$1.678 (0.379) \cdot 10^{-4}$
0.30	$9.889 (0.172) \cdot 10^{-4}$	$6.761 (0.423) \cdot 10^{-4}$	$6.753 (1.552) \cdot 10^{-4}$
0.40	$2.260 (0.027) \cdot 10^{-3}$	$2.007 (0.124) \cdot 10^{-3}$	$2.029 (0.474) \cdot 10^{-3}$
0.50	$4.088 (0.047) \cdot 10^{-3}$	$4.579 (0.265) \cdot 10^{-3}$	$4.669 (1.065) \cdot 10^{-3}$
0.60	$6.340 (0.075) \cdot 10^{-3}$	$8.078 (0.421) \cdot 10^{-3}$	$8.184 (1.775) \cdot 10^{-3}$
0.70	$9.220 (0.125) \cdot 10^{-3}$	$1.114 (0.054) \cdot 10^{-2}$	$1.104 (0.231) \cdot 10^{-2}$
0.80	$1.247 (0.043) \cdot 10^{-2}$	$1.239 (0.065) \cdot 10^{-2}$	$1.213 (0.266) \cdot 10^{-2}$
0.90	$1.385 (0.007) \cdot 10^{-2}$	$1.157 (0.077) \cdot 10^{-2}$	$1.165 (0.292) \cdot 10^{-2}$
1.00	$9.277 (0.093) \cdot 10^{-3}$	$9.409 (0.863) \cdot 10^{-3}$	$1.039 (0.307) \cdot 10^{-2}$
$T = 313.15$ K			
0.00	$4.860 (0.060) \cdot 10^{-6}$	$4.847 (0.637) \cdot 10^{-6}$	$4.340 (1.334) \cdot 10^{-6}$
0.10	$2.358 (0.070) \cdot 10^{-5}$	$4.027 (0.405) \cdot 10^{-5}$	$3.779 (0.932) \cdot 10^{-5}$
0.20	$2.914 (0.071) \cdot 10^{-4}$	$2.220 (0.191) \cdot 10^{-4}$	$2.146 (0.483) \cdot 10^{-4}$
0.30	$1.332 (0.047) \cdot 10^{-3}$	$8.724 (0.690) \cdot 10^{-4}$	$8.628 (1.981) \cdot 10^{-4}$
0.40	$2.860 (0.123) \cdot 10^{-3}$	$2.577 (0.188) \cdot 10^{-3}$	$2.617 (0.609) \cdot 10^{-3}$
0.50	$5.239 (0.104) \cdot 10^{-3}$	$5.863 (0.380) \cdot 10^{-3}$	$6.115 (1.382) \cdot 10^{-3}$
0.60	$8.172 (0.169) \cdot 10^{-3}$	$1.027 (0.057) \cdot 10^{-2}$	$1.077 (0.230) \cdot 10^{-2}$
0.70	$1.154 (0.020) \cdot 10^{-2}$	$1.394 (0.070) \cdot 10^{-2}$	$1.429 (0.293) \cdot 10^{-2}$
0.80	$1.519 (0.026) \cdot 10^{-2}$	$1.517 (0.079) \cdot 10^{-2}$	$1.534 (0.328) \cdot 10^{-2}$
0.90	$1.689 (0.069) \cdot 10^{-2}$	$1.388 (0.091) \cdot 10^{-2}$	$1.445 (0.354) \cdot 10^{-2}$
1.00	$1.195 (0.034) \cdot 10^{-2}$	$1.111 (0.100) \cdot 10^{-2}$	$1.274 (0.370) \cdot 10^{-2}$

^a Values in parentheses are standard deviations. Those of model-calculated values are computed from the relevant variance-covariance matrix according to the general error propagation equation.